Development of nanomedicines for inflammation disorders : evaluation of pharmacological efficacy on preclinical models

Flavio Dormont

NNT : 2019SACLS451

Development of nanomedicines for inflammatory disorders: evaluation of squalene-based nanoparticles in pre-clinical models

Thèse de doctorat de l'Université Paris-Saclay
préparée à l'Université Paris-Sud

École doctorale n°569
Innovation thérapeutique : du fondamental à l'appliqué (ITFA)
Spécialité de doctorat : Pharmacotechnie et biopharmacie

Thèse présentée et soutenue à Châtenay-Malabry, le 15 Novembre 2019, par

Flavio Dormont

Composition du Jury :

Fabienne Testard Chercheuse, CEA (LIONS)	Président
María José Blanco Prieto Professeur, Universidad de Navarra	Rapporteur
Stefaan de Smedt Professeur, Ghent University	Rapporteur
Thomas Pons Chargé de Recherche, ESPCI (– UMR 8213)	Examinateur
Patrick Couvreur Professeur, Université Paris-Sud (– UMR 8612)	Directeur de thèse
Mariana Varna Maitre de Conférence, Université Paris-Sud (– UMR 8612)	Co-Directeur de thèse

Thèse de doctorat

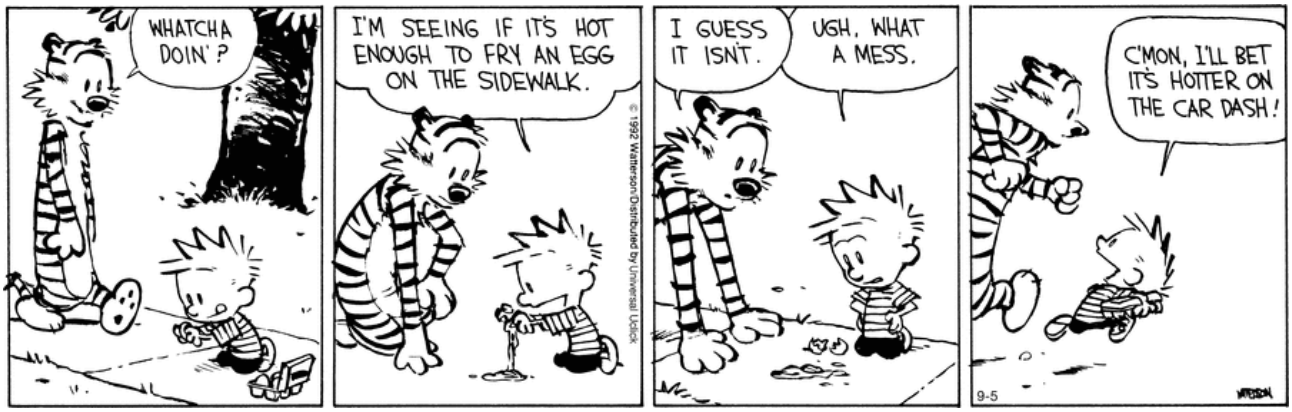
WHATCHA DOIN'?
I'M SEEING IF IT'S HOT ENOUGH TO FRY AN EGG ON THE SIDEWALK.
© 1992 Watterson/Distributed by Universal Uclick
I GUESS IT ISN'T.
UGH, WHAT A MESS.
C'MON, I'LL BET IT'S HOTTER ON THE CAR DASH!
9-5
WATTERSON

Remerciements

On dit souvent qu'un doctorat est un travail long et solitaire où l'on fait face, seul, aux nombreuses difficultés de la recherche académique. A l'issue de la rédaction de cette thèse, je suis convaincu que ceci est loin d'être le cas. Je n'aurais jamais pu mener à terme ce travail sans l'aide inestimable de mes nombreux collaborateurs et mentors, auprès de qui j'ai tant appris.

Je tiens tout d'abord à remercier **Patrick**, mon directeur de thèse, pour m'avoir donné la chance de travailler au sein d'une équipe formidable et sur des sujets si passionnants. A travers nos discussions, vous avez toujours su laisser libre cours à ma curiosité scientifique tout en la canalisant par vos remarques et suggestions qui poussaient mon exigence expérimentale et professionnelle. Malgré votre emploi du temps chargé vous avez toujours su me faire sentir suivi, encouragé et apprécié. Je ne compte aussi plus le nombre de fois où je suis venu me perdre en conversations dans votre bureau, qu'elles soient à propos de science, de voyages ou à propos de votre passé de dopeur de pigeons de course. Pour tout cela et plus encore je vous dis un grand merci.

Je souhaite également témoigner toute ma gratitude à, **Mariana**, ma co-directrice de thèse. Depuis le premier jour de cette épreuve tu as été à mes côtés, me préparant, me poussant dans mes connaissances scientifiques, me suivant dans mes avancées, toujours disponible et réactive. Je n'étais surement pas la personne la plus facile à encadrer, mais tu as toujours fait preuve de gentillesse et d'attention à mon égard. L'abnégation et l'énergie que tu mets dans ton travail m'ont stimulé en permanence au cours de cette thèse. J'essaierai de conserver la générosité et le sens du détail que j'ai appris à tes côtés, ce sont des atouts précieux.

Je tiens aussi à remercier l'ensemble des membres de mon jury de thèse : **Pr. Maria Jose Blanco Prieto** et **Pr. Stefaan de Smedt** for doing me the honor of reviewing my work as rapporteurs ; **Dr. Thomas Pons** et **Dr. Fabienne Testard** pour avoir accepté de porter un regard critique sur mon travail en tant que qu'examinateurs.

Je remercie par ailleurs la Fondation pour la Recherche Médicale, pour avoir financé ce travail de thèse et bien voulu placer sa confiance en moi, dans le projet et dans notre équipe.

J'adresse aussi de chaleureux remerciements à **Elias**, pour son accueil au sein de l'Institut Galien. Contrairement à d'autres thésards, je ne connaissais pas le laboratoire de mes années de master ou autre et pourtant j'y ai été accueilli à bras ouverts. En tant que directeur de l'Institut vous contribuez à la création et au maintien de cette magnifique « tour de Babel » comme vous l'appelez, où se mélangent langues, cultures et personnalités finissant par créer un lieu de travail si enrichissant tant sur le plan personnel que professionnel.

J'ai en effet été entouré de personnes remarquables au sein de l'institut, sans qui je n'aurai jamais pu mener mon travail à bout : **Didier**, notre « encyclopédie chimique » à tous, qui m'a tant aidé à me débourber de mes déboires d'impuretés, mais en qui j'ai aussi rencontré une personne d'une culture rare et d'une disponibilité à toutes épreuves. Un grand merci pour tout ; **Simona**, merci pour avoir partagé avec moi ton expertise du squalène, pour nos discussions si enrichissantes et pour tes délicieux gâteaux qui vont beaucoup me manquer ; **Sinda**, pour avoir toujours pris le temps de faire progresser mes connaissances chimiques, pour t'être penchée sur mes problèmes de synthèse ou pour m'avoir demandé si souvent comment ça allait au passage d'une porte de labo. Merci ; **Catherine,** qui m'a accompagné durant toutes mes études en animalerie, et qui arrivait à faire passer un peu plus vite une dure journée de labeur en salle de manip. Merci pour toute ton expertise, ta gentillesse et ta disponibilité, elles m'ont énormément aidé ; **Juliette**, avec qui j'ai tant échangé sur la culture cellulaire et qui a guidé mes premiers pas dans le monde des ROS et de la cytométrie ; **Stéphanie** qui sauvait nos cellules au rythme des coupures d'électricité et me croisait toujours avec un son grand sourire ; **Julie** notre experte TEM qui garnissait l'air du labo et de la cafet' par ses thés menthe-fraise ; **Nicolas** qui savait toujours à qui s'adresser pour de nouvelles questions techniques et qui au passage d'une discussion autour d'un café a toujours su me suggérer des articles ou idées intéressantes pour faire avancer mes recherches ; **Julien** merci pour les discussions intéressantes, les photos en congrès et les tweet ; **Franceline** d'une gentillesse extraordinaire et avec qui j'ai eu la chance de partager des projets de recherches (et mes passages de cellules), merci pour ta générosité et ta collaboration à mon travail ; **Nada** avec qui c'était toujours agréable de partager un labo, pour discuter de sciences, ou de la vie. Un grand merci aussi à **Sylvie, Marie-Claude, Patricia et Dominique**, pour avoir toujours répondu à mes questions administratives avec bonne humeur et sans perdre patience quand je revenais cinq fois sur le même sujet.

Merci également aux responsables des plateformes de la faculté de pharmacie, notamment

Karine, avec qui j'ai fait des dizaines de HPLC et qui nous a permis d'arriver à bout des impuretés du squalène, **Delphine** toujours disponible pour m'aider à mettre en place des expériences de fluorimétrie au dernier moment, merci pour ta disponibilité et ta gentillesse ; **Valérie Nicolas** pour vos explications et protocoles limpides en microscopie confocale ; **Audrey** pour ton aide à l'identification de composés squalenés ; **Françoise** avec qui j'ai pu mettre en place de belles expériences d'histologie.

Je tiens également à remercier les participants au projet européen NanoHeart, tout particulièrement **Serge** notre partenaire industriel qui a accepté de se lancer dans l'aventure de la synthèse à grande échelle des dérivés squalénés. Ton honnêteté, ton expérience et ta transparence nous ont permis de faire de grandes avancées sur le sujet et je t'en remercie grandement ; **Maria** merci de m'avoir accueilli au sein de ton laboratoire et pour votre travail sur les études pré-cliniques avec l'adénosine-squalène, j'ai énormément apprécié échanger avec toi, tant sur le plan scientifique que personnel ; **Laura** et **Elisa** encore désolé d'avoir doublé votre nombre de groupes d'études sur les rats, j'espère pouvoir me racheter avec quelques pinxos à Pamplona bientôt. **Caroline** et **Julie,** merci aussi pour votre accueil au sein de vos entités respectives en Belgique, ça a été un grand plaisir de collaborer avec vous.

Ces trois années auront aussi et surtout été enrichies par la présence des nombreux étudiants de l'Institut Galien. Par votre enthousiasme, votre sympathie et votre amitié vous avez rendu chaque moment passé parmi vous un vrai plaisir que j'emporte avec moi. **Raul** mon compagnon de tous les jours, péruvien en cachète et apiculteur en reconversion. Tout cela aurait été bien difficile sans toi. Je laisse à nos déclarations enivrées le témoignage de mon affection et tiens simplement ici à te remercier pour ton amitié, ta loyauté et ton soutien, elles ont été pour moi une source de force insoupçonnée ; **Federica**, Emofede, Reine des glaces et des soirées, qui a la gentillesse de corriger mon italien par des risées à peine contenues, qui marche aussi vite que moi dans les couloirs et a plus de vêtements rangés dans ma cave que j'en ai dans mon armoire. Promis, l'année prochaine il ne pleuvra pas tous les jours en Sicile. Merci pour tous les duckfaces et les fous rire ; **Arnaud**, avec qui j'ai suivi (par intermittence) un entrainement physique intensif, et que j'ai bassiné à longueur de semaines avec mes théories sur le métabolisme et la nutrition. Merci pour ta compagnie et pour nos nombreuses discussions, scientifique ou autres, mais fait réparer la portière de ta rape car ; **Romain**, cher compagnon de bureau, que j'ai également bassiné avec mes théories diverses et variées et qui a toujours eu l'amabilité de m'écouter sans hausser les yeux au ciel. Toi plus que tout autre aura contribué au travail de

cette thèse et je t'en remercie infiniment, ça a été un plaisir de bosser avec toi et de se retrouver tous les jours dans notre petit bureau pour discuter de tout et de rien, partager nos opinions et s'entraider ; **Serra** aka Sooo niiice qui aura eu en l'espace d'un an-et-demi 5 pots de départ et d'arrivée, traversé 3 bureaux différents et illuminé autant de personnes par sa bonne humeur et son sourire. Merci d'avoir transformé mon bureau en salon de thé, et d'avoir fait de moi un membre des « Girls » ; **Céline** dont le regard désapprobateur suffisait en une seconde à me faire savoir quand je faisais ou disais n'importe quoi. Je suis bien content qu'on ait apprit à se connaitre au fur et à mesure de ces années de thèse, même si tu m'as terrifié avec tes talons bruyants pendant toute ma thèse ; **Quentin,** le français de souche, avec son accent blédard et la barbe hirsute. Merci pour tous les sushis, les bonnes discussions à la cantine et l'aide en DH22. Quand tu veux on fait un foot samedi matin après le Thirsty Mad Cat ; **Barbara** avec qui j'ai partagé ma passion des jeux de cartes et qui aura presque réussi à m'initier à Magic. OnePlus power ; **Balthazar**, Baltou, respo blague lourde, avec qui c'était toujours un plaisir de partager une (quelques) pintes aux 3 marches ; **Eléonore** pour ta gentillesse et ta disponibilité, dommage que on ait pas eu l'occasion de faire toutes les études que l'on avait prévu ensemble ; **Justin** qui me rappelle mes jours en Corée, entouré de personnes qui parlaient une langue que je ne comprenais pas et combien un sourire ou une simple conversation peuvent aider à s'intégrer ; **Marie** chère compagne d'adénosine-squalène, qui m'a toujours inspiré par son exigence scientifique et partageait mes problématiques. C'était toujours un plaisir de travailler et de discuter avec toi ; **Gianpiero** mon modèle préféré, membre de la team du 15e, meilleure caisse de résonance pour râler et toujours de bon conseil. Merci pour ton soutien dans les moments difficiles qu'on a traversé, et pour avoir été la première personne à m'accueillir au labo avec ton grand sourire Colgate de star ; **Daniele,** Naughty Bear, tu me dois encore des shooters. Merci de me rappeler de ce qui peut m'attendre après la thèse, pour les chansons, les coccole et pour tes précieux conseils de synthèse. Ca me manque de prendre des verres avec toi ; **Jiao** thank you for the time together in the lab and for your precious advice, I hope everything goes okay in China and we can meet again some day ; **Alex** pour m'avoir introduit à mon bar préféré et pour ta bonne humeur; **Tanguy** pour tes conseils sur de nombreuses expériences ; **Alessandro** pour tes suggestions de publication ; **Marion** pour avoir subventionné mon addiction au chocolat ; **Johanna** pour m'avoir toujours accueilli avec le sourire malgré le fait que j'avais volé ton agitateur et pour tous les gâteaux que je venais quémander dans ton bureau ; **Clélia** pour être toujours la dernière à partir en soirée ; **Justine** pour les sourires journaliers et la réorganisation du labo ; **Maelle** pour me rappeler que je ressemble à un kéké et me motiver à aller au sport ; **Flora** pour ta gentillesse et pour m'avoir

débloqué la DH22 pendant mes tests ELISA critiques ; **Théo**, mon compagnon de l'ESPCI, bon courage pour la suite ; **Maud** qui, venant dans mon bureau me demander comment allait mes expériences, avec une simplicité et une douceur déconcertante, réussissant toujours à me redonner le punch ; **Ichem** pour te soucier toi aussi de l'avancée de mon travail et ta gentillesse ; **Eliot** et **Manon** premiers stagiaires avec qui j'ai travaillé sur l'adénosine-squalène et qui soulevaient les premiers soucis. Bref, Il est difficile de citer **tous les doctorants, post-doctorants et stagiaires** qui m'on influencé de près ou de loin, pourtant vous avez tous participé à créer cette superbe ambiance de travail qui rendait plaisant (malgré la localisation géographique) le fait de partir pour le labo tous les matins.

Au terme de ce parcours, je remercie enfin **ma famille et mes amis**, qui m'apportent tant chaque jour et dont les attentions et encouragements m'ont accompagné tout au long de ces années. Je suis particulièrement redevable à mes parents, **Didier** et **Alessandra**, pour leur soutien moral et matériel et pour leur confiance indéfectible dans mes choix. J'ai enfin une pensée toute particulière pour ma grand-mère, **Simone,** dont la mémoire et l'influence ne sont pas étrangères à mes choix scientifiques.

Table of Contents

General Introduction

Inflammation is associated with many pathological conditions such as sepsis, ischemia/reperfusion injuries or atherosclerosis. Inflammatory disorders drive the genesis and pathophysiology of these complex maladies for which efficient treatments are still lacking. Current therapies aimed at alleviating these inflammatory disorders are often limited by side effects, poor specificity and the introduction of immune-deficient states.

Advances in drug delivery have afforded numerous tools which help to adapt the administration strategy of an active pharmaceutical agent taking into account its therapeutic target. Notably, nanomedicines, or nanoparticle-based delivery agents, have afforded a host of breakthroughs in oncology and diagnostics. By improving drug targeting and protecting the active pharmaceutical agents from metabolisation, nanomedicines can enhance a drug's therapeutic index resulting in improved patient outcomes. With these promising advances, however, come noteworthy drawbacks such as the infamous low drug loading of some nanomedicine formulations, complicated industrial translation and control of drug release.

To answer these limitations, Pr Couvreur's team has developed since 2004 a novel encapsulation strategy, so-called « squalenoylation ». Coupling active therapeutic agents with a derivative of squalene- an endogenous, biocompatible and biodegradable lipid- yields stable nanoparticles, with high drug loading efficiency and low toxicity. The resulting nanomedicines usually present improved pharmacokinetics compared to the free drug and a more targeted biodistribution. Squalene bioconjugates have been used coupled to adenosine, an endogenous modulator of inflammation, in pre-clinical models of ischemic stroke and spinal chord injury, with promising results.

Another advantage of squalene prodrug-based nanocarriers is that they afford the possibility to encapsulate multiple drugs in the same therapeutic system, thus allowing multidrug therapy. This is an important tool in the context of inflammatory disorders, where often multiple factors converge to drive disease progression. For instance, it has been established that uncontrolled

inflammation is often driven by continuous positive feedback loops between pro-inflammatory signaling and oxidative stress. There are currently no effective ways to counter this crosstalk in a targeted manner. Therefore, part of the focus of this doctoral thesis was to develop and test on preclinical models, squalene prodrug-based nanoparticles for inflammation control through a powerful two-drug neutralization process: adenosine as an endogenous inflammation mediator and tocopherol (VitE) for efficient protection against oxidative stress. Not only could a two drug therapy improve disease outcome by inhibiting multiple, self-reinforcing, pathogenic processes, but the nanoparticle formulation could provide an interesting targeting ability to the loci of uncontrolled inflammation.

In a bibliographic introduction, first we describe the different systems that have been investigated so far to mitigate the uncontrolled inflammatory processes that occur during sepsis. We shortly outline the pathogenesis of the disease and address where current therapies have failed, before reviewing recent advances made in the field of nanomedicine to overcome these shortcomings. In the second bibliographic part, we evaluate the use of biomaterials in the context of cardiovascular diseases. These include nanosystems that were used for the prevention of atherosclerosis as well as its acute manifestation in heart ischemia and infarction. We describe how the two diseases progress and tie into each other, where and how nanomaterials can play a therapeutic role, and promising avenues of research.

Our experimental section was divided in three chapters.

In the first experimental chapter, we describe the development of a novel multidrug squalene formulation to mitigate uncontrolled inflammation. By encapsulating adenosine and tocopherol in the same therapeutic agent, these novel nanoparticles had the potential to efficiently address the crosstalk between inflammation and oxidative stress while limiting side effects resulting from high doses of adenosine. After characterizing the physico-chemical properties of our formulation, its anti-inflammatory and anti-oxidant effects were evaluated in *in vitro* models of oxidative stress and inflammation. In parallel, the *in* vivo biodistribution of these squalene-based multidrug nanoparticles was studied and showed a marked targeting property for inflamed tissue. Consequently, we evaluated the therapeutic potential of these squalene-adenosine/tocopherol (SQAd/VitE) nanoparticles in two *in vivo* models of inflammatory endotoxemia. Animals treated with SQAd/VitE nanoparticles had a significantly improved survival to the inflammatory insult and showed lowered signs of side effects compared to free

drug controls.

In a second experimental chapter, we studied whether the targeting ability of squalene-based nanoparticles for inflamed tissue could translate to other models of inflammatory disease. For this proof of concept, the biodistribution of fluorescent squalene nanoparticles was evaluated in an *in vivo* model of atherosclerosis using ApoE$^{-/-}$ mice. Our initial results show that squalene nanoparticles could indeed accumulate specifically in the lipid rich atherosclerotic plaque and interact with macrophages. Current studies aim at elucidating the mechanism of this accumulation more precisely.

Finally, in a third experimental chapter, we evaluated the feasibility of industrial scale-up for the synthesis of squalene bioconjugates. Indeed, while nanomedicine is poised to bring momentous advances in the fight against many maladies, it is still stifled by unrealistic industrial production of systems that have often become too complex or too expensive to efficiently manufacture at the industrial scale. In an effort to facilitate the translation of squalene-based nanoassemblies from lab scale experiments to the larger multicenter studies needed for regulatory approval, we associated with an industrial partner to study industrially produced squalene-adenosine nanoparticles. Our experiments showed that minute differences in the composition of squalene-adenosine bioconjugates could result in significantly different physico-chemical and biological properties of the obtained nanoparticles, which could lead too poor reproducibility and unreliable pre-clinical data. Solving these issues constituted an important step forward in the pharmaceutical development of squalene-based therapeutic agents.

Overall, this work opens new therapeutic possibilities and avenues of study by showing how the differential biodistribution of squalene-based nanoassemblies can be used to target and efficiently mitigate uncontrolled inflammation.

Bibliographic Introduction

Nanomedicines for the management of Sepsis

Flavio Dormont, Mariana Varna, Patrick Couvreur

Institut Galien Paris-Sud, CNRS, Univ. Paris-Sud, Université Paris-Saclay, Faculté de Pharmacie, 92296 Châtenay-Malabry, France

Nanomedicines for the Management of Sepsis

Abstract

Sepsis, resulting from uncontrolled inflammatory responses to bacterial infections, continues to cause high morbidity and mortality worldwide. Currently, effective sepsis treatments are lacking in the clinic and primary care remains primarily supportive. Numerous new pharmacological treatments have been attempted but the complexities of sepsis pathophysiology, poor relevancy of pre-clinical models and patient heterogenicity have stifled hopes for an efficient treatment of the disease. Over the past decade, nanotechnology based therapeutic systems have been developed to improve sepsis treatment. By enabling specific targeting, protection from early metabolization and interaction with pathogen associated molecules, several encouraging findings have been described. Provided herein is a review of this young field of science, of the complexities of sepsis treatment and future perpectives for the field of nanomedicine applied to uncontrolled inflammation.

I. Introduction

Sepsis is a highly complex syndrome that is caused by uncontrolled inflammation resulting from an unbalanced host response to infection (1). While its definition and clinical diagnosis are ever-evolving, sepsis has most recently been defined as an auto-inflammatory disease. When clinical factors such as systematic arterial hypotension or hyperlactataemia are involved, the syndrome is called “septic shock”. Sepsis is most frequently encountered in intensive care units (ICUs), where it occurs to nearly 40% of patients entering ICUs in Europe with a mortality rate of nearly 30%(2, 3). Current treatment of sepsis mainly revolves around the administration of antibiotics to curb the source of infection and early administration of intravenous fluids and vasopressors to maintain intravascular volume and tone. Where current clinical and pharmaceutical capabilities lack, are in preventing the numerous vicious cycles of anomalies involving hyper-inflammation, oxidative stress, disseminated tissue ischemia, vascular leakage, and organ dysfunctions that happen during sepsis and ultimately lead to death. In fact, patients are essentially “on their own” when fighting against a septic insult, with intensive care practitioners often relegated to a mere supporting cast role.

This state of affairs is often explained by the fact that the pathophysiology of sepsis is complex and poorly understood. Although the topic has been reviewed extensively(4, 5), a simplified overview is provided herein. During sepsis, certain microbial products, such as lipopolysaccharides (LPS) or peptidoglycans are capable of activating the innate immune system and endothelium. These pathogen-associated molecular patterns (PAMPs) activate immune cells through a multitude of pattern recognition receptors, most notably Toll-like receptors (TLRs) such as TLR2, TLR4, TLR5 or TLR9 found on monocytes, macrophages and many other types of cells. Once activated, these cells secrete a variety of inflammatory mediators such as cytokines (TNF-α, IL-6), chemokines (IL-8), reactive oxygen species (ROS), nitric oxide and damage-associated molecular patterns (DAMPs). The recruitment and migration of immune cells such as polymorphonuclear leukocytes (i.e. neutrophils) then transfers the oxidative burst performed by the innate immune system to tissues and cells where it results in disturbed signaling, oxidative damage, hypoxia and further tissue injury.

Cytokine induced tissue factor expression in endothelial cells activates the coagulation pathway which, along with excessive platelet activation, results in widespread vascular coagulation and further tissue damage. These numerous pathological processes are at the center of the pathophysiology of sepsis, however it is unclear which, if any, are the main effectors of sepsis

mortality. Rather, they seem to constitute a network of interconnected disease phenomena, organized into positive-feedback loops that amplify the initial inflammatory response and drive the disease into generalized shock and organ failure.

II. Current therapies

Once sepsis has been diagnosed, antibiotic therapies are initiated to help fight the primary infection. If a patient is identified as entering septic shock, intensive care practitioners mainly focus on normalizing several aspects of patient physiology. An influential single center study was published in 2001(6) that randomized a group of 263 patients with sepsis and hypotension within one to two hours of admission to the emergency department to either standard of care or "Early goal directed therapy" (EGTD) for the first six hours. The developed EGTD aimed to achieve, in addition to standard-of-care (8-12 mm Hg venous pressure by crystalloid administration, 65-90 mm Hg arterial pressure by vasopressor/vasodilator administration, urine output of 0.5 mL/kg/h by fluid administration) a central venous oxygen saturation of 70% using red blood cells transfusions and dobutamine administration at an initial dose of 2.5 µg/kg/min. The EGTD group had a diminished mortality of 31% vs 47% mortality for the non EGTD treated group. This has now become standard of care with many centers adopting EGDT methodology along with early detection of systemic inflammation(7). The adoption of low-tidal volume, lung protective ventilation in patients with sepsis has also been a factor in the improvement of patient outcomes(8).

While EGTD-based fluid resuscitation and antimicrobial therapies have afforded consistent improvements in survival after sepsis(4), no proven effective molecular treatments of sepsis have been implemented so far. Early preclinical studies on anti-TNF-α antibodies(9, 10) were the first to generate excitement with the hypothesis that blocking pro-inflammatory cytokine cascades in sepsis would reduce mortality. However, subsequent clinical trials failed to prove a significant improvement in survival with patients receiving solely anti-TNF-α treatment(11). Similarly, corticosteroids were reported as early as 1976 to reduce mortality in septic shock dramatically(12), however, there is still no consensus about their efficacy after larger clinical trials(13). Other specific therapeutic interventions have covered (i) the use of anti-virulence factors aimed at sequestering bacterial components such as LPS from the blood stream(14, 15), (ii) agents targeting coagulopathy(16, 17) to limit disseminated vascular coagulation and (iii) antioxidants for ROS scavenging and mitochondrial protection(18, 19). Unfortunately, in almost every case, early preclinical and clinical successes failed to be confirmed and replicated

in larger phase III trial.

III. Why it hasn't worked so far

There are many reasons why novel drug development efforts in sepsis have yielded poor results and much has been written about this subject(20). Apart from the usual challenges of optimizing pharmacokinetics, relevancy of preclinical models or patient heterogenicity, some issues merit to be highlighted here.

One example is with antioxidant therapies aimed at limiting oxidative shock during sepsis. Although many promising results have been obtained from animal models, a benefit from anti-oxidant therapy in sepsis has rarely been found in human clinical trials(19). Kohen and Nyska(21) clearly explain the shortcomings of anti-oxidant therapy as follows: "Taking into consideration the high reactivity of ROS, their short life span, their continuous production in close proximity to biological targets and their ability to be modified into other more reactive species, one realizes that, in order to cope with these deleterious metabolites, the anti-oxidant should be administered to the body continuously, in high concentrations and targeted to the biological site susceptible to oxidative damage." Moreover, the delivery of anti-oxidants into the intracellular space is limited by mechanisms, such as the intracellular redox buffer(22), regulating the cytosolic redox state in order to maintain normal functioning of the cell. Therefore, even if long-term supplementation raises blood anti-oxidants, it will have a limited effect on intracellular levels or redox status. Hence, the majority of anti-oxidants perform their actions predominantly in plasma, which may have beneficial effects during the hyper-inflammatory stage of sepsis but are ineffective at protecting cells and tissues.

Similarly, although anti-bacterial therapy has had some success, its effective implementation in the context of sepsis is complicated by compromised cardiovascular, hepatic and renal functions. The pharmacokinetics of the administered treatments are often altered so much that administration of excessive dosages leading to adverse side effects are common(23). Furthermore, bacteria have developed systems to evade common antibiotic therapy, such as intracellular localization or bacterial DNA recombination. More than ever, the current era is characterized by frequent drug resistance of pathogens requiring the use of high doses of antibiotics, generating toxicity and driving resistance. Studies have demonstrated that the outcome of sepsis is worse if the infecting micro-organism is not sensitive to the antibiotic treatment(24).

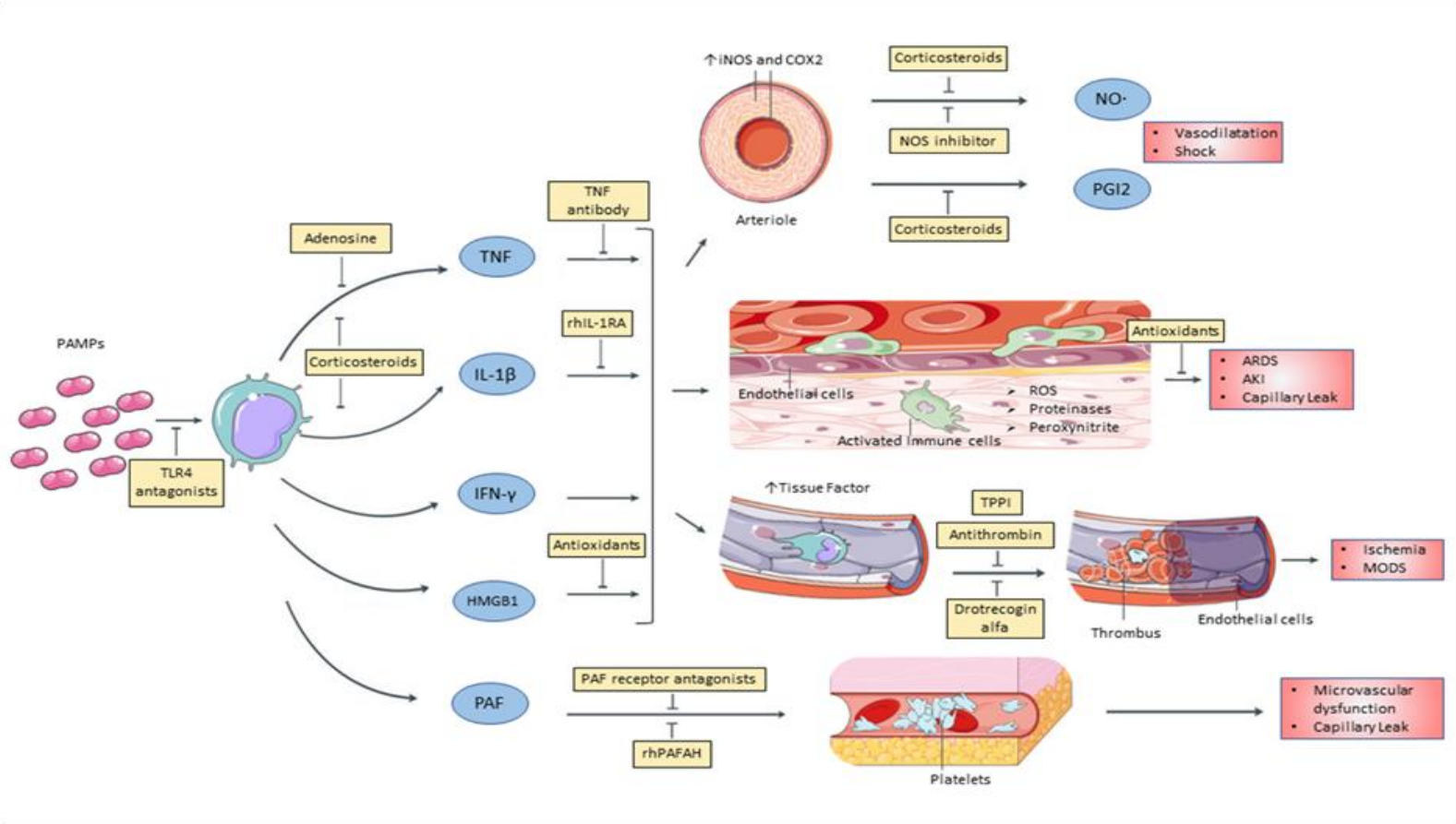

Figure 1: Pathogenesis of sepsis and attempted treatments. Pathogen associated molecular patterns (PAMPs) interact with Toll-like receptors on macrophages. This triggers the release of pro-inflammatory molecules such as tumor necrosis factor (TNF-α), interleukin-1β (IL-1β). These molecules activate endothelial and smooth muscle cells throughout the body, where they promote inducible nitric oxide synthase (iNOS) and Prostaglandin-endoperoxide synthase 2 (COX-2) producing ROS, NO· and prostaglandin. Together, these potent vasodilators severely alter vascular tone, resulting in widespread vasodilatation and shock. Activated endothelium also expresses various vascular adhesion molecules such as ICAM-1 and VCAM-1, leading to vascular sequestration of activated immune cells at the sites of inflammation. These cells deploy a vast array of molecular messengers and stress molecules which result in tissue damage, ROS-mediated mitochondrial dysfunction, capillary leak and eventually pathological conditions such as acute respiratory distress syndrome (ARDS) or acute kidney injury (AKI). Stress molecules increase the expression of tissue factor, triggering a coagulation cascade which results in disseminated vascular thrombosis, ischemia and eventually multiple organ dysfunction syndrome (MODS). Activated macrophages also release platelet-activating factor (PAF), which results in widespread platelet aggregation, microvascular dysfunction and capillary leakage.

Another example is found in the case of adenosine, where preclinical studies have provided insights into the role of the various adenosine receptors (A1, A2A, A2B, A3) in the physiological response of the organism to sepsis. Indeed, adenosine has been shown to reduce vascular leakage at inflamed sites through A2B receptor activation(25), diminish neutrophil recruitment by inhibiting both selectin and integrin-mediated adhesive events(26, 27) and promote the anti-inflammatory effects of effector T cells(28). In general, adenosine receptor activation preserves tissue function and prevents tissue injury in insults where inflammation and the immune system have a major role to play such as ischemia, reperfusion injury, arthritis, chronic obstructive pulmonary disease and sepsis. As such, several agonists of adenosine receptors have been developed and investigated for efficacy. Like adenosine, however, these compounds carry potential issues related to cardiovascular side effects and the wide tissue distribution of their cognate receptors limits their usefulness in the treatment of inflammatory diseases. Additionally, because of the ubiquity of its catabolic enzymes cAMP, and adenosine deaminase (ADA), adenosine has an extremely short half-life in the blood (<10 s) requiring the use of high doses which limit its therapeutic use, too.

IV. Where nanomedicine could help

In the context of sepsis, nanomedicines may provide distinctive advantages over usual small drug molecules in at least three areas. They afford prolonged blood residence time and protection from early metabolization to compounds that would otherwise suffer from poor bioavailability. Their differential biodistribution allows the specific targeting of injured tissue and cells through passive mechanisms or specific targeting by surface functionalization. And by encapsulating several therapeutic agents they allow the delivery of multidrug therapies that may concurrently inhibit different pathways of disease progression and efficiently manage septic insults. Indeed, sepsis pathophysiology affords several phenomena that can be exploited by nanomedicine. Being essentially an inflammatory condition, with immune cells as the main mediators and effectors of injury, nanomedicines can be used to target specific cells in order to inhibit or alter pathological processes without influencing other tissues(29, 30). The inflammatory environment of sepsis also allows nanoparticles to passively target the loci of inflammation due to the endothelial permeability that exists there. Indeed, during acute inflammation, different activated immune cells release proteases and inflammatory cytokines which increase the vascular permeability by degrading the endothelial extracellular matrix and inducing the dissolution of intercellular VE-cadherin tight junctions. Macromolecules tend to

passively and preferentially accumulate at these sites of enhanced vascular permeability and are then retained (Figure 2). This enhanced permeability and retention (EPR) effect has been recognized as a major breakthrough in antitumoral targeting, but has just started to be exploited in infection and inflammation. The following sections describe how nanoparticles have been used so far in the management of sepsis and advances in the field.

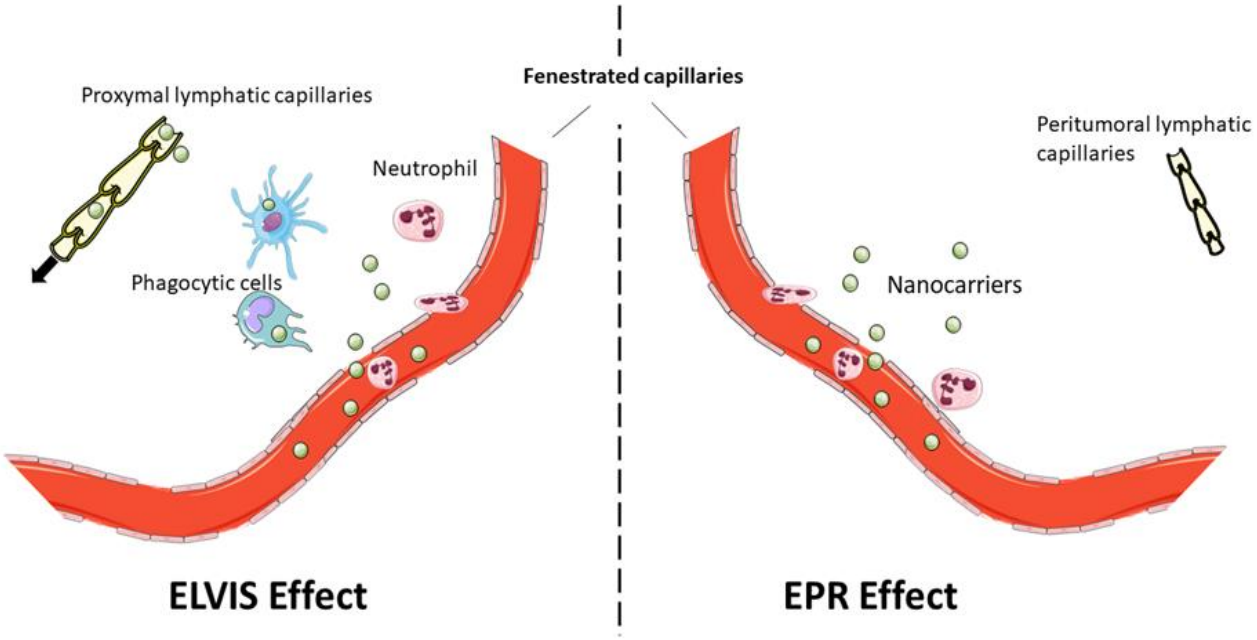

Figure 2: **Mechanisms of passive drug targeting.** Tumors and inflammation have many common features. One hallmark of both is enhanced vascular permeability, which is mediated by various factors including bradykinin, nitric oxide, inflammatory cytokines and abnormal vascular growth. The absence of effective lymphatic drainage is a characteristic of tumors which leads to extravasated macromolecules to accumulate at the tumor site, this is called the EPR effect. During inflammation, proximal lymphatic capillaries readily clear debris and retention only occurs through increased interstitial pressure or cell-mediated sequestration. Phagocytic cells resident in inflamed tissue are thus key players in inflamed tissue targeting in a mechanism called Extravasation through Leaky Vasculature and Inflammatory cell-mediatation Sequestration (ELVIS).

V. Immuno-modulating nanomedicines

The common denominator of many nanomedicine based immune-modulating treatments in sepsis is their targeted nature. Indeed, after the failure of several clinical trials of anti-inflammatory agents, a growing understanding that immuno-modulation in sepsis should be targeted both in time and space has emerged. For this reason, nanomedicine based therapeutic systems have usually been engineered to specifically interact with activated cells, enacting a

therapeutic response but avoiding the introduction of a secondary immune-compromised state.

Thus, recent drug development efforts have reported the use of Sialic acid-binding immunoglobulin-like lectins (Siglecs) targeted nanoparticles capable of downregulating the acute inflammatory response in murine models of sepsis and pulmonary inflammation(31). Siglecs are cell membrane bound receptors found on hematopoietic cells and capable of inhibiting pro-inflammatory Toll-like receptor signaling. In order to target the Siglecs on activated macrophages and monocytes, PLGA-based NPs were surface functionalized using a sialic acid, N-acetyl neuraminic acid (NANA). The NANA-NPs were more efficient at inducing Siglecs activation and IL-10 dependent anti-inflammatory signaling than free NANA, due to the surface display of the sialic acid. This resulted in a significant survival advantage in treated animals (100% vs 0%) with signs of abrogated inflammation such as diminished TNF-α levels and increased IL-10.

Another study targeted endothelial inflammation by using bovine serum albumin NPs interacting specifically with adherent neutrophils(32). The NPs were used as carriers of piceatannol, a tyrosine kinase inhibitor used to reverse the TNF-α activated adhesion of neutrophils to the inflamed endothelium. Interestingly, the albumin NPs (100 nm) were readily taken up by neutrophils adherent to the inflamed endothelial cells via Fcγ receptors -a receptor recognizing opsonization antibodies- but not by resting neutrophils or other cells. Indeed, because Fcγ receptors are highly expressed in adherent neutrophils(33), theses nanoparticles were able to selectively affect the pro-inflammatory subpopulation of neutrophils without affecting the essential host-defence function of circulating neutrophils. In a mouse model of LPS-induced lung inflammation, the NPs significantly reduced myeloperoxidase (MPO) activity in the lungs, a marker of neutrophil infiltration, and reduced acute lung injury.

More recently, nanoparticles with targeting abilities towards the infection environment were tested for sepsis management(34). During sepsis, endothelial cells rapidly expresses several adhesion molecules, such as intercellular adhesion molecule-1 (ICAM-1)(35). In a mouse model of induced sepsis by intraperitoneal injection of a lethal dose of bacteria, these nanoparticles afforded a significant increase of survival to the septic insult. Practically, the nanoparticles were designed by using a pH/enzyme-responsive amphiphilic block copolymers consisting of biotinylated poly(ethylene glycol)-b-poly(β-amino ester)-b-poly(ethylene glycol) grafted with PEGylated lipid (Biotin-PEG-b-PAE(-g-PEGb-DSPE)-b-PEG-Biotin) for targeting the inflamed

endothelium both passively via EPR effect and actively after surface decoration with an antimouse ICAM-1 antibody. Once the nanoparticles accumulated into the inflamed site, the unique microenvironment of low pH (~pH 6)(36), bacterial enzymes(37) and activated cells triggered the release of an antiobiotic (ciprofloxacin) together with an anti-inflammatory agent ((2-[(aminocarbonyl)amino]-5-(4-fluorophenyl)- 3-thiophenecarboxamide) for an efficient 'on demand' multidrug therapy.

Concurrently, carriers of natural origin called exosomes have been the focus of attention for use in sepsis therapy(38). Exosomes are extracellular vesicles that are produced in the endosomal compartment of most cells and used to shuttle proteins or RNAs to specific target cells. Because of this, exosomes are of interest in the treatment of sepsis as accurate drug carriers(39). For instance, bone marrow-derived dendritic cells can selectively downregulate inflammatory gene expression by releasing exosomes containing microRNA (miRNA) miR-146 to be specifically uptaken by target dendritic cells. When administered as a prophylactic measure to LPS-challenged mice, miR-146-containing exosomes reduced the TNF-α and IL-6 production and regulated inflammation by functional transfer between immune cells(40). In another study, exosomes containing miR-223, a miRNA down-regulator of pro-inflammatory cytokine production in cardiomyocytes, were injected in cecal ligation and puncture (CLP)-challenged mice resulting in improved survival and diminished markers of inflammation in the hearts of treated animals(41). While these studies demonstrate the promising, targeted nature of exosomal delivery, the industrial development of these innovative nanocarriers is still in its infancy(42) and other carriers of miRNA have been explored for the treatment of sepsis. For instance, miR-126, an exosomal miRNA impacting endothelial homeostasis and postulated to improve outcomes during sepsis, was also recently administered in deacetylated poly-N-acetyl glucosamine (DEAC-pGlcNAc) based nanoparticles to CLP-challenged mice. DEAC-pGlcNAc also display anti-microbial activity which makes it another interesting candidate for drug delivery during sepsis. These NPs significantly improved survival in compared to PBS-treated controls(43).

VI. Nanomedicines for the sequestration of pathogen-associated molecular patterns

Pathogen associated molecular patterns are an important pathogenic trigger during sepsis which induce the systemic inflammatory response. Their amount in the blood usually strongly correlates with the severity of the inflammatory response and as such effective endotoxin removal is a critical component of successful sepsis management. This neutralization process however presents various challenges. While many PAMPs are architecturally similar, they vary in their precise structure across bacterial strains, which poses difficulties for structure-based neutralization strategies relying on specific ligand interactions.

Because of their high surface-to-volume ratio, nanoparticles are ideally suited to act as antagonists to toxins by sequestering pathogen associated molecular patterns from the blood stream. *In vivo,* bacterial toxins naturally target sphingolipid and cholesterol-rich domains of cellular membranes as they confer specificity for animal cells as opposed to bacterial cell membranes. Based on this idea, liposomes were engineered to effectively compete with host cells for toxin binding by comprising higher than *in vivo* relative concentrations of selected lipids(44). Once bound to liposomes, the bacterial toxins were unable to affect mammalian cells in vitro. When used in mice infected by *Staphylococcus aureus*, the liposomes significantly improved survival rate and reduced TNF-α levels and bacterial loads in the blood and lungs of treated animals. The study showed that the liposomes themselves were not bactericidal but rather acted by sequestering PAMPs and thus limited the toxin-induced tissue damage that occurred during bacterial clearance(44). This study highlighted how nanocarriers could be used in creative ways for therapeutic avenues making use of their particular composition.

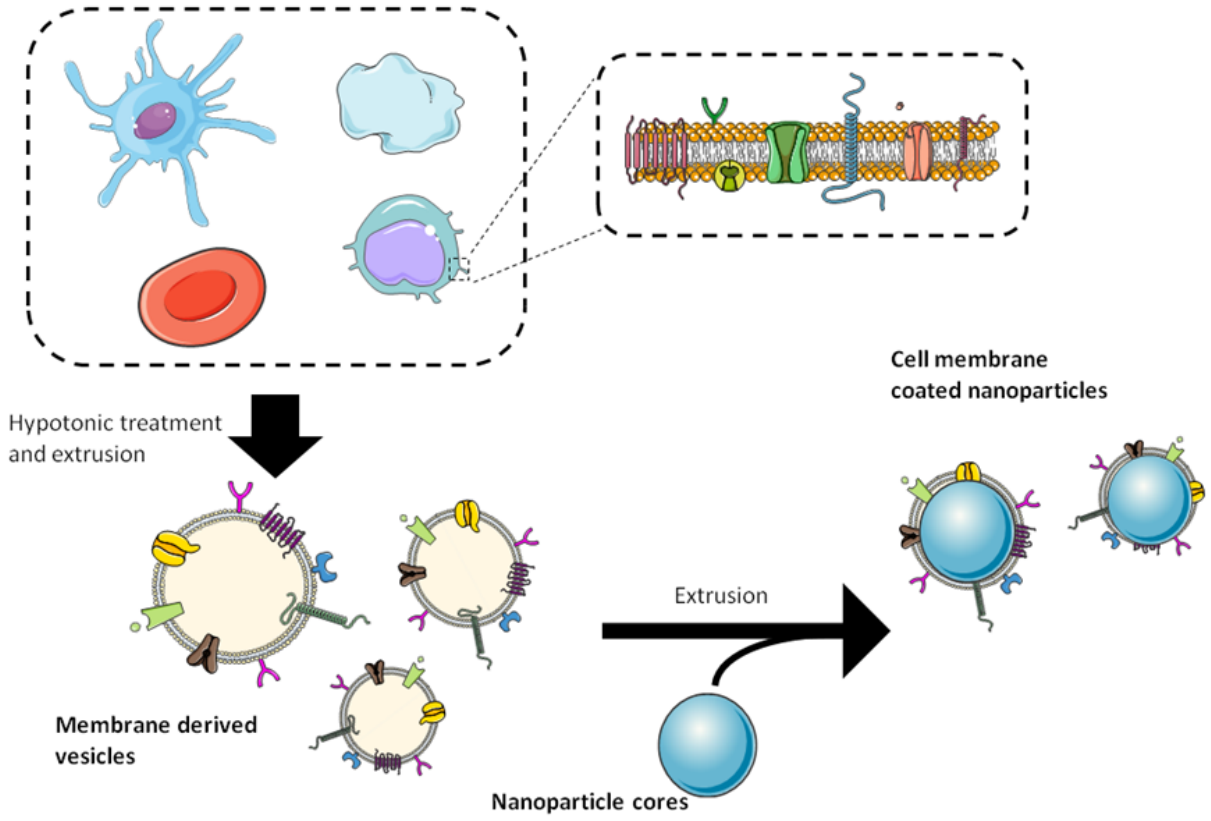

Figure 3: General technique for preparation of cell-membrane coated nanoparticles. Host cells are given a hypotonic treatment to empty their contents, yielding membrane derived vesicles. These vesicles are extruded together with nanoparticle cores to yield cell membrane coated derived nanoparticles through Van der Walls interaction between the membrane and nanoparticle coating

More recently, coating nanoparticles with endogenous cell membranes has emerged as a novel biomimetic technique, enabling a broad range of biodetoxification applications (Figure 3). In a seminal study, PLGA-based nanoparticles that were surface modified with red blood cells membranes (RBC-NPs) were found to capture circulating toxins and could diminish toxin virulence effects(45). The RBC-NPs were prepared by fusing empty RBC membrane vesicles onto PLGA nanoparticles through an extrusion approach(46). Interestingly, these RBC-NPs were found to interact with different types of bacterial toxins in a similar manner to the host cells. This allowed the development of an efficient detoxification platform without the need to specifically target the molecular structure of toxins, which is still the case with existing monoclonal antibodies, small molecule inhibitors or other polymer-based techniques. Subsequently, other types of nanoparticle surface modifications based on the same technique were used for the treatment of sepsis. For instance, J774 macrophage cell membrane modified

PLGA NPs were used on LPS-challenged mice(47). These biomimetic nanoparticles were efficient at sequestering LPS from the bloodstream, and also acted as targets for pro-inflammatory cytokines, essentially preventing their downstream inflammation cascade. A similar study using mice endogenous macrophage membranes to encapsulate iron oxide nanoclusters for sequestration of LPS in a mouse endotoxemia model was also reported recently(48). The macrophage membrane could act as a bait to selectively capture LPS *in vivo*, while the iron oxide cores could afford eventual magnetic separation of the captured LPS through extra-corporal circulation devices, which the study showed *in vitro*(48).

Techniques relying on cell membrane coating of nanoparticles are promising and offer many advantages for targeting and sequestering PAMPs. Focus should start to be put on developing large-scale, reliable production methods for these systems to start envisioning their transition to the clinics.

VII. Anti-bacterial nanomedicines

Recent studies have shown that encapsulating antibiotic agents inside of nanomedicines can improve several factors such as their selectivity, delivery and biodistribution(49-51). Trigger-dependent release of antibiotics has also been demonstrated by using pH or enzyme responsive nanoparticle delivery platforms(52). Given the importance of fighting the primary infection during sepsis without inducing further lesions or therapeutic side effects, some of these new antibacterial systems were evaluated in models of sepsis.

Opportunistic bacteria interact with platelets by both direct and indirect adherence mechanisms for tissue localization and immune evasion(53). As such, in a technique similar to the above described cell-membrane coating, platelet-membrane coated PLGA nanoparticles (PNPs) were used for targeted antibiotic delivery to bacteria (54). *In vitro,* the PNPs showed increased retention on bacteria compared to bare NPs or NPs coated with RBCs when interacting with MRSA252, a strain of methicillin-resistant *Staphylococcus aureus*. *In vivo,* mice systemically challenged with $6x10^6$ colony-forming units (CFU) of MRSA252 received daily injections of PNPs loaded with the antibiotic vancomycin, the supposition being that PNPs would efficiently deliver vancomycin bacteria due to the natural interaction of bacteria with platelets. In comparison to free vancomycin or vancomycin loaded nude PLGA NPs, vancomycin loaded PNPs showed significantly higher antibiotic potency -as measured by the number of detected CFU- in the heart, lung, liver and spleen, reflecting membrane-specific modulation of

nanoparticle antibiotic performance(54).

More recently, new types of antimicrobial agents termed “structurally nanoengineered antimicrobial peptide polymers” or SNAPPs were reported to exhibit sub-μM activity against multi-drug resistant Gram-negative bacteria(55). In a model of peritonitis with multidrug-resistant bacterial strains, the SNAPPs showed important bactericidal activity and improved survival of the animals. The antimicrobial activity of these novel polymers was shown to proceed via a multimodal mechanism including destabilization of the bacterial membrane and activation of ‘apoptosis-like’ death pathways. By interacting with bacteria in such a multifaceted, non-specific manner, these nanoparticles could provide a new class of antimicrobial agents able to affect drug resistant organisms.

VIII. Antioxidant nanomedicines

Because of the importance of oxidative stress and the production of ROS during sepsis, as mediators of inflammation and tissue injury, antioxidants nanoparticles were among the first treatment option to be considered. Notably, Ceria (CeO_2) nanoparticles have been shown to have potent enzyme-like autocatalytic antioxidant properties(56, 57). Consequently, modified Ce NPs incorporating Zircon ion (Zr^{4+}) for enhanced antioxidant activity were evaluated in both LPS endotoxemia and CLP models of sepsis(58). In both models, the NPs afforded enhanced survival, reduced oxidative stress and had significant anti-inflammatory activity as shown by reduced tissue infiltration of immune cells. Although these nanoparticles exhibited interesting pre-clinical results, there is still debate whether inorganic nanoparticles can realistically be used in the clinics. The discontinuation of iron oxide-based nanoparticles products due to safety issues serving as testimony of the complicated translation of this technology.

Another example of antioxidant nanoparticles makes use of organic radical containing nanoparticles (RNPs)(59). RNPs are composed of an antioxidative block copolymer (PEG-b-PMOT) possessing 2,2,6,6-tetramethylpiperidine-1-oxyl (TEMPO) as a side chain of the hydrophobic segment (PMOT) and poly(ethylene glycol) (PEG) as the hydrophilic segment. TEMPO is a stable radical which has strong ROS scavenging properties thanks to its catalytic reaction with superoxide ions in physiological conditions(60, 61). The covalently conjugated TEMPO in RNPs showed prolonged blood circulation properties thanks to the PEG coating of the nanoparticles. When RNPs were used to co-encapsulate TEMPO with the antibiotic amoxicillin, they significantly protected tissues from oxidative damage and improved the

survival of mice infected with lethal doses of *Listeria monocytogenes*. Although treatment with antioxidant nanoparticles alone did not eliminate bacteria, combined treatment with amoxicillin was found to significantly improve survival rate of the treated mice as compared to the amoxicillin-only control group. More importantly, the antioxidant nanoparticles were shown to reduce the oxidative stress linked to bacterial infection. These findings highlight the potential of combination therapies combining antioxidant nanoparticles with other agents to prevent severe inflammation caused by bacterial infections.

Other studies have focused on the delivery of melatonin for antioxidant therapy in models of sepsis. Melatonin is a multifunctional hormone than can function as an endogenous radical scavenger through its interaction with toxic reactants such as peroxyl radicals, singlet oxygen species, hydrogen peroxide or hydroxyl radicals(62, 63). In addition, melatonin may induce upregulation of the antioxidant activity of several key enzymes such as heme oxygenase-1 (HO-1)(64) or glutathione peroxidase(65) (66). As such, previous studies have indicated that systemic administration of melatonin can have a therapeutic benefit, reducing sepsis-induced tissue injury(67). This type of approach however, is limited by the short half-life of melatonin in the blood circulation (<30 min) and its low bioavailability. In an early study, Li Volti et al.(68) developed PLGA nanoparticles encapsulating melatonin for evaluation in a peritoneal fecal instillation sepsis model. Although the nanoparticles suffered from poor drug-loading (~0.6% w/w drug/polymer ratio), they were successful in limiting sepsis induced oxidative stress and tissue injury. The melatonin NPs decreased lipid hydroperoxides content in tissue homogenates and induced higher HO-1 expression compared to vehicle or free melatonin controls(68). More recent efforts describe the use of ROS responsive polymeric nanoparticles delivering melatonin in LPS induced endotoxemia mouse model(69). By using a redox-sensitive polypropylenesulfide polymer backbone, the nanoparticles could selectively disassemble at site of oxidative stress and on-demand delivery of melatonin. This resulted in the liver in reduced markers of inflammation (IL-6 and IL-1β) and oxidative stress (MDA and MPO). However, the influence on survival of these redox-sensitive melatonin nanocarriers was not investigated.

IX. Conclusions and Perspectives

The application of nanoparticles to sepsis therapy is a young area of research, with the first studies on the subject appearing in the early 2010s. As was summarized in this review, a number of nanomedicines have been developed in recent years at a pre-clinical stage, taking advantage of the tools afforded by nanoparticles for the management of sepsis. The field is steadily growing and poised to bring interesting new treatments to the clinics. With the development of robust and reliable formulations should come the first clinical trials aimed at bringing this exciting technology to patients. However, learning from past failures, several caveats should be taken into consideration when developing nanoparticles for such therapeutic application. Similar to limitations in small molecule research, animal models of sepsis and acute inflammation should be carefully selected for their relevancy to the target pathology. Dozens of animal models of sepsis have been described and reviewed in the literature. While intoxication models (based on LPS or other purified PAMP) are interesting tools to evaluate the pathophysiology of the disease, in studies related to therapeutic intervention, investigators should privilege true infection models with live bacterial populations. The “gold standard” in this context remains the rodent model of bacterial peritonitis, caecal ligation and puncture (CLP), which reproduces a number of key features of human sepsis, including the circulation profile of some inflammatory cytokines, vascular dysfunction and the development of acute lung injury. Nevertheless, animal models, and typically rodent models, are limited by very steep dose-response curves to the initial septic insult. So much so that small alterations to the initial inflammatory process can significantly alter survival. Furthermore, in rodents mortality to sepsis models typically evolve quickly, in the first 48 hours, in mechanisms that are highly dependent on TNF-α. Contrary to this fulminant process, sepsis-induced organ dysfunction in humans often evolves over days or weeks after the initial infection. In view of this, new “humanized-mice” models have been described in the literature. These mice develop a complete lineage of human cells of the innate and adaptive immune systems, potentially conferring a closer response to human patients(70, 71) in sepsis models. Another limitation that should be taken into account is the time of treatment. In some notable cases, small-molecule treatments were advanced into clinical trials based on limited data showing improved survival when the compound was used as a pre-treatment before LPS challenge(72). Treating a patient before a septic insult is not possible in a clinical setting where one of the challenges is the timely identification of sepsis. This, in turn, constitutes another challenge for the successful

translation of novel therapeutics to patients undergoing sepsis, where patient heterogenicity is a clinical reality not present in animal models. It is, in fact, important to recognize that different clinical conditions at different stages of the disease and with different biochemical profiles can be classified under the term “sepsis”. Post-hoc analyses of numerous clinical trials have started to shed light on the fact that some pharmacological approaches for sepsis could be beneficial to a certain subset of patients while harmful to others(73).

More specific to nanomedicine, the field has also historically been limited by poor industrial translation due to the complexity of the materials used(74). In a sense, reporting drug-delivery systems with exotic features seems to have prevailed over the desire to treat a disease effectively with a simple, robust and safe formulation(75). Fragile supramolecular structures or materials that require unrealistic industrial productions limit the scope of the developed nanoparticles. The complexities of industrial scale-up should be taken into account from the initial stages of design in order to improve the chances of ever seeing nanomedicine-based products reach the clinics. In this regard, inorganic nanoparticle-based systems still have a ways to go, with several FDA approved formulations having been retired due to safety reasons. Development efforts in this field should focus on finding safe, biocompatible materials that could be approved for use in humans.

Active Molecule	Carrier	Animal Model	Protocol	Targeting	Mechanism	Ref
Sialic acid	PLGA NP	CLP Intratracheal LPS	2 mg/kg i.p. 20 µg/kg intratracheal	Active, sialic acid	Anti-inflammatory	(31)
Pineatannol	Albumin NP	LPS inflammation	4.3 mg/kg i.v.	Active, Fcγ mediated	Anti-inflammatory	(32)
ciprofloxacin + IKK2 inhibitor	PEG-b-PEA(-gPEGb-DSPE)	Bacteremia i.p.	1.5 mg/kg i.v.	Passive, EPR Active, ICAM-1	Antibacterial + Anti-inflammatory	(34)
miR-146	Exosome	LPS endotoxemia	1 mg/kg i.v.	Active, exosome mediated	Anti-inflammatory	(40)
miR-223	Exosome	CLP	2 mg/kg i.v.	Active, exosome mediated	Anti-inflammatory	(41)
miR-126	Exosome	CLP	5 mg/kg NP i.v. (7 µg/kg miRNA) x2	Active, exosome mediated	Anti-inflammatory	(43)
MGFE8	Exosome	CLP	20 µg/kg i.v.	Active, exosome mediated	Clearance of apoptotic endothelium	(76)
/	Liposomes	Bacteremia i.p.	100 mg/kg i.v.	Passive, circulating toxins	Endotoxin antagonist	(44)
/	RBC-coated NPs	a-toxin endotoxemia	80 mg/kg i.v.	Passive, circulating toxins	Endotoxin antagonist	(45)
/	Macrophage-coated NPs	LPS endotoxemia	300 mg/kg i.v.	Passive, circulating toxins	Endotoxin antagonist	(47)
Ce4+/Zr4+	Ceria NPs	CLP	2 mg/kg i.v.	Passive, EPR	Antioxidant	(58)
TEMPO + amoxicillin	PEG-PMOT	Bacteremia i.p.	200 mg/kg i.p.	Passive	Antioxidant	(59)

Table 1. Nanomedicines for the pre-clinical treatment of sepsis

X. References

1. J.-L. Vincent, S. M. Opal, J. C. Marshall,K. J. Tracey, Sepsis definitions: time for change. *Lancet (London, England)*. 381, 774 (2013)
2. J.-L. Vincent, Y. Sakr, C. L. Sprung, V. M. Ranieri*, et al.*, Sepsis in European intensive care units: results of the SOAP study. *Critical care medicine*. 34, 344-353 (2006)
3. R. S. Hotchkiss, L. L. Moldawer, S. M. Opal, K. Reinhart*, et al.*, Sepsis and septic shock. *Nature reviews Disease primers*. 2, 16045 (2016)
4. R. S. Hotchkiss,I. E. Karl, The pathophysiology and treatment of sepsis. *New England Journal of Medicine*. 348, 138-150 (2003)
5. T. Van Der Poll, F. L. Van De Veerdonk, B. P. Scicluna,M. G. Netea, The immunopathology of sepsis and potential therapeutic targets. *Nature Reviews Immunology*. 17, 407 (2017)
6. E. Rivers, B. Nguyen, S. Havstad, J. Ressler*, et al.*, Early goal-directed therapy in the treatment of severe sepsis and septic shock. *New England Journal of Medicine*. 345, 1368-1377 (2001)

7. D. F. Gaieski, M. E. Mikkelsen, R. A. Band, J. M. Pines*, et al.*, Impact of time to antibiotics on survival in patients with severe sepsis or septic shock in whom early goal-directed therapy was initiated in the emergency department. *Critical care medicine*. 38, 1045-1053 (2010)
8. V. M. Ranieri, P. M. Suter, C. Tortorella, R. De Tullio*, et al.*, Effect of mechanical ventilation on inflammatory mediators in patients with acute respiratory distress syndrome: a randomized controlled trial. *Jama*. 282, 54-61 (1999)
9. K. J. Tracey, Y. Fong, D. G. Hesse, K. R. Manogue*, et al.*, Anti-cachectin/TNF monoclonal antibodies prevent septic shock during lethal bacteraemia. *Nature*. 330, 662 (1987)
10. J. C. Fisher, S. M. Opal, J.-F. Dhainaut, S. T. Stephens*, et al.*, Influence of an anti-tumor necrosis factor monoclonal antibody on cytokine levels in patients with sepsis. The CB0006 Sepsis Syndrome Study Group. *Critical care medicine*. 21, 318-327 (1993)
11. E. Abraham, R. Wunderink, H. Silverman, T. M. Perl*, et al.*, Efficacy and safety of monoclonal antibody to human tumor necrosis factor α in patients with sepsis syndrome: a randomized, controlled, double-blind, multicenter clinical trial. *Jama*. 273, 934-941 (1995)
12. W. Schumer, Steroids in the treatment of clinical septic shock. *Annals of surgery*. 184, 333 (1976)
13. C. L. Sprung, P. V. Caralis, E. H. Marcial, M. Pierce*, et al.*, The effects of high-dose corticosteroids in patients with septic shock: a prospective, controlled study. *New England Journal of Medicine*. 311, 1137-1143 (1984)
14. E. Lachman, S. Pitsoe,S. Gaffin, Anti-lipopolysaccharide immunotherapy in management of septic shock of obstetric and gynaecological origin. *The Lancet*. 323, 981-983 (1984)
15. E. J. Ziegler, J. A. Mccutchan, J. Fierer, M. P. Glauser*, et al.*, Treatment of gram-negative bacteremia and shock with human antiserum to a mutant Escherichia coli. *New England Journal of Medicine*. 307, 1225-1230 (1982)
16. E. Abraham, K. Reinhart, S. Opal, I. Demeyer*, et al.*, Efficacy and safety of tifacogin (recombinant tissue factor pathway inhibitor) in severe sepsis: a randomized controlled trial. *Jama*. 290, 238-247 (2003)
17. G. Bernard, J.-L. Vincent, P.-F. Laterre, S. P. Larosa*, et al.*, for the recombinant human activated protein C worldwide evaluation in severe sepsis (PROWESS) study group. *N Engl J Med*. 344, 699-709 (2001)
18. A. Putzu, A.-M. Daems, J. C. Lopez-Delgado, V. F. Giordano*, et al.*, The Effect of Vitamin C on Clinical Outcome in Critically Ill Patients: A Systematic Review With Meta-Analysis of Randomized Controlled Trials. *Critical care medicine*. 47, 774-783 (2019)
19. V. Mishra, Oxidative stress and role of antioxidant supplementation in critical illness. *Clinical laboratory*. 53, 199-209 (2007)
20. M. P. Fink,H. S. Warren, Strategies to improve drug development for sepsis. *Nature Reviews Drug Discovery*. 13, 741 (2014)
21. R. Kohen,A. Nyska, Invited review: Oxidation of biological systems: oxidative stress phenomena, antioxidants, redox reactions, and methods for their quantification. *Toxicologic pathology*. 30, 620-650 (2002)
22. H. R. López-Mirabal,J. R. Winther, Redox characteristics of the eukaryotic cytosol. *Biochimica et Biophysica Acta (BBA)-Molecular Cell Research*. 1783, 629-640 (2008)
23. P. De Paepe, F. M. Belpaire,W. A. Buylaert, Pharmacokinetic and pharmacodynamic considerations when treating patients with sepsis and septic shock. *Clinical pharmacokinetics*. 41, 1135-1151 (2002)
24. S. Harbarth, J. Garbino, J. Pugin, J. A. Romand*, et al.*, Inappropriate initial antimicrobial therapy and its effect on survival in a clinical trial of immunomodulating therapy for severe sepsis. *The American journal of medicine*. 115, 529-535 (2003)
25. L. F. Thompson, H. K. Eltzschig, J. C. Ibla, C. J. Van De Wiele*, et al.*, Crucial role for ecto-5′-nucleotidase (CD73) in vascular leakage during hypoxia. *Journal of Experimental Medicine*. 200, 1395-1405 (2004)
26. G. W. Sullivan, D. D. Lee, W. G. Ross, J. A. Divietro*, et al.*, Activation of A2A adenosine receptors inhibits expression of α4/β1 integrin (very late antigen-4) on stimulated human neutrophils. *Journal of leukocyte biology*. 75, 127-134 (2004)

27. D. A. Bullough, M. J. Magill, G. S. Firestein,K. M. Mullane, Adenosine activates A2 receptors to inhibit neutrophil adhesion and injury to isolated cardiac myocytes. *The Journal of Immunology*. 155, 2579-2586 (1995)
28. G. Haskó, B. Csóka, Z. H. Németh, E. S. Vizi*, et al.*, A2B adenosine receptors in immunity and inflammation. *Trends in immunology*. 30, 263-270 (2009)
29. B. S. Zolnik, A. Gonzalez-Fernandez, N. Sadrieh,M. A. Dobrovolskaia, Minireview: nanoparticles and the immune system. *Endocrinology*. 151, 458-465 (2010)
30. J. Du, Y. S. Zhang, D. Hobson,P. Hydbring, Nanoparticles for immune system targeting. *Drug discovery today*. 22, 1295-1301 (2017)
31. S. Spence, M. K. Greene, F. Fay, E. Hams*, et al.*, Targeting Siglecs with a sialic acid–decorated nanoparticle abrogates inflammation. *Science translational medicine*. 7, 303ra140-303ra140 (2015)
32. Z. Wang, J. Li, J. Cho,A. B. Malik, Prevention of vascular inflammation by nanoparticle targeting of adherent neutrophils. *Nature nanotechnology*. 9, 204 (2014)
33. K. Nakatani, S. Takeshita, H. Tsujimoto, Y. Kawamura*, et al.*, Regulation of the expression of Fcγ receptor on circulating neutrophils and monocytes in Kawasaki disease. *Clinical and experimental immunology*. 117, 418 (1999)
34. C. Y. Zhang, J. Gao,Z. Wang, Bioresponsive Nanoparticles Targeted to Infectious Microenvironments for Sepsis Management. *Advanced Materials*. 30, 1803618 (2018)
35. C. A. Dinarello, Anti-inflammatory agents: present and future. *Cell*. 140, 935-950 (2010)
36. A. F. Radovic-Moreno, T. K. Lu, V. A. Puscasu, C. J. Yoon*, et al.*, Surface charge-switching polymeric nanoparticles for bacterial cell wall-targeted delivery of antibiotics. *ACS nano*. 6, 4279-4287 (2012)
37. M.-H. Xiong, Y. Bao, X.-Z. Yang, Y.-C. Wang*, et al.*, Lipase-sensitive polymeric triple-layered nanogel for “on-demand” drug delivery. *Journal of the American Chemical Society*. 134, 4355-4362 (2012)
38. N. Terrasini,V. Lionetti, Exosomes in critical illness. *Critical care medicine*. 45, 1054-1060 (2017)
39. J. Wu, Y. Wang,L. Li, Functional significance of exosomes applied in sepsis: A novel approach to therapy. *Biochimica et Biophysica Acta (BBA)-Molecular Basis of Disease*. 1863, 292-297 (2017)
40. M. Alexander, R. Hu, M. C. Runtsch, D. A. Kagele*, et al.*, Exosome-delivered microRNAs modulate the inflammatory response to endotoxin. *Nature communications*. 6, 7321 (2015)
41. X. Wang, H. Gu, D. Qin, L. Yang*, et al.*, Exosomal miR-223 contributes to mesenchymal stem cell-elicited cardioprotection in polymicrobial sepsis. *Scientific reports*. 5, 13721 (2015)
42. I. L. Colao, R. Corteling, D. Bracewell,I. Wall, Manufacturing exosomes: a promising therapeutic platform. *Trends in molecular medicine*. 24, 242-256 (2018)
43. J. N. J. Buie, Y. Zhou, A. J. Goodwin, J. A. Cook*, et al.*, Application of Deacetylated Poly-N-Acetyl Glucosamine Nanoparticles for the Delivery of miR-126 for the Treatment of Cecal Ligation and Puncture-Induced Sepsis. *Inflammation*. 42, 170-184 (2019)
44. B. D. Henry, D. R. Neill, K. A. Becker, S. Gore*, et al.*, Engineered liposomes sequester bacterial exotoxins and protect from severe invasive infections in mice. *Nature biotechnology*. 33, 81 (2015)
45. C.-M. J. Hu, R. H. Fang, J. Copp, B. T. Luk*, et al.*, A biomimetic nanosponge that absorbs pore-forming toxins. *Nature nanotechnology*. 8, 336 (2013)
46. C.-M. J. Hu, L. Zhang, S. Aryal, C. Cheung*, et al.*, Erythrocyte membrane-camouflaged polymeric nanoparticles as a biomimetic delivery platform. *Proceedings of the National Academy of Sciences*. 108, 10980-10985 (2011)
47. S. Thamphiwatana, P. Angsantikul, T. Escajadillo, Q. Zhang*, et al.*, Macrophage-like nanoparticles concurrently absorbing endotoxins and proinflammatory cytokines for sepsis management. *Proceedings of the National Academy of Sciences*. 114, 11488-11493 (2017)
48. S. Shen, F. Han, A. Yuan, L. Wu*, et al.*, Engineered nanoparticles disguised as macrophages for trapping lipopolysaccharide and preventing endotoxemia. *Biomaterials*. 189, 60-68 (2019)
49. N. Abed,P. Couvreur, Nanocarriers for antibiotics: A promising solution to treat intracellular bacterial infections. *International journal of antimicrobial agents*. 43, 485-496 (2014)
50. A. J. Huh,Y. J. Kwon, “Nanoantibiotics”: a new paradigm for treating infectious diseases using nanomaterials in the antibiotics resistant era. *Journal of controlled release*. 156, 128-145 (2011)
51. Z. Drulis-Kawa,A. Dorotkiewicz-Jach, Liposomes as delivery systems for antibiotics. *International journal of pharmaceutics*. 387, 187-198 (2010)

52. G. Baier, A. Cavallaro, K. Vasilev, V. MailäNder*, et al.*, Enzyme responsive hyaluronic acid nanocapsules containing polyhexanide and their exposure to bacteria to prevent infection. *Biomacromolecules*. 14, 1103-1112 (2013)
53. J. R. Fitzgerald, T. J. Foster,D. Cox, The interaction of bacterial pathogens with platelets. *Nature Reviews Microbiology*. 4, 445 (2006)
54. C.-M. J. Hu, R. H. Fang, K.-C. Wang, B. T. Luk*, et al.*, Nanoparticle biointerfacing by platelet membrane cloaking. *Nature*. 526, 118 (2015)
55. S. J. Lam, N. M. O'brien-Simpson, N. Pantarat, A. Sulistio*, et al.*, Combating multidrug-resistant Gram-negative bacteria with structurally nanoengineered antimicrobial peptide polymers. *Nature microbiology*. 1, 16162 (2016)
56. C. K. Kim, T. Kim, I. Y. Choi, M. Soh*, et al.*, Ceria nanoparticles that can protect against ischemic stroke. *Angewandte Chemie International Edition*. 51, 11039-11043 (2012)
57. J. Chen, S. Patil, S. Seal,J. F. Mcginnis, Rare earth nanoparticles prevent retinal degeneration induced by intracellular peroxides. *Nature nanotechnology*. 1, 142 (2006)
58. M. Soh, D. W. Kang, H. G. Jeong, D. Kim*, et al.*, Ceria–Zirconia Nanoparticles as an Enhanced Multi-Antioxidant for Sepsis Treatment. *Angewandte Chemie International Edition*. 56, 11399-11403 (2017)
59. Y. Ikeda, K. Shoji, C. P. Feliciano, S. Saito*, et al.*, Antioxidative nanoparticles significantly enhance therapeutic efficacy of an antibacterial therapy against Listeria monocytogenes infection. *Molecular pharmaceutics*. 15, 1126-1132 (2018)
60. E. E. Voest, E. Van Faassen,J. J. Marx, An electron paramagnetic resonance study of the antioxidant properties of the nitroxide free radical TEMPO. *Free Radical Biology and Medicine*. 15, 589-595 (1993)
61. H. D. Black, W. Xu, E. Hortle, S. I. Roberston*, et al.*, The cyclic nitroxide antioxidant 4-methoxy-TEMPO decreases mycobacterial burden in vivo through host and bacterial targets. *Free Radical Biology and Medicine*. (2019)
62. A. Galano, On the direct scavenging activity of melatonin towards hydroxyl and a series of peroxyl radicals. *Physical Chemistry Chemical Physics*. 13, 7178-7188 (2011)
63. E. A. De Almeida, G. R. Martinez, C. F. Klitzke, M. H. De Medeiros*, et al.*, Oxidation of melatonin by singlet molecular oxygen (O2 (1Δg)) produces N1-acetyl-N2-formyl-5-methoxykynurenine. *Journal of pineal research*. 35, 131-137 (2003)
64. K. J. Kwon, J. N. Kim, M. K. Kim, J. Lee*, et al.*, Melatonin synergistically increases resveratrol-induced heme oxygenase-1 expression through the inhibition of ubiquitin-dependent proteasome pathway: a possible role in neuroprotection. *Journal of pineal research*. 50, 110-123 (2011)
65. W. Szaroma,K. Dziubek, Changes in the amount of reduced glutathione and activity of antioxidant enzymes in chosen mouse organs influenced by zymosan and melatonin administration. *Acta Biologica Hungarica*. 62, 133-141 (2011)
66. V. Dubey, D. Mishra, A. Asthana,N. K. Jain, Transdermal delivery of a pineal hormone: melatonin via elastic liposomes. *Biomaterials*. 27, 3491-3496 (2006)
67. H. Volt, J. A. García, C. Doerrier, M. E. Díaz-Casado*, et al.*, Same molecule but different expression: aging and sepsis trigger NLRP3 inflammasome activation, a target of melatonin. *Journal of pineal research*. 60, 193-205 (2016)
68. G. Li Volti, T. Musumeci, R. Pignatello, P. Murabito*, et al.*, Antioxidant potential of different melatonin-loaded nanomedicines in an experimental model of sepsis. *Experimental Biology and Medicine*. 237, 670-677 (2012)
69. G. Chen, H. Deng, X. Song, M. Lu*, et al.*, Reactive oxygen species-responsive polymeric nanoparticles for alleviating sepsis-induced acute liver injury in mice. *Biomaterials*. 144, 30-41 (2017)
70. L. D. Shultz, F. Ishikawa,D. L. Greiner, Humanized mice in translational biomedical research. *Nature Reviews Immunology*. 7, 118 (2007)
71. K. Laudanski, N. Lapko, M. Zawadka, B. X. Zhou*, et al.*, The clinical and immunological performance of 28 days survival model of cecal ligation and puncture in humanized mice. *PloS one*. 12, e0180377 (2017)
72. E. Whalley, J. Solomon, D. Modafferi, K. Bonham*, et al.*, CP-0127, a novel potent bradykinin antagonist, increases survival in rat and rabbit models of endotoxin shock. *Agents and actions. Supplements*. 38, 413-420 (1992)

73. A. M. P. Van Ton, M. Kox, W. F. Abdo,P. Pickkers, Precision immunotherapy for sepsis. *Frontiers in immunology*. 9, (2018)
74. F. Dormont, M. Rouquette, C. Mahatsekake, F. Gobeaux*, et al.*, Translation of nanomedicines from lab to industrial scale synthesis: The case of squalene-adenosine nanoparticles. *Journal of Controlled Release*. 307, 302-314 (2019)
75. J. C. Leroux, Drug delivery: too much complexity, not enough reproducibility? *Angewandte Chemie International Edition*. 56, 15170-15171 (2017)
76. M. Miksa, R. Wu, W. Dong, H. Komura*, et al.*, Immature dendritic cell-derived exosomes rescue septic animals via milk fat globule epidermal growth factor VIII. *The Journal of immunology*. 183, 5983-5990 (2009)

Bibliographic Introduction

Nanoplumbers: Biomaterials to fight cardiovascular diseases

Flavio Dormont, Mariana Varna, Patrick Couvreur

Institut Galien Paris-Sud, CNRS, Univ. Paris-Sud, Université Paris-Saclay, Faculté de Pharmacie, 92296 Châtenay-Malabry, France

Published in Materials Today, March 2018

Nanoplumbers: Biomaterials to fight cardiovascular diseases

Abstract

The adequate management of cardiovascular diseases remains one of the major challenges of modern medicine. Nanomaterials may offer new and unique treatment opportunities that transcend the shortcomings of currently available therapies. Conventional administration of drugs is mainly based on the systemic delivery of therapeutic molecules, often leading to their non-specific distribution throughout the body, decreasing their efficacy and sometimes resulting in deleterious side effects. Through the precise control of the physicochemical properties of nanomaterials, such as size, drug loading and surface functionalization, nanoencapsulation of select therapeutic agents may enhance drug delivery and release at the sites of disease, ultimately increasing their effectiveness. Different biomaterials loaded with therapeutic drugs have been engineered for cardiovascular nanotherapy and evaluated in preclinical models. This review highlights how nanomedicines (*i.e.,* nanoparticles and drugs) offer interesting perspectives in the treatment of atherosclerosis and heart ischemia, potentially affording new tools in the fight against cardiovascular diseases.

I. Introduction

The rapid development of materials science, nanotechnology and bioengineering has yielded an entirely novel field of research that is set to bring momentous advances in the fight against a range of conditions (1). Nanomedicine, that is the use of nanoparticules (NPs) for the prevention, the treatment and/or the imaging of diseases, now covers a range of challenging therapeutic applications, mainly in oncology. With a size usually ranging a few hundred nanometers, nanoparticles may be composed of either organic, inorganic or even hybrid organic-inorganic materials. Their size allows them to selectively carry payloads and escape renal clearance while their composition can provide novel applications using the properties of their constitutive materials. Furthermore, they exhibit a high surface-to-volume ratio, allowing extensive surface modification with a variety of ligands to tailor their fates *in-vivo* (2). The design of nanomedicines is often motivated by the need to modify the pharmacodynamic and pharmacokinetic profiles of established drugs. By encapsulating and targeting therapeutic agents, nanotechnology has the potential to create new treatment opportunities for a host of diseases.

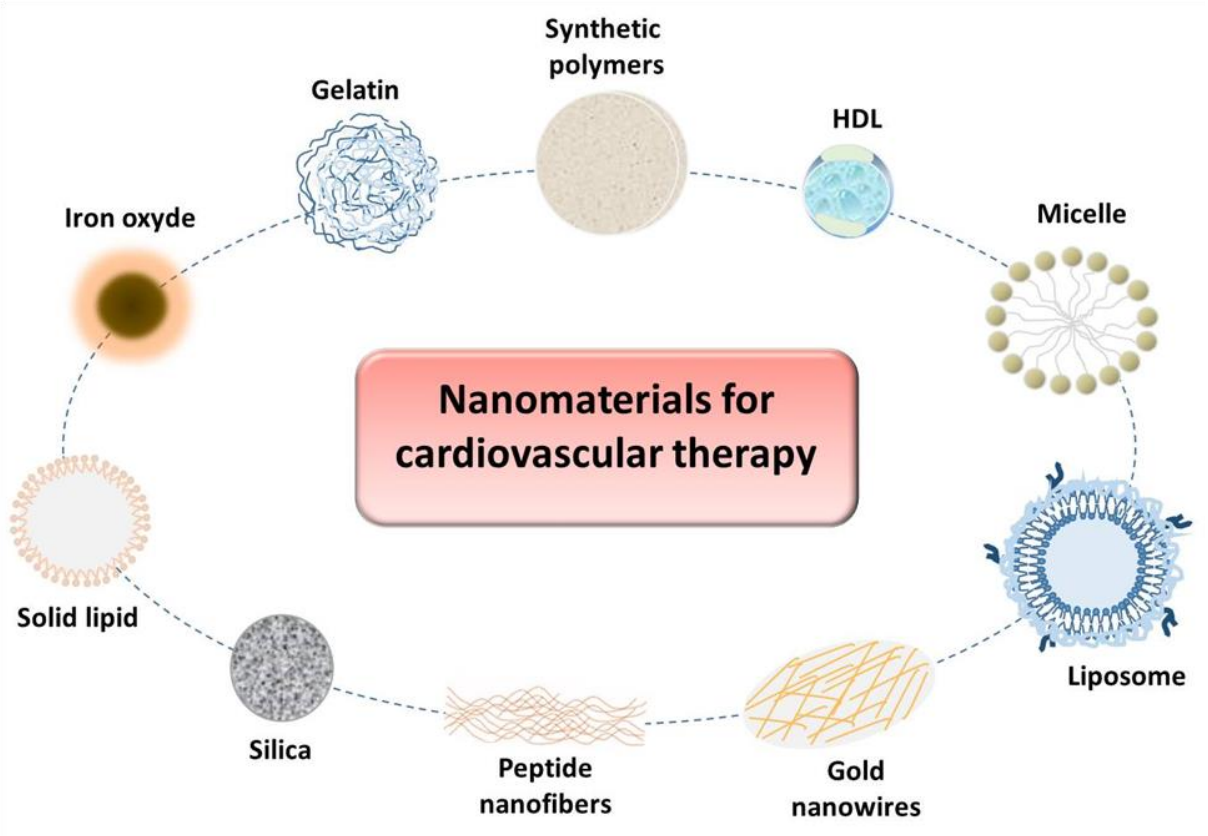

Several preparation methods have been developed to synthesize nanoparticles made of a wide variety of materials (3-10). Among lipid based strategies, liposomes, which are phospholipidic bilayered vesicles surrounding an aqueous core (Fig. 1), have beenextensively used since their discovery by Bangham *et al.,* fifty years ago (11-13).

The safety of the materials used for liposome synthesis represents an important advantage, while the main limitation pertains to their poor stability in the blood flow (14). Polymer nanoparticles (Fig. 1), represent another type of useful drug nanocarriers with the advantage of being more resistant than lipid-based formulations. The promise of these NPs also lies in the wide

Figure 1: Schematic representation of various nanomaterials for cardiovascular

variety of polymers that can be used to tailor the properties of the drug delivery nanosystem. Disadvantages are linked to their often slow biodegradability, manufacturing cost and possible toxicity due to residual solvent (15). Inorganic nanomedicines (Fig.1) such as metallic, fullerenes or silica-based, are less used for therapeutic purposes in the cardiovascular field, due to safety concerns.

With two families of therapeutic nanocarriers, liposomes (Doxil^{R}, Daunosone) (16) and albumin NPs (Abraxane^{R}) (17), now firmly established in clinical oncological practice and dozens of other therapeutic applications currently undergoing clinical trials (18), nanomedicine now enters an exciting time in its growth and development. As the paths to clinical translation become clearer (19), nanomedicine is gradually extending beyond oncological applications and find use in other areas of medicine where there is a strong need for novel therapeutics. These promises, however, need to be accompanied by a careful study of the fate of nanocarriers *in vivo* (20), a precise understanding of their biocompatibility and interaction with the disease when the short-comings of prevalent animal models also deserve evaluation.

Of particular interest is the potential of nanoparticles in the management of cardiovascular diseases, from which, by 2030, more than 23 million people will die annually (21). For this reason, the development of new strategies for the therapy of cardiovascular diseases remains

essential. It is the aim of this review to give a global outlook and discuss the preclinical advances obtained in the application of nanomedicine to the cardiovascular field. We have focused on nanomedicines dedicated to therapy of atherosclerotic plaque, the main underpinning of cardiovascular diseases and to therapy against injuries induced by myocardial ischemia, the main cause of cardiovascular mortality and disability in the world (22).

II. From atherosclerosis to myocardial infarction

The atherosclerotic process is characterised by a remodelling of arteries leading to progressive sub-endothelial accumulation of lipids and development of atherosclerotic plaques. Atherosclerosis is a multifactorial and slowly progressing physio-pathological disease which develops in large and mid-sized arteries at predisposed regions (*e.g.,* near branch points and along inner curvature) characterized by disturbed blood flow dynamics (23-25) leading to inflammation and endothelial cell dysfunction (26). In this inflammatory condition, low-density lipoproteins (LDLs)-derived cholesterol, pass through the endothelium into the subendothelial space, where they undergo oxidative modifications by radical oxygen species leading to oxidised LDL (oxLDLs) (Fig. 2).

The inflammatory process is accompanied by the attachment of monocytes to the endothelial cells expressing adhesion molecules (*e.g.,* ICAM-1, VCAM-1, Selectins) and their subsequent penetration into the subendothelial space where they differentiate into macrophages. These macrophages, expressing scavenger receptors (SR-A/B and CD36) start to ingest the oxLDLs, allowing them to evolve into “foam cells”. In advanced plaques, characterized by the development of a fibrous cap and the presence of a necrotic core, the hypoxic and inflammatory environments promote the development of fragile and defective blood vessels. These neovessels prone to leakage, promote intraplaque hemorrhages, thus accelerating plaque growth and instability (26). Plaque rupture induces contact between the necrotic core and the blood, leading to the formation of a thrombus (27).

Atherosclerosis alone is rarely fatal, while the complications induced by thrombosis (*e.g.,* myocardial infarction) are the most common causes of death and disabilities in the world (22, 28). During myocardial ischemia, the infarcted area is poorly supplied with blood, which creates an hypoxic environment. In these conditions, ischemic myocardium undergoes a variety of metabolic changes (Fig.3) which consist in the shutdown of the aerobic metabolism,

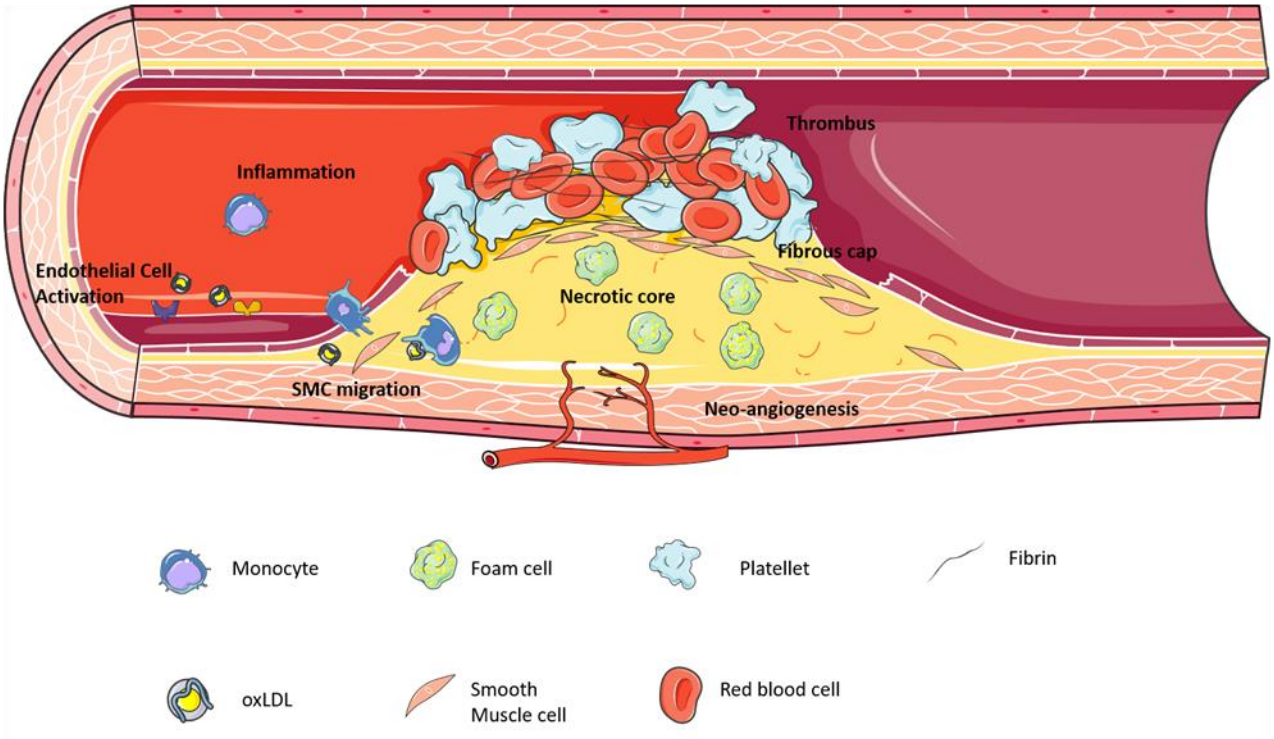

Figure 2: The main steps in atherosclerotic plaque development. The risk factors (e.g., hypertension, dyslipidemia) lead to activation of endothelial cells that start to express adhesion molecules (e.g., VCAM, P-Selectins). The monocytes can then adhere to the activated endothelium and accumulate into the subendothelial space where are transformed in macrophages, start to ingest oxidized LDL (oxLDL) and become foam cells. In this inflammatory environment, the smooth muscle cells (SMCs) migrate, proliferate and produce collagen. New fragile neovessels are formed and may bleed, causing intraplaque hemorrhages and participating in plaque growth. At the advanced stage of atherosclerosis, a fibrous cap is formed encapsulating a necrotic core. Plaque rupture induces contact between the necrotic core and the blood, leading to the formation of a thrombus.

depletion of ATP stores and the onset of anaerobic glycolysis (29). These changes culminate with the cell death in the absence of blood flow restoration (reperfusion). Although prompt reperfusion therapy has been shown to reduce morbidity, it is also recognized to be associated with adverse events such as reactive oxygen species (ROS) overproduction, inflammation,

cardiomyocytes hypercontracture, and opening of mitochondrial permeability transition pore (mPTP) that initiate the apoptotic program (30) (Fig. 3). In response to chemoattractants (*e.g.,* ROS, cytokines or complement activation), neutrophils adhere to the endothelium and release degradative enzymes and ROS, amplifying the damages induced onto cells. These changes provoke cardiac remodelling. In these conditions, the extracellular matrix degrades step by step, leading to cardiomyocyte loss and their replacement by collagen, resulting in the formation of scar tissue (29).

Insights into the processes involved in atherosclerosis initiation and development, have led to a number of treatments for its clinical manifestations. The pharmacological standard of care for at-risk patients includes lowering plasma lipid levels by orally administered drugs (*e.g.,* statins, fibrates) (31) which act on lipid metabolism (32). However, conventional drugs are unsuccessful at protecting against acute ischemic events or preventing cellular uptake of oxidized lipoproteins (33). In the case that atherosclerotic plaque growth progresses to occlusion, a surgical care option is based on the use of stents to physically enlarge the lumen of vessels (34). In practice, significant residual risk remains in patients treated with these conventional drugs that in essence, do not cure atherosclerosis but merely mitigate its development.

Accordingly, diverse pharmacological therapeutic strategies have been explored for the treatment of atherosclerotic plaque and myocardial ischemia/reperfusion lesions but most tend to be afflicted with significant drawbacks. Many systemic anti-inflammatory strategies such as corticosteroids, anti-cytokines agents (35, 36), nonsteroidal anti-inflammatory drugs or anti-chemokines (37) have been employed to target the central role played by inflammation in atherosclerosis and myocardial infarction. Most of these drugs exert a number of off-target effects that limit their use as potential therapeutics (38). Notably, systemic inhibition of inflammation is hampered by important side effects because many of the molecular targets have important roles in host defense. Additionally, many of these pharmacological strategies have fallen short in clinical settings (39-41) due to rapid degradation and metabolization of active molecules, insufficient accumulation into the targeted areas or deficient intracellular penetration of drugs. Reflecting the complex interplay between inflammation pathways and cardiovascular diseases, more specific anti-inflammatory formulations need to be developed.
Antioxidants therapies, as potential inhibitors of lipid oxidation, one of the root causes of

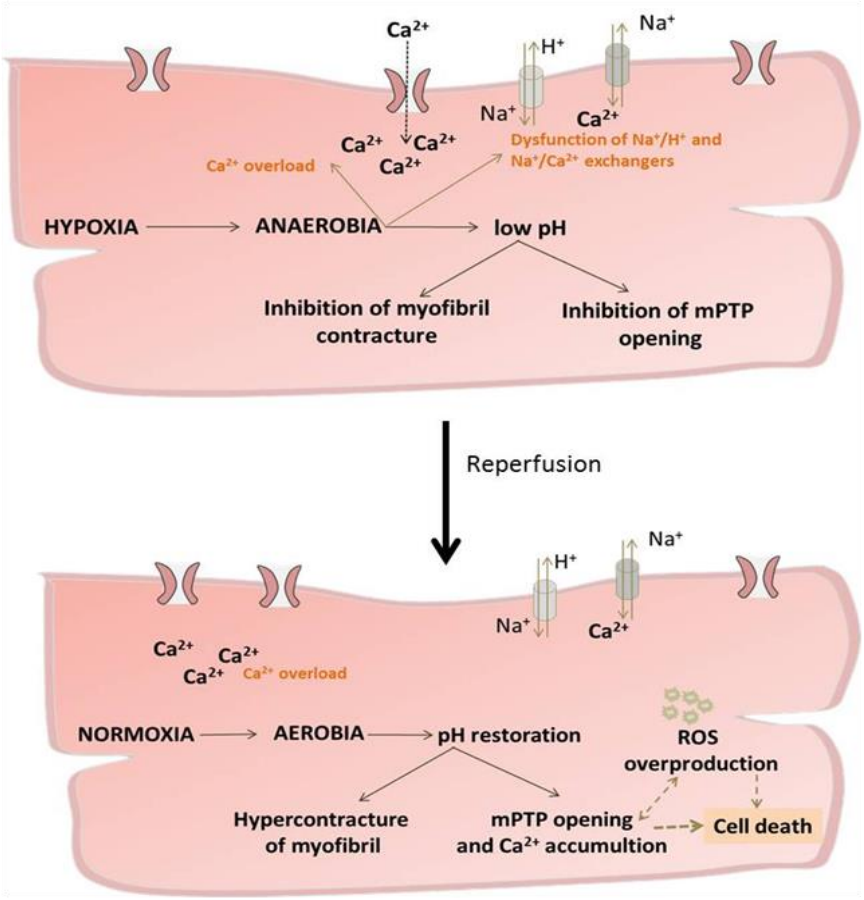

Figure 3: Schematic illustration of the main modifications of myocardial ischemia/reperfusion injuries. During acute myocardial ischemia (hypoxic conditions), the lack of oxygen switches cell metabolism to anaerobic respiration, leading to lactate production and a low intracellular pH. This induces intracellular Ca^{2+} overload and Na^{+}/H^{+} and Na^{+}/Ca^{2+} exchangers dysfunction. The low pH during ischemia prevents the opening of the mPTP and cardiomyocyte hypercontracture. At reperfusion time (normoxic conditions) the reactivation of electron transport chain result in washout of lactic acid and thus pH correction which lead to mPTP opening. This allow Ca^{2+} to penetrate into the mitochondria, leading to Cytochrome C releasing in parallel to ROS overproduction. Together these modifications contribute to cell death.

atherosclerosis and myocardial infarction, have also been evaluated in clinical trials (42) but have shown mitigated results in preventing the onset of the disease (43). For later stage cardiovascular diseases, anti-platelet therapies (44) have been considered to prevent clot formation and aid in asymptomatic clot breakup.

Despite these numerous efforts, the pharmacological treatment of cardiovascular diseases remains insufficient. Currently, it is estimated that more than 70 % of acute coronary events cannot be prevented with available drug therapy (38). Also, available therapy is unable to

restore, albeit partially, cardiac function after myocardial infarction. This leads to the progressive structural remodeling (*i.e.,* wall thinning, scar formation and cardiomyocyte hypertrophy) and deterioration of heart muscle function characteristic of chronic myocardial infarction, which often results in congestive heart failure.

In this context, nanomedicines may represent a promising alternative to small-molecules, owing to their ability to specifically target pathological processes *versus* the uncontrolled distribution of drugs when administrated using conventional galenical formulations. Hence, various therapeutic agents have been encapsulated into NPs to improve their delivery and retention at disease sites, incl. statins, thrombolytic drugs, pro- and anti-angiogenic proteins or genes, purines, antioxidants or anti-inflammatory molecules. Magnetic responsive nanoparticles combined with the application of a magnetic field were also employed to guide stem cells towards the ischemic area and to avoid some of the limitations observed in clinical trials (*e.g.,* lung trapping and low retention into the infarcted area).

III. Rationale for using nanomedicines

The concomitant development of nanotechnology and a more precise understanding of the processes involved in atherosclerosis and myocardial infarction have paved the way for new nanomedicine-based therapeutic approaches. However, the design and use of nanomedicines raises new issues to be solved before their successful translation to the clinic. The first is related to the nanoparticle's constitutive material itself, which must be biocompatible and biodegradable without inducing inflammatory processes. Secondly, nanomedicines should be stable at body temperature with the ability to target and accumulate into diseased areas.
Progresses in materials chemistry and the versatility of the preparation processes involved in nanomaterial synthesis allow the physicochemical properties of NPs to be precisely controlled to obtain the desired size, surface charge, shape and functionalization, ultimately influencing their fates *in vivo*. Particle size plays an important role in tissue distribution as demonstrated by different studies (45, 46). In general, NPs smaller than 10 nm show a widespread organ distribution while larger particles (up to 250 nm) accumulate principally in the liver and spleen (46). Particle shape also influences the toxicity of nanocarriers and it has been established that spherical nanoparticles are less toxic compared to non-spherical ones (47, 48). Surface charge of nanocarriers also plays an important role, in that positively charged NPs show increased cellular uptake compared to negatively charged or neutral NPs (49).

Due to their high surface energy, nanoparticles adsorb proteins and other biomolecules by Vroman effect upon intravenous injection, forming the so-called protein corona. While the formation of this corona is related to the physicochemical characteristics of the nanocarriers (50-52) its composition is influenced by numerous factors that are difficult to control *in vivo* and alter the behaviour of nanomaterials (53, 54). In fact, the formation of a protein layer at the surface of the nanoparticles confers them a new 'biological identity'. At first underestimated, the significance of these protein interactions has gradually been recognized to greatly affect nanoparticles biodistribution, blood clearance, targeting ability and drug release (53). It was initially perceived that the presence of a protein corona mainly resulted in rapid clearance of nanomaterials from the blood circulation and reduced therapeutic efficacy (55-57). Early strategies that addressed the issue of protein corona have mostly attempted to prevent its formation and to increase NPs blood circulation time by coating their surface with hydrophilic polymers to induce a steric stabilization, thus reducing interaction with blood proteins. PEGylation, a process where poly(ethylene) glycol chains are attached onto the surface of the NPs to provide them with long circulation properties is a popular and typical example of this approach (58, 59).

Recent findings, however, have shown that rather than the presence or absence of proteins at the surface of NPs, it is the proteomic make-up of the corona that appears to influence the biological fate of NPs (60). For instance, Walkey and colleagues have suggested that PEG did not eliminate serum protein adsorption, but selectively suppressed the adsorption of specific proteins, resulting in a minimized macrophage uptake (61). Further, it was observed that the corona composition was influenced by the individual's plasma protein composition which varies according to a number of factors such as age, genetic background, lifestyle and disease (62-64).

Accordingly, the concept of "personalized protein corona" has been introduced in the

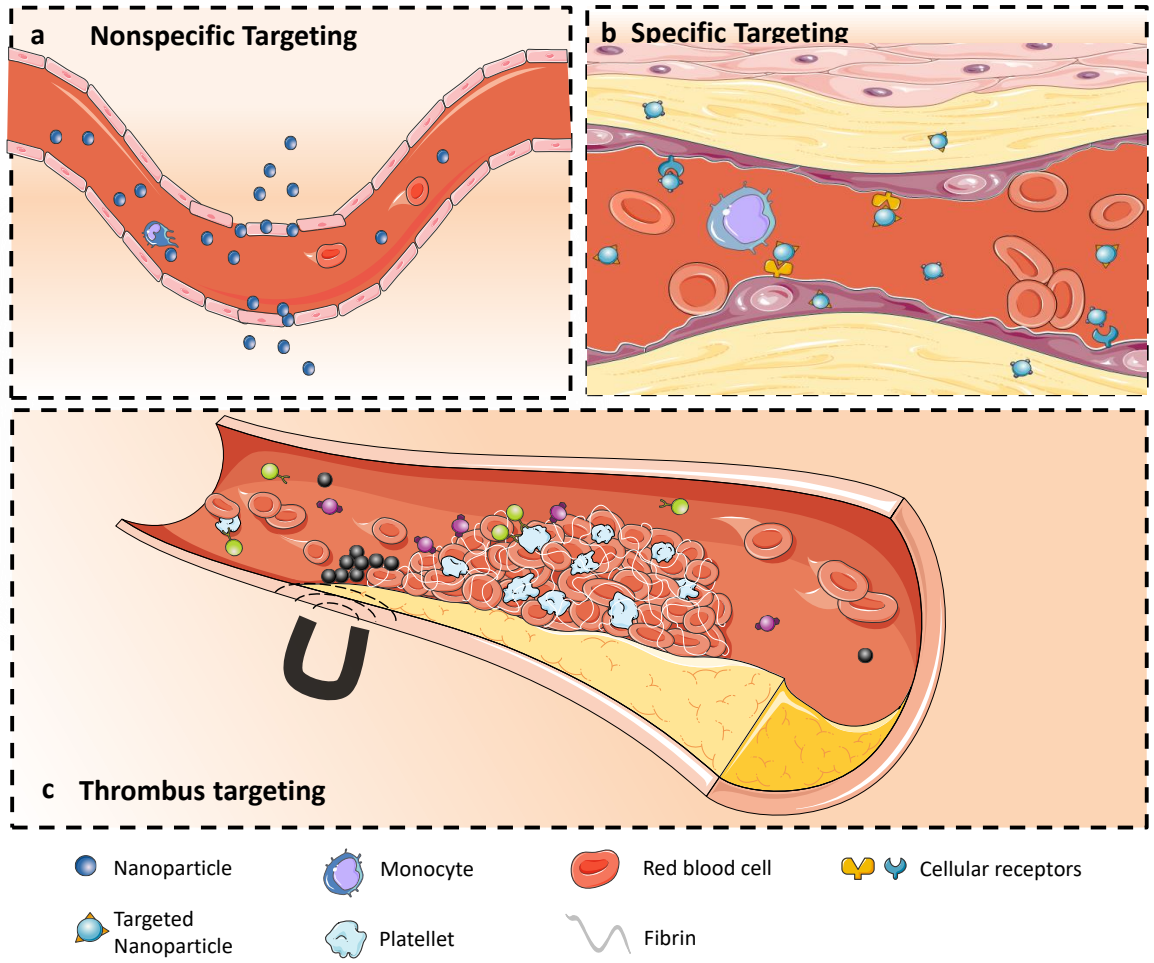

Figure 4: Targeting principles for cardiovascular diseases. Nanomedicines can target the sites of disease through multiple mechanisms. Pathological conditions in atherosclerotic plaque and during myocardial infarction increase the permeability of the endothelium and are often accompanied by upregulation of specific cell-surface receptors. Non-specific targeting (**a**) occurs through the Enhanced Permeation and Retention effect which occurs non-discriminately for nanocarriers circulating in the bloodstream allowing for their extravasation and local sites of damaged vasculature. Specific targeting (**b**) of different components (vasculature, cellular matrix, disease markers) can be achieved by active targeting thanks to ligands attached to nanocarriers. When a thrombus forms (**c**) magnetic targeting, accumulation, or specific targeting of constitutive elements of the thrombus can direct nanomedicines to the blockage site.

scientific literature, with the growing understanding that NPs should undergo disease and patient specific design for more efficient and safe clinical applications. In fact, discounting the central, albeit complex, role that personalized protein coronas play in the *in vivo* behavior of NPs could be a major hurdle for the clinical translation of nanomedicines.

Making use of the numerous cellular and molecular events associated with cardiovascular

lesion sites (65), namely hypoxia-induced neovascularization (66), endothelial dysfunction (67), permeability of the vasculature (68) and up-regulation of adhesion molecules (23), nanoparticle-based treatments were demonstrated to allow efficient targeting of the affected sites. The main targeting approaches in cardiovascular diseases can be divided into passive delivery (Fig. 4), through the enhanced permeability and retention effect (EPR) (69, 70) and active targeting using surface functionalized nanoparticles interacting with specific ligands at the target site (Fig. 4) (71, 72).

The enhanced permeability and retention effect has been comprehensively investigated in tumor tissue (73). Interestingly, the mechanisms that give rise to it in cancer also seem to occur in atherosclerosis (74). In both cases, inflammatory state and local hypoxia induce the production of angiogenic factors (VEGF), leading to the rapid formation of blood vessels. Where normal vascular physiology usually yields well-aligned cells backed by a smooth muscle layer and joined by tight endothelial junctions, the newly formed vessels are usually abnormal in form and architecture. They lack supporting cells, are fragile and leaky with large gaps that allow local extravasation of plasma proteins and nanoparticles which accumulate at the disease site, due to an underdeveloped lymphatic drainage system. Additionally, tissue inflammation causes continuous leukocyte recruitment and pro-inflammatory cytokine release which also contribute to endothelial permeability. Concerning the ischemic myocardium, local ischemia also induces vascular permeability on its own. Cardiac blood vessels, which are usually lined by a continuous endothelial wall, become leaky and/or disrupted due to hypoxia and inflammation**,** as shown by several studies. For instance, by using Magnetic Resonance Imaging (MRI), Geelen *et al*., (69), have convincingly demonstrated in a mouse cardiac ischemia-reperfusion injury model, that lipid-based nanocarriers (*i.e.,* liposomes and micelles) loaded with gadolinium accumulated massively in injured myocardium in a passive and specific manner over a time period of 24 hours.

The mechanism behind the EPR effect is still a matter of debate (68) and some investigators have started to question the validity of the model describing it, proposing that the accumulation of nanoparticles is caused by different, more dynamic processes related to vascular bursts in the compromised vasculature for instance (75). Nevertheless, the above mentioned permeability of the endothelium at the disease sites of atherosclerosis and myocardial ischemia can be exploited by long-circulating nanomaterials to achieve the efficient targeting of pathological areas with compromised vasculature (76-79).

Apart from exploiting the vascular permeability associated with intra-lesion vessels, the surface of nanoparticles can be equipped with specific ligands (antibodies, peptides, folates, etc.) allowing the targeting of specific receptors at the disease site. Knowledge of disease markers and attachment of complimentary ligands can increase the interaction of those NPs that do reach the target site, thus improving therapeutic activity (80). In the case of atherosclerotic plaques, functionalization of the nanomaterial's surface allows for the targeting of different plaque components at different stages of the disease. For instance, endothelial adhesion molecules expressed at the luminal side of the endothelium from the early stages of the disease can be targeted by ligand decorated nanoparticles (81-83). Other than endothelial cells, targeted nanosystems have been developed against macrophage-specific receptors (84, 85) and extracellular matrix proteins (86) (*e.g.,* collagen IV). When plaque is ruptured and a thrombus forms, specific components like fibrin (87) or platelets (88) may also be targeted.

During ischemia and immediately after reperfusion, cell adhesion molecules (*e.g.,* Selectin, ICAM, CD11, CD18) are up-regulated at the luminal surface of the microvasculature in the border zone of the infarctus. Thus, selective delivery is also becoming possible at this level by NPs surface functionalization with antibodies, able to specifically recognize these adhesion molecules (23, 25). Other specific targets may also be considered. As an illustration, Liu *et al*. (89), have engineered anti-cTN1 antibody modified liposomes, since cardiac troponin (cTN1) is also overexpressed during myocardial ischemia. These targeted liposomes were used to deliver efficiently anti-miR-1 antisense oligonucleotides with alleviation of arrhythmogenesis after cardiac ischemia.

Another strategy to target the heart is through specific peptides. Discovered by *in vivo* phage display technology, various peptides have indeed been used to identify heart specific markers in normal (90) or ischemic myocardium (91). Interestingly, liposomes loaded with CRPPR peptide showed an increased accumulation into injured rather than healthy myocardium (92). Cardiac accumulation was also demonstrated with NPs made of cationic polymers decorated with ischemic myocardium targeted peptide (93).

Due to the ability of nanoparticles to improve drug delivery and biodistribution, some classes of molecules have been considered for encapsulation and their efficacy tested *in vivo* in different animal models of atherosclerosis (Table1) or heart ischemia (Table 2).

IV. Nanomedicines for managing lipid levels

Elevated low density lipoprotein (LDL) levels are correlated to an increased risk of coronary artery disease. Long term statin administration remains the gold standard for cholesterol lowering therapy. Further, clinical trials have demonstrated a significant benefit of high dose statin therapy versus the standard-dose treatment in preventing cardiovascular events (94). However, high-dose statin treatments have been shown to induce unwanted side effects (95) prompting the US Food and Drug Administration (FDA) to issue new safety guidelines for their use. This, along with the fact that many individuals treated with statins do not achieve their target levels of LDL cholesterol, has prompted new research in the field of LDL lowering therapeutics.

ApoB is a component apolipoprotein of LDL and is required for assembling LDL in the liver. As such, inhibiting ApoB production holds promise in reducing LDL-dependent vascular inflammation. Because, as a large lipid-associated protein, ApoB is difficult to target with conventional therapies (96), a strategy based on RNA interference through the use of siRNA (small interfering RNA) strands can be used to silence ApoB expression and consequently reduce LDL blood levels (97).

siRNA therapeutics hold immense promise but are limited by two inherent inefficiencies. First, the non-specific effects of siRNA, such as off-target effects (98), and a propensity to induce an innate immune response via Toll-like receptors activation. Second, siRNA delivery issues caused by inefficient intracellular penetration resulting from hydrophilicity and polyanionic nature, poor stability in circulation and unfavourable distribution towards non-target cell types (99). Therefore, considerable efforts have been made to improve siRNA delivery by the use of nanocarriers (100) as reviewed in detail elsewhere (101, 102).

Nanocarriers are ideally suited as they can be used to protect siRNA from degradation by exonucleases and carry these small fragments of nucleic acids to sites of interest In a seminal study, ApoB specific siRNAs were encapsulated into stable nucleic acid lipid particles (SNALP) and administered intravenously to cynomolgus monkeys (2.5 mg/kg). 48h after administration, a reduced ApoB RNA expression, up to 90%, was observed in the liver of the animals. The effect lasted up to 11 days, showing reductions in ApoB protein, cholesterol and LDL plasma levels (97). More recently, ApoB specific siRNA was encapsulated in lipid nanoparticles and administered to lean cynomolgus monkeys in a single dose at 2.5 mg/kg. ApoB knockdown was observed and the phenotypic effects on serum lipid levels resulted in a significant decrease in plasma levels of LDL (96).

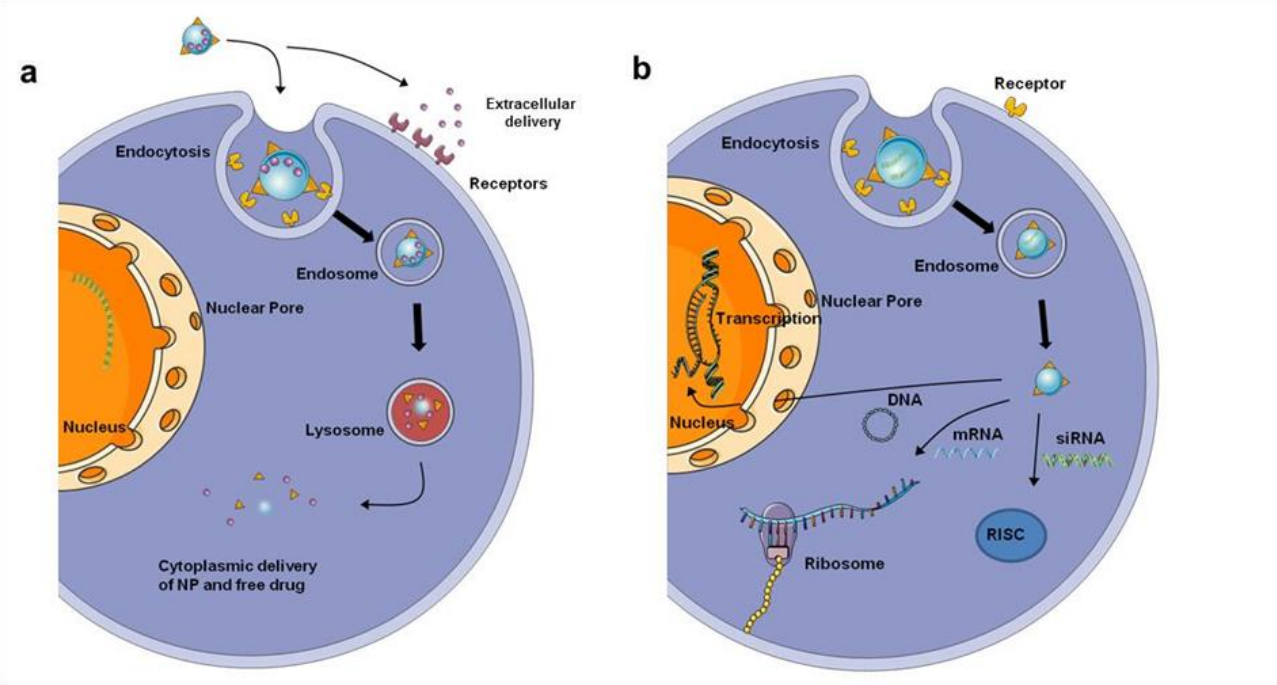

Figure 5: Mechanisms of drug and genetic material delivery by nanocarriers. (a) Upon reaching their cellular targets, nanomedicines can release therapeutic agents at the cell vicinity or inside the cell. Cells usually uptake nanomedicines by endocytosis after the nanocarrier interacts with specific membrane receptors. This leads to the formation of an endosome that becomes increasingly acidic through V-ATPase action, fuses with other endosomes and pre-lysosomal vesicles containing degrading enzymes, eventually evolving into a lysosome prone to carrier degradation and drug release into the cytoplasm. (b) For genetic material delivery the mechanisms differ following the type of gene therapy enacted by the therapeutic agent. Cytoplasmic delivery of mRNA and siRNA respectively activate ribosomal translation and RNA-induced silencing complex (RISC) pathways. For DNA delivery the nanocarrier should be designed to resist the degrading conditions found in the endosome to allow for endosomal escape and direct targeting of nuclear pore complexes through nuclear localization signals.

Concurrently, pro-protein convertase substilisin/kexin type 9 (PCSK9) protein, an endogenous regulator of LDL receptors in the liver has garnered interest in the regulation of LDL levels. Therapeutic silencing of PCSK9 induces a higher density of LDL receptors in the liver, thus lowering LDL plasma levels and conferring atheroprotection (103). In an elegant study, Frank-Kamenetsky *et al.,* (104) demonstrated in various pre-clinical animal models, that the encapsulation of PCSK9 siRNA into lipid nanoparticles decreased the level of PCSK9 in the liver, lowered plasma concentrations of LDL cholesterol and had little effect on HDL-cholesterol and

liver triglyceride levels. This approach underwent a phase 1 clinical trial (105) suggesting that selective inhibition of PCSK9 synthesis by liposomal RNA interference provides a potentially safe mechanism to reduce LDL cholesterol concentration in healthy individuals.

Contrary to LDL, high density lipoprotein (HDL) an endogenous lipidic nanoparticle (7-13 nm in size) are known to possess atheroprotective capacities by participating in reverse cholesterol transport from atherosclerotic plaque macrophages to the liver (106). Direct administration of endogenous HDL or recombinant forms (rHDL) was considered to reduce cholesterol levels and thus atherosclerotic plaque development. In rabbits, these NPs showed a regression of atherosclerotic lesions (107, 108). Late, rHDL NPs were tested in clinical trials and a significant regression of coronary artery diseases was observed (109). Even if interesting, these rHDL nanoparticles are expensive, difficult to synthesize and mass produce, which has hampered further clinical development (74). More recent attempts have focused on the use of so-called "mimetic" HDL nanoparticles made for instance of a polylactide-co-glycolide (PLGA) core and a coating composed of lipids and ApoA, a constitutive protein of HDL (110). While the PLGA core provided sustained drug delivery, the coating endowed the nanoparticles with biological capabilities similar to those found on native HDL (*e.g.,* macrophage targeting and cholesterol efflux capacities) (110). Additionally, the PEGylation of ApoA in HDL mimetic nanoparticles has been shown to markedly improve their plasma half-life and enhance their anti-atherogenic properties in a hypercholesterolemic ApoE$^{-/-}$ mouse model (111).

V. Nanomedicine and anti-inflammatory therapy

Inflammation is recognized as having a major role in both atherosclerosis, and myocardial ischemia/ reperfusion injury (82). As such different anti-inflammatory therapies have been developed, or are currently undergoing clinical trials (112, 113). However, these therapies cannot target a specific area since they are distributed throughout the whole body when injected. To further improve the treatment, different strategies have been developed through nanoparticle engineered systems. Monocyte recruitment to the arterial wall through chemokine binding at the monocyte CCR2 receptor site and recognition of upregulated endothelial cell adhesion molecules with subsequent differentiation of monocytes into intra-lesion macrophages, is one of the hallmarks of atherosclerosis and one of the therapeutic pathways targeted by nanomedicine.

Upon systemic injection, nanomaterials interact strongly with circulating monocytes and tend to accumulate in the spleen, which contains a large monocyte reservoir and subsequently dispatches these cells to sites of local inflammation (114). Accordingly, studies have demonstrated that siRNA encapsulated in integrin targeted liposomes that accumulate in the spleen could efficiently enact local silencing of CCR2 expression. This nanosystem reduced monocyte recruitment at sites of inflammation (115). The same method was used in the treatment of myocardial infarcts in ApoE$^{-/-}$ atherosclerotic mice models by co-encapsulation of CCR2 siRNA with an MRI (Magnetic Resonance Imaging) sensor. This monocyte targeting with RNA interference attenuated left ventricular dilation and resulted in reduced post-MI heart failure, while allowing companion imaging of treatment response (116).
Another modality to inhibit CCR2 and to reduce monocyte infiltration into atherosclerotic plaque relies on the use of chemokine receptor antagonists. CCR2 antagonists were loaded in VCAM-1 directed target sensitive liposomes to reduce adhesion and transmigration of monocytes at activated endothelium (117). These nanocarriers have a specific phospholipid bilayer composition, which upon target recognition and binding, exhibit destabilization immediately followed by cargo release. This is desirable when inhibition of chemokine/chemokine receptor interaction at the cell's surface is sought after and uptake of the nanocarrier by the endothelial cells should be avoided.

Monocytes also rely on endothelial cell adhesion molecules for recruitment into the arterial wall. Studies have suggested that inhibiting adhesion molecules function could have beneficial effects on inflammatory cell recruitment (118). Recently, novel polymeric nanoparticles based on epoxide modified low molecular weight polyethyleneimines were identified for selective *in vivo* delivery of siRNA to endothelial cells (119). This formulation was used at low doses (up to 0.02 mg kg^{-1}) for simultaneous *in-vivo* silencing of 5 genes (Tie1, Tie2, VEcad, VEGFR-2, and ICAM2). Interestingly, this endothelial cell targeted silencing was enacted without significantly reducing gene expression in hepatocytes, pulmonary endothelial cells, or other immune cells, thus limiting off-target effects. In ApoE$^{-/-}$ mice, the same nanoformulation allowed for the efficient silencing of multiple cell adhesion molecules involved in leukocyte adhesion (VCAM1) transmigration (*ICAM1, ICAM2)* and rolling (*Sele*, and *Selp*) (120).

TABLE 1

Experimental animal models and protocols used in literature for demonstrating atheroprotection of various nanomedicines.

Active molecule	Carrier	Size (nm)	Animal model	Protocol	Main results	Refs
Lipid management						
LDL						
siRNA	LNP	nd	Cyonomolgus monkey	• Bolus i.v. injection	• 80% silencing of liver ApoB mRNA and ApoB-100 protein was achieved with a single bolus 1 mg/kg	[97]
siRNA	LNP	~50 nm	Rodent and non human primate	• In rodents tail vein injection, in NHP 30 min i.v. injection of 5 mg/kg formulation of LNP	• Liver-specific siRNA silencing of PCSK9 associated with up to 60% reduction in plasma cholesterol concentrations	[104]
siRNA	LNP	nd	Cyonomolgus monkey	• Peripheral vein bolus injection of 2.5 mg/kg	• 80% silencing of ApoB and 60% reduction in plasma LDL levels	[96]
HDL						
HDL mimetic	ApoA coated PLGA	~40 nm	$ApoE^{-/-}$ mice	• Tail vein injection of 2 mg of NPs	• Accumulation of PLGA-HDL nanoparticles in atherosclerotic plaques • Specific targeting of plaque macrophages • Good cholesterol efflux	[110]
Anti-inflammatory						
CCR2						
siRNA	LNP	~80 nm	$ApoE^{-/-}$ mice	• 0.5 mg/kg/day twice a week for 3 weeks	• Reduced monocyte/macrophage number in atherosclerotic plaques by 82%. • 38% reduction of lesion size in the aortic root	[115]
Cell adhesion molecules						
siRNA	PEI NP	nd	$ApoE^{-/-}$ mice	• Three intravenous injections of 3 mg/kg cumulative siRNA dose over 2 weeks by tail vein injection	• 50% reduction of myeloid cells recruited to aorta. Good silencing of several cell adhesion molecules	[120]
Glucocorticosteroids						
Dexamethasone (DXM)	Biogel embedded with PLGA NPs	nd	$ApoE^{-/-}$ mice	• 0.5 mg of DXM loaded in PLGA NPs embedded in biogel painted on atherosclerotic lesions	• Fibrous cap thickening • 25% reduction of plaque macrophage content • Lower VCAM 1 expression	[131]
Prednisolone phosphate (PLP)	Liposomes	~100 nm	Rabbits	• Ear vein injection of 15 mg/kg loaded PLP	• 40% decrease in plaque macrophage content after only 2 days of treatment	[129]
Endogenous pro resolving peptides						
Ac2-26	Col IV targeted PEG-PLGA	~100 nm	$LDLr^{-/-}$ mice	• Once per week i.v. injection of 10 μg NP loaded Ac2-26	• Subendothelial collagen increase • Superoxide suppression in lesions • Necrotic area decrease	[137]
IL-10	Col IV targeted PEG-PLGA	~100 nm	$LDLr^{-/-}$ mice	• Once per week intravenous injection of 5 μg of NP loaded IL-10	• Increased fibrous cap thickness and necrotic core decrease	[136]
Statins						
Pitavastatin	rHDL	~30 nm	$ApoE^{-/-}$ mice	• Long term treatment: i.v. injection 15 mg/kg twice per week of rHDL loaded pitavastatin for 12 weeks • Short term treatment: four i.v. injections of 60 mg/kg of rHDL loaded pitavastatin within 1 week	• Long term: 34% decrease of total plaque area; 57% decrease of plaque macrophage content • Short term: 31% decrease of total plaque area. 84% decrease of plaque macrophage content. • Decrease of inflammation related gene expression	[123]
Pitavastatin	PLGA	~160 nm	$ApoE^{-/-}$ mice	• 0.012 mg pitavastatin once per week administered by tail vein intravenous injection	• Inhibition of plaque destabilization and rupture • Inhibition of inflammatory monocyte recruitment	[125]

LNP: lipid nanoparticle; siRNA: small interfering RNA; PCSK9: pro-protein convertase substilisin/kexin type 9; LDL: low density lipoprotein; HDL: high density lipoprotein; PLGA: poly(lactic-co-glycolic acid); PEG-PLGA: poly(ethyleneglycol)-block-poly(lactic-

These nanoparticles showed preferential uptake into plaque endothelial cells where the treatment, at a cumulative dose of 3 mg/kg, synergistically suppressed cell adhesion molecules expression. This resulted in a 50% reduction in monocyte recruitment to aortic plaque compared to controls, while blood monocyte levels remained constant. Although the molecular mechanism governing the preferential accumulation of these NPs into endothelial cells remains unknown, it was suggested that it may be due to interactions with serum proteins, which can promote delivery to certain cell types (118, 120).

As mentioned above, statins are widely used for their lipid lowering ability while they also exert anti-inflammatory effects at high doses, but with severe side effects (121, 122). Local delivery of statins to plaque tissue for achieving local anti-inflammatory effect was carried out by encapsulation into synthetic HDL particles derived from recombinant human ApoA (123). In a 3 month, long-term low dose oral treatment (15mg/kg), these HDL nanoparticles were able to reduce the plaque inflammation, to affect mRNA expression of genes related to inflammation and to decrease inflammatory protease activity on a $ApoE^{-/-}$ mouse model. Another report confirmed the findings of this initial study (124). Similarly, statins were also delivered in PLGA nanoparticles, resulting in decreased monocyte recruitment by inhibiting cytokine mediated chemotaxis and increased plaque stability by inhibiting matrix metalloprotease activity (125). It was found that these polymeric nanoparticles were rapidly taken-up by circulating and splenic leukocytes and accumulated in macrophages at atherosclerotic lesions sites. In another experiment performed by the same group, pitavastatin loaded PLGA nanoparticles were administered at the time of reperfusion in a rat model of myocardial ischemia. A reduction of the infarct size was observed 24 h after injection, as well as, an improvement of left ventricular function 4 weeks post-myocardial infarction, when free pitavastatin showed no therapeutic efficacy (126). Since pitavastatin accumulated into infarcted myocardium, it was suggested that it could exert protective effects by activation of PI3K/Akt pathway and inhibition of inflammation and cardiomyocyte death.

TABLE 2

Experimental animal models and protocols used in literature for demonstrating cardioprotection of various nanomedicines.

Active molecule	Carrier	Size (nm)	Animal model	Protocol	Main results	Refs
Thrombolytic drug delivery						
tPA	Gelatin	~100 nm	Pig, distal balloon occlusion	• i.v. injection of NPs over 5 min; trans-thoracically US continuous wave (1.0 MHz, 1.0 W/cm^2) for up to 60 min	• Recanalization in 9 of 10 swine within 30 min	[88]
SK	Liposomes	nd	Dog, AMI obtained with autologus thrombus	• An initial bolus preceded by an i.v. infusion until recanalization was observed	• Reduced time to obtain reperfusion (32 min *vs* 78 min for SK alone)	[157]
SK	Polymer	~810 nm	Dog, AMI obtained with autologus thrombus	• Initial bolus in the first minute, preceded by a constant infusion of remaining formulation over 2 h period	• Accelerated thrombolysis and blood flow restoration	[159]
Pro-angiogenic molecules delivery						
VEGF	Liposome-targeted P-Selectin	~180 nm	Rat, MI after LAD	• Liposomes injected immediately after MI, *via* tail vein	• Significant improvement in cardiac function and vascular structure at 4 weeks after MI	[182]
VEGF	Lecithin/Pluronic F-127	~270 nm	Rat, MI after LAD	• 2 weeks after the infarction a thoracothomy was done and NPs were injected into the epicardium	• Enhancement of vascularization 4 weeks after treatment	[183]
VEGF (gene delivery)	PLGA bearing VEGF plasmid DNA	~100–300 nm	Rabbit, MI after LAD	• 1 h after left coronary artery occlusion, injection of NPs-VEGF gene into the border zone surrounding the infarct	• 4 weeks after MI: increased of capillaries numbers • Improvement of cardiac function	[199]
VEGF (gene-adenoviral vectors)	Magnetic NPs	~100–200 nm	Rat, MI after LAD	• i.v. injection after 24 h of MI	• Improvement of heart function 4 weeks after surgery	[196]
PGF	Chitosan-alginate	~100–200 nm	Rat, MI after LAD	• Intramyocardial injection of NPs 5 min after ligation	Increases of LV function and vascular density • Decrease of scar area formation	[186]
PGF	PLGA	~233 nm	Rat, MI after LAD	• NPs injected directly into the border zone of the myocardium	• 6 weeks after MI: significant reduction of infarct size • Improved cardiac function	[187
IGF	PLGA	~74 nm	Mice, MI after LAD	• Directly injected into the heart after MI	• Reduced infarct size 21 days after MI	[189]
PDGF	Peptide nanofibers	nd	Rat, MI after LAD	• Injection into infarcted border zone 1 min after LAD	• 4 months after MI: improvement of vascular density and blood flow and absence of toxicity	[192]
PDGF	Peptide nanofibers	~10 nm	Rat, MI after LAD	• Injection into infarcted border zone after LAD	• Reduced apoptosis in infarcted myocardium	[193]
Epo	Liposomes coated with Sialyl Lewis X	~100 nm	Rabbits with MI for 30 min	• Injection of lipo-Epo at reperfusion; analysis at 24 h, 48 h, 7 and 14 days	• Accumulation of targeted liposomes in the border area of myocardium • The LV function and remodeling were improved • The number of CD31 positive microvessels was significantly greater	[148]

Anti-oxidants molecules delivery						
CoQ10	Liposome	~177 nm	Rabbit with AMI for 30 min and reperfusion for 3 hours	• Brief infusion of liposomes through coronary arteries before occlusion	• 3 h after reperfusion: reduction of area at risk	[205]
CoQ10	Liposome	nd	Rat, isolated hearts	• i.v. administration 15 min prior I/R	• Improvement of tolerance to ischemia reperfusion injuries	[204]
Purine delivery						
ATP	Liposomes	~189 nm	Rat, isolated heart	• Liposomes were infused over a 1 min period prior the onset of ischemia; isolated hearts with global ischemia for 25 min and reperfusion for 30 min	• Improvement of both systolic and diastolic functions	[211]
ATP	Liposomes	~200 nm	Rabbit with AMI for 30 min	• Liposomes were administered by intracoronary infusion followed by 30 min of occlusion and 3 h of reperfusion	• 3 h after reperfusion: reduction of area at risk	[209]
ATP	Liposomes coated with monoclonal 2G4 antibody against cardiac myosin	~189 nm	Rat, isolated heart	• Liposomes were infused over a 1 min period prior the onset of ischemia; isolated hearts with global ischemia for 25 min and reperfusion for 30 min	Improved accumulation of coated liposomes; recovery of mechanical functions of myocardium	[210]
Ade	Liposomes	~134 nm	Rats with MI for 10 min	• i.v. infusion for a 10 min period starting from 5 min before reperfusion	• Accumulation of liposomes due to EPR effect • 3 h after reperfusion: limitation of infarct size	[223]
Ade	Silica	~6–13 nm	Rat with MI for 30 min followed by 60 min of reperfusion	• Ade adsorbed on the surface of the silica NPs; i.v. infusion for 10 min starting 5 min prior to reperfusion	• Reduction of infarct size area	[224]
Anti-inflammatory drugs delivery						
PGE_1	Liposome	nd	Dog with LAD for 2 h	• i.v. bolus administration during coronary occlusion	• Reduction of infarct size • Inhibition of neutrophils infiltration	[140]
Pitavastatin	PLGA	~159	Rat, MI with LAD for 30 min or 45 min	• i.v. injection of NPs at the time of reperfusion	• 24 h after reperfusion: reduced MI size by inhibiting inflammation and cardiomyocyte apoptosis	[126]

tPA: tissue plasminogen activator; SK: streptokinase; US: ultrasound; AMI: acute myocardial infarction; VEGF: vascular endothelial growth factor; PLGA: poly-lactic-co-glycolic acid; MI: myocardial infarction; LAD: left anterior descending artery; PGF: platelet growth factor; IGF: insulin growth facto; PDGF: platelet derived growth factor; Epo: erythropoietin; LV: left ventricle; CoQ10: coenzyme Q10; ATP: adenosine triphosphate; Ade: adenosine; PGE_1: prostaglandin E_1; nd: not determined.

Glucocorticoids are a class of steroid hormones which have the ability to effectively suppress inflammation through binding to the glucocorticoid receptor present on every cell. With systemic delivery, glucocorticoids have a host of pleiotropic effects, including potentially harmful side effects like osteoporosis, glaucoma and insulin resistance, which limit their long-term administration (127). Interestingly, the delivery of glucocorticoids in liposomal formulations was found to significantly reduce side effects. For instance, Dexamethasone (DXM) was loaded into liposomes of different sizes and injected intravenously into atherogenic mice (128). Compared to free DXM and to liposomes with other sizes, 200 nm liposomes showed a significant decrease in aortic cholesterol content. DXM liposomes showed a substantial dose advantage, with a higher antiatherogenic effect at 55 μg/kg compared to free DXM at 550 μg/kg which was explained by a higher macrophage uptake of 200 nm liposomes in atherosclerotic lesions. In another study (129), prednisolone (another glucocorticoid) and a MRI contrast agent were encapsulated in long circulating PEGylated liposomes to enhance the blood circulation time and accumulation in inflamed sites. In a rabbit model, a significant decrease in the inflammatory response was observed over a week (129), which correlated with decreased intimal macrophage contents. These liposomes had less side effects compared to free prednisolone phosphate in rats and caused a decreased inflammatory response of the artery wall after intravenous administration in hyperlipidemic rabbits (130). Another approach that has been undertaken for the delivery of glucocorticoids, is through local delivery to the vascular wall via a bioadhesive gel (131). Indeed, DXM loaded into biodegradable nanoparticles and delivered to the lesion via a bioadhesive gel displayed slow drug elution, resulting a reduced inflammation. Furthermore, this material was observed to promote characteristics of plaque healing by remodelling and strengthening the fibrous cap on atherosclerotic plaques (131).

Recently, attempts have been made to stimulate endogenous mechanisms orchestrating the resolution of inflammation (132, 133). Following the onset of inflammation, the resolution phase aims to restore tissue function and homeostasis by clearing pathogens, pro-inflammatory debris and cytokines. The defective enacting of this important regulatory process has been shown to be a major pathogenic pathway in the progression of atherosclerosis (134). In the innate setting, resolution is mediated by pro-resolving lipids (*e.g.*, (lipoxins, resolvins, maresins, and protectins) and protein mediators such as interleukin-10 (IL-10) and annexin A1 (135). Thus, Ac2-26, an annexin A1 mimetic peptide, was encapsulated in biodegradable diblock PEG-PLGA collagen IV-targeted nanoparticles and evaluated in a $LDLr^{-/-}$ mouse model of atherosclerosis for efficient plaque localized release and anti-inflammatory therapy. These NPs

were shown to enhance resolution *in vivo* (136) and led to a marked improvement in key advanced plaque properties, including an increase in the protective collagen layer overlying atherosclerotic lesions, a diminishment of plaque related oxidative stress and a decrease of the necrotic areas in arterial plaques (137). More recently, similar collagen IV-targeted NPs loaded with IL-10, were shown to prevent vulnerable plaque formation in a $LDLr^{-/-}$ mouse model of atherosclerosis by similarly increasing fibrous cap thickness and decreasing necrotic core size (138).

Other molecules have been evaluated for their anti-inflammatory capacities in myocardial ischemia/reperfusion injuries. Prostaglandin E_1 (PGE_1), a potent vasodilator, was shown to reduce experimental infarct size when administered by slow infusion and at low-dose, by inhibiting pro-inflammatory cytokine productions, such as IL-6 and IL-8 (139). However, PGE_1 is rapidly metabolized in the lungs and induces tachycardia and/or hypotension. To minimize these drawbacks, Feld *et al.,* encapsulated PGE_1 into liposomes (lipo-PGE_1), showing that intravenous bolus administration of liposomal PGE_1 reduced the infarct size in an open-chest canine model with 2 hours left anterior descending coronary occlusion. In parallel, an improvement of myocardial blood flow during reperfusion without adverse hemodynamic effects was noted (140). This cardioprotective activity resulted from an anti-inflammatory activity on neutrophil functions. A similar therapeutic efficacy was obtained on a porcine model with 2 h myocardial infarction and 3 hours reperfusion. In these experiments, lipo-PGE_1 were found to decrease serum pro-inflammatory cytokines IL-6 and TNF-α (141). These liposomal PGE_1 were further evaluated in clinics, in patients with ST-segment elevation myocardial infarction (STEMI) after primary percutaneous coronary intervention (PCI). The major finding of this study was that intravenous administration of 20 µg of Lipo-PGE_1 prior to PCI, could improve myocardial microcirculation without any clinical adverse effect (142).

Erythropoietin (Epo), a small circulating protein hormone, which stimulates angiogenesis and displays anti-inflammatory and anti-apoptotic activity, demonstrated a cardioprotective effect in rats with experimental heart failure (143, 144). However, clinical trials failed to show any reduction in myocardial infarction size, even at long term after the administration of large doses of Epo (145, 146), which also induced adverse events (147). To limit such undesirable side effects, Yamada *et al.*(148) have prepared Epo-encapsulated liposomes, surface decorated with Sialyl $Lewis^X$ (SLX) for P-Selectin recognition. After intravenous injection in rabbits subjected to 30 min myocardial ischemia, a significant improvement of left ventricular function, a

reduction of myocardial infarct size and an activation of pro-survival pathways were noticed.

By mimicking apoptotic cells, phosphatidylserine (PS)-presenting liposomes represents another approach to reduce inflammatory processes. The resident and recruited macrophages may, indeed, recognize apoptotic cells via phosphatidylserine at their surface to clear them and, at the same time, to produce an anti-inflammatory consequence. When PS-liposomes were injected in a rat model of acute myocardial infarction, a trend in the secretion of anti-inflammatory cytokines was detected 3 days after, resulting in small scar areas which prevented ventricular dilatation and remodelling (149).

The above examples illustrate some of the experimental therapeutic strategies employing nanomedicines to restrain deleterious effects of inflammation during atherosclerosis and heart ischemia/reperfusion. In general, pharmacological and/or toxicological improvement is observed, even if the application of nanoparticles as drug delivery systems in cardiovascular diseases is emerging in only very few clinical trials.

VI. Nanomedicines for thrombolytic therapy

Plaque rupture and thrombus formation remain the primary causes of vessel occlusion that leads to acute ST-segment elevation myocardial infarction (STEMI). Although contemporary guidelines recommend primary percutaneous coronary intervention (PCI) as the preferred reperfusion strategy, this approach is limited to the PCI-capable hospital (150).
The greatest advantage of thrombolytic drugs (*e.g.,* streptokinase, urokinase or tissue plasminogen activator) is their ease of administration outside of hospital settings (151). However, when injected into the systemic circulation, these molecules distribute rapidly throughout the body and/or are quickly degraded by natural inhibitors present into the blood (*e.g.,* alpha 2 antiplasmine, alpha-2-macroglobuline, anti-C1 esterase, PAI-1) (152, 153). High quantities of thrombolytic agents are therefore needed to be injected to achieve significant therapeutic effect, but such high dosage results in undesirable side effects, like intracranial hemorrhages (154). To protect the drug and to concentrate it into the thrombus, different strategies based on the use of nanocarriers have been tested in preclinical models (28).

Non-targeted nanomedicines

A few decades ago, it was reported that positive and neutral charged liposomes tended to

accumulate in regions of myocardial infarction (155, 156). Based on this property, Streptokinase (157) or rtPA (69) were encapsulated into liposomes. A prolonged circulation time and a better fibrinolytic activity was noted compared to the free drugs. Some difficulties are, however, noted with these systems, since liposomes have a limited stability in systemic circulation and present a risk of premature drug release (158). Thus, streptokinase was further encapsulated into a water-soluble double emulsion polymer (PVA and PEG) nanoparticles. In a canine model of autologous coronary artery thrombosis, the encapsulated streptokinase demonstrated an accelerated thrombolysis comparatively to free streptokinase and a reduction of bleeding complications (159). Chitosan, another water soluble polymer, was applied to prepare urokinase-loaded nanoparticles by using an ionic cross-linking method. Compared to free urokinase, an increased capacity of clot lysis was observed when injected into rabbits with jugular thrombosis (160).

Targeted nanomedicines

An interesting modality to enhance the accumulation of nanoparticles charged with thrombolytic drugs is through their active targeting. An example is the use of RGD peptide (arginine-glycine-aspartic acid), in order to target GPIIb/IIIa receptor expressed at the surface of the activated platelets in thrombi. Thus, targeted liposomes loaded with either streptokinase (161) or rtPA (162) showed an enhanced accumulation into thrombus and an increased thrombolytic activity compared to non-targeted carriers. Similar results were observed with PLGA nanocarriers covered with a chitosan shell, loaded with rtPA and functionalized with RGD peptide linked to nanoparticle surface via a carbodiimide bond (163). Later, gelatin nanoparticles loaded with recombinant tissue plasminogen activator (rtPA, monteplase) and Zn^{2+} ions have been prepared (164). Gelatin was used as encapsulation material due to its preferential binding to von Willebrand factors (vWF) at the surface of platelets, ubiquitously found in thrombi, while Zn^{2+} ions may suppress rtPA activity, as long as they are present in the nanoparticles. In swine with acute myocardial infarction (AMI) treated with these nanoparticles, the application of a trans-thoracic continuous wave (1.0 MHz ultrasound) showed good recovery of blood flow in nine of ten swine within 30 minutes (88). These results were explained by the convergent effect of ultrasounds and drug. The ultrasounds were acting by inducing both the release of rtPA from gelatin nanoparticles and the breakage of the blood clot into small fragments, promoting the penetration of tPA molecules into the thrombus (165).

Magnetic nanomedicines

Another strategy to increase the quantity of thrombolytic drugs into the thrombus is the use of magnetic carriers made of a magnetite (Fe3O4) core that responds to an external magnetic field. Magnetic NPs coated with polyacrylic acid (PAA) (166) or with poly(aniline-co-N-[1-one-butyric acid] aniline) (167) were covalently coupled with an amino group of rtPA. The administration of rtPA loaded on magnetic nanoparticles associated with a magnetic guidance resulted in high blood flow recovery with a five-fold lower dosage, (*i.e.,* 0.2 mg/kg), comparatively to 1 mg/kg required for thrombolysis with free rtPA (168).

By using these different options for delivering thrombolytic drugs *in vivo*, it is possible to bypass the limitations of the free drugs (*e.g.,* protection against rapid degradation, enhanced accumulation into the clot). Moreover, reducing the injected dose represents important advantages, since the high doses used in clinics to obtain recanalization, often induce intracranial hemorrhages.

VII. Nanomedicines and anti-angiogenic therapy

Another strategy to stop atherosclerotic plaque destabilization and eventual rupture is through the inhibition of the microvessels that develop from the *vasa vassorum* to supply the plaque in nutrients. Integrin $\alpha_v\beta_3$ represents a possible target since it is transiently expressed during plaque growth (169). A first study made by Winter *et al.,* (170) demonstrated the feasibility of this strategy by using $\alpha_v\beta_3$ integrin targeted paramagnetic nanoparticles loaded with fumagillin. This study demonstrated for the first time the inhibition of proliferation of intraplaque neoangiogenesis from *vasa vasorum* in hyperlipidaemic rabbits, one week after the anti-angiogenic nanoparticles administration. These results obtained at a very low dose of fumagillin were shown to minimise the neurocognitive adverse effects of this compound. Moreover, the combination of free atorvastatin, a drug which is known to reduce intraplaque angiogenesis (171) and $\alpha_v\beta_3$ targeted fumagillin nanoparticles reduced the neovascularisation of the plaque up to 8 weeks in atherosclerotic rabbit models (172).
More recently echogenic liposomes loaded with Bevacizumab, an FDA-approved monoclonal antibody against VEGF, showed an effective delivery of the drug on *ex vivo* atheromatous carotid arteries under ultrasound exposure. This has led to an increased release of Bevacizumab from liposomes into porcine carotid tissue (173).

VIII. Nanomedicines for pro-angiogenic therapy

After cardiac ischemia, important dysfunctions in the blood vessels are often observed, leading to the impossibility to restore the blood flow. It was reported that in the presence of pro-angiogenic factors, such as fibroblast growth factor (FGF) or vascular endothelial growth factor (VEGF), new microvessels may emerge from pre-existing capillaries (174). With this aim, pro-angiogenic VEGF proteins were administered to patients, at low ($17ng/kg^{-1}/min^{-1}$) or high-dose ($50ng/kg^{-1}/min^{-1}$), after heart ischemia to promote cardiac tissue repair and salvage (175). This study showed that the low or high-dose of VEGF did not improve cardiac function, comparatively to a placebo-treated group. Moreover, the administration of large systemic doses of VEGF has resulted in serious side effects, such as the development of neoplasms or diabetic retinopathy (176, 177). These disappointing results are probably due to the rapid enzymatic degradation of these proteins and to their low residence time in the infarcted tissue (178, 179). Alternative approaches have considered the possibility to deliver genes encoding for pro-angiogenic proteins. Most of gene therapy tested in clinical trials consisted in the injection of *VEGF* or *FGF* plasmids (180, 181), but transfection efficiency, stability and long term expression of delivered genes were disappointing and needed improvement.

To overcome these obstacles, new modalities for growth factors delivery into the cardiac tissue remain an important challenge. Thus, liposomes containing VEGF and functionalized with antibodies against P-selectin were injected intravenously into rats, immediately after the induction of heart ischemia. Four weeks after treatment, rats receiving these immunoliposomes clearly showed significant improvements in cardiac function compared to untreated rats, in parallel to an increased number of perfused blood vessels in the infarcted area (182). However, since drug leakage from liposomes may occur rapidly after intravenous infusion, hybrid nanoparticles (270 nm) were constructed with a Pluronic F-127 triblock co-polymer shell and a lecithin core encapsulating 5 µg of rhVEGF (recombinant human VEGF). Of note, Pluronic F-127 is a polymer able to undergo thermal gelation under physiological conditions. These nanoparticles were injected into the ischemic border zone of rats subjected to myocardial infarction. Four weeks after treatment, animals exhibited evident cardioprotective effect manifested by new blood vessels formation and cardiac function improvement (183).

The placental induced growth factor (PIGF) is another pro-angiogenic protein reported to stimulate angiogenesis and to improve cardiac function by mediating endothelial cells growth, survival and migration (184, 185). Binsalamah *et al.* (186) have developed biodegradable and

biocompatible chitosan-alginate nanoparticles loaded with recombinant human PIGF (rhPIGF). These nanoparticles were injected into the peri-infarct myocardium area of rats, 15 minutes after the induction of an acute myocardial infarction. A cardioprotective effect was observed 8 weeks later, manifested by an improved blood flow in the myocardial infarction boarder zone, a decrease of scar tissue and a significant increase in left ventricular function with enhanced vascular density. A significant cardioprotective effect of PIGF was also observed after loading into poly lactic-co-glycolic acid (PLGA)-nanoparticles and injection into the infarction boarder zone of rats. This was attributed to the slow release of PIGF from nanoparticles during a period of 15 days (187).

Insulin like growth factor (IGF-1) is a pro-angiogenic factor, known to induce cardiomyocytes growth and survival (188). To evaluate the cardioprotection after acute myocardial infarction, Chang *et al*. (189) have developed 60 nm-sized PLGA nanoparticles loaded with IGF-1, taking advantage of electrostatic interactions for drug loading, which preserved the biological functions of IGF-1. A single intramyocardial injection was sufficient to reduce infarct size and to prevent cardiomyocytes apoptosis. The PLGA-NPs induced a slow release of IGF-1 during at least 24 hours but not beyond 3 days following the injection. This study confirmed the ability of PLGA-NPs to perform a prolonged delivery of pro-angiogenic proteins into the heart to provide better cardioprotection.

Self-assembling peptide nanofibers (SAPNF) represent another very original approach for sustained delivery of pro-angiogenic factors into myocardium (190). A characteristic of these peptides nanofibers is that upon exposure at physiological pH, they can self-assemble into stable tri-dimensional network structures (191). SAPNF loaded with human platelet-derived growth factor (PDGF) were intramyocardially injected into rats immediately after coronary ligation. A significant reduction of the infarcted volume was observed four months later. Noteworthy, apart from the observed improvement in vascular density and blood flow, absence of any pulmonary toxicity was noted, which is one of the major inconvenient of PDGF therapy (192). Similarly, a cardioprotective effect was observed after treatment with peptide-nanofibers charged with VEGF (193, 194) which was, once again, explained by the slow degradation of the nanofibers, resulting in sustained delivery of pro-angiogenic proteins.

Other than the direct injection of pro-angiogenic molecules, a second strategy is based on the modulation of gene expression, obtained by introducing exogenous DNA, mRNA, siRNA, miRNA

or oligonucleotides into cells (195). Adenoviral vector conjugated to magnetic nanobeads is another kind of carrier for triggering expression of VEGF gene in acute myocardial infarction. By using an epicardial magnet, adenoviral vectors conjugated to nanobeads were successfully concentrated in the infarcted heart after intravenous administration and a strong therapeutic gene expression was detected together with improvement of cardiac functions. These results highlighted that the $VEGF_{165}$ gene could be successfully expressed in endothelial cells which captured the nanocarrier (196).

However, gene therapy through the use of viral systems may also induce undesirable side effects, such as a host immune response against viral components, a risk of potential chromosomal insertion of viral sequences, a limitation of DNA for encapsulation and high cost production (197).

A second option for pro-angiogenic gene therapy is represented by non-viral systems such as liposomes or nanoparticles (Fig.5b) (198). Thus, PLGA nanoparticles bearing $VEGF_{165}$ plasmid DNA were developed by Yi *et al.,* (199). A significant increase in the number of capillaries was noted at four weeks after nanoparticles administration on a rabbit with one hour left coronary occlusion. In a more recent study, a nanocomplex formed by graphene oxide loaded with $VEGF_{165}$ gene was formulated and incorporated in methacrylated gelatin hydrogel. When injected into the peri-infarct area of rats with myocardial infarction, this nanocomplex induced an increased capillary density and a reduction in scar area, seven days post-administration (200).

Although these preclinical data suggest, without ambiguousness, that a cardioprotective effect can be obtained after treatment with proangiogenic proteins or genes loaded into nanoparticles, the protocols generally used are either complicated or very invasive, which will need improvements before clinical application. On the other hand, if these initial preclinical results may be encouraging, several limitations remain to overcome in order to achieve clinical application of nanoparticle based gene therapy (195). Among these limitations are included the rapid RES uptake, the inflammation, the possible aggregation in blood and a nonspecific effect in othertissues.

IX. Nanomedicines for Antioxidants delivery

As already mentioned before, reactive oxygen species (ROS) play an important role in the pathogenesis of atherosclerosis and myocardial ischemia/reperfusion injuries. ROS participate

to key molecular events in atherosclerosis including oxidative modification of lipoproteins and phospholipids, endothelial cell activation, and macrophage infiltration/activation and smooth muscle cell migration and proliferation.

Several antioxidants such as CoQ_{10}, beta carotene, lycopene, quercetin, resveterol, vitamin C and vitamin E have shown therapeutic benefits in atherosclerosis or in myocardial ischemia/reperfusion injuries. Antioxidants are molecules which counteract ROS due to their scavenging capabilities, thus preventing oxidative damages to the cell (201). However, clinical studies have shown inconsistent results because these molecules have poor stability, short half-life in plasma and insufficient diffusion into cells when administered through conventional delivery modes (43).

During heart ischemia/reperfusion (I/R) radical oxygen species (ROS) are produced in high quantities, mainly by neutrophils and in lower quantity by cardiomyocytes and endothelial cells. Such high amounts of ROS induce membrane damages, fragmentation, lipid peroxidation and/or random cross linking of DNA, leading to cell death (202). Thus, to preserve the cardiac function and to limit deleterious effects of I/R injuries, administration of antioxidant based therapy has been given consideration.

In this context, the most investigated antioxidant molecule is CoQ_{10}. The fully reduced form of CoQ_{10} (ubiquinol) shows antioxidant properties by acting as an hydrogen atom donor, preventing lipid peroxidation propagation, as well as, protein and DNA oxidation (203). The first study concerning the pharmacological efficacy of CoQ_{10} encapsulated into liposomes demonstrated a protective effect on isolated rat heart after ischemia/reperfusion (204). This cardioprotective effect has been explained by the antioxidant and membrane stabilizing properties of encapsulated CoQ_{10}. The pharmacological efficacy was also attributed to the essential role of this molecule in cells by acting as an electron and proton carrier coupled to ATP synthesis. Later, Verma *et al.*, (205) demonstrated a similar protective effect of CoQ_{10} when loaded into liposomes and administered to rabbits subjected to 30 minutes coronary artery occlusion and 3 hours reperfusion. A significant reduction of total area at risk was observed in animals receiving CoQ_{10} liposomes compared to controls (*i.e.,* 30% of the total area at risk as compared to 70% in the Krebs-Henseleit buffer-treated group). The efficacy of CoQ_{10} liposomal formulation was explained by a mechanism based on «plug and seal » of the damaged cell membranes (206).

In another approach, Nox2, the catalytic subunit of NADPH-oxidase, has been chosen as target since it is the major source of cardiac ROS production in the heart. Indeed, it was shown that

mice lacking *NOX2* gene were protected from ischemic injuries (207). Thus, Nox2 specific siRNA have been encapsulated into polyketal nanoparticles for gene silencing and inactivation of NADPH-oxidase in cardiac macrophages. The intramyocardial immediate injection of these nanostructures in mice with experimental myocardial ischemia showed a significant recovery of cardiac function, as demonstrated by echocardiography collected three days post-injection (208). However, this study did not investigate the exact mechanism behind the beneficial restoration of the cardiac function observed in Nox2-siRNA treated animals and it did not demonstrate the *in vivo* knock down of Nox-mRNA expression in macrophages. Additionally, the long term effects of polyketal nanostructures need to be evaluated, especially from a toxicological and metabolic point of view.

X. Nanomedicines for purines delivery

During myocardial ischemia a variable area of myocardium is deprived of nutrients and oxygen. In these conditions, the loss of oxidative phosphorylation decreases considerably the generation of ATP, resulting in failure of the ATP-dependent ion pumps. If such depletion prolongs, the ion balance across the cell membrane becomes lost, leading to cell death (29). Experimental studies (209-211) have shown that the administration of exogenous ATP has some cardioprotective effect *via* the attenuation of cell death during cardiac ischemia and reperfusion. However, the pharmacological efficacy of this approach is limited by (i) the rapid hydrolysis of ATP by extracellular ectonucleotidases (*e.g.,* CD39) in adenosine diphosphate (ADP), adenosine monophosphate (AMP), and adenosine (212, 213) and (ii) the strong hydrophilic character of ATP, which makes this molecule unable to cross biological membranes (214). In order to overtake these limitations, some research efforts have focused on the encapsulation of ATP into liposomes (214, 215). Thus, positively charged liposomes loaded with ATP were administered in dogs with myocardial ischemia and found to accumulate in ischemic tissue (216). A diminution of the size of the ischemic area was also demonstrated by Torchilin's group (210, 211). In this study, ATP loaded PEGylated liposomes showed a cardioprotective effect in both, isolated rat heart model (211) and in rabbits subjected to 30 minutes coronary artery occlusion (209). The same group has further developed ATP-immunoliposomes decorated with monoclonal 2G4 anti-myosin antibody, demonstrating enhanced pharmacological activity in myocardial ischemia in an isolated rat heart model (210). Adenosine, a catabolite of ATP, exerts beneficial effects during heart ischemia and reperfusion. Adenosine inhibits neutrophil adhesion to the endothelium, reduces cytokines release and

radical oxygen species formation, thus displaying anti-inflammatory and anti-apoptotic activity on cardiomyocytes (217). However, because adenosine is rapidly metabolized in the blood after intravenous administration, high doses of adenosine are required to obtain cardioprotection (218, 219) which is associated with severe adverse effects (*i.e.,* hypertension, reflex tachycardia, chest pain etc.), hampering the use of this molecule for therapeutic purposes (220-222). To circumvent the above mentioned limitations, Takahama *et al.* (223) have encapsulated adenosine into PEGylated liposomes before administration to rats with transient myocardial ischemia, for a 10-minutes period, starting from 5 minutes before the onset of reperfusion. The accumulation of adenosine-liposomes into infarcted areas was associated with infarct size limitation, as compared to the treatment using free adenosine. Silica nanoparticles represent another kind of nanoparticle for adenosine delivery (224). In this study, adenosine was adsorbed onto the surface of the nanoparticles and infused into rats undergoing 30 minutes of ischemia, for a period of 10 minutes, starting 5 minutes prior reperfusion. The area of the infarct was reduced comparatively to animals receiving only adenosine (224). However, silica nanoparticles are known to promote inflammation which represents an important limitation of this approach (225, 226).

Some more extensive investigations are still necessary to better understand the mechanisms of release and action of purines derivatives when delivered as nanoparticles.

XI. Stents coated with nanoparticles as delivery systems

The use of stents to keep open a stenotic vessel has demonstrated a beneficial effect in patients with heart ischemia, even if in-stent restenosis due to abnormal cell growth into the vessel lumina and thrombosis represent the major failures of this treatment. Thus, stents coated with different drugs (drug eluting stents (DESs)) have been developed to prevent smooth muscle cell growth and proliferation, as well as, inflammation and thrombogenesis. A series of investigations have focused on the use of stents coated with antiproliferative agents such as sirolimus, everolimus, zotarolimus, paclitaxel, dexamethasone or statins. The DESs use synthetic or natural polymers (biodegradable or non-biodegradable) as a foundation upon which are incorporated active molecules. They have demonstrated to be effective in reducing late restenosis but current DESs lack the capacity to adjust the drug dose and release kinetics appropriately, according to the disease status of the treated vessel. Recently, a new generation of DES coated with nanoparticles as delivery systems have been developed and preclinically evaluated (227, 228). Interestingly, these new nanoparticles coated DESs were found to be

more efficient for the treatment of restenosis, because local delivery could reach specific cell types in sufficient concentrations over time, thus achieving lower systemic toxicity. For example, imatinib mesylate (a PDGF receptor tyrosine kinase inhibitor) (227) and statins (known to inhibit the proliferation of vascular smooth muscle cells) (228) were encapsulated into bioabsorbable polymeric NPs-eluting stent. Both systems showed an attenuated in-stent restenosis when administered in a porcine coronary artery model. However, these studies were performed in normal pigs without pre-existing atherosclerotic lesions, which makes the comparison with clinical situation quite difficult. Moreover, both studies did not evaluate the long term efficacy and toxicity of these new medical devices.

Currently, paclitaxel loaded albumin nanoparticles (SNAPIST-I (229) and SNAPIST-III) and paclitaxel loaded liposomes were tested in clinical trials (https://clinicaltrials.gov) for the prevention of in-stent restenosis. In SNAPIST-I study, the patients received a single dose of paclitaxel-loaded nanoparticles administered *via* intracoronary catheter, immediately following percutaneous transluminal coronary angioplasty/stenting or balloon angioplasty. Systemic treatment was well tolerated at doses below 70 mg/m^2 with no significant adverse effects (229, 230).
We do not include additional details on nanoparticles drug eluting stents for the prevention and treatment of coronary restenosis because this subject has already been addressed previously in excellent reviews (231, 232).

XII. Nanoparticular systems for heart regeneration

In recent years, cell therapy has received increased attention for cardiac repair after heart ischemia. The injection of stem cells could allow for regeneration of the heart tissue and may limit the chronic aspect of heart infarction. Adult stem cells, such as autologous bone marrow derived stem cells (233), mesenchymal stem cell-like (234), peripheral blood endothelial progenitor cells (235, 236) or resident cardiac stem cells (237) have been tested in clinical trials.

It has resulted, however, that grafted cell generally have low retention during and immediately after intracoronary or intramyocardial injections. Some studies highlighted apoptosis as the culprit underlying low engraftment (238), while other investigations showed that the venous drainage and the contraction of the beating heart accounted for significant loss of transplanted

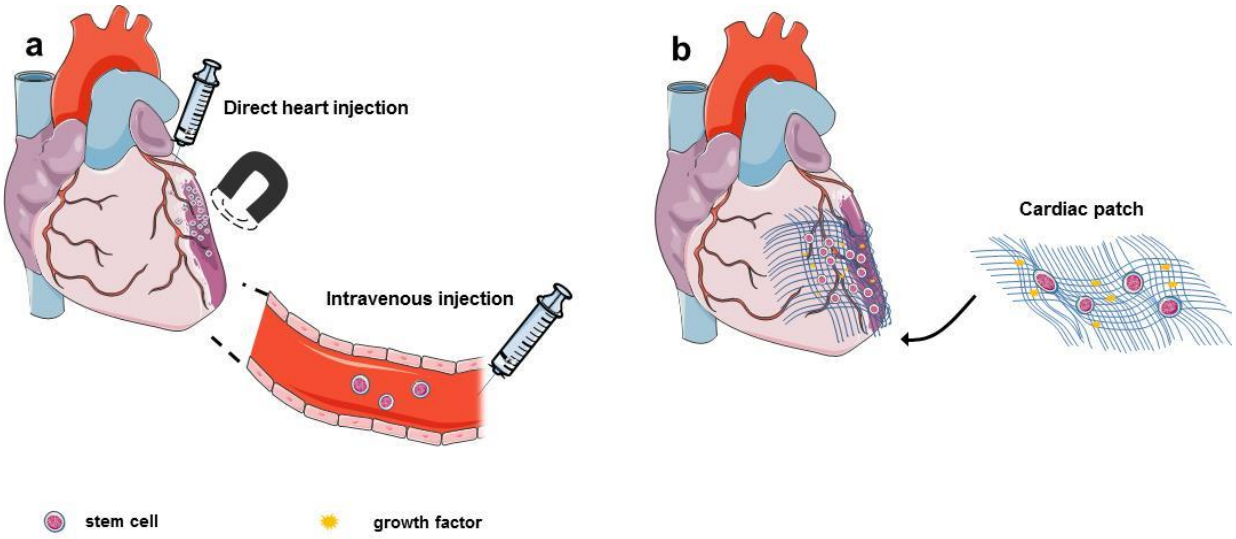

Figure 5: Heart tissue regeneration using nanostructured materials. For heart tissue regeneration, one of the main challenges lies in ensuring localization of stem cells and growth factors at the infarct site. (a) Other than direct injection into the heart, stem cells can be loaded with superparamagnetic SPIO nanoparticles which allow for magnetic attraction and retention at the lesion site after intravenous injection. (b) Cardiac patches are another method allowing for efficient retention of stem cells at the infarct zone.

cells (239, 240). In other words, the majority of transplanted cells are washed out along with myocardium contraction. It was even reported that only 1.5% (range 0.2%-3.3%) of transplanted stem cells accumulated in the myocardium 2 h after administration in patients (241).

Magnetic attraction of superparamagnetic iron oxide nanoparticles (SPIONs) or magnetic microspheres loaded stem cells has been considered in order to concentrate and retain cells in the targeted tissue (Fig.6a and Table 3). The cell uptake of SPIONs occurs via endocytosis after incubation at different time intervals before injection into animals (242, 243) and did not affect the overall cell viability (244). Enhancement of cell retention and improvement of cardiac function was confirmed by qRTPCR and immunohistochemistry in different studies (245, 246). Numerous studies have underlined the importance of MRI to detect and localize iron labelled stem cells after injection into rats (247) or mice (248) with heart ischemia. However, if at early

time (24 hours) after transplantation of SPIO-labelled mesenchymal stem cells, the engrafted cells were detected at the site of injection, later (few weeks), they were no more visible in the scar tissue because SPIONs were captured by macrophages. These finding suggests that SPIONs may not be a reliable marker to monitor the transplanted stem cells in the long term (244, 249). An interesting strategy to follow-up the transplanted cells survival is the use of markers for bioluminescence imaging. However, this approach requires the creation of stable cell lines expressing firefly luciferase (250). More recently, an interesting alternative has been proposed, consisting in living contrast agents such as magneto-endosymbionts derived from Magnetotactic bacteria (251). After injection into the cardiac infarcted area of mice, iCPMs labelled with magneto-endosymbionts were cleared and no more visible within one week after cell death.

Cardiosphere-derived cells (CDCs), a natural mixture of cardiac stem cells and supporting cell types, were also used for cardiac repair (242). Cheng *et al,.* (252) have employed a magnetic field to counteract the venous washout and to improve rat cardiosphere-derived cells retention when labelled with superparamagnetic microspheres particles (0.9 µm) and injected into the heart of rats with experimental open chest myocardial infarction. With this therapeutic modality, a beneficial effect was observed three weeks after intracoronary administration of these human cardiospheres-derived cells. Later, the same authors demonstrated better ejection fraction after autologous intracoronary injection of CDCs in rats with ischemia and reperfusion after being subjected to an external 1.3 Tesla circular NdFeB magnet (253). However, the risk of capillary occlusion with the cardiac spheres should not be underestimated and may represent a limitation of this approach.

In another study, iron oxide nanoparticles were conjugated with two types of antibodies: one against CD45 antigen expressed on bone marrow-derived stem cells and another directed towards CD34-positive cells of injured cardiomyocytes (254). After loading onto stem cells and injection under influence of a magnetic field, such nanoconstructions allowed antibodies to link the therapeutic stem cells to the injured cells. This resulted in a significant reduction of scar tissue formation in rats with heart ischemia and reperfusion. However, it remains unclear if magnetic accumulation of stem cells could also enhance the risk of coronary micro-embolization and additional experiments are certainly needed to evaluate the real benefit/risk ratio, especially at later time points after treatment.

TABLE 3

Preclinical examples of homing stem cells with magnetic nanoparticles, microspheres or nanofibers for cardioprotection.

Origin of stem cell	Carrier characteristics	Protocols	Main results	Refs.
Rat, MSC from BM	Iron NPs (SPIO), 62 nm	• 1 × 10^6 magnetic MSC injected into the left cardiac vein of rat with MI • 0.6 Tesla magnet placed above the heart	• At 3 weeks: 2.73–2.87 fold enhancement of cell engraftment retention of transplanted cells • Improvement of cardiac function • Attenuation of left ventricular remodeling	[245]
Rat, MSC from BM	Iron NPs (Ferumoxide (Endorem)	• Injection of 2 × 10^6 SPIO labeled MSCs 7 days after MI	• At 4 weeks: SPIO labeled MSC are in macrophages • Attenuation of left ventricular dilatation and dysfunction of the myocardium	[244]
Human cord blood-derived endothelial progenitor cells	Iron NPs, 8 nm, citrate coated	• Rats with MI for 30 min followed by 20 min of reperfusion • Intraventricular injection of SPIO labeled cells • External magnetic field application on chest cavity	• Detection of cells 24 h later • Enhancement of myocardial retention of labeled cells	[246]
Rat, cardiospheres derived cells	Iron microspheres	• 1.3 Tesla magnet application on rats with MI • Injection directly into myocardium at 4 sites around the border zone	• At 3 weeks: accumulation around ischemic zone • Attenuation of left ventricular remodeling	[252]
Rat, cardiospheres-derived cells	Fluorescence conjugated superparamagnetic microspheres	• Rat with ischemia 45 min and reperfusion • 20 min later after reperfusion injection of 1, 3 or 5 × 10^5 cells into left ventricular cavity intracoronary injection of NPs • Application of an external magnetic field 1.3 Tesla	• Enhancement of cell engraftment persisted for at least 3 weeks • Reduced scar tissue, enhancement of cell therapy benefits	[253]
Human cardiospheres derived stem cells	Iron NPs (Ferumoxytol)	• Rats with MI for 45 min and reperfusion • Intracoronary injection of labeled cells	• 3 weeks after: left ventricular remodeling attenuation • Enhanced angiogenesis	[242]
Rat, BM derived stem cells	Iron NPs (Ferumoxytol), coated with carboxylated dextran polymer, ~95.7 nm, zeta potential −9.6 mV	• Iron NPs conjugated with CD45 and CD34 against stem cells • i.v. infusion into rats with MI for 3 hours and 20 min reperfusion	• Reduction of scar tissue formation • Augmentation of cardiac function	[254]
Autologus MNC from BM	Peptide nanofibers	• Injection of 1 × 10^8 cells intramyocardially into MI pig model	• At 28 days after treatment: improved diastolic function • Reduced ventricular remodeling	[257]
Cardiomyoblasts cell line	Superparamagnetic iron oxide (Feridex)	• Labeling of cells with Feridex or transfected with Fluc	• A strong signal detection difference between BLI and MRI (half-life = 2.65 days over 6 days and 16.8 days over 80 days respectively)	[251]

MSC: mesenchymal stem cells; BM: bone marrow; SPIO: superparamagnetic iron oxide; MNC: mononuclear cells.

Even if the safety issues related to intravenously injected magnetically responsive stem cells may still represent a matter of debate, the major advantages of this method lie in the non-invasive administration of a reduced number of cells, actively homed to the injured myocardium.

Another method for regenerative cardiac tissue engineering is the implementation of cardiac patches for treating damaged heart tissue (Fig. 6b). Cardiac patches are, indeed, considered a promising strategy for enhancing stem cell therapy of myocardial infarction by allowing better retention of stem cells in the infarcted area, as well as, local delivery of bioactive molecules (*e.g.* growth factors) (255).

The materials used can be either natural or synthetic. Among natural biomaterials largely used are collagen, fibrin and hyaluronan but also polysaccharides, such as alginate, chitosan or dextran. Another type of natural biomaterial is represented by decellularized extracellular matrix (ECM). The major advantages of these natural biomaterials are their biocompatibility

and ability to mimic native ECM which can help in tissue regeneration.

Self-assembling peptide nanofibers represent an interesting approach to improve cell therapy for myocardial infarction. Indeed, nanofibers loaded with insulin-like growth factor (IGF1) combined with neonatal cardiomyocytes and injected into the infarct zone of rats with experimental ischemia, have shown a cardioprotective effect as well. It was hypothesized that the slow local delivery of IGF1 activated critical survival pathways and improved transplanted cell growth (256). A similar cardioprotective effect was also observed in pigs with experimental cardiac ischemia, when receiving autologous bone marrow mononuclear cells (MNC) combined with self-assembling peptide nanofibers. It was hypothesized that nanofibers could act as a scaffold for the MNC, allowing their adhesion and differentiation (257). Very recently (258), it was found that epicardial cells expressed follistatin-like 1 (Fstl1), a protein with a potent cardiogenic activity. However, Fstl1 epicardial expression declines following myocardial infarction. Interestingly, the application of human Fstl 1 protein via an epicardial 3D collagen nano-fibrilar patch was observed to stimulate cell cycle entry and division of pre-existing cardiomyocytes in mouse and swine model of myocardial infarction.

On the other hand, synthetic materials offer a better control of patches structure, porosity, and mechanical strength. For example, nanofibers made of tri-dimensional polymeric matrices of polylactic-co-glycolic were used in cell based therapies for inducing repair after myocardial infarction (259, 260), allowing for cellular integration and minimal inflammation. As a result, enhanced neovascularisation, reduced fibrosis and ameliorated ventricular function have been noted. Also, nanofibers were used to deliver growth factors to enhance neovascularisation and ameliorate blood flow.

Comparable results were obtained with porous patches made of Poly(ε-caprolactone)/gelatine seeded with mesenchymal stem cells (261, 262) or bone marrow stem cells (263) and implanted into the epicardium of rats with experimental ischemia. Four weeks after implantation, it was observed that the transplanted cells were able to migrate towards scar tissue (262).

Interestingly, cardiovascular patches may also be loaded with gold nanoparticles to provide conductive capacity. In an original approach, cardiac patches were engineered by seeding cardiac cells from neonatal rats within 3D porous alginate scaffolds. It was demonstrated that incorporating gold nanowires within the alginate scaffolds could improve electrical communication between adjacent cardiac cells which succeeded to contract synchronously (264). Later, other types of scaffolds gathering together gold nanoparticles and neonatal

cardiac cells seeded on a decellularised matrix (265) or on a chitosan thermosensitive hydrogel (266) were proposed for cardiac tissue engineering. Recently, three-dimensional macroporous and flexible nanoelectronic scaffolds with synthetic or natural biomaterials were developed to mimic the cardiac tissue structure in a cardiomyocytes culture (253, 267).
For more information on the use of cardiac patches, nanostructured or not, excellent detailed reviews already exist (268-271).

These preclinical results obtained with different nanomedicines are encouraging for cardiac therapy after myocardial infarction. Special attention should be paid on the fact that cell implantation success is strongly influenced by the retention and proliferation of the surviving cell fraction, where extensive cell death after transplantation is induced by a lack of blood vessels (due to ischemia) and by anoikis (death due to matrix detachment) (272).

XIII. Conclusion and future perspectives

Even if nanomaterials offer new opportunities for the treatment of chronic atherosclerosis and myocardial ischemia/reperfusion, preclinical studies remain still few in number for the different drug categories. Despite the *in vivo* pre-clinical proofs of concept reported in this review, there are currently no FDA approved nanomedicines for the treatment of cardiovascular diseases. At present, only a few nanosystems are in clinical trials. Such is the case for prednisolone-containing liposomes in atherosclerotic plaque treatment (Phase 2) (273) and for paclitaxel loaded albumin or liposomes for the prevention of in-stent restenosis (Phase 3) (229).

The reason why the encouraging preclinical findings with nanomedicines in different animal models of atherosclerosis are not systematically validated in clinical trials remains an open question. A reason for this is linked to the relevance of the animal models used to validate initial *in-vivo* efficacy. For instance, the accelerated development of atherosclerosis in animal models has been shown to create atherosclerotic lesions with somewhat different properties from those found in humans (67). Concerning heart ischemia, the failure to translate the observed cardioprotective effects in the clinical setting may stem from non-relevant preclinical studies which are often performed on young healthy animals, while patients with heart ischemia are generally old and have a number of comorbidity factors (*i.e.,* diabetes, hypertension, hypercholesterolemia ...).

Also, most investigations assess nanomedicines after relatively short periods of time following reperfusion, whereas a much longer period is needed to accurately evaluate the effects of these nanomedicines on the heart functionality, regeneration and their potential toxicity.

In fact, a high proportion of the literature solely focuses on the treatment of acute MI. Encouraging advances have been made in this field, but the treatment of chronic myocardial infarction *(e.g.,* growth factor and stem cell therapy for cardiac regeneration) remains a potentially fertile area of study in the treatment of cardiovascular diseases using nanomaterials. The final goal concerns the regeneration of functional myocardial tissue, unlike acute MI mitigation which essentially aims at salvaging the heart ischemic tissue.

Another reason for the disappointing clinical translation of cardiovascular nanomedicines is linked to the modes of administration tested in preclinical models, when the few strategies available should be better evaluated with human physiology in mind. Local drug delivery has an important advantage, as it allows to easily concentrate the drug at the disease site. It seems, however, that such an approach, while well suited for growth factors or for stem cells injected intramyocardially or into the border zone of necrotic areas, shows some limits. Although relatively easy to implement in preclinical models, its clinical translation remains more complicated because of the invasiveness of the method. Additionally, direct myocardial injection is often volume-limited and suffers from the tendency of the heart to circulate injected therapeutics. Another strategy for the delivery of therapeutics to the myocardium is through an intracoronary catheter. In fact, percutaneous coronary intervention provides a unique opportunity for the administration of nanomedicines at the critical time of reperfusion. While this strategy is less invasive it can also be less adequate when the coronary arteries are compromised (72, 274). As such, there is an urgent need for more standardisation of preclinical studies and protocols in order to allow for the pertinent selection of the most effective nanomedicines.

The most common strategy remains intravenous administration of the nanocarriers, less invasive and easier to implement than both local and intracoronary delivery modalities. Its main drawbacks lie in the insufficient accumulation of drug at lesions sites. Through the use of actively and passively targeted nanoparticles, nanomedicines can circumvent some of these hurdles but investigators should remain conscious of the discrepancies between animal models and humans.

Failure in this sense may result in the differences observed between animal and human trials such as in the case of the EPR effect which is less observed in humans than in animals, due to

excessive interstitial pressure or poor status of endothelial vessels in ischemic zones. In fact, to ensure successful clinical application of nanomedicines, the choice of the administration mode should also carefully be thought out from the initial design stages of the nanosystem depending on the therapeutic agent (*e.g*., drugs, genes or cells) and the targeted pathway.

Likewise, to be efficient, nanomedicines for atherosclerosis and myocardial ischemia must fulfil several criteria. Most importantly, the materials used for nanoparticle formulation need to be biocompatible and biodegradable, while the nanoparticles themselves should have adequate size, blood residence time and stability to target multiple lesion sites. It follows that the physico-chemical characteristics of nanomedicines should to be finely controlled to allow for reproducibility of obtained therapeutic results. Moreover, the formation of a protein corona may directly impact the biological identity of nanomedicines, which may in turn drastically alter their biodistribution and efficacy. The issue of the “personalized protein corona” could also represent another key factor. Discrepancies in blood protein make-up among species and individuals, resulting in variability of NPs targeting, drug release and bioavailability should be reported and better taken into account when developing nanomedicines. Thus, a more precise understanding of nanoparticles interaction with the blood environment is necessary to advance the predictable clinical translation of nanomedicines. The interaction with certain types of cells such as macrophages or endothelial cells should also be well mastered for optimum therapeutic efficacy. Additionally, a detailed knowledge of the disease at different stages of development is essential in order to develop a targeted specific treatment for personalized cardiovascular medicine.

Nanoparticles toxicity, especially in acute conditions, may also remain an important issue. Ideally, nanocarriers allow to target the site of disease, carry and release their payload in a controllable fashion, and eventually are degraded by the body’s metabolic processes into non-toxic metabolites. Great strides have been made towards the development of FDA approved biocompatible materials for use in clinical medicine. However, some research remains to be done. Notably, it is known that due to complement activation after intravenous injection, nanoparticles may induce reactions known as "C activation-related pseudoallergy" or CARPA (275, 276). The liver accumulation of high amounts of nanoparticles may also affect hepatic functions. Concerning the cardiovascular system, upon systemic injection, the heart is one of the first organs to be exposed to NPs. However, in normal conditions, the nanoparticles do not accumulate in this tissue and cause little cardiac toxicity. In general, encapsulation into nanoparticles or liposomes of anticancer drugs with a cardiac toxicity profile even results in an

important reduction of cardiac toxicity (277).However, in ischemic conditions, nanoparticles may accumulate into the heart (through the EPR effect), and new toxicological risks deserve to be investigated. Even if some data already exist in the literature concerning the cardiotoxicity of some nanomaterials, like for silica, carbon and some metallic nanoparticles (278, 279), they remain too scarce. The search for specific cardiotoxicity of nanoparticles in ischemic conditions represents therefore an interesting research area for the future.

Finally translation from bench to bedside is further hampered by the complex architectural design of many nanomedicines, like those with engineered surface functionalization or stimuli-responsive capabilities. Such complexity often results in difficulties for performing reproducible sample preparation and scaling-up. It is the opinion of the authors that future research should concentrate more on the construction of elementary nanocarriers, pharmaceutically more easy to develop and whose preparation is transposable to the industrial scale. There is, therefore, still considerable room for the development of novel biomaterials that could prove intrinsically superior to currently used nanoformulations. For example, we have previously reported the design of biocompatible drug-squalene materials which spontaneously self-assemble in water to form nanoparticles with high drug loading and absence of burst release, acting as efficient drug carriers and displaying targeting abilities due to their similitude with endogenous molecules (280, 281). Also, since the mechanisms of ischemia/reperfusion are well known today, it would be interesting to develop multidrug nanomedicines able to interfere with different processes such as angiogenesis, inflammation and free radical generation.

If considerable progresses have already been made possible, thanks to multidisciplinary approaches combining the complementary skills of chemists, material scientists, physico-chemists, drug delivery researchers and pharmacologists, there is still a requisite to bring more expertise from pharmaceutical developers, clinicians and regulatory officers to bridge the gap of nanomedicines from bench to bedside.

XIV. References

1. M. O. Guler,A. B. Tekinay, Nanomaterials for Medicine. *Therapeutic Nanomaterials*. 1 (2016)
2. D. T. Bui, J. Nicolas, A. Maksimenko, D. Desmaele*, et al.*, Multifunctional squalene-based prodrug nanoparticles for targeted cancer therapy. *Chem Commun (Camb)*. 50, 5336-5338 (2014)
3. F. Caruso, Nanoengineering of particle surfaces. *Advanced Materials*. 13, 11-22 (2001)
4. H. Fessi, F. Puisieux, J. P. Devissaguet, N. Ammoury*, et al.*, Nanocapsule formation by interfacial polymer deposition following solvent displacement. *International journal of pharmaceutics*. 55, R1-R4 (1989)
5. R. A. Jain, The manufacturing techniques of various drug loaded biodegradable poly (lactide-co-glycolide)(PLGA) devices. *Biomaterials*. 21, 2475-2490 (2000)
6. R. Karnik, F. Gu, P. Basto, C. Cannizzaro*, et al.*, Microfluidic platform for controlled synthesis of polymeric nanoparticles. *Nano letters*. 8, 2906-2912 (2008)
7. K. Landfester, The generation of nanoparticles in miniemulsions. *Advanced Materials*. 13, 765-768 (2001)
8. Y. Lee, J. Lee, C. J. Bae, J. G. Park*, et al.*, Large-scale synthesis of uniform and crystalline magnetite nanoparticles using reverse micelles as nanoreactors under reflux conditions. *Advanced Functional Materials*. 15, 503-509 (2005)
9. J. Park, K. An, Y. Hwang, J.-G. Park*, et al.*, Ultra-large-scale syntheses of monodisperse nanocrystals. *Nature materials*. 3, 891-895 (2004)
10. C. Vauthier,K. Bouchemal, Methods for the preparation and manufacture of polymeric nanoparticles. *Pharmaceutical research*. 26, 1025-1058 (2009)
11. A. D. Bangham, M. M. Standish,N. Miller, Cation permeability of phospholipid model membranes: effect of narcotics. *Nature*. 208, 1295-1297 (1965)
12. A. D. Bangham, M. M. Standish,J. C. Watkins, Diffusion of univalent ions across the lamellae of swollen phospholipids. *J Mol Biol*. 13, 238-252 (1965)
13. A. D. Bangham, M. M. Standish,G. Weissmann, The action of steroids and streptolysin S on the permeability of phospholipid structures to cations. *J Mol Biol*. 13, 253-259 (1965)
14. V. P. Torchilin, Recent advances with liposomes as pharmaceutical carriers. *Nat Rev Drug Discov*. 4, 145-160 (2005)
15. X. Y. Lu, D. C. Wu, Z. J. Li,G. Q. Chen, Polymer nanoparticles. *Prog Mol Biol Transl Sci*. 104, 299-323 (2011)
16. Y. Barenholz, Doxil(R)--the first FDA-approved nano-drug: lessons learned. *J Control Release*. 160, 117-134 (2012)
17. F. Kratz, Albumin as a drug carrier: design of prodrugs, drug conjugates and nanoparticles. *Journal of Controlled Release*. 132, 171-183 (2008)
18. J. Shi, P. W. Kantoff, R. Wooster,O. C. Farokhzad, Cancer nanomedicine: progress, challenges and opportunities. *Nature Reviews Cancer*. 17, 20-37 (2016)
19. V. Weissig, T. K. Pettinger,N. Murdock, Nanopharmaceuticals (part 1): products on the market. *Int J Nanomedicine*. 9, 4357-4373 (2014)
20. N. Bertrand,J.-C. Leroux, The journey of a drug-carrier in the body: An anatomo-physiological perspective. *Journal of Controlled Release*. 161, 152-163 (2012)
21. C. D. Mathers,D. Loncar, Projections of global mortality and burden of disease from 2002 to 2030. *PLoS Med*. 3, e442 (2006)
22. J. A. Finegold, P. Asaria,D. P. Francis, Mortality from ischaemic heart disease by country, region, and age: statistics from World Health Organisation and United Nations. *Int J Cardiol*. 168, 934-945 (2013)
23. J. F. Bentzon, F. Otsuka, R. Virmani,E. Falk, Mechanisms of plaque formation and rupture. *Circ Res*. 114, 1852-1866 (2014)
24. K. J. Moore,I. Tabas, Macrophages in the pathogenesis of atherosclerosis. *Cell*. 145, 341-355 (2011)

25. C. Silvestre-Roig, M. P. De Winther, C. Weber, M. J. Daemen*, et al.*, Atherosclerotic plaque destabilization: mechanisms, models, and therapeutic strategies. *Circ Res*. 114, 214-226 (2014)
26. C. Weber,H. Noels, Atherosclerosis: current pathogenesis and therapeutic options. *Nat Med*. 17, 1410-1422 (2011)
27. B. Furie,B. C. Furie, Mechanisms of thrombus formation. *N Engl J Med*. 359, 938-949 (2008)
28. M. Varna, M. Juenet, R. Bayles, M. Mazighi*, et al.*, Nanomedicine as a strategy to fight thrombotic diseases. *Future Science OA*. 1, (2015)
29. D. J. Hausenloy,D. M. Yellon, Myocardial ischemia-reperfusion injury: a neglected therapeutic target. *J Clin Invest*. 123, 92-100 (2013)
30. C. P. Baines, The mitochondrial permeability transition pore and ischemia-reperfusion injury. *Basic Res Cardiol*. 104, 181-188 (2009)
31. E. Bruckert,D. Rosenbaum, Lowering LDL-cholesterol through diet: potential role in the statin era. *Curr Opin Lipidol*. 22, 43-48 (2011)
32. O. S. Descamps, J. De Sutter, M. Guillaume,L. Missault, Where does the interplay between cholesterol absorption and synthesis in the context of statin and/or ezetimibe treatment stand today? *Atherosclerosis*. 217, 308-321 (2011)
33. C. Baigent, A. Keech, P. M. Kearney, L. Blackwell*, et al.*, Efficacy and safety of cholesterol-lowering treatment: prospective meta-analysis of data from 90,056 participants in 14 randomised trials of statins. *Lancet*. 366, 1267-1278 (2005)
34. K. H. Bonaa, J. Mannsverk, R. Wiseth, L. Aaberge*, et al.*, Drug-Eluting or Bare-Metal Stents for Coronary Artery Disease. *N Engl J Med*. 375, 1242-1252 (2016)
35. O. Ovchinnikova, A. Gylfe, L. Bailey, A. Nordstrom*, et al.*, Osteoprotegerin Promotes Fibrous Cap Formation in Atherosclerotic Lesions of ApoE-Deficient Mice--Brief Report. *Arteriosclerosis, Thrombosis, and Vascular Biology*. 29, 1478-1480 (2009)
36. J. S. Smolen, A. Beaulieu, A. Rubbert-Roth, C. Ramos-Remus*, et al.*, Effect of interleukin-6 receptor inhibition with tocilizumab in patients with rheumatoid arthritis (OPTION study): a double-blind, placebo-controlled, randomised trial. *The Lancet*. 371, 987-997 (2008)
37. J. Rolin,A. A. Maghazachi, Implications of chemokines, chemokine receptors, and inflammatory lipids in atherosclerosis. *Journal of Leukocyte Biology*. 95, 575-585 (2014)
38. R. Klingenberg,G. K. Hansson, Treating inflammation in atherosclerotic cardiovascular disease: emerging therapies. *European Heart Journal*. 30, 2838-2844 (2009)
39. D. Atar, H. Arheden, A. Berdeaux, J. L. Bonnet*, et al.*, Effect of intravenous TRO40303 as an adjunct to primary percutaneous coronary intervention for acute ST-elevation myocardial infarction: MITOCARE study results. *Eur Heart J*. 36, 112-119 (2015)
40. D. J. Hausenloy, H. Erik Botker, G. Condorelli, P. Ferdinandy*, et al.*, Translating cardioprotection for patient benefit: position paper from the Working Group of Cellular Biology of the Heart of the European Society of Cardiology. *Cardiovasc Res*. 98, 7-27 (2013)
41. V. Sharma, R. M. Bell,D. M. Yellon, Targeting reperfusion injury in acute myocardial infarction: a review of reperfusion injury pharmacotherapy. *Expert Opin Pharmacother*. 13, 1153-1175 (2012)
42. A. M. Gotto, Antioxidants, statins, and atherosclerosis. *Journal of the American College of Cardiology*. 41, 1205-1210 (2003)
43. S. R. Steinhubl, Why have antioxidants failed in clinical trials? *Am J Cardiol*. 101, 14D-19D (2008)
44. F. Krotz, H. Y. Sohn,V. Klauss, Antiplatelet drugs in cardiological practice: established strategies and new developments. *Vasc Health Risk Manag*. 4, 637-645 (2008)
45. W. H. De Jong, W. I. Hagens, P. Krystek, M. C. Burger*, et al.*, Particle size-dependent organ distribution of gold nanoparticles after intravenous administration. *Biomaterials*. 29, 1912-1919 (2008)
46. E. Blanco, H. Shen,M. Ferrari, Principles of nanoparticle design for overcoming biological barriers to drug delivery. *Nature biotechnology*. 33, 941-951 (2015)
47. J. A. Champion,S. Mitragotri, Role of target geometry in phagocytosis. *Proc Natl Acad Sci U S A*. 103, 4930-4934 (2006)
48. M. K. Lee, S. J. Lim,C. K. Kim, Preparation, characterization and in vitro cytotoxicity of paclitaxel-loaded sterically stabilized solid lipid nanoparticles. *Biomaterials*. 28, 2137-2146 (2007)

49. C. M. Goodman, C. D. Mccusker, T. Yilmaz,V. M. Rotello, Toxicity of gold nanoparticles functionalized with cationic and anionic side chains. *Bioconjug Chem*. 15, 897-900 (2004)
50. G. Maiorano, S. Sabella, B. Sorce, V. Brunetti*, et al.*, Effects of cell culture media on the dynamic formation of protein-nanoparticle complexes and influence on the cellular response. *ACS Nano*. 4, 7481-7491 (2010)
51. A. Albanese, P. S. Tang,W. C. Chan, The effect of nanoparticle size, shape, and surface chemistry on biological systems. *Annu Rev Biomed Eng*. 14, 1-16 (2012)
52. Z. J. Deng, M. Liang, M. Monteiro, I. Toth*, et al.*, Nanoparticle-induced unfolding of fibrinogen promotes Mac-1 receptor activation and inflammation. *Nat Nanotechnol*. 6, 39-44 (2011)
53. V. Mirshafiee, M. Mahmoudi, K. Lou, J. Cheng*, et al.*, Protein corona significantly reduces active targeting yield. *Chem Commun (Camb)*. 49, 2557-2559 (2013)
54. A. Salvati, A. S. Pitek, M. P. Monopoli, K. Prapainop*, et al.*, Transferrin-functionalized nanoparticles lose their targeting capabilities when a biomolecule corona adsorbs on the surface. *Nat Nanotechnol*. 8, 137-143 (2013)
55. C. Corbo, R. Molinaro, A. Parodi, N. E. Toledano Furman*, et al.*, The impact of nanoparticle protein corona on cytotoxicity, immunotoxicity and target drug delivery. *Nanomedicine (Lond)*. 11, 81-100 (2016)
56. C. C. Fleischer,C. K. Payne, Nanoparticle-cell interactions: molecular structure of the protein corona and cellular outcomes. *Acc Chem Res*. 47, 2651-2659 (2014)
57. R. M. Pearson, V. V. Juettner,S. Hong, Biomolecular corona on nanoparticles: a survey of recent literature and its implications in targeted drug delivery. *Front Chem*. 2, 108 (2014)
58. A. S. Karakoti, S. Das, S. Thevuthasan,S. Seal, PEGylated inorganic nanoparticles. *Angew Chem Int Ed Engl*. 50, 1980-1994 (2011)
59. R. Mathaes, G. Winter, A. Besheer,J. Engert, Influence of particle geometry and PEGylation on phagocytosis of particulate carriers. *International Journal of Pharmaceutics*. 465, 159-164 (2014)
60. S. Schottler, G. Becker, S. Winzen, T. Steinbach*, et al.*, Protein adsorption is required for stealth effect of poly(ethylene glycol)- and poly(phosphoester)-coated nanocarriers. *Nat Nanotechnol*. 11, 372-377 (2016)
61. C. D. Walkey, J. B. Olsen, H. Guo, A. Emili*, et al.*, Nanoparticle size and surface chemistry determine serum protein adsorption and macrophage uptake. *J Am Chem Soc*. 134, 2139-2147 (2012)
62. G. Engstrom, P. Lind, B. Hedblad, L. Stavenow*, et al.*, Effects of cholesterol and inflammation-sensitive plasma proteins on incidence of myocardial infarction and stroke in men. *Circulation*. 105, 2632-2637 (2002)
63. M. I. Setyawati, C. Y. Tay, D. Docter, R. H. Stauber*, et al.*, Understanding and exploiting nanoparticles' intimacy with the blood vessel and blood. *Chem Soc Rev*. 44, 8174-8199 (2015)
64. V. Colapicchioni, M. Tilio, L. Digiacomo, V. Gambini*, et al.*, Personalized liposome-protein corona in the blood of breast, gastric and pancreatic cancer patients. *Int J Biochem Cell Biol*. 75, 180-187 (2016)
65. P. Libby, P. M. Ridker,G. K. Hansson, Inflammation in Atherosclerosis. *Journal of the American College of Cardiology*. 54, 2129-2138 (2009)
66. P. R. Moreno, Neovascularization in Human Atherosclerosis. *Circulation*. 113, 2245-2252 (2006)
67. B. L. Chung, M. J. Toth, N. Kamaly, Y. J. Sei*, et al.*, Nanomedicines for Endothelial Disorders. *Nano Today*. 10, 759-776 (2015)
68. J. Fang, H. Nakamura,H. Maeda, The EPR effect: Unique features of tumor blood vessels for drug delivery, factors involved, and limitations and augmentation of the effect. *Advanced Drug Delivery Reviews*. 63, 136-151 (2011)
69. T. Geelen, L. E. Paulis, B. F. Coolen, K. Nicolay*, et al.*, Passive targeting of lipid-based nanoparticles to mouse cardiac ischemia-reperfusion injury. *Contrast Media Mol Imaging*. 8, 117-126 (2013)
70. A. N. Lukyanov, W. C. Hartner,V. P. Torchilin, Increased accumulation of PEG-PE micelles in the area of experimental myocardial infarction in rabbits. *J Control Release*. 94, 187-193 (2004)
71. P. Couvreur, Nanoparticles in drug delivery: Past, present and future. *Advanced Drug Delivery Reviews*. 65, 21-23 (2013)
72. S. I. Cameron W Evans,Hool, The potential for nanotechnology to improve delivery of therapy to the acute ischemic heart. *Nanomedicine*. (2016)

73. H. Maeda, K. Tsukigawa,J. Fang, A Retrospective 30 Years After Discovery of the Enhanced Permeability and Retention Effect of Solid Tumors: Next-Generation Chemotherapeutics and Photodynamic Therapy—Problems, Solutions, and Prospects. *Microcirculation*. 23, 173-182 (2016)
74. M. E. Lobatto, V. Fuster, Z. A. Fayad,W. J. Mulder, Perspectives and opportunities for nanomedicine in the management of atherosclerosis. *Nat Rev Drug Discov*. 10, 835-852 (2011)
75. Y. Matsumoto, J. W. Nichols, K. Toh, T. Nomoto*, et al.*, Vascular bursts enhance permeability of tumour blood vessels and improve nanoparticle delivery. *Nature Nanotechnology*. 11, 533-538 (2016)
76. C. K. Kim, T. Kim, I. Y. Choi, M. Soh*, et al.*, Ceria nanoparticles that can protect against ischemic stroke. *Angew Chem Int Ed Engl*. 51, 11039-11043 (2012)
77. J. Kreuter, Drug delivery to the central nervous system by polymeric nanoparticles: what do we know? *Adv Drug Deliv Rev*. 71, 2-14 (2014)
78. H. L. Wong, X. Y. Wu,R. Bendayan, Nanotechnological advances for the delivery of CNS therapeutics. *Adv Drug Deliv Rev*. 64, 686-700 (2012)
79. U. Flogel, Z. Ding, H. Hardung, S. Jander*, et al.*, In Vivo Monitoring of Inflammation After Cardiac and Cerebral Ischemia by Fluorine Magnetic Resonance Imaging. *Circulation*. 118, 140-148 (2008)
80. D. B. Kirpotin, Antibody Targeting of Long-Circulating Lipidic Nanoparticles Does Not Increase Tumor Localization but Does Increase Internalization in Animal Models. *Cancer Research*. 66, 6732-6740 (2006)
81. S. Blankenberg, S. Barbaux,L. Tiret, Adhesion molecules and atherosclerosis. *Atherosclerosis*. 170, 191-203 (2003)
82. M. Nahrendorf, F. A. Jaffer, K. A. Kelly, D. E. Sosnovik*, et al.*, Noninvasive Vascular Cell Adhesion Molecule-1 Imaging Identifies Inflammatory Activation of Cells in Atherosclerosis. *Circulation*. 114, 1504-1511 (2006)
83. M. I. Cybulsky, K. Iiyama, H. Li, S. Zhu*, et al.*, A major role for VCAM-1, but not ICAM-1, in early atherosclerosis. *J Clin Invest*. 107, 1255-1262 (2001)
84. W. J. M. Mulder, G. J. Strijkers, K. C. Briley-Saboe, J. C. Frias*, et al.*, Molecular imaging of macrophages in atherosclerotic plaques using bimodal PEG-micelles. *Magnetic Resonance in Medicine*. 58, 1164-1170 (2007)
85. V. Amirbekian, M. J. Lipinski, K. C. Briley-Saebo, S. Amirbekian*, et al.*, Detecting and assessing macrophagesin vivoto evaluate atherosclerosis noninvasively using molecular MRI. *Proceedings of the National Academy of Sciences*. 104, 961-966 (2007)
86. J. M. Chan, L. Zhang, R. Tong, D. Ghosh*, et al.*, Spatiotemporal controlled delivery of nanoparticles to injured vasculature. *Proceedings of the National Academy of Sciences*. 107, 2213-2218 (2010)
87. X. X. Sun, W. Li, X. W. Zhang, M. Qi*, et al.*, In Vivo Targeting and Imaging of Atherosclerosis Using Multifunctional Virus-Like Particles of Simian Virus 40. *Nano Letters*. 16, 6164-6171 (2016)
88. H. Kawata, Y. Uesugi, T. Soeda, Y. Takemoto*, et al.*, A new drug delivery system for intravenous coronary thrombolysis with thrombus targeting and stealth activity recoverable by ultrasound. *J Am Coll Cardiol*. 60, 2550-2557 (2012)
89. M. Liu, M. Li, S. Sun, B. Li*, et al.*, The use of antibody modified liposomes loaded with AMO-1 to deliver oligonucleotides to ischemic myocardium for arrhythmia therapy. *Biomaterials*. 35, 3697-3707 (2014)
90. L. Zhang, J. A. Hoffman,E. Ruoslahti, Molecular profiling of heart endothelial cells. *Circulation*. 112, 1601-1611 (2005)
91. S. Kanki, D. E. Jaalouk, S. Lee, A. Y. Yu*, et al.*, Identification of targeting peptides for ischemic myocardium by in vivo phage display. *J Mol Cell Cardiol*. 50, 841-848 (2011)
92. H. Zhang, N. Li, P. Sirish, L. Mahakian*, et al.*, The cargo of CRPPR-conjugated liposomes crosses the intact murine cardiac endothelium. *J Control Release*. 163, 10-17 (2012)
93. Y. W. Won, A. N. Mcginn, M. Lee, D. A. Bull*, et al.*, Targeted gene delivery to ischemic myocardium by homing peptide-guided polymeric carrier. *Mol Pharm*. 10, 378-385 (2013)
94. C. P. Cannon, B. A. Steinberg, S. A. Murphy, J. L. Mega*, et al.*, Meta-Analysis of Cardiovascular Outcomes Trials Comparing Intensive Versus Moderate Statin Therapy. *Journal of the American College of Cardiology*. 48, 438-445 (2006)

95. R. Collins, C. Reith, J. Emberson, J. Armitage*, et al.*, Interpretation of the evidence for the efficacy and safety of statin therapy. *Lancet*. 388, 2532-2561 (2016)
96. M. S. Hamza, C. Kumar, S. M. Chia, V. Anandalakshmi*, et al.*, Alterations in the hepatic transcriptional landscape after RNAi mediated ApoB silencing in cynomolgus monkeys. *Atherosclerosis*. 242, 383-395 (2015)
97. T. S. Zimmermann, A. C. H. Lee, A. Akinc, B. Bramlage*, et al.*, RNAi-mediated gene silencing in non-human primates. *Nature*. 441, 111-114 (2006)
98. D. Semizarov, L. Frost, A. Sarthy, P. Kroeger*, et al.*, Specificity of short interfering RNA determined through gene expression signatures. *Proceedings of the National Academy of Sciences*. 100, 6347-6352 (2003)
99. I. Dunham, A. Kundaje, S. F. Aldred, P. J. Collins*, et al.*, An integrated encyclopedia of DNA elements in the human genome. *Nature*. 489, 57-74 (2012)
100. J. F. Gohy,Y. Zhao, Photo-responsive block copolymer micelles: design and behavior. *Chem Soc Rev*. 42, 7117-7129 (2013)
101. J. M. Williford, J. Wu, Y. Ren, M. M. Archang*, et al.*, Recent advances in nanoparticle-mediated siRNA delivery. *Annu Rev Biomed Eng*. 16, 347-370 (2014)
102. H. J. Kim, A. Kim, K. Miyata,K. Kataoka, Recent progress in development of siRNA delivery vehicles for cancer therapy. *Adv Drug Deliv Rev*. 104, 61-77 (2016)
103. D. Urban, J. Pöss, M. Böhm,U. Laufs, Targeting the Proprotein Convertase Subtilisin/Kexin Type 9 for the Treatment of Dyslipidemia and Atherosclerosis. *Journal of the American College of Cardiology*. 62, 1401-1408 (2013)
104. M. Frank-Kamenetsky, A. Grefhorst, N. N. Anderson, T. S. Racie*, et al.*, Therapeutic RNAi targeting PCSK9 acutely lowers plasma cholesterol in rodents and LDL cholesterol in nonhuman primates. *Proceedings of the National Academy of Sciences*. 105, 11915-11920 (2008)
105. K. Fitzgerald, M. Frank-Kamenetsky, S. Shulga-Morskaya, A. Liebow*, et al.*, Effect of an RNA interference drug on the synthesis of proprotein convertase subtilisin/kexin type 9 (PCSK9) and the concentration of serum LDL cholesterol in healthy volunteers: a randomised, single-blind, placebo-controlled, phase 1 trial. *The Lancet*. 383, 60-68 (2014)
106. H. Wang, J. Wang, X. Deng, H. Sun*, et al.*, Biodistribution of carbon single-wall carbon nanotubes in mice. *J Nanosci Nanotechnol*. 4, 1019-1024 (2004)
107. J. J. Badimon, L. Badimon,V. Fuster, Regression of atherosclerotic lesions by high density lipoprotein plasma fraction in the cholesterol-fed rabbit. *J Clin Invest*. 85, 1234-1241 (1990)
108. J. J. Badimon, L. Badimon, A. Galvez, R. Dische*, et al.*, High density lipoprotein plasma fractions inhibit aortic fatty streaks in cholesterol-fed rabbits. *Lab Invest*. 60, 455-461 (1989)
109. S. E. Nissen, T. Tsunoda, E. M. Tuzcu, P. Schoenhagen*, et al.*, Effect of recombinant ApoA-I Milano on coronary atherosclerosis in patients with acute coronary syndromes: a randomized controlled trial. *JAMA*. 290, 2292-2300 (2003)
110. B. L. Sanchez-Gaytan, F. Fay, M. E. Lobatto, J. Tang*, et al.*, HDL-Mimetic PLGA Nanoparticle To Target Atherosclerosis Plaque Macrophages. *Bioconjugate Chemistry*. 26, 443-451 (2015)
111. A. J. Murphy, S. Funt, D. Gorman, A. R. Tall*, et al.*, Pegylation of High-Density Lipoprotein Decreases Plasma Clearance and Enhances Antiatherogenic Activity. *Circulation Research*. 113, e1-e9 (2013)
112. M. Back, C. Weber,E. Lutgens, Regulation of atherosclerotic plaque inflammation. *J Intern Med*. 278, 462-482 (2015)
113. P. M. Ridker,T. F. Luscher, Anti-inflammatory therapies for cardiovascular disease. *Eur Heart J*. 35, 1782-1791 (2014)
114. F. K. Swirski, M. Nahrendorf, M. Etzrodt, M. Wildgruber*, et al.*, Identification of Splenic Reservoir Monocytes and Their Deployment to Inflammatory Sites. *Science*. 325, 612-616 (2009)
115. F. Leuschner, P. Dutta, R. Gorbatov, T. I. Novobrantseva*, et al.*, Therapeutic siRNA silencing in inflammatory monocytes in mice. *Nature Biotechnology*. 29, 1005-1010 (2011)
116. M. E. J. K. Maulik D. Majmudar, Phd; Timo Heidt, Md; Florian Leuschner, Md;, B. B. F. S. Jessica Truelove, Bs; Rostic Gorbatov, Bs; Yoshiko Iwamoto, Bs; Partha Dutta, Phd;, M. G. C. Gregory Wojtkiewicz, Phd; Matt Sebas, Bs; Anna Borodovsky, Phd;, P. M. W. N. Kevin Fitzgerald, Phd; Gerhard

Dickneite, Phd;*, et al.*, Monocyte-Directed RNAi Targeting CCR2 Improves Infarct Healing in Atherosclerosis-Prone Mice. *Circulation*. (2013)

117. Manuela Calin A, Daniela Stan a, Martin Schlesinger B, Viorel Simion a, Mariana Deleanu, Cristina Ana Constantinescu a, Ana-Maria Gana, Monica Madalina Pirvulescu a, Elena Butoi, Ileana Manduteanua, Marian Bota C, Marius Enachescu C, Lubor Borsig D, Gerd Bendas B, Maya Simionescu, VCAM-1 directed target-sensitive liposomes carrying CCR2 antagonists bind to activated endothelium and reduce adhesion and transmigration of monocytes.pdf. *European Journal of Pharmateucis and Biopharmaceutics*. (2015)
118. Z. M. Dong, S. M. Chapman, A. A. Brown, P. S. Frenette*, et al.*, The combined role of P- and E-selectins in atherosclerosis. *J Clin Invest*. 102, 145-152 (1998)
119. J. E. Dahlman, C. Barnes, O. F. Khan, A. Thiriot*, et al.*, In vivo endothelial siRNA delivery using polymeric nanoparticles with low molecular weight. *Nat Nanotechnol*. 9, 648-655 (2014)
120. H. B. Sager, P. Dutta, J. E. Dahlman, M. Hulsmans*, et al.*, RNAi targeting multiple cell adhesion molecules reduces immune cell recruitment and vascular inflammation after myocardial infarction. *Science Translational Medicine*. 8, 11 (2016)
121. S. Steffens,F. Mach, Drug Insight: immunomodulatory effects of statins—potential benefits for renal patients? *Nature Clinical Practice Nephrology*. 2, 378-387 (2006)
122. D. X. Bu, G. Griffin,A. H. Lichtman, Mechanisms for the anti-inflammatory effects of statins. *Curr Opin Lipidol*. 22, 165-170 (2011)
123. R. Duivenvoorden, J. Tang, D. P. Cormode, A. J. Mieszawska*, et al.*, A statin-loaded reconstituted high-density lipoprotein nanoparticle inhibits atherosclerotic plaque inflammation. *Nat Commun*. 5, 3065 (2014)
124. Jun Tang, 2 Mark E. Lobatto,1,3 Laurien Hassing,1,3 Susanne Van Der Staay,1,3, Sarian M. Van Rijs, 3 Claudia Calcagno,1 Mounia S. Braza,1 Samantha Baxter,1, B. L. S.-G. Francois Fay, 1 Raphaël Duivenvoorden,3 Hendrik B. Sager,4, W. L. Yaritzy M. Astudillo, 1,2 Sarayu Ramachandran,1 Gert Storm,6,7 Carlos Pérez-Medina,1*, et al.*, <Inhibiting macrophage proliferation suppresses atherosclerotic plaque inflammation.pdf>. *Science Advances* (2015)
125. S. Katsuki, T. Matoba, S. Nakashiro, K. Sato*, et al.*, Nanoparticle-Mediated Delivery of Pitavastatin Inhibits Atherosclerotic Plaque Destabilization/Rupture in Mice by Regulating the Recruitment of Inflammatory Monocytes. *Circulation*. 129, 896-906 (2013)
126. K. Nagaoka, T. Matoba, Y. Mao, Y. Nakano*, et al.*, A New Therapeutic Modality for Acute Myocardial Infarction: Nanoparticle-Mediated Delivery of Pitavastatin Induces Cardioprotection from Ischemia-Reperfusion Injury via Activation of PI3K/Akt Pathway and Anti-Inflammation in a Rat Model. *PLoS One*. 10, e0132451 (2015)
127. P. J. Barnes, Glucocorticosteroids: current and future directions. *Br J Pharmacol*. 163, 29-43 (2011)
128. S. Chono, Y. Tauchi, Y. Deguchi,K. Morimoto, Efficient drug delivery to atherosclerotic lesions and the antiatherosclerotic effect by dexamethasone incorporated into liposomes in atherogenic mice. *Journal of drug targeting*. 13, 267-276 (2005)
129. Z. a. F. Mark E. Lobatto, *,† Stephane Silvera,† Esad Vucic,†, V. M. Claudia Calcagno, † Stephen D. Dickson,† Klaas Nicolay,‡, R. M. S. Manuela Banciu, § Josbert M. Metselaar,§ Louis Van, H.-S. W. Bloois, | John T. Fallon,| James H. Rudd,†,⊥ Valentin Fuster,#,∇*, et al.*, Multimodal Clinical Imaging To Longitudinally Assess a Nanomedical Anti-Inflammatory Treatment in Experimental Atherosclerosis.pdf. *Molecular Pharmaceutics*. (2010)
130. J. Koga, T. Matoba,K. Egashira, Anti-inflammatory Nanoparticle for Prevention of Atherosclerotic Vascular Diseases. *J Atheroscler Thromb*. 23, 757-765 (2016)
131. B. Christian J. Kastrupa, Matthias Nahrendorfc, Jose Luiz Figueiredoc, Haeshin Leed, Swetha Kambhampatia,, S.-W. C. Timothy Leea, Rostic Gorbatovc, Yoshiko Iwamotoc, Tram T. Danga, Partha Duttac, Ju Hun Yeonb,, F. Hao Chenga, Christopher D. Pritcharda, Arturo J. Vegasa, Cory D. Siegelc, Samantha Macdougalla, Michael Okonkwoa,,J. R. S. Anh Thaia, Arthur J. Couryh, Ralph Weisslederc, Robert Langera,I,1, and Daniel G. Andersona,I, <Painting blood vessels and atherosclerotic plaques with an adhesive drug depot.pdf>. *Proc Natl Acad Sci U S A*. (2012)

132. A. Ortega-Gómez, M. Perretti,O. Soehnlein, Resolution of inflammation: an integrated view. *EMBO Molecular Medicine*. 5, 661-674 (2013)
133. L. V. Norling, M. Spite, R. Yang, R. J. Flower*, et al.*, Cutting Edge: Humanized Nano-Proresolving Medicines Mimic Inflammation-Resolution and Enhance Wound Healing. *The Journal of Immunology*. 186, 5543-5547 (2011)
134. I. Tabas,C. K. Glass, Anti-Inflammatory Therapy in Chronic Disease: Challenges and Opportunities. *Science*. 339, 166-172 (2013)
135. M. A. Sugimoto, J. P. Vago, M. M. Teixeira,L. P. Sousa, Annexin A1 and the Resolution of Inflammation: Modulation of Neutrophil Recruitment, Apoptosis, and Clearance. *Journal of Immunology Research*. 2016, 1-13 (2016)
136. G. F. Nazila Kamaly, Manikandan Subramanianb, Suresh Gaddea, Aleksandar Pesica, Louis Cheunga,,R. L. Zahi Adel Fayadc, Ira Tabas, and Omid Cameron Farokhzad, Development and in vivo efficacy of targeted polymeric inflammation-resolving nanoparticles.pdf. *Proc Natl Acad Sci U S A*. (2013

)
137. G. Fredman, N. Kamaly, S. Spolitu, J. Milton*, et al.*, Targeted nanoparticles containing the proresolving peptide Ac2-26 protect against advanced atherosclerosis in hypercholesterolemic mice. *Science Translational Medicine*. 7, 275ra220-275ra220 (2015)
138. N. Kamaly, G. Fredman, J. J. R. Fojas, M. Subramanian*, et al.*, Targeted Interleukin-10 Nanotherapeutics Developed with a Microfluidic Chip Enhance Resolution of Inflammation in Advanced Atherosclerosis. *ACS Nano*. 10, 5280-5292 (2016)
139. T. Kawamura, N. Nara, M. Kadosaki, K. Inada*, et al.*, Prostaglandin E1 reduces myocardial reperfusion injury by inhibiting proinflammatory cytokines production during cardiac surgery. *Crit Care Med*. 28, 2201-2208 (2000)
140. S. Feld, G. Li, A. Wu, P. Felli*, et al.*, Reduction of canine infarct size by bolus intravenous administration of liposomal prostaglandin E1: comparison with control, placebo liposomes, and continuous intravenous infusion of prostaglandin E1. *Am Heart J*. 132, 747-757 (1996)
141. J. H. Li, P. Yang, A. L. Li, Y. Wang*, et al.*, Cardioprotective effect of liposomal prostaglandin E1 on a porcine model of myocardial infarction reperfusion no-reflow. *J Zhejiang Univ Sci B*. 12, 638-643 (2011)
142. L. Y. Wei, X. H. Fu, W. Li, X. L. Bi*, et al.*, Effect of Intravenous Administration of Liposomal Prostaglandin E1 on Microcirculation in Patients with ST Elevation Myocardial Infarction Undergoing Primary Percutaneous Intervention. *Chin Med J (Engl)*. 128, 1147-1150 (2015)
143. P. Van Der Meer, E. Lipsic, R. H. Henning, K. Boddeus*, et al.*, Erythropoietin induces neovascularization and improves cardiac function in rats with heart failure after myocardial infarction. *J Am Coll Cardiol*. 46, 125-133 (2005)
144. C. Moon, M. Krawczyk, D. Paik, E. G. Lakatta*, et al.*, Cardioprotection by recombinant human erythropoietin following acute experimental myocardial infarction: dose response and therapeutic window. *Cardiovasc Drugs Ther*. 19, 243-250 (2005)
145. I. Ott, S. Schulz, J. Mehilli, S. Fichtner*, et al.*, Erythropoietin in patients with acute ST-segment elevation myocardial infarction undergoing primary percutaneous coronary intervention: a randomized, double-blind trial. *Circ Cardiovasc Interv*. 3, 408-413 (2010)
146. S. S. Najjar, S. V. Rao, C. Melloni, S. V. Raman*, et al.*, Intravenous erythropoietin in patients with ST-segment elevation myocardial infarction: REVEAL: a randomized controlled trial. *JAMA*. 305, 1863-1872 (2011)
147. F. Prunier, L. Biere, M. Gilard, J. Boschat*, et al.*, Single high-dose erythropoietin administration immediately after reperfusion in patients with ST-segment elevation myocardial infarction: results of the erythropoietin in myocardial infarction trial. *Am Heart J*. 163, 200-207 e201 (2012)
148. Y. Yamada, H. Kobayashi, M. Iwasa, S. Sumi*, et al.*, Postinfarct active cardiac-targeted delivery of erythropoietin by liposomes with sialyl Lewis X repairs infarcted myocardium in rabbits. *Am J Physiol Heart Circ Physiol*. 304, H1124-1133 (2013)

149. T. Harel-Adar, T. Ben Mordechai, Y. Amsalem, M. S. Feinberg*, et al.*, Modulation of cardiac macrophages by phosphatidylserine-presenting liposomes improves infarct repair. *Proc Natl Acad Sci U S A*. 108, 1827-1832 (2011)
150. S. T. S. E. a. M. I. O. T. E. S. O. C. Task Force on the Management Of, P. G. Steg, S. K. James, D. Atar*, et al.*, ESC Guidelines for the management of acute myocardial infarction in patients presenting with ST-segment elevation. *Eur Heart J*. 33, 2569-2619 (2012)
151. G. De Luca, H. Suryapranata,P. Marino, Reperfusion strategies in acute ST-elevation myocardial infarction: an overview of current status. *Prog Cardiovasc Dis*. 50, 352-382 (2008)
152. Y. M. Fortenberry, Plasminogen activator inhibitor-1 inhibitors: a patent review (2006-present). *Expert Opin Ther Pat*. 23, 801-815 (2013)
153. B. Van De Craen, P. J. Declerck,A. Gils, The Biochemistry, Physiology and Pathological roles of PAI-1 and the requirements for PAI-1 inhibition in vivo. *Thromb Res*. 130, 576-585 (2012)
154. J. C. Copin, D. J. Bengualid, R. F. Da Silva, O. Kargiotis*, et al.*, Recombinant tissue plasminogen activator induces blood-brain barrier breakdown by a matrix metalloproteinase-9-independent pathway after transient focal cerebral ischemia in mouse. *Eur J Neurosci*. 34, 1085-1092 (2011)
155. V. J. Caride,B. L. Zaret, Liposome accumulation in regions of experimental myocardial infarction. *Science*. 198, 735-738 (1977)
156. T. M. Mueller, M. L. Marcus, H. E. Mayer, J. K. Williams*, et al.*, Liposome concentration in canine ischemic myocardium and depolarized myocardial cells. *Circ Res*. 49, 405-415 (1981)
157. O. R. E. Nguyen P, Johnson a, Patterson E,,A. B. R. Whitsett T, Accelerated Thrombolysis and Reperfusion in a Canine Model of Myocardial Infarction by Liposomal Encapsulation of Streptokinase. *Circulation Research* 66, 875-878 (1990)
158. A. C. Silva, C. M. Lopes, J. M. Lobo,M. H. Amaral, Delivery Systems for Biopharmaceuticals. Part I: Nanoparticles and Microparticles. *Curr Pharm Biotechnol*. 16, 940-954 (2015)
159. J. K. Leach, E. Patterson,E. A. O'rear, Encapsulation of a plasminogen activator speeds reperfusion, lessens infarct and reduces blood loss in a canine model of coronary artery thrombosis. *Thromb Haemost*. 91, 1213-1218 (2004)
160. H. J. Jin, H. Zhang, M. L. Sun, B. G. Zhang*, et al.*, Urokinase-coated chitosan nanoparticles for thrombolytic therapy: preparation and pharmacodynamics in vivo. *J Thromb Thrombolysis*. 36, 458-468 (2013)
161. B. Vaidya, G. P. Agrawal,S. P. Vyas, Platelets directed liposomes for the delivery of streptokinase: development and characterization. *Eur J Pharm Sci*. 44, 589-594 (2011)
162. S. Absar, K. Nahar, Y. M. Kwon,F. Ahsan, Thrombus-targeted nanocarrier attenuates bleeding complications associated with conventional thrombolytic therapy. *Pharm Res*. 30, 1663-1676 (2013)
163. J. Zhou, D. Guo, Y. Zhang, W. Wu*, et al.*, Construction and evaluation of Fe(3)O(4)-based PLGA nanoparticles carrying rtPA used in the detection of thrombosis and in targeted thrombolysis. *ACS Appl Mater Interfaces*. 6, 5566-5576 (2014)
164. Y. Uesugi, H. Kawata, Y. Saito,Y. Tabata, Ultrasound-responsive thrombus treatment with zinc-stabilized gelatin nano-complexes of tissue-type plasminogen activator. *J Drug Target*. 20, 224-234 (2012)
165. A. V. Alexandrov, Ultrasound identification and lysis of clots. *Stroke*. 35, 2722-2725 (2004)
166. Y. H. Ma, S. Y. Wu, T. Wu, Y. J. Chang*, et al.*, Magnetically targeted thrombolysis with recombinant tissue plasminogen activator bound to polyacrylic acid-coated nanoparticles. *Biomaterials*. 30, 3343-3351 (2009)
167. H. W. Yang, M. Y. Hua, K. J. Lin, S. P. Wey*, et al.*, Bioconjugation of recombinant tissue plasminogen activator to magnetic nanocarriers for targeted thrombolysis. *Int J Nanomedicine*. 7, 5159-5173 (2012)
168. J. P. Chen, P. C. Yang, Y. H. Ma,T. Wu, Characterization of chitosan magnetic nanoparticles for in situ delivery of tissue plasminogen activator. *Carbohydrate Polymers*. 84, 364-372 (2011)
169. S. D. Caruthers, T. Cyrus, P. M. Winter, S. A. Wickline*, et al.*, Anti-angiogenic perfluorocarbon nanoparticles for diagnosis and treatment of atherosclerosis. *Wiley Interdiscip Rev Nanomed Nanobiotechnol*. 1, 311-323 (2009)

170. P. M. Winter, A. M. Neubauer, S. D. Caruthers, T. D. Harris*, et al.*, Endothelial alpha(v)beta3 integrin-targeted fumagillin nanoparticles inhibit angiogenesis in atherosclerosis. *Arterioscler Thromb Vasc Biol*. 26, 2103-2109 (2006)
171. M. Koutouzis, A. Nomikos, S. Nikolidakis, V. Tzavara*, et al.*, Statin treated patients have reduced intraplaque angiogenesis in carotid endarterectomy specimens. *Atherosclerosis*. 192, 457-463 (2007)
172. P. M. Winter, S. D. Caruthers, H. Zhang, T. A. Williams*, et al.*, Antiangiogenic synergism of integrin-targeted fumagillin nanoparticles and atorvastatin in atherosclerosis. *JACC Cardiovasc Imaging*. 1, 624-634 (2008)
173. J. T. Sutton, K. J. Haworth, S. K. Shanmukhappa, M. R. Moody*, et al.*, Delivery of bevacizumab to atheromatous porcine carotid tissue using echogenic liposomes. *Drug Deliv*. 23, 3594-3605 (2016)
174. C. Cochain, K. M. Channon,J. S. Silvestre, Angiogenesis in the infarcted myocardium. *Antioxid Redox Signal*. 18, 1100-1113 (2013)
175. T. D. Henry, B. H. Annex, G. R. Mckendall, M. A. Azrin*, et al.*, The VIVA trial: Vascular endothelial growth factor in Ischemia for Vascular Angiogenesis. *Circulation*. 107, 1359-1365 (2003)
176. S. E. Epstein, R. Kornowski, S. Fuchs,H. F. Dvorak, Angiogenesis therapy: amidst the hype, the neglected potential for serious side effects. *Circulation*. 104, 115-119 (2001)
177. S. Yla-Herttuala, T. T. Rissanen, I. Vajanto,J. Hartikainen, Vascular endothelial growth factors: biology and current status of clinical applications in cardiovascular medicine. *J Am Coll Cardiol*. 49, 1015-1026 (2007)
178. S. M. Jay,R. T. Lee, Protein engineering for cardiovascular therapeutics: untapped potential for cardiac repair. *Circ Res*. 113, 933-943 (2013)
179. M. Simons,J. A. Ware, Therapeutic angiogenesis in cardiovascular disease. *Nat Rev Drug Discov*. 2, 863-871 (2003)
180. D. W. Losordo, P. R. Vale, R. C. Hendel, C. E. Milliken*, et al.*, Phase 1/2 placebo-controlled, double-blind, dose-escalating trial of myocardial vascular endothelial growth factor 2 gene transfer by catheter delivery in patients with chronic myocardial ischemia. *Circulation*. 105, 2012-2018 (2002)
181. P. R. Vale, D. W. Losordo, C. E. Milliken, M. Maysky*, et al.*, Left ventricular electromechanical mapping to assess efficacy of phVEGF(165) gene transfer for therapeutic angiogenesis in chronic myocardial ischemia. *Circulation*. 102, 965-974 (2000)
182. R. C. Scott, J. M. Rosano, Z. Ivanov, B. Wang*, et al.*, Targeting VEGF-encapsulated immunoliposomes to MI heart improves vascularity and cardiac function. *FASEB J*. 23, 3361-3367 (2009)
183. K. S. Oh, J. Y. Song, S. J. Yoon, Y. Park*, et al.*, Temperature-induced gel formation of core/shell nanoparticles for the regeneration of ischemic heart. *J Control Release*. 146, 207-211 (2010)
184. H. Iwasaki, A. Kawamoto, M. Tjwa, M. Horii*, et al.*, PlGF repairs myocardial ischemia through mechanisms of angiogenesis, cardioprotection and recruitment of myo-angiogenic competent marrow progenitors. *PLoS One*. 6, e24872 (2011)
185. N. Beohar, J. Rapp, S. Pandya,D. W. Losordo, Rebuilding the damaged heart: the potential of cytokines and growth factors in the treatment of ischemic heart disease. *J Am Coll Cardiol*. 56, 1287-1297 (2010)
186. Z. M. Binsalamah, A. Paul, A. A. Khan, S. Prakash*, et al.*, Intramyocardial sustained delivery of placental growth factor using nanoparticles as a vehicle for delivery in the rat infarct model. *Int J Nanomedicine*. 6, 2667-2678 (2011)
187. Z. X. Lu, L. L. Mao, F. Lian, J. He*, et al.*, Cardioprotective activity of placental growth factor in a rat model of acute myocardial infarction: nanoparticle-based delivery versus direct myocardial injection. *BMC Cardiovasc Disord*. 14, 53 (2014)
188. R. Troncoso, C. Ibarra, J. M. Vicencio, E. Jaimovich*, et al.*, New insights into IGF-1 signaling in the heart. *Trends Endocrinol Metab*. 25, 128-137 (2014)
189. M. Y. Chang, Y. J. Yang, C. H. Chang, A. C. Tang*, et al.*, Functionalized nanoparticles provide early cardioprotection after acute myocardial infarction. *J Control Release*. 170, 287-294 (2013)
190. M. E. Davis, J. P. Motion, D. A. Narmoneva, T. Takahashi*, et al.*, Injectable self-assembling peptide nanofibers create intramyocardial microenvironments for endothelial cells. *Circulation*. 111, 442-450 (2005)

191. S. Zhang, Fabrication of novel biomaterials through molecular self-assembly. *Nat Biotechnol*. 21, 1171-1178 (2003)
192. P. C. Hsieh, M. E. Davis, J. Gannon, C. Macgillivray*, et al.*, Controlled delivery of PDGF-BB for myocardial protection using injectable self-assembling peptide nanofibers. *J Clin Invest*. 116, 237-248 (2006)
193. H. D. Guo, G. H. Cui, J. J. Yang, C. Wang*, et al.*, Sustained delivery of VEGF from designer self-assembling peptides improves cardiac function after myocardial infarction. *Biochem Biophys Res Commun*. 424, 105-111 (2012)
194. Y. D. Lin, C. Y. Luo, Y. N. Hu, M. L. Yeh*, et al.*, Instructive nanofiber scaffolds with VEGF create a microenvironment for arteriogenesis and cardiac repair. *Sci Transl Med*. 4, 146ra109 (2012)
195. H. Yin, R. L. Kanasty, A. A. Eltoukhy, A. J. Vegas*, et al.*, Non-viral vectors for gene-based therapy. *Nat Rev Genet*. 15, 541-555 (2014)
196. Y. Zhang, W. Li, L. Ou, W. Wang*, et al.*, Targeted delivery of human VEGF gene via complexes of magnetic nanoparticle-adenoviral vectors enhanced cardiac regeneration. *PLoS One*. 7, e39490 (2012)
197. J. W. Yockman, A. Kastenmeier, H. M. Erickson, J. G. Brumbach*, et al.*, Novel polymer carriers and gene constructs for treatment of myocardial ischemia and infarction. *J Control Release*. 132, 260-266 (2008)
198. M. Y. Rincon, T. Vandendriessche,M. K. Chuah, Gene therapy for cardiovascular disease: advances in vector development, targeting, and delivery for clinical translation. *Cardiovasc Res*. 108, 4-20 (2015)
199. F. Yi, H. Wu,G. L. Jia, Formulation and characterization of poly (D,L-lactide-co-glycolide) nanoparticle containing vascular endothelial growth factor for gene delivery. *J Clin Pharm Ther*. 31, 43-48 (2006)
200. A. Paul, A. Hasan, H. A. Kindi, A. K. Gaharwar*, et al.*, Injectable graphene oxide/hydrogel-based angiogenic gene delivery system for vasculogenesis and cardiac repair. *ACS Nano*. 8, 8050-8062 (2014)
201. K. Goszcz, S. J. Deakin, G. G. Duthie, D. Stewart*, et al.*, Antioxidants in Cardiovascular Therapy: Panacea or False Hope? *Front Cardiovasc Med*. 2, 29 (2015)
202. D. V. Ratnam, D. D. Ankola, V. Bhardwaj, D. K. Sahana*, et al.*, Role of antioxidants in prophylaxis and therapy: A pharmaceutical perspective. *J Control Release*. 113, 189-207 (2006)
203. A. Ayer, P. Macdonald,R. Stocker, CoQ(1)(0) Function and Role in Heart Failure and Ischemic Heart Disease. *Annu Rev Nutr*. 35, 175-213 (2015)
204. K. Niibori, H. Yokoyama, J. A. Crestanello,G. J. Whitman, Acute administration of liposomal coenzyme Q10 increases myocardial tissue levels and improves tolerance to ischemia reperfusion injury. *J Surg Res*. 79, 141-145 (1998)
205. D. D. Verma, W. C. Hartner, V. Thakkar, T. S. Levchenko*, et al.*, Protective effect of coenzyme Q10-loaded liposomes on the myocardium in rabbits with an acute experimental myocardial infarction. *Pharm Res*. 24, 2131-2137 (2007)
206. B. A. Khaw, V. P. Torchilin, I. Vural,J. Narula, Plug and seal: prevention of hypoxic cardiocyte death by sealing membrane lesions with antimyosin-liposomes. *Nat Med*. 1, 1195-1198 (1995)
207. Y. H. Looi, D. J. Grieve, A. Siva, S. J. Walker*, et al.*, Involvement of Nox2 NADPH oxidase in adverse cardiac remodeling after myocardial infarction. *Hypertension*. 51, 319-325 (2008)
208. I. Somasuntharam, A. V. Boopathy, R. S. Khan, M. D. Martinez*, et al.*, Delivery of Nox2-NADPH oxidase siRNA with polyketal nanoparticles for improving cardiac function following myocardial infarction. *Biomaterials*. 34, 7790-7798 (2013)
209. D. D. Verma, W. C. Hartner, T. S. Levchenko, E. A. Bernstein*, et al.*, ATP-loaded liposomes effectively protect the myocardium in rabbits with an acute experimental myocardial infarction. *Pharm Res*. 22, 2115-2120 (2005)
210. D. D. Verma, T. S. Levchenko, E. A. Bernstein, D. Mongayt*, et al.*, ATP-loaded immunoliposomes specific for cardiac myosin provide improved protection of the mechanical functions of myocardium from global ischemia in an isolated rat heart model. *J Drug Target*. 14, 273-280 (2006)
211. D. D. Verma, T. S. Levchenko, E. A. Bernstein,V. P. Torchilin, ATP-loaded liposomes effectively protect mechanical functions of the myocardium from global ischemia in an isolated rat heart model. *J Control Release*. 108, 460-471 (2005)

212. J. L. Gordon, Extracellular ATP: effects, sources and fate. *Biochem J*. 233, 309-319 (1986)
213. H. K. Eltzschig, M. V. Sitkovsky,S. C. Robson, Purinergic signaling during inflammation. *N Engl J Med*. 367, 2322-2333 (2012)
214. F. Puisieux, E. Fattal, M. Lahiani, J. Auger*, et al.*, Liposomes, an interesting tool to deliver a bioenergetic substrate (ATP). in vitro and in vivo studies. *J Drug Target*. 2, 443-448 (1994)
215. W. Liang, T. S. Levchenko,V. P. Torchilin, Encapsulation of ATP into liposomes by different methods: optimization of the procedure. *J Microencapsul*. 21, 251-261 (2004)
216. G. X. Xu, X. H. Xie, F. Y. Liu, D. L. Zang*, et al.*, Adenosine triphosphate liposomes: encapsulation and distribution studies. *Pharm Res*. 7, 553-557 (1990)
217. J. P. Headrick, B. Hack,K. J. Ashton, Acute adenosinergic cardioprotection in ischemic-reperfused hearts. *Am J Physiol Heart Circ Physiol*. 285, H1797-1818 (2003)
218. H. K. Eltzschig, Adenosine: an old drug newly discovered. *Anesthesiology*. 111, 904-915 (2009)
219. M. V. Cohen,J. M. Downey, Adenosine: trigger and mediator of cardioprotection. *Basic Res Cardiol*. 103, 203-215 (2008)
220. R. A. Kloner, M. B. Forman, R. J. Gibbons, A. M. Ross*, et al.*, Impact of time to therapy and reperfusion modality on the efficacy of adenosine in acute myocardial infarction: the AMISTAD-2 trial. *Eur Heart J*. 27, 2400-2405 (2006)
221. A. M. Ross, R. J. Gibbons, G. W. Stone, R. A. Kloner*, et al.*, A randomized, double-blinded, placebo-controlled multicenter trial of adenosine as an adjunct to reperfusion in the treatment of acute myocardial infarction (AMISTAD-II). *J Am Coll Cardiol*. 45, 1775-1780 (2005)
222. J. Wang, Y. D. Chen, G. Zhi, Y. Xu*, et al.*, Beneficial effect of adenosine on myocardial perfusion in patients treated with primary percutaneous coronary intervention for acute myocardial infarction. *Clin Exp Pharmacol Physiol*. 39, 247-252 (2012)
223. H. Takahama, T. Minamino, H. Asanuma, M. Fujita*, et al.*, Prolonged targeting of ischemic/reperfused myocardium by liposomal adenosine augments cardioprotection in rats. *J Am Coll Cardiol*. 53, 709-717 (2009)
224. M. Galagudza, D. Korolev, V. Postnov, E. Naumisheva*, et al.*, Passive targeting of ischemic-reperfused myocardium with adenosine-loaded silica nanoparticles. *Int J Nanomedicine*. 7, 1671-1678 (2012)
225. A. Nemmar, S. Albarwani, S. Beegam, P. Yuvaraju*, et al.*, Amorphous silica nanoparticles impair vascular homeostasis and induce systemic inflammation. *Int J Nanomedicine*. 9, 2779-2789 (2014)
226. C. Guo, Y. Xia, P. Niu, L. Jiang*, et al.*, Silica nanoparticles induce oxidative stress, inflammation, and endothelial dysfunction in vitro via activation of the MAPK/Nrf2 pathway and nuclear factor-kappaB signaling. *Int J Nanomedicine*. 10, 1463-1477 (2015)
227. S. Masuda, K. Nakano, K. Funakoshi, G. Zhao*, et al.*, Imatinib mesylate-incorporated nanoparticle-eluting stent attenuates in-stent neointimal formation in porcine coronary arteries. *J Atheroscler Thromb*. 18, 1043-1053 (2011)
228. N. Tsukie, K. Nakano, T. Matoba, S. Masuda*, et al.*, Pitavastatin-incorporated nanoparticle-eluting stents attenuate in-stent stenosis without delayed endothelial healing effects in a porcine coronary artery model. *J Atheroscler Thromb*. 20, 32-45 (2013)
229. J. Margolis, J. Mcdonald, R. Heuser, P. Klinke*, et al.*, Systemic nanoparticle paclitaxel (nab-paclitaxel) for in-stent restenosis I (SNAPIST-I): a first-in-human safety and dose-finding study. *Clin Cardiol*. 30, 165-170 (2007)
230. G. Mcdowell, M. Slevin,J. Krupinski, Nanotechnology for the treatment of coronary in stent restenosis: a clinical perspective. *Vasc Cell*. 3, 8 (2011)
231. R. X. Yin, D. Z. Yang,J. Z. Wu, Nanoparticle drug- and gene-eluting stents for the prevention and treatment of coronary restenosis. *Theranostics*. 4, 175-200 (2014)
232. K. M. Lekshmi, H. L. Che, C. S. Cho,I. K. Park, Drug- and Gene-eluting Stents for Preventing Coronary Restenosis. *Chonnam Med J*. 53, 14-27 (2017)
233. A. Mozid, C. Yeo, S. Arnous, E. Ako*, et al.*, Safety and feasibility of intramyocardial versus intracoronary delivery of autologous cell therapy in advanced heart failure: the REGENERATE-IHD pilot study. *Regen Med*. 9, 269-278 (2014)

234. J. H. Houtgraaf, W. K. Den Dekker, B. M. Van Dalen, T. Springeling*, et al.*, First experience in humans using adipose tissue-derived regenerative cells in the treatment of patients with ST-segment elevation myocardial infarction. *J Am Coll Cardiol*. 59, 539-540 (2012)
235. B. Assmus, V. Schachinger, C. Teupe, M. Britten*, et al.*, Transplantation of Progenitor Cells and Regeneration Enhancement in Acute Myocardial Infarction (TOPCARE-AMI). *Circulation*. 106, 3009-3017 (2002)
236. X. Gu, Y. Xie, J. Gu, L. Sun*, et al.*, Repeated intracoronary infusion of peripheral blood stem cells with G-CSF in patients with refractory ischemic heart failure--a pilot study. *Circ J*. 75, 955-963 (2011)
237. R. R. Makkar, R. R. Smith, K. Cheng, K. Malliaras*, et al.*, Intracoronary cardiosphere-derived cells for heart regeneration after myocardial infarction (CADUCEUS): a prospective, randomised phase 1 trial. *Lancet*. 379, 895-904 (2012)
238. L. Ye, H. Haider, C. Guo,E. K. Sim, Cell-based VEGF delivery prevents donor cell apoptosis after transplantation. *Ann Thorac Surg*. 83, 1233-1234; author reply 1234 (2007)
239. C. J. Teng, J. Luo, R. C. Chiu,D. Shum-Tim, Massive mechanical loss of microspheres with direct intramyocardial injection in the beating heart: implications for cellular cardiomyoplasty. *J Thorac Cardiovasc Surg*. 132, 628-632 (2006)
240. J. Terrovitis, R. Lautamaki, M. Bonios, J. Fox*, et al.*, Noninvasive quantification and optimization of acute cell retention by in vivo positron emission tomography after intramyocardial cardiac-derived stem cell delivery. *J Am Coll Cardiol*. 54, 1619-1626 (2009)
241. W. J. Kang, H. J. Kang, H. S. Kim, J. K. Chung*, et al.*, Tissue distribution of 18F-FDG-labeled peripheral hematopoietic stem cells after intracoronary administration in patients with myocardial infarction. *J Nucl Med*. 47, 1295-1301 (2006)
242. A. C. Vandergriff, T. M. Hensley, E. T. Henry, D. Shen*, et al.*, Magnetic targeting of cardiosphere-derived stem cells with ferumoxytol nanoparticles for treating rats with myocardial infarction. *Biomaterials*. 35, 8528-8539 (2014)
243. J. Cores, T. G. Caranasos,K. Cheng, Magnetically Targeted Stem Cell Delivery for Regenerative Medicine. *J Funct Biomater*. 6, 526-546 (2015)
244. Y. Amsalem, Y. Mardor, M. S. Feinberg, N. Landa*, et al.*, Iron-oxide labeling and outcome of transplanted mesenchymal stem cells in the infarcted myocardium. *Circulation*. 116, I38-45 (2007)
245. Z. Huang, Y. Shen, A. Sun, G. Huang*, et al.*, Magnetic targeting enhances retrograde cell retention in a rat model of myocardial infarction. *Stem Cell Res Ther*. 4, 149 (2013)
246. A. Chaudeurge, C. Wilhelm, A. Chen-Tournoux, P. Farahmand*, et al.*, Can magnetic targeting of magnetically labeled circulating cells optimize intramyocardial cell retention? *Cell Transplant*. 21, 679-691 (2012)
247. Y. J. Kim, Y. M. Huh, K. O. Choe, B. W. Choi*, et al.*, In vivo magnetic resonance imaging of injected mesenchymal stem cells in rat myocardial infarction; simultaneous cell tracking and left ventricular function measurement. *Int J Cardiovasc Imaging*. 25 Suppl 1, 99-109 (2009)
248. E. Kustermann, W. Roell, M. Breitbach, S. Wecker*, et al.*, Stem cell implantation in ischemic mouse heart: a high-resolution magnetic resonance imaging investigation. *NMR Biomed*. 18, 362-370 (2005)
249. J. Terrovitis, M. Stuber, A. Youssef, S. Preece*, et al.*, Magnetic resonance imaging overestimates ferumoxide-labeled stem cell survival after transplantation in the heart. *Circulation*. 117, 1555-1562 (2008)
250. I. Y. Chen, J. M. Greve, O. Gheysens, J. K. Willmann*, et al.*, Comparison of optical bioluminescence reporter gene and superparamagnetic iron oxide MR contrast agent as cell markers for noninvasive imaging of cardiac cell transplantation. *Mol Imaging Biol*. 11, 178-187 (2009)
251. M. Mahmoudi, A. Tachibana, A. B. Goldstone, Y. J. Woo*, et al.*, Novel MRI Contrast Agent from Magnetotactic Bacteria Enables In Vivo Tracking of iPSC-derived Cardiomyocytes. *Sci Rep*. 6, 26960 (2016)
252. K. Cheng, T. S. Li, K. Malliaras, D. R. Davis*, et al.*, Magnetic targeting enhances engraftment and functional benefit of iron-labeled cardiosphere-derived cells in myocardial infarction. *Circ Res*. 106, 1570-1581 (2010)

253. K. Cheng, K. Malliaras, T. S. Li, B. Sun*, et al.*, Magnetic enhancement of cell retention, engraftment, and functional benefit after intracoronary delivery of cardiac-derived stem cells in a rat model of ischemia/reperfusion. *Cell Transplant*. 21, 1121-1135 (2012)
254. K. Cheng, D. Shen, M. T. Hensley, R. Middleton*, et al.*, Magnetic antibody-linked nanomatchmakers for therapeutic cell targeting. *Nat Commun*. 5, 4880 (2014)
255. Q. L. Wang, H. J. Wang, Z. H. Li, Y. L. Wang*, et al.*, Mesenchymal stem cell-loaded cardiac patch promotes epicardial activation and repair of the infarcted myocardium. *J Cell Mol Med*. (2017)
256. M. E. Davis, P. C. Hsieh, T. Takahashi, Q. Song*, et al.*, Local myocardial insulin-like growth factor 1 (IGF-1) delivery with biotinylated peptide nanofibers improves cell therapy for myocardial infarction. *Proc Natl Acad Sci U S A*. 103, 8155-8160 (2006)
257. Y. D. Lin, M. L. Yeh, Y. J. Yang, D. C. Tsai*, et al.*, Intramyocardial peptide nanofiber injection improves postinfarction ventricular remodeling and efficacy of bone marrow cell therapy in pigs. *Circulation*. 122, S132-141 (2010)
258. K. Wei, V. Serpooshan, C. Hurtado, M. Diez-Cunado*, et al.*, Epicardial FSTL1 reconstitution regenerates the adult mammalian heart. *Nature*. 525, 479-485 (2015)
259. D. Castellano, M. Blanes, B. Marco, I. Cerrada*, et al.*, A comparison of electrospun polymers reveals poly(3-hydroxybutyrate) fiber as a superior scaffold for cardiac repair. *Stem Cells Dev*. 23, 1479-1490 (2014)
260. K. L. Fujimoto, J. Guan, H. Oshima, T. Sakai*, et al.*, In vivo evaluation of a porous, elastic, biodegradable patch for reconstructive cardiac procedures. *Ann Thorac Surg*. 83, 648-654 (2007)
261. J. Jin, S. I. Jeong, Y. M. Shin, K. S. Lim*, et al.*, Transplantation of mesenchymal stem cells within a poly(lactide-co-epsilon-caprolactone) scaffold improves cardiac function in a rat myocardial infarction model. *Eur J Heart Fail*. 11, 147-153 (2009)
262. D. Kai, Q. L. Wang, H. J. Wang, M. P. Prabhakaran*, et al.*, Stem cell-loaded nanofibrous patch promotes the regeneration of infarcted myocardium with functional improvement in rat model. *Acta Biomater*. 10, 2727-2738 (2014)
263. H. Piao, J. S. Kwon, S. Piao, J. H. Sohn*, et al.*, Effects of cardiac patches engineered with bone marrow-derived mononuclear cells and PGCL scaffolds in a rat myocardial infarction model. *Biomaterials*. 28, 641-649 (2007)
264. T. Dvir, B. P. Timko, M. D. Brigham, S. R. Naik*, et al.*, Nanowired three-dimensional cardiac patches. *Nat Nanotechnol*. 6, 720-725 (2011)
265. M. Shevach, S. Fleischer, A. Shapira,T. Dvir, Gold nanoparticle-decellularized matrix hybrids for cardiac tissue engineering. *Nano Lett*. 14, 5792-5796 (2014)
266. P. Baei, S. Jalili-Firoozinezhad, S. Rajabi-Zeleti, M. Tafazzoli-Shadpour*, et al.*, Electrically conductive gold nanoparticle-chitosan thermosensitive hydrogels for cardiac tissue engineering. *Mater Sci Eng C Mater Biol Appl*. 63, 131-141 (2016)
267. R. Feiner, L. Engel, S. Fleischer, M. Malki*, et al.*, Engineered hybrid cardiac patches with multifunctional electronics for online monitoring and regulation of tissue function. *Nat Mater*. 15, 679-685 (2016)
268. M. M. Nguyen, N. C. Gianneschi,K. L. Christman, Developing injectable nanomaterials to repair the heart. *Curr Opin Biotechnol*. 34, 225-231 (2015)
269. J. Han, J. Park,B. S. Kim, Integration of mesenchymal stem cells with nanobiomaterials for the repair of myocardial infarction. *Adv Drug Deliv Rev*. 95, 15-28 (2015)
270. S. Pascual-Gil, E. Garbayo, P. Diaz-Herraez, F. Prosper*, et al.*, Heart regeneration after myocardial infarction using synthetic biomaterials. *J Control Release*. 203, 23-38 (2015)
271. R. Amezcua, A. Shirolkar, C. Fraze,D. A. Stout, Nanomaterials for Cardiac Myocyte Tissue Engineering. *Nanomaterials (Basel)*. 6, (2016)
272. J. J. Chong,C. E. Murry, Cardiac regeneration using pluripotent stem cells--progression to large animal models. *Stem Cell Res*. 13, 654-665 (2014)
273. F. M. Van Der Valk, D. F. Van Wijk, M. E. Lobatto, H. J. Verberne*, et al.*, Prednisolone-containing liposomes accumulate in human atherosclerotic macrophages upon intravenous administration. *Nanomedicine*. 11, 1039-1046 (2015)

274. D. J. Lundy, K. H. Chen, E. K. Toh,P. C. Hsieh, Distribution of Systemically Administered Nanoparticles Reveals a Size-Dependent Effect Immediately following Cardiac Ischaemia-Reperfusion Injury. *Sci Rep*. 6, 25613 (2016)
275. J. Szebeni, Complement activation-related pseudoallergy caused by liposomes, micellar carriers of intravenous drugs, and radiocontrast agents. *Crit Rev Ther Drug Carrier Syst*. 18, 567-606 (2001)
276. J. Szebeni, Complement activation-related pseudoallergy: a new class of drug-induced acute immune toxicity. *Toxicology*. 216, 106-121 (2005)
277. U. Bulbake, S. Doppalapudi, N. Kommineni,W. Khan, Liposomal Formulations in Clinical Use: An Updated Review. *Pharmaceutics*. 9, (2017)
278. H. B. Bostan, R. Rezaee, M. G. Valokala, K. Tsarouhas*, et al.*, Cardiotoxicity of nano-particles. *Life Sci*. 165, 91-99 (2016)
279. C. E. Guerrero-Beltran, J. Bernal-Ramirez, O. Lozano, Y. Oropeza-Almazan*, et al.*, Silica nanoparticles induce cardiotoxicity interfering with energetic status and Ca2+ handling in adult rat cardiomyocytes. *Am J Physiol Heart Circ Physiol*. 312, H645-H661 (2017)
280. A. Gaudin, M. Yemisci, H. Eroglu, S. Lepetre-Mouelhi*, et al.*, Squalenoyl adenosine nanoparticles provide neuroprotection after stroke and spinal cord injury. *Nat Nanotechnol*. 9, 1054-1062 (2014)
281. A. Maksimenko, F. Dosio, J. Mougin, A. Ferrero*, et al.*, A unique squalenoylated and nonpegylated doxorubicin nanomedicine with systemic long-circulating properties and anticancer activity. *Proc Natl Acad Sci U S A*. 111, E217-226 (2014)

Chapter 1

Squalene-based multidrug nanoparticles for improved mitigation of uncontrolled inflammation

Flavio Dormont[a], Romain Brusini[a], Catherine Cailleau[a], Franceline Reynaud[a,b], Arnaud Peramo[a], Julie Mougin[a], Françoise Gaudin[c], Mariana Varna[a], Patrick Couvreur[a]*

[a] Institut Galien Paris-Sud, CNRS UMR 8612, Université Paris-Sud, Université Paris-Saclay, 92296 Châtenay-Malabry, France

[b] School of Pharmacy, Federal University of Rio de Janeiro, 21944-59 Rio de Janeiro, Brazil

[c] UMS31, Plateforme PHIC, Institut Paris-Saclay d'Innovation Thérapeutique (IPSIT), *92140* Clamart, France

Under Revision at Science Advances

Squalene-based multidrug nanoparticles for improved mitigation of uncontrolled inflammation

Abstract

During uncontrolled inflammation, the production of various reactive oxidant species in excess of endogenous antioxidant defense mechanisms promotes the development of oxidative stress, with significant biological consequences. In recent years, evidence has emerged that this oxidative stress plays a crucial role in the development and perpetuation of the pro-inflammatory state. Currently, effective treatments against this crosstalk between inflammation and oxidative stress are lacking, and patient care remains primarily selective of one or the other. Here we report on the development of multidrug nanoparticles for the mitigation of uncontrolled inflammation. The nanoparticles are made by conjugating squalene, an endogenous lipid, to adenosine, an endogenous immunomodulator, thus yielding a biocompatible pro-drug based nanocarrier. This prodrug nanocarrier was used to encapsulate α-tocopherol, a natural antioxidant, yielding high drug loading, biocompatible, multidrug nanoparticles. By exploiting the vascular endothelial barrier dysfunction at sites of acute inflammation, these multidrug nanoparticles could (i) deliver the therapeutic agents in a targeted manner, (ii) improve their bioavailability, and (iii) enact potent antioxidant and anti-inflammatory action. In mouse models of LPS-induced endotoxemic shock, treatment with these multifunctional squalene-based nanoparticles, termed SQAd/VitE NPs, reduced oxidative stress, curtailed pro-inflammatory signaling and ultimately conferred a significant survival advantage to infected animals. Selectively delivering adenosine and antioxidants together could serve as a novel approach for the treatment of acute inflammation with reduced-side effects and high therapeutic potential.

Significance Statement

Growing evidence has indicated that uncontrolled inflammation is often driven by continuous positive feedback loops between pro-inflammatory signaling and oxidative stress. There are currently no effective ways to counter this crosstalk in a targeted manner. Herein, we demonstrate the therapeutic potential of squalene prodrug-based nanoparticles for inflammation control through a powerful two-drug neutralization process: adenosine as a potent inflammation mediator and tocopherol for efficient protection against oxidative stress. The multidrug nanoparticles are able to target the site of acute inflammation because of the vascular permeability that appears there. This therapeutic option may provide a first-in class adenosine and antioxidant based treatment that may ultimately improve the clinical outcome of patients suffering from uncontrolled inflammatory disorders.

I. Introduction

Uncontrolled inflammation is a key health challenge, and is associated with numerous diseases(1-3). A growing understanding of the pathophysiology accompanying acute inflammation can help devise novel therapeutics for inflammatory diseases(4). Of particular relevance, is that severe inflammation is associated with significant alterations to redox balance(5), inducing oxidative stress to tissues and cells. Evidence accumulated over the past two decades has pointed to significant connections between inflammation and oxidative stress, both processes contributing to fuel one another, thereby establishing a vicious cycle able to perpetuate and propagate the inflammatory response(6, 7).

Inhibiting pathological inflammatory responses and the crosstalk between oxidative stress and inflammation presents various challenges(8). For instance, while potent anti-inflammatory agents –such as corticosteroids- already exist, these have fallen short in acute inflammatory conditions such as sepsis, because of their negative effects on tissue repair and the reported adrenocortical insufficiency common in sepsis patients(9). Adenosine, an endogenous purine, and adenosine receptor agonists have shown promise by promoting the resolution of inflammation(10, 11), but their systemic administration is associated with rapid clearance(12) and unacceptable medical side effects(13) related to untargeted adenosine receptor activation. Similarly, antioxidant supplementation has been attempted(14-17) to scavenge reactive species during acute inflammation, but remains limited by poor pharmacodynamics and tissue penetration(18). Recently, multidrug treatments of low-dose hydrocortisone with antioxidants have emerged as a promising approach for the mitigation of uncontrolled inflammation(19), simultaneously inhibiting pro-inflammatory cascades and scavenging reactive oxygen species. However, so far, most of the antioxidants used in this context perform their action predominantly in the plasma. While this is useful during the initial hyper-inflammatory stages of the body response, it is ineffective at inhibiting the pathological redox cycles happening inside cells and tissues(18) - as plasma antioxidant levels poorly correlate with intracellular antioxidant levels(20).

To improve on these issues, and taking into account the potential of adenosine and multidrug therapies for the resolution of inflammation, we propose here a novel prodrug-based nanoparticle formulation, enabling the targeted delivery of adenosine and tocopherol to the sites of acute inflammation. We show that the bioconjugation of adenosine to squalene, an

endogenous lipid, and further nanoformulation with tocopherol led to the formation of stable multidrug nanoparticles allowing: (i) efficient encapsulation of both drugs, (ii) reduced side-effects and (iii) promising anti-inflammatory and protective effects in models of endotoxemia and lethal systemic shock. Furthermore, we also report evidence that these squalene-based nanoparticles could target inflamed tissues in multiple murine models of inflammation for selective adenosine receptor activation and antioxidant action. These functionalities together enabled a therapeutic intervention with significant potential for the antioxidant management of acute inflammatory diseases and improved the use of adenosine as a pro-resolving pharmaceutical agent.

II. Materials and Methods

1. Preparation of Squalene based Nanoparticles.

Squalene-adenosine (SQAd) was synthesized as previously described (21) and the resulting nanoparticles were prepared using the nanoprecipitation technique. Briefly, SQAd was dissolved in absolute ethanol (6 mg/mL), and added dropwise under strong stirring to a 5% (wt/vol) dextrose solution. Ethanol was then completely evaporated using a Rotavapor (90 rpm, 40 °C, 42 mbar) to obtain an aqueous suspension of pure SQAd nanoparticles (2mg/mL). Multidrug SQAd/VitE nanoparticles (50:50 wt%) were obtained by dissolving SQAd (3 mg/mL) and VitE (3 mg/mL) (α-tocopherol, Sigma-Aldrich) in absolute ethanol and adding the solution dropwise under strong stirring to a 5% dextrose solution with subsequent ethanol evaporation to obtain an aqueous suspension of SQAd/VitE nanoparticles (2 mg/mL). Fluorescent nanoparticles were obtained by the same procedure, except 1% (wt/wt) of fluorescent probe (SQ conjugated Rhodamine B (SQRho)) or 1,1′-dioctadecyl-3,3,3′,3′-tetramethylindodicarbocyanine perchlorate (DiD) was added to the ethanolic phase. All NP sizes (hydrodynamic diameter) and surface charges (zeta potential) were measured using a Malvern Zetasizer Nano ZS 6.12 (173° scattering angle, 25 °C). For the size measurements by dynamic light scattering (DLS), a good attenuator value (7−9) was obtained when suspending 20 µL of NPs in 1 mL of distilled water. The mean diameter for each preparation resulted from the average of three measurements of 60 s each. For zeta potential measurements, 70 µL of NPs was dissolved in 2 mL of KCl 1 mM, before filling the measurement cell. The mean zeta potential for each preparation resulted from the average of three independent measurements in automatic mode, followed by application of the Smoluchowski equation. Morphology was observed by cryogenic TEM (cryoTEM). For this, drops of the NP suspensions (2mg/mL) were

deposited on EM grids covered with a holey carbon film (Quantifoil R2/2) previously treated with a plasma glow discharge. Observations were conducted at low temperature (−180°C) on a JEOL 2010 FEG microscope operated at 200 kV. Images were recorded with a Gatan camera.

2. Encapsulation efficiency experiment.

SQAd/VitE NPs with different VitE content were formulated in 5 % dextrose solution and subsequently washed with water twice, using a ultrafiltration device (molecular weight cut-off 100,000). NPs were dissolved in ethanol and measured by HPLC to determine VitE content. A high-performance liquid chromatograph Waters Alliance 1695 (Waters, Milford, MA), equipped with a Waters DAD 2996 photodiode array detector, Hewlett-Packard computer with a Waters Empower 3 software and a Waters autosampler with a 50 μL loop was used, with simultaneous spectra detection wavelengths from 200-600 nm recorded for all peaks. A Waters Xselect LC-18 column (2.1 x 150 mm, 3.5 μm) was used with a non-gradient mobile phase of acetonitrile and methanol (v/v 50/50) at a constant flow rate of 1 mL/min. The VitE peak was measured at a wavelength of 216 nm and quantitatively determined by comparing with a standard curve.

3. Intracellular ROS detection assay.

H9c2 cells (50 000 cells/well) were seeded in a 12-well plate and cultured for 24 h at 37°C. The cells were treated for 2 hours with SQAd/VitE NPs or controls diluted in culture medium at a concentration of 10 μg/mL for standard tests or according to the described dose for dose-response experiments. Cells were washed with PBS and incubated with medium containing hydrogen peroxide (H_2O_2, final concentration 0.5 mM). After 30 min, H_2O_2 containing medium was removed and the cells were washed with PBS. Intracellular ROS production was detected using Abcam Cellular ROS Assay Kit (Deep Red) per manufacturer instructions. Briefly, the ROS detection probe was diluted in PBS and cells were incubated with this staining solution for 30 min. Staining solution was removed, cells were washed with PBS and treated with 300 μL of 0.25% trypsin solution for 5 min at 37 °C. The trypsin solution was inhibited by adding 0.7 mL of medium and cell fluorescence was recorded using an Accuri flow cytometer C6 (Accuri Cytometers Ltd.). Necrotic cell death was assessed by propidium iodide staining at 10 μg/mL.

4. Nitric oxide assay.

Nitrite ($NO2^-$) release was assessed with freshly prepared Griess reagent. Briefly, in 96-well

plates (20 000 cells/well) RAW264.7 cells were treated for 2 hours with SQAd/VitE NPs or controls diluted in culture medium at a concentration of 10 µg/mL. LPS was added at a final concentration of 1 µg/mL for 24 h for macrophage stimulation. For co-treatment experiments, SQAd/VitE NPs treatment was also performed concurrently to LPS stimulation. After LPS stimulation, the Griess reagent was added in equal volume to culture supernatants. The absorbance at 550 nm was measured on a Perkin Elmer absorbance reader after 10 min of incubation in the dark at room temperature. The $NO2^-$ concentrations were determined using standard curves prepared from sodium nitrite (NaNO2) at various concentrations.

5. *In vitro* evaluation of pro-inflammatory cytokines production.

LPS stimulation and drug treatments were performed in the same way than with Nitric oxide assays. After LPS stimulation for 24 h, cell supernatants were retrieved and centrifuged for 5 min at 1000 g to remove cell debris. Inflammatory cytokines production was evaluated using a Biolegend ELISA mouse TNF-α cytokine detection kit per manufacturer instructions (BioLegend, USA). Supernatants were diluted 20X with Assay Diluent prior to detection experiment.

6. Animal Care.

Male C57BL/6J and female BALB/c mice were purchased from Janvier Labs (France) for systemic inflammation and biodistribution studies, respectively. Animals were housed in a standard controlled environment (22° ± 1°C, 60% relative humidity, 12-hour light/dark cycles) with food and water available ad libitum. Experiments were approved by the Animal Care Committee of the University Paris-Sud, in accordance with principles of laboratory animal care and European legislation 2010/63/EU. All efforts were made to reduce animal numbers and minimize their suffering, as defined in the specific agreement (registration no. APAFIS#16257).

7. Biodistribution studies.

For the paw inflammation study, experiments were performed on 18 weeks old female BALB/c mice. Paw inflammation was caused by intraplantar injection in the right paw of 100 ng of LPS (Sigma-Aldrich O111:B4) dissolved at 5 mg/mL in physiological saline (NaCl, 0.9%). Animals received a control injection of 20 µL saline in the left paw. *In vivo* imaging biodistribution studies were performed after two hours, following intravenous injection of fluorescent

SQAd/VitE NPs (100 µL, 2 mg/mL, containing 1% DiD) or control fluorescent DiD solution (100 µL, 20 µg/mL in 5% dextrose solution). The biodistribution of the NPs was recorded at 0.5, 2, 4 and 24 hours with the IVIS Lumina LT Series III system (Caliper Life Sciences) using 640 nm excitation and 695 nm emission filters. During imaging, mice were kept on the imaging stage under anesthesia with 2% isofluorane gas in oxygen flow (1 liter/min) and were imaged in ventral position. Images and measures of fluorescence signals were acquired and analyzed with Living Imaging software (Caliper Life Sciences).

For the systemic inflammation study, experiments were performed on 12-week old male C57BL/6J mice. Systemic inflammation was caused by i.p. injection of LPS (Sigma-Aldrich O111:B4) at a dose of 7.5 mg/kg. Non-inflamed control animals did not receive the LPS injection. After two hours, animals received intravenous injection of fluorescent SQAd/VitE NPs (100 µL, 2 mg/mL, containing 1% SQRho) or control fluorescent rhodamine B solution (100µL, 20 µg/mL in 5% dextrose solution). After 24 hours, animals were deeply anesthetized with an i.p. sodium pentobarbital injection before euthanasia by intracardial perfusion of 40 mL of saline (8 mL/min), until the fluid exiting the right atrium was entirely clear. The liver, heart, lungs, kidneys and spleen were excised and immediately imaged with the IVIS imager using 560 nm excitation and 620 nm emission filters. Images and measures of fluorescence signals were acquired and analyzed with Living Imaging software (Caliper Life Sciences).

8. *In vivo* efficacy.

The therapeutic efficacy of SQAd/VitE NPs was evaluated *in vivo* in a mouse endotoxemia model with 8-12 week-old male C57BL/6J mice. To evaluate the efficacy through cytokine production, endotoxemia was induced by intraperitoneal injection of a 7.5 mg/kg dose of LPS (Sigma O111:B4) diluted at 1.875 mg/mL in buffered saline. Mice injected with LPS alone were used as controls. 30 min after LPS injection, SQAd/VitE NPs (15 mg/kg SQAd, (ie. equiv 5.5 mg/kg Ad and 15 mg/kg VitE), SQAd NPs (15 mg/kg SQAd, equiv 5.5 mg/kg Ad) or free Ad/VitE (5.5 mg/kg Ad and 15 mg/kg VitE with 1% Pluronic® F-123 vehicle) were intravenously injected via the suborbital vein. Following the injections, blood samples (~100 µL) were collected at predetermined time points via submandibular puncture before terminal cardiac puncture and organ collection. Plasma was obtained by centrifuging blood samples at 2000 rcf for 10 min and stored at −78°C before further analysis. In the plasma, cytokines, including IL-10 and TNF-α, were quantified by Biolegend ELISA mouse kit per manufacturer instructions. Organ homogenates were obtained with a Heidolph Instruments (Germany) RZR-2021 organ

homogenizer in PBS at a concentration of 500 mg/mL. Pro-inflammatory cytokines in organ homogenates were quantified using a cytometric bead array per manufacturer's instruction (BD Biosciences). For MDA content in the lungs, 10 mg of lung tissues were homogenized on ice in 300 µL of MDA lysis buffer containing 3 µL BHT antioxidant solution as per manufacturer instruction (Biovision, Lipid Peroxidation MDA Fluometric Assay Kit). To evaluate efficacy through survival in the lethal LPS model, mice were sensitized to the lethal effects of LPS with D-galactosamine hydrochloride (Roth, Germany) via i.p. injection of a 8 mg dose concurrently to LPS injection at 2 µg/kg. After 30 min, nanoparticles or free drugs as controls were injected intravenously. Signs of disease severity were evaluated at predetermined time-points using a previously described disease scoring system(22). For histological evaluation, organs were fixed for 24 h in 4% PFA and then embedded in paraffin. Sections (5µm) were deparaffinized and stained with hematoxylin-eosin (H&E, VWR, France). Slides were scanned with a digital slide scanner NanoZoomer 2.0-RS (Hamamatsu, Japan), which allowed an overall view of the samples. Images were digitally captured from the scan slides using the NDP.view2 software (Hamamatsu).

9. Blood pressure measurements.

For blood pressure measurements a Kent Scientific (Torrington, USA) Coda tail-cuff VPR blood pressure measurement system was used. C57BL/6J mice were acclimated to the procedure for two days before measurements to avoid undue stress and experimental artifact. For all measurements, an experimental session of 10 acclimation cycles and 10 measurement cycles was used. Only measurement cycles that passed Coda software acceptance criteria were retained. For animals that received free Ad/VitE or SQAd/VitE (30 mg/kg or equivalent), the blood pressure measurement was started immediately after i.v. injection.

III. Results and Discussion

1. Preparation SQAd/VitE NPs

The preparation of squalene-adenosine/tocopherol nanoparticles (SQAd/VitE NPs) first required conjugation of adenosine to squalenic acid as previously described(21). This conjugation step was performed with moderate yield (45%) and afforded SQAd which could then be used as a prodrug-based nanocarrier for tocopherol (Fig. 1A-B). The second step in the preparation of multidrug squalene-based nanoparticles consisted in encapsulating tocopherol (VitE) in SQAd nanoparticles which was performed by a nanoprecipitation technique. Following nanoprecipitation and solvent removal, the VitE content of the nanoparticles was evaluated.

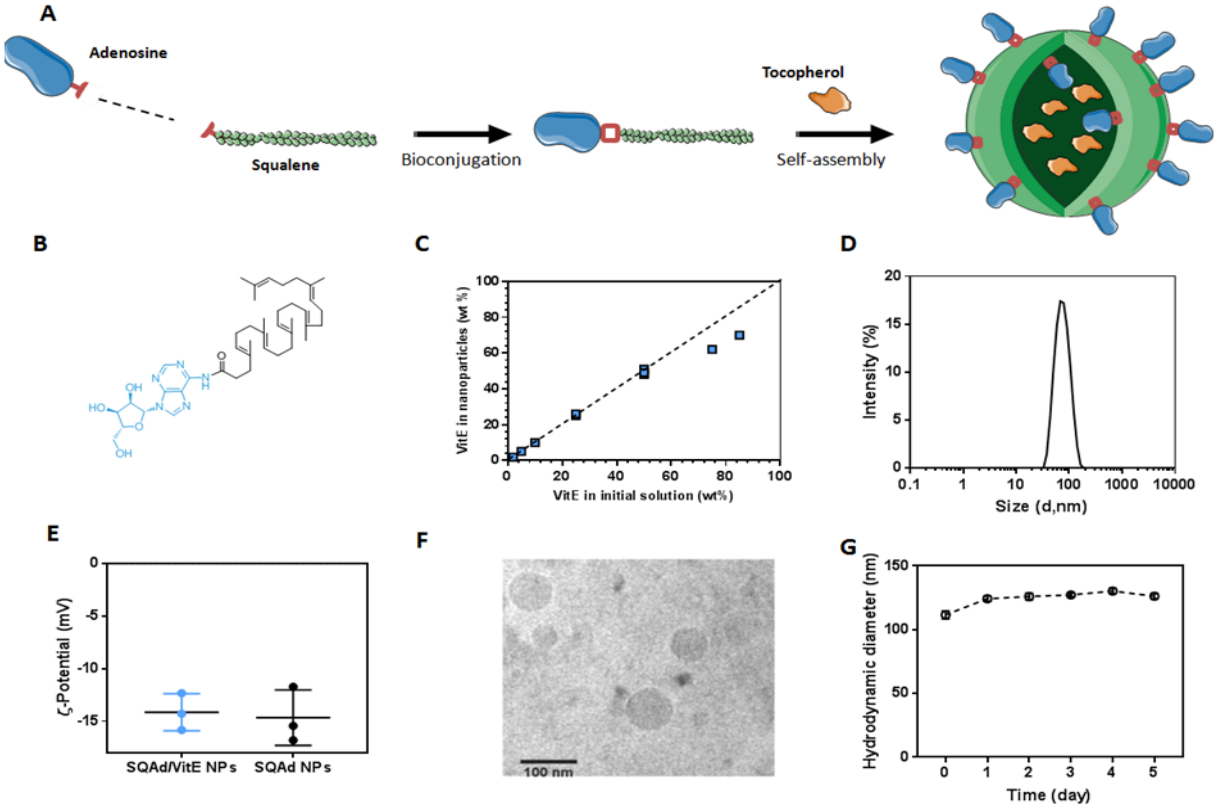

Figure 1. Formulation and characterization of multidrug squalene-adenosine/VitE nanoparticles (SQAd/VitE NPs). (**A**) Schematic representation of SQAd bioconjugation and VitE encapsulation to afford SQAd/VitE NPs. (**B**) Structure of squalene-adenosine, with adenosine moiety in blue. (**C**) VitE encapsulation efficiency in SQAd/VitE NPs as measured by HPLC. (**D**) Hydrodynamic size of SQAd/VitE NPs (diameter, nanometers) measured by dynamic light scattering (DLS). (**E**) Measurement of surface ζ-potential of SQAd/VitE and SQAd NPs. (**F**) Cryo-TEM images of SQAd/VitE NPs (scale bar: 100 nm). (**G**) Stability of SQAd/VitE NPs in 50% FBS over 5 days as measured by DLS.

For SQAd/VitE nanoformulations containing 50 wt% VitE or less, most of the VitE present in the precursor organic solution was found to be incorporated in the nanoparticles (Fig. 1C). For the rest of this study, we used the SQAd/VitE NPs formulation which afforded the highest total drug loading with proper colloidal stability, ie. SQAd/VitE (50:50) %wt. The total drug loading of the multidrug NPs was therefore 68.6 wt%: 50 wt% VitE and 18.6 wt% Ad. When measured by dynamic light scattering (DLS), the multidrug SQAd/VitE NPs displayed a uniform size distribution with a mean hydrodynamic diameter of 71.2 ± 3 nm and a polydispersity index inferior to 0.2 (Fig. 1D). Surface zeta potential was measured to be -14.29 ± 1.01 (s.e.m.) mV, similar to SQAd NP only (-15.45 ± 1.52 mV), ensuring proper colloidal stability (Fig. 1E). The obtained multi-drug nanoparticles were also observed by Cryo-TEM imaging, revealing uniform nanoparticles (Fig. 1F). Following their formulation, SQAd/VitE NPs were suspended in 50% serum, and showed satisfactory colloidal stability over 5 days (Fig. 1G).

Squalene is an endogenous precursor of cholesterol which forms stable colloidal phases in water(23). VitE is insoluble in water and usually co-localizes with cholesterol in low-density lipoproteins in vivo(24). Accordingly, our results showed that VitE was efficiently encapsulated in SQAd nanoparticles to form stable multidrug nanoparticles. Overall, the preparation of SQAd/VitE nanoparticles is very straightforward since it simply requires an ethanolic solution of SQAd and VitE to be added in water medium before ethanol evaporation. This procedure didn't require any excipients which makes the scaling-up affordable. Noteworthy, this may represent an asset over the current trend of developing ever more sophisticated nanomedicines, whose physico-chemical complexity represents an important factor to slow the speed and even the feasibility of nanomedicines translation into the clinic.

2. Biodistribution Studies

To investigate if squalene nanoparticles could improve the bioavailability of the encapsulated therapeutic agents and direct them to the inflammation foci, we evaluated the *in vivo* biodistribution of SQAd/VitE NPs in two different models, one of local acute inflammation and one of systemic inflammation. First, the *in vivo* circulation and biodistribution of SQAd/VitE NPs was followed after intravenous injection of fluorescent DiD (1,1'-dioctadecyl-3,3,3',3'-tetramethylindodicarbocyanine, 4- chlorobenzenesulfonate salt) – labeled SQAd/VitE NPs in a

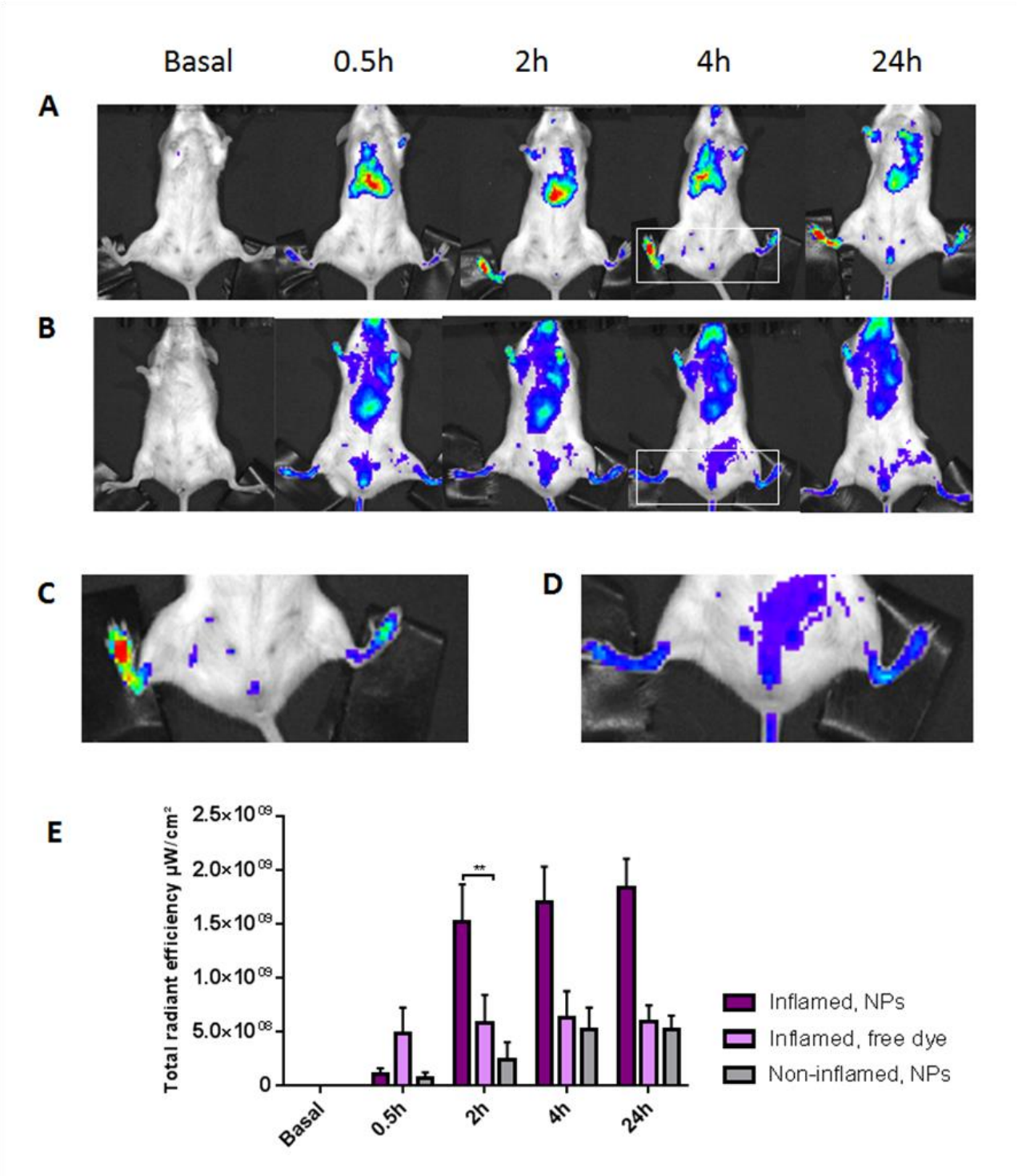

Figure 2: IVIS Lumina scan of mice after intravenous administration of fluorescent SQAd/VitE NPs or control fluorescent dye solution (ventral view). (A) Biodistribution of fluorescent SQAd/VitE NPs in mice with inflamed right hind paw and non-inflamed left hind paw. (B) Biodistribution of the free dye in mice with inflamed right hind paw. (C) Zoom of group A at 4 hours. (D) Zoom of group B at 4 hours. (E) Analysis of the measured total radiant efficiency in the region of interest. n=3 mice per group. Data are mean ± SD. *P<0.05, **P<0.01 (Student's t-test).

murine lipopolysaccharide (LPS)-induced paw inflammation model. Animals received 100 ng of LPS in their right paw and a control saline injection in the left paw. The fluorescence in tissues was monitored non-invasively up to 24 hours, from the abdomen side using a IVIS Lumina. The real-time *in vivo* imaging showed that, in comparison with the control healthy left paw, an increase of two to three times in the radiant efficiency of the inflamed right paw could be detected after intravenous injection of fluorescent SQAd/VitE NPs (Fig. 2A-E). In a control experiment, when the mice received a free DiD solution, no significant accumulation of fluorescence was observed in the inflamed paw (Fig. 2B).

In a second study, we evaluated the ability of SQAd/VitE NPs to accumulate in organs in a model of LPS-induced sepsis. Loss of endothelial integrity is one of the hallmarks of sepsis and LPS injection has been shown to induce capillary leakage in a β1-integrin dependent mechanism(25). Here, rhodamine B covalently linked to squalene (SQRho, Supp. Fig. S1-S2) was used as a fluorescent marker for SQAd/VitE NPs. Animals received LPS intraperitoneally, and after 2h, an intravenous injection of fluorescent SQAd/VitE NPs. After 24 hours, the mice were deeply anesthetized and intracardially perfused with 40 mL of PBS to remove blood. The fluorescence signal in the different organs was measured using an IVIS Lumina. Mice that did not receive an LPS challenge were used as non-inflamed controls. The fluorescent imaging showed that, in comparison with healthy mice, LPS inflamed animals had a significant increase in levels of total radiant efficiency in the lungs, liver and kidneys (Fig. 3). In a control experiment, when LPS-treated mice were intravenously injected with a free rhodamine probe solution, no significant accumulation occurred in the studied organs except the kidney, most probably because of the renal clearance of rhodamine.

During inflammation, neutrophils interact with the vascular endothelium leading to barrier dysfunction and increased permeability. This constitutes a unique opportunity for nanomedicines to accumulate at the sites of organ injury and selectively deliver therapeutic agents through enhanced permeation and retention effects(26). In the present *in vivo* studies, SQAd/VitE NPs were found to accumulate at the sites of acute inflammation and endothelial dysfunction in models of both local and systemic inflammation. When injected in vivo, free adenosine is readily catabolized into inosine and hypoxanthine, resulting in an extremely short blood half-life of 10 sec(12). This requires adenosine to be administered continuously and in high doses to achieve a pharmacological response, resulting in side effects related to the unchecked activation of the ubiquitous adenosine receptors. The targeted accumulation

achieved by SQAd/VitE NPs could therefore potentially limit the side effects induced by adenosine treatment and enhance the bioavailability of both drugs at the sites of inflammation for improved therapeutic action.

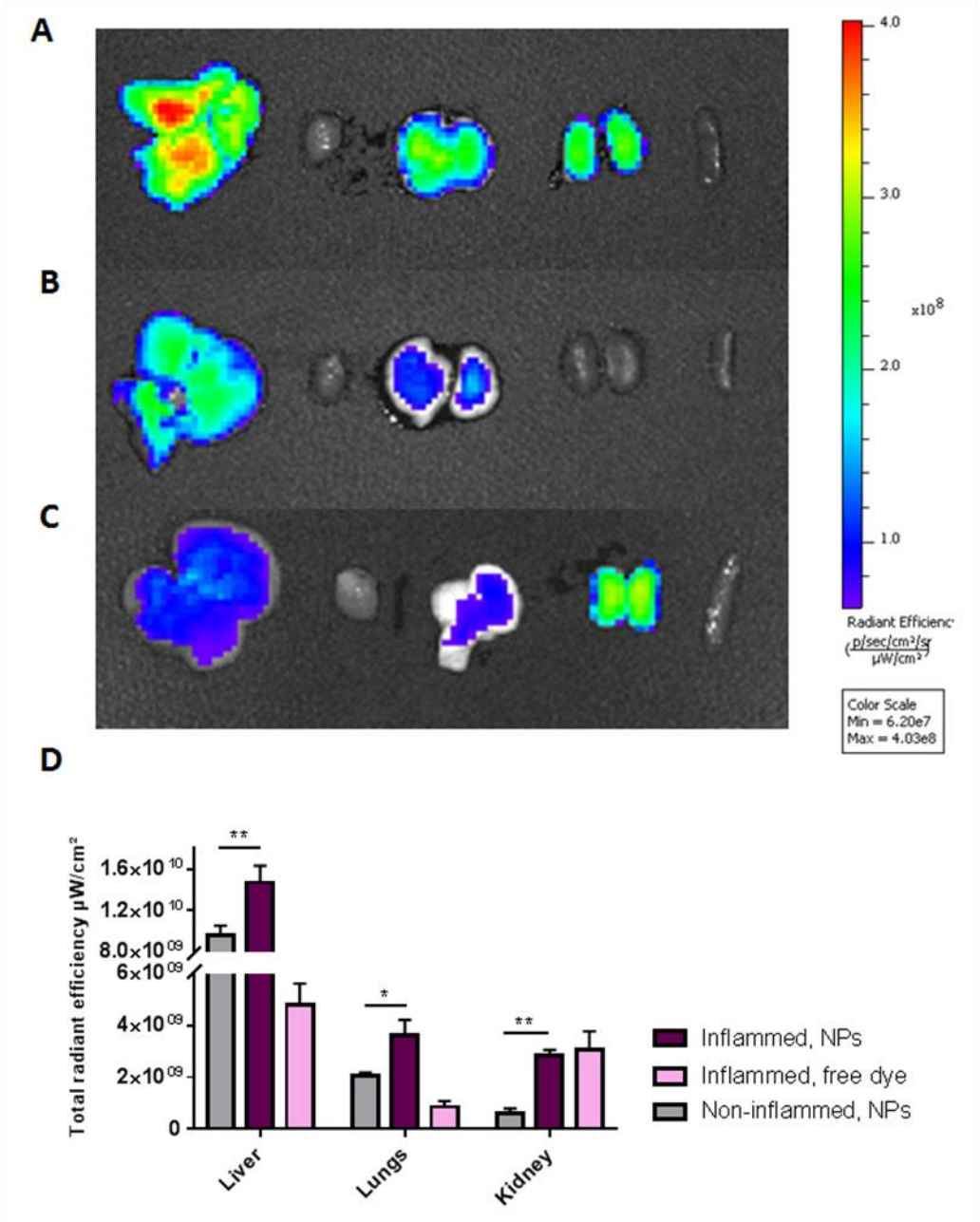

Figure 3. Ex-vivo IVIS Lumina scan of mice organs after intravenous administration of fluorescent SQAd/VitE NPs in a septic shock model. Organs displayed from left to right Liver, Heart, Lungs, Kidneys, Spleen (**A**) Biodistribution of fluorescent SQAd/VitE NPs labeled in mice that received a LPS challenge. (**B**) Biodistribution of fluorescent SQAd/VitE NPs in non-inflamed mice (did not receive LPS challenge). (**C**) Biodistribution of free dye in mice that received a LPS challenge. (**D**) Analysis of the measured total radiant efficiency in the different organs. *n*=3 mice per group. Data are mean ± SD. **P*<0.05, ***P*<0.01 (Student's *t*-test).

3. In vitro evaluation

To investigate whether SQAd/VitE NPs could effectively enact protection against oxidative stress, we first developed an *in vitro* model of oxidative insult. In inflamed tissue, immune cells produce reactive oxygen species such as hydrogen peroxide (H_2O_2) that can cross the cellular membrane and produce intracellular oxidative stress(27) to tissue cells. When H9c2 murine cardiac cells were incubated with H_2O_2 for 30 min, a strong increase in intracellular ROS was detected by flow cytometry using a ROS sensitive fluorescent probe. Treatment with SQAd/VitE NPs was efficient at limiting intracellular ROS production in a dose dependent manner (Fig. 4A-B). While SQAd NPs controls did not provide this protection, free drug Ad/VitE in the medium did induce some protection against the oxidative insult, most probably because of the antioxidant action of VitE. Interestingly, this effect was less pronounced than with SQAd/VitE NPs. The reduction in intracellular ROS correlated positively with improved cell survival to the oxidative insult as measured by propidium iodide straining. In SQAd/VitE NPs treated samples, only 20 % of cells were found to be necrotic, while non treated cell populations contained 80 % of necrotic cells (Fig. 4C-D). SQAd/VitE NPs were found to be readily taken up by cells (Supp. Fig. S3), likely through LDL receptor-mediated mechanisms as shown previously with SQAd only nanoparticles(28). Thus, after accumulating at the sites of inflammation, SQAd/VitE NPs are most likely able to enter cells, where they can deliver their therapeutic cargo intracellularly. As it has been suggested(18, 29), and as demonstrated here, the intracellular delivery of the antioxidant VitE improved its capacity to diminish oxidative stress. This cellular uptake also likely allows SQAd/VitE NPs to generate the active adenosine in a localized manner after hydrolysis of SQAd(30).

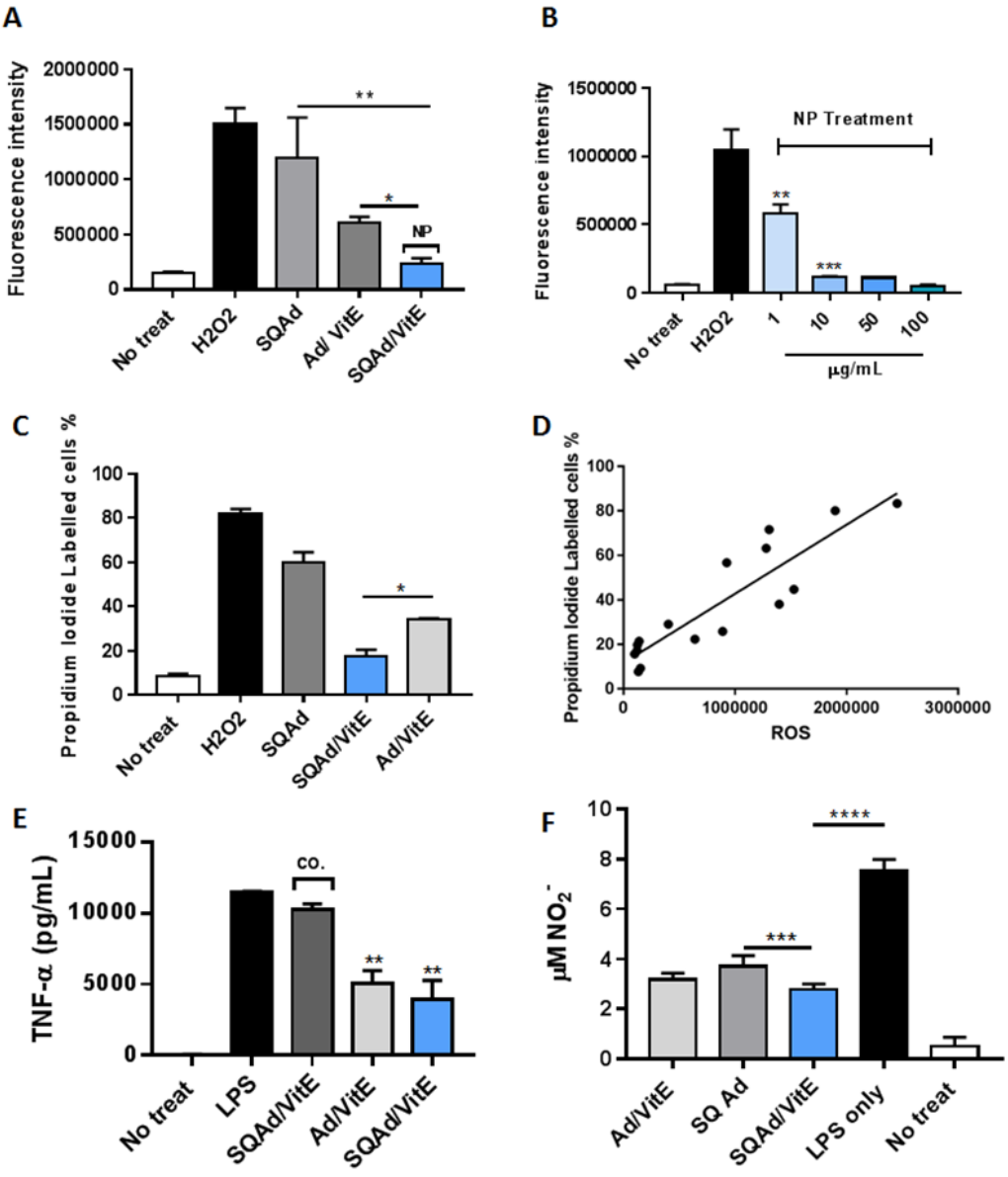

Figure 4. *In vitro* antioxidant and anti-inflammatory properties of SQAd/VitE NPs. (**A**) Fluorescent detection of ROS in H9c2 cells showing that SQAd/VitE NPs efficiently scavenge intracellular ROS compared to free-drug or single-drug controls. (**B**) Dose dependence of the ROS protective effect of SQAd/VitE NPs on H9c2 cells. (**C**) Evaluation of necrotic cell death by propidium iodide staining. (**D**) Correlation of necrotic cell death with the amount of detected intracellular ROS. (**E**) Quantification of pro-inflammatory cytokine TNF-α production in LPS stimulated RAW 264.7 cells treated with SQAd/VitE NPs or controls. Co: SQAd/VitE NPs treatment concurrently to LPS challenge. (**F**) Evaluation of nitrite content in cell medium following LPS stimulation of RAW 264.7 macrophages with or without SQAd/VitE NPs treatment and controls. Data are the mean ± SD n=3 independent experiments. **P*<0.05, ***P*<0.01,

We next evaluated the ability of SQAd/VitE NPs to efficiently inhibit pro-inflammatory signaling.

For this, RAW 264.7 macrophages were used in an *in vitro* LPS-induced inflammation model. RAW macrophages respond to LPS stimulation by releasing pro-inflammatory cytokines(11, 31). Accordingly, when RAW macrophages were stimulated with 1 µg/mL of LPS, a significant increase in TNF-α cytokine was measured in the supernatant. This pro-inflammatory response was inhibited by treatment with SQAd/VitE NPs at a concentration of 10 µg/mL for two hours. Here, SQAd and SQAd/VitE nanoparticles had similar effects on the release of inflammatory cytokines, indicating that adenosine could be the main effector of the observed anti-inflammatory effect (Fig. 4E). Interestingly, when SQAd/VitE treatment was performed simultaneously to the LPS challenge, no significant inhibition of pro-inflammatory signaling was observed, contrary to free drug Ad/VitE. This substantiated the idea that SQAd is not active as an anti-inflammatory agent but needs to be activated in situ to perform anti-inflammatory activity(30).

LPS stimulation of macrophages also causes overproduction of nitric oxide by inducible nitric oxide synthase (iNOS)(32), which results in further pro-inflammatory signaling and oxidative stress by reactive nitrogen species (NOx)(33, 34). Thus, Raw 264.7 macrophages were stimulated with LPS and nitrite accumulation was monitored by Griess reagent to evaluate the consequence of SQAd/VitE NPs treatment on NOx formation. Stimulation by 1 µg/mL LPS resulted in 7.5 µM nitrite content in the supernatant, but NOx production was significantly inhibited after incubation of SQAd/VitE NPs at 10 µg/mL (Fig. 4F). Free drugs Ad/VitE controls also showed efficient inhibition of nitrite accumulation, which likely resulted from free adenosine, acting on its cognate receptors A2A and A2B, inhibiting iNOS expression(35, 36). Interestingly here, there was no difference between pre-treated cells or cells incubated with SQAd/VitE simultaneously to the LPS challenge (data not shown). Noteworthy, nitrite production was significantly lower in SQAd/VitE NPs treated cells compared to cells that only received SQAd. This indicated a synergistic action of SQAd and VitE, concurrently inhibiting the production of NO· and trapping the produced reactive nitrogen species.

Overall, these results showed that multidrug SQAd/VitE NPs could effectively scavenge ROS in a concentration-dependent manner and established effective pro-resolving action through the combined effects of SQAd and VitE *in vitro*. By using a prodrug-based nanoformulation, SQAd/VitE NPs did not trigger adenosine signaling until adenosine release, which could limit deleterious side effects associated with adenosine therapy.

4. In vivo efficacy of SQAd/VitE NPs in endotoxemia model

We then proceeded to evaluate the *in vivo* ability of SQAd/VitE NPs to promote the resolution of inflammation in mice by examining their effect on the acute inflammatory response to endotoxin. In the blood, recognition of LPS by circulating macrophages activates the redox-controlled nuclear factor-κB (NF-κB) by Toll-like receptor 4 (TLR4) mediated mechanisms(37). This event potentiates downstream inflammation cascades, resulting in the pathological "cytokine storm". In our experiments, LPS was injected in mice intraperitoneally, after which blood and organs were collected at various time points to measure the levels of pro-inflammatory and anti-inflammatory cytokines by enzyme-linked immunosorbent assay

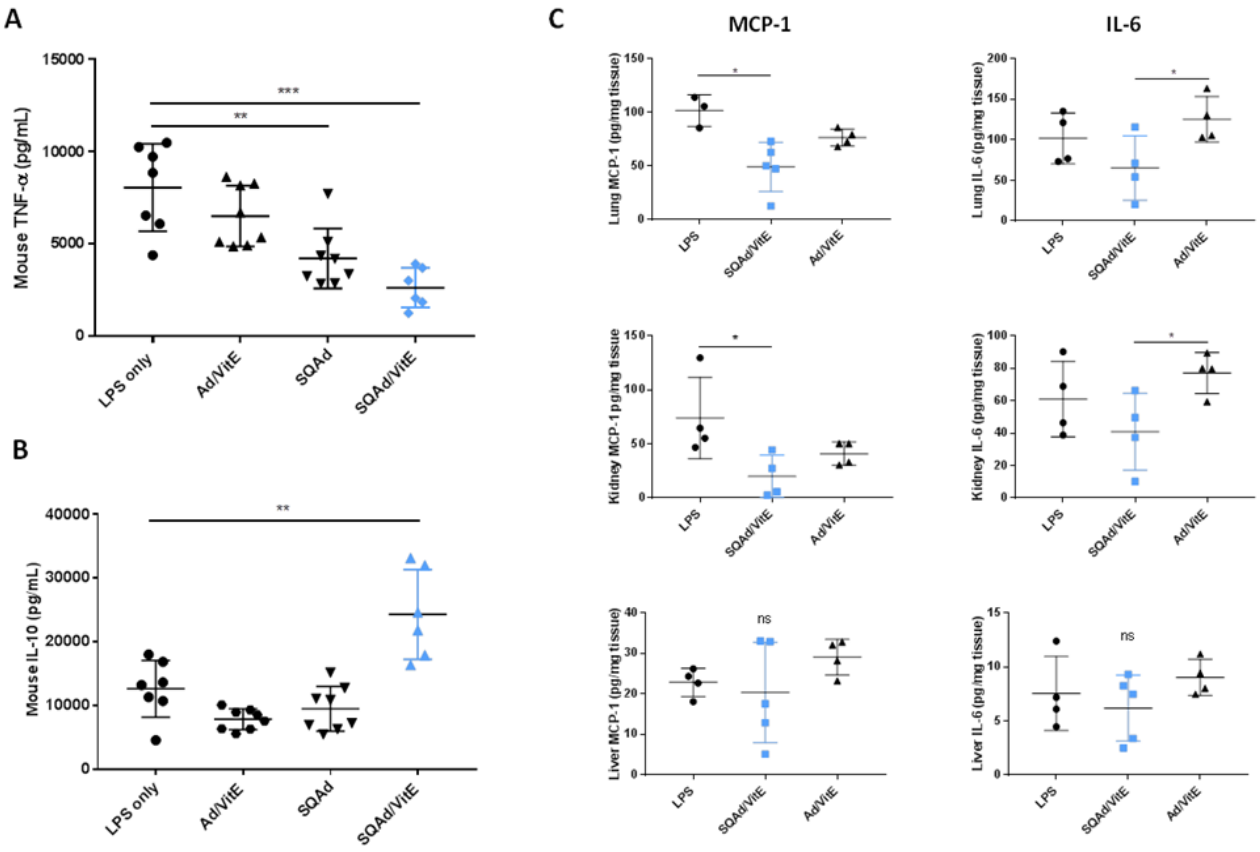

Figure 5. *In vivo* influence of SQAd/VitE NPs on inflammatory cytokines. (**A**) Mouse TNF-α in plasma 1 h after LPS challenge as measured by ELISA. (**B**) Mouse IL-10 in plasma 1 h after LPS challenge as measured by ELISA. (**C**) Pro-inflammatory cytokines including MCP-1 and IL-6 from the Lungs, Liver and Kidneys (n=4), 4 hours after LPS challenge as measured by cytometric bead array. n=4 to 8 mice per group. Data are mean ± SD. ns: non significant,*P<0.05, **P<0.01,***P<0.001 (Student's t-test with Welch's correction, not assuming equal SD).

(*ELISA*). In the blood, pro-inflammatory cytokine levels reached a maximum 1 hour after the LPS challenge, while anti-inflammatory cytokines followed with a peak 2 hours after LPS injection (Supp. Fig. S4). In the treatment group where SQAd/VitE NPs were injected at a dose of 30 mg/kg (corresponding to 5.5 mg/kg of adenosine and 15 mg/kg of VitE), a significant decrease in TNF-α together with an increase in anti-inflammatory IL-10 could be observed, comparatively to control groups that received either no treatment, free drugs Ad/VitE or SQAd NPs only at equivalent doses (Fig. 5A-B). This effect took place in a dose dependent manner (Supp. Fig. S5). Next, we evaluated in organ homogenates the levels of two key pro-inflammatory cytokines MCP-1 and IL-6, responsible, respectively, for recruiting immune cells to the sites of inflammation and mediating the acute phase response (38, 39). In the lungs and kidneys, four hours after the initial LPS challenge, treatment with SQAd/VitE NPs at 30 mg/kg significantly reduced the amount of MCP-1 and IL-6 compared to non-treated or free drugs treated controls (Fig. 5C). In the liver, results failed to reach significance but a tendency for mitigated acute inflammation could be observed.

We next evaluated the antioxidant effects of SQAd/VitE NPs *in vivo*, by measuring the amount of lipid peroxidation products in the lungs following the LPS challenge. During acute systemic inflammation, the immune cells recruited by the extensive pulmonary capillary bed induce high levels of oxidative stress in the lungs, resulting in substantial lipid peroxidation(40, 41). LPS challenge resulted in an increase in lipid peroxidation products as measured by reaction of malondialdehyde (MDA) with thiobarbituric acid (TBARS test) (5.5 nmol MDA/mg protein vs 2.75 nmol MDA/mg protein). This increase was significantly mitigated in the SQAd/VitE NPs treatment group where, MDA levels reached only 4.04 nmol MDA/mg protein (Fig. 6A).

Together, these *in vivo* studies demonstrated an efficient and targeted resolution of inflammation by multidrug SQAd/VitE NPs. While single SQAd NPs did display some efficacy at inhibiting plasma TNF-α, they did not reach the therapeutic efficacy of SQAd/VitE NPs. Contrary to what was observed in *in vitro* studies, *in vivo* free drug Ad/VitE controls consistently failed to induce a significant therapeutic response. This could be explained by the quick metabolization of Ad after a bolus injection (42) and poor bioavailability of VitE. Our prodrug-based nanoparticles thus increased the efficacy of both drugs by simultaneously delivering them to the sites of inflammation.

5. Side effects and efficacy in lethal LPS model

To further validate the *in vivo* capability of SQAd/VitE NPs, we then investigated the hemodynamic effects of SQAd/VitE NPs comparatively to free drugs Ad/VitE. The effects of a

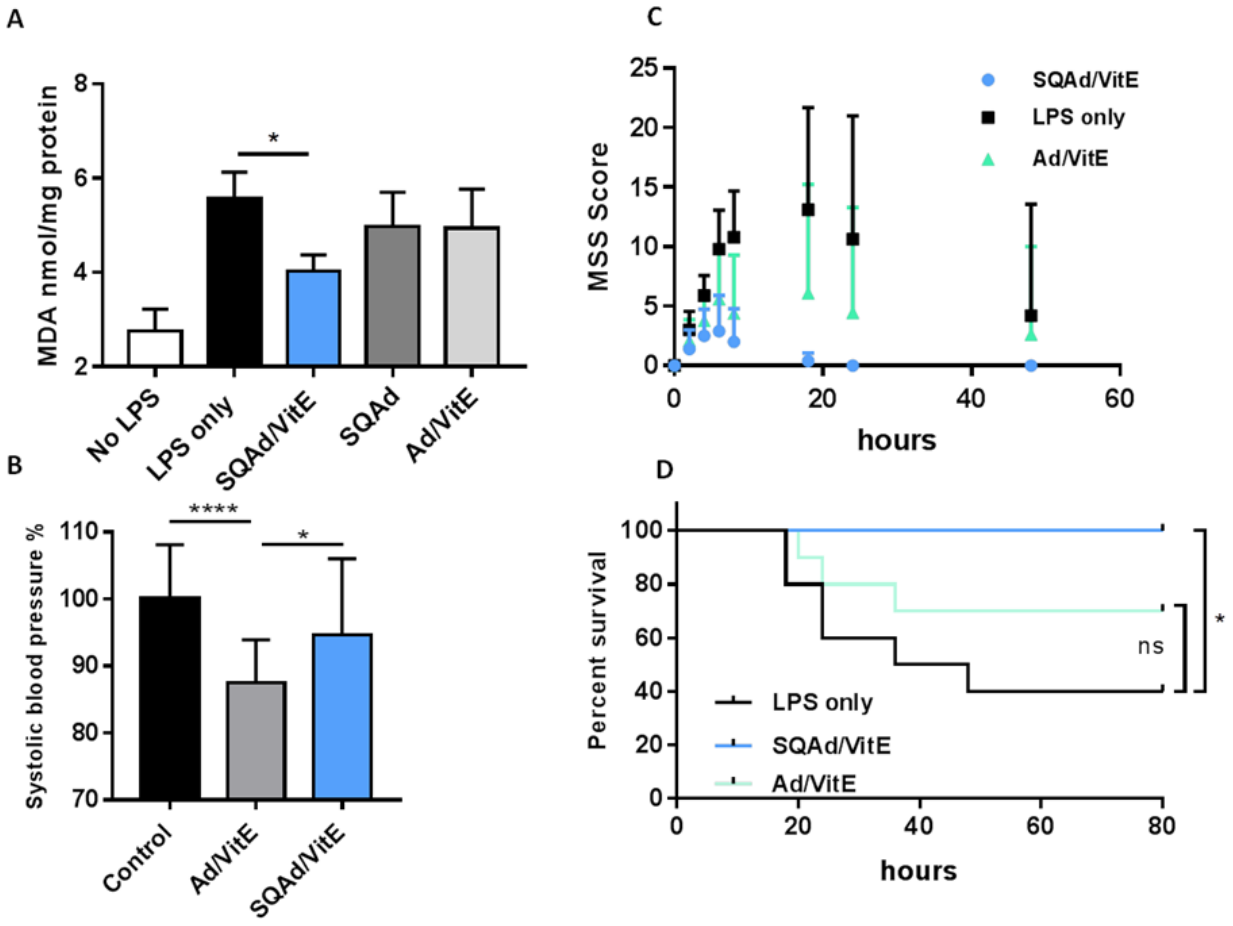

Figure 6. *In vivo* therapeutic efficacy of SQAd/VitE NPs in endotoxemia models. (**A**) Level of lipid peroxidation in the lungs as measured by TBARS quantification of MDA. *n*=3 mice per group (**B**) Systolic blood pressure determination as % of control. *n*=3 animals per group, five measurements per animal. (**C**) MSS clinical score of animals undergoing LPS endotoxemic shock *n*=10 mice per group. (**D**) Survival followed after lethal LPS injection for 80 hours. *n*=10 mice per group. Data are the mean ± SD. ns: non significant, **P*<0.05, ***P*<0.01, ****P*<0.001, *****P*<0.0001 (Student's *t*-test).For survival evaluation, a Log-rank (Mantel-Cox) test was used giving a *P* value *P*=0.0130.

single injection of SQAd/VitE NPs on blood pressure were measured non-invasively. While the nanoparticle encapsulated drugs had no significant effect on blood pressure compared to non-treated controls, free drugs Ad/VitE induced a measurable decrease in blood pressure due to adenosine, in accordance with published literature (Fig. 6B)(43). These results confirmed that the SQAd/VitE nanoparticle formulation helped to protect animals from the deleterious side effects induced by adenosine therapy.

We therefore proceeded to evaluate the efficacy of SQAd/VitE NPs in a model of lethal LPS

challenge(44). Mice in the treatment groups received either SQAd/VitE NPs at a dose of 30 mg/kg or free drugs Ad/VitE at an equivalent dose. In the group treated with SQAd/VitE NPs, all mice survived the lethal LPS challenge, whereas free drug Ad/VitE failed to significantly improve the survival rate, compared to the untreated control animals (Fig. 6D). Improvements in the clinical scores of the animals paralleled the improvements in survival rates for all groups (Fig. 6C). Finally, the consequence of the treatment with SQAd/VitE NPs was histologically investigated regarding signs of inflammation. In the previous LPS lethality model, organs from either SQAd/VitE NPs treated mice or LPS-only treated controls were harvested at the 24 hours point and analyzed for histological signs of tissue stress following hematoxylin and eosin staining. Inflammatory changes including, mononuclear cell infiltration, endothelial disruption and hemorrhage were noticeably reduced in animals that received SQAd/VitE NPs treatment (Fig. 7). In the liver, non-treated animals displayed severe injuries which were not observed in SQAd/VitE NPs treated animals (see also Supp.Fig.S6); these included hemorrhagic sinusal occlusion, advanced hepatocellular stress and disseminated steatosis. In the lungs, although both animal groups showed signs of inflammatory stress, the non-treated animals displayed more advanced loss of structure, alveolar thickening and hemorrhage (Fig. 7).

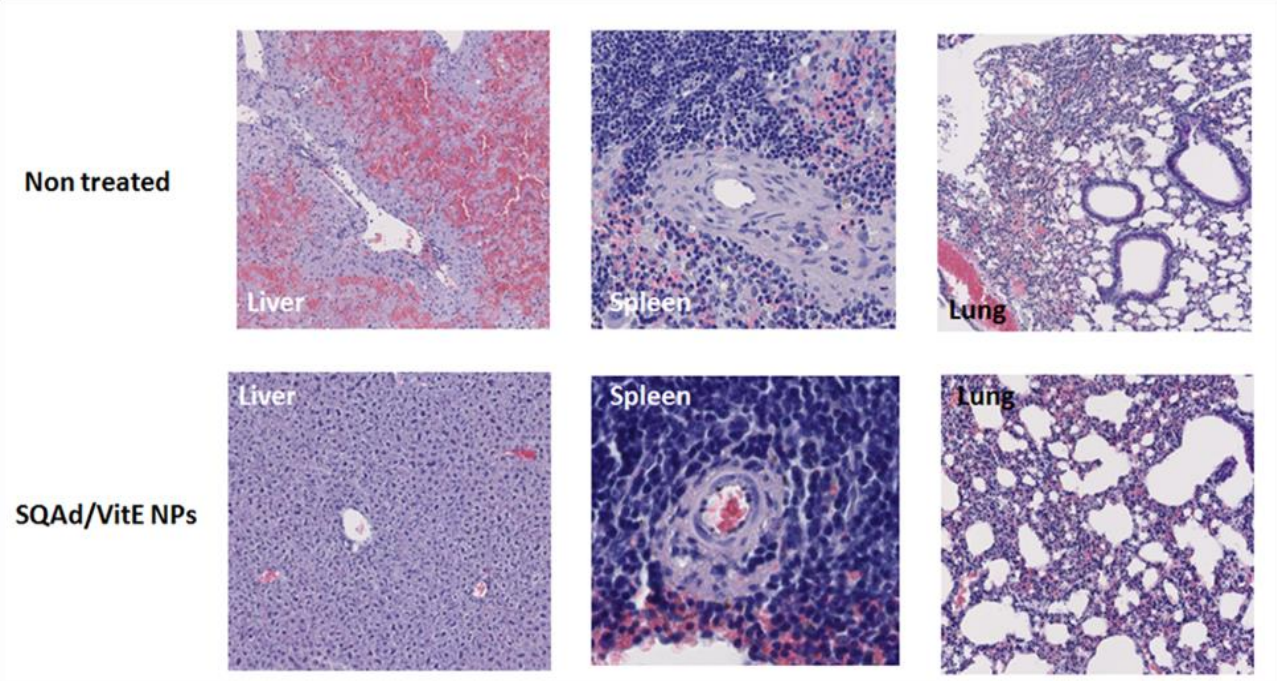

Figure 7. Representative histological images of organ tissue after lethal LPS challenge. Top row contains Liver, spleen and lung samples of animals having received only LPS challenge, bottom row same organs of animals having received SQAd/VitE (30 mg/kg) after LPS challenge. Liver: Non treated groups show widespread hemorrhage and inflammatory cell infiltration. Spleen: Loss of endothelial cells in capillaries correlated with inflammatory stress. Lungs: Alveolar thickening and severe loss of structure in non treated animals.

IV. Conclusion

We presented here the first example of targeted delivery of adenosine, and of multidrug anti-inflammatory/antioxidant nanoparticles, for the mitigation of inflammation. Bioconjugation of adenosine to squalene allowed to obtain a prodrug-based nanocarrier, which, after nanoformulation with VitE yielded stable multidrug nanoparticles improving the bioavailability of both drugs with significant pharmaceutical activity in models of acute inflammatory injury. With the ability to specifically target and deliver adenosine at tissue foci of acute inflammation and the capacity to react with intracellular reactive species at the target site, SQAd/VitE NPs represent a promising therapeutic intervention overcoming limitations of both conventional adenosine and antioxidant therapy. Our extensive in vivo data supports this hypothesis which opens the way to explore the plethora of available specific adenosine receptor

agonists and antioxidants. Overall, these squalene based multidrug nanoparticles represent a unique approach for inhibiting the pathological crosstalk between oxidative stress and inflammation, delivering synergistic therapeutic agents at the loci of inflammation, and thus afford a new tool in the fight against the complex and multi-factorial phenomenon of uncontrolled inflammation.

Acknowledgments

The authors gratefully acknowledge the financial support from the 7th EuroNanoMed-II call for proposals, project NanoHeart n°ANR-16-ENM2-0005-01. This work was further supported by la Fondation pour la Recherche Médicale (FRM) grant number ECO20160736101. The authors also wish to thank Pr. Paul Van Tassel for helpful corrections to the manuscript.

V. References

1. H. Gomez, C. Ince, D. De Backer, P. Pickkers*, et al.*, A unified theory of sepsis-induced acute kidney injury: inflammation, microcirculatory dysfunction, bioenergetics and the tubular cell adaptation to injury. *Shock (Augusta, Ga.)*. 41, 3 (2014)
2. F. Dormont, M. Varna,P. Couvreur, Nanoplumbers: biomaterials to fight cardiovascular diseases. *Materials Today*. 21, 122-143 (2018)
3. R. B. Goodman, J. Pugin, J. S. Lee,M. A. Matthay, Cytokine-mediated inflammation in acute lung injury. *Cytokine & growth factor reviews*. 14, 523-535 (2003)
4. T. Van Der Poll, F. L. Van De Veerdonk, B. P. Scicluna,M. G. Netea, The immunopathology of sepsis and potential therapeutic targets. *Nature Reviews Immunology*. 17, 407 (2017)
5. C. A. Prauchner, Oxidative stress in sepsis: pathophysiological implications justifying antioxidant co-therapy. *Burns*. 43, 471-485 (2017)
6. S. K. Biswas, Does the interdependence between oxidative stress and inflammation explain the antioxidant paradox? *Oxidative medicine and cellular longevity*. 2016, (2016)
7. J. Lugrin, N. Rosenblatt-Velin, R. Parapanov,L. Liaudet, The role of oxidative stress during inflammatory processes. *Biological chemistry*. 395, 203-230 (2014)
8. A. Dandekar, R. Mendez,K. Zhang (2015) Cross talk between ER stress, oxidative stress, and inflammation in health and disease. *Stress Responses*, (Springer), 205-214.
9. B. Gibbison, J. A. López-López, J. P. Higgins, T. Miller*, et al.*, Corticosteroids in septic shock: a systematic review and network meta-analysis. *Critical Care*. 21, 78 (2017)
10. B. N. Cronstein,G. Haskó, Regulation of inflammation by adenosine. *Frontiers in immunology*. 4, 85 (2013)
11. G. Hasko, C. Szabó, Z. H. Németh, V. Kvetan*, et al.*, Adenosine receptor agonists differentially regulate IL-10, TNF-alpha, and nitric oxide production in RAW 264.7 macrophages and in endotoxemic mice. *The Journal of Immunology*. 157, 4634-4640 (1996)

12. U. Söderbäck, A. Sollevi,B. Fredholm, The disappearance of adenosine from blood and platelet suspension in relation to the platelet cyclic AMP content. *Acta physiologica scandinavica*. 129, 189-194 (1987)
13. L. Belardinelli, J. Linden,R. M. Berne, The cardiac effects of adenosine. *Progress in cardiovascular diseases*. 32, 73-97 (1989)
14. H. Mangge, K. Becker, D. Fuchs,J. M. Gostner, Antioxidants, inflammation and cardiovascular disease. *World journal of cardiology*. 6, 462 (2014)
15. H. F. Goode, H. C. Cowley, B. E. Walker, P. D. Howdle*, et al.*, Decreased antioxidant status and increased lipid peroxidation in patients with septic shock and secondary organ dysfunction. *Critical care medicine*. 23, 646-651 (1995)
16. M. M. Berger,R. L. Chioléro, Antioxidant supplementation in sepsis and systemic inflammatory response syndrome. *Critical care medicine*. 35, S584-S590 (2007)
17. E. Borrelli, P. Roux-Lombard, G. E. Grau, E. Girardin*, et al.*, Plasma concentrations of cytokines, their soluble receptors, and antioxidant vitamins can predict the development of multiple organ failure in patients at risk. *Critical care medicine*. 24, 392-397 (1996)
18. M. É. Andrades, A. Morina, S. Spasić,I. Spasojević, Bench-to-bedside review: sepsis-from the redox point of view. *Critical Care*. 15, 230 (2011)
19. P. E. Marik, V. Khangoora, R. Rivera, M. H. Hooper*, et al.*, Hydrocortisone, vitamin C, and thiamine for the treatment of severe sepsis and septic shock: a retrospective before-after study. *Chest*. 151, 1229-1238 (2017)
20. N. Lane, A unifying view of ageing and disease: the double-agent theory. *Journal of Theoretical Biology*. 225, 531-540 (2003)
21. F. Dormont, M. Rouquette, C. Mahatsekake, F. Gobeaux*, et al.*, Translation of nanomedicines from lab to industrial scale synthesis: The case of squalene-adenosine nanoparticles. *Journal of Controlled Release*. (2019)
22. B. Shrum, R. V. Anantha, S. X. Xu, M. Donnelly*, et al.*, A robust scoring system to evaluate sepsis severity in an animal model. *BMC research notes*. 7, 233 (2014)
23. D. Desmaële, R. Gref,P. Couvreur, Squalenoylation: a generic platform for nanoparticular drug delivery. *Journal of controlled release*. 161, 609-618 (2012)
24. H. Esterbauer, M. Dieber-Rotheneder, G. Striegl,G. Waeg, Role of vitamin E in preventing the oxidation of low-density lipoprotein. *The American journal of clinical nutrition*. 53, 314S-321S (1991)
25. L. Hakanpaa, E. A. Kiss, G. Jacquemet, I. Miinalainen*, et al.*, Targeting β1-integrin inhibits vascular leakage in endotoxemia. *Proceedings of the National Academy of Sciences*. 115, E6467-E6476 (2018)
26. E. A. Azzopardi, E. L. Ferguson,D. W. Thomas, The enhanced permeability retention effect: a new paradigm for drug targeting in infection. *Journal of Antimicrobial Chemotherapy*. 68, 257-274 (2012)
27. B. Halliwell,J. M. Gutteridge (2015) *Free radicals in biology and medicine* (Oxford University Press, USA).
28. A. Gaudin, O. Tagit, D. Sobot, S. Lepetre-Mouelhi*, et al.*, Transport mechanisms of squalenoyl-adenosine nanoparticles across the blood–brain barrier. *Chemistry of Materials*. 27, 3636-3647 (2015)
29. H. F. Galley, Bench-to-bedside review: targeting antioxidants to mitochondria in sepsis. *Critical care*. 14, 230 (2010)
30. M. Rouquette, S. Lepetre-Mouelhi, O. Dufrançais, X. Yang*, et al.*, Squalene-adenosine nanoparticles: ligands of adenosine receptors or adenosine prodrug? *Journal of Pharmacology and Experimental Therapeutics*. 369, 144-151 (2019)
31. D. J. Wadleigh, S. T. Reddy, E. Kopp, S. Ghosh*, et al.*, Transcriptional activation of the cyclooxygenase-2 gene in endotoxin-treated RAW 264.7 macrophages. *Journal of Biological Chemistry*. 275, 6259-6266 (2000)
32. A. T. Jacobs,L. J. Ignarro, Lipopolysaccharide-induced expression of interferon-β mediates the timing of inducible nitric-oxide synthase induction in RAW 264.7 macrophages. *Journal of Biological Chemistry*. 276, 47950-47957 (2001)
33. R. Korhonen, A. Lahti, H. Kankaanranta,E. Moilanen, Nitric oxide production and signaling in inflammation. *Current Drug Targets-Inflammation & Allergy*. 4, 471-479 (2005)

34. K. Hensley, K. A. Robinson, S. P. Gabbita, S. Salsman*, et al.*, Reactive oxygen species, cell signaling, and cell injury. *Free Radical Biology and Medicine*. 28, 1456-1462 (2000)
35. C. Brodie, P. M. Blumberg,K. A. Jacobson, Activation of the A2A adenosine receptor inhibits nitric oxide production in glial cells. *FEBS letters*. 429, 139-142 (1998)
36. D. Yang, Y. Zhang, H. G. Nguyen, M. Koupenova*, et al.*, The A 2B adenosine receptor protects against inflammation and excessive vascular adhesion. *The Journal of clinical investigation*. 116, 1913-1923 (2006)
37. M. A. Dobrovolskaia,S. N. Vogel, Toll receptors, CD14, and macrophage activation and deactivation by LPS. *Microbes and Infection*. 4, 903-914 (2002)
38. S. L. Deshmane, S. Kremlev, S. Amini,B. E. Sawaya, Monocyte chemoattractant protein-1 (MCP-1): an overview. *Journal of interferon & cytokine research*. 29, 313-326 (2009)
39. P. Damas, D. Ledoux, M. Nys, Y. Vrindts*, et al.*, Cytokine serum level during severe sepsis in human IL-6 as a marker of severity. *Annals of surgery*. 215, 356 (1992)
40. C.-W. Chow, M. T. Herrera Abreu, T. Suzuki,G. P. Downey, Oxidative stress and acute lung injury. *American journal of respiratory cell and molecular biology*. 29, 427-431 (2003)
41. K. Sato, M. B. Kadiiska, A. J. Ghio, J. Corbett*, et al.*, In vivo lipid-derived free radical formation by NADPH oxidase in acute lung injury induced by lipopolysaccharide: a model for ARDS. *The FASEB Journal*. 16, 1713-1720 (2002)
42. E. Snoeck, K. Ver Donck, P. Jacqmin, H. Van Belle*, et al.*, Physiological red blood cell kinetic model to explain the apparent discrepancy between adenosine breakdown inhibition and nucleoside transporter occupancy of draflazine. *Journal of Pharmacology and Experimental Therapeutics*. 286, 142-149 (1998)
43. U. Flögel, S. Burghoff, P. L. Van Lent, S. Temme*, et al.*, Selective activation of adenosine A2A receptors on immune cells by a CD73-dependent prodrug suppresses joint inflammation in experimental rheumatoid arthritis. *Science translational medicine*. 4, 146ra108-146ra108 (2012)
44. B. E. Barton,J. V. Jackson, Protective role of interleukin 6 in the lipopolysaccharide-galactosamine septic shock model. *Infection and immunity*. 61, 1496-1499 (1993)

Supplementary Data

Synthesis of SQRho

SQRho was synthesized by direct acylation of the piperazine-rhodamine B after *in situ* formation of chloroformate mixed anhydride of trisnorsqualenic acid.

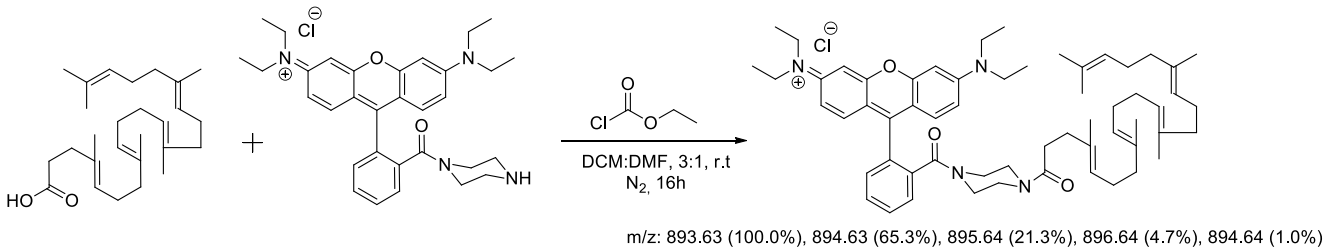

Supp. Fig. S1. Synthesis scheme for SQRho

To a solution of ethyl chloroformate (30 µL, 0.33 mmol) in anhydrous DCM (1 mL) was added Et3N (90 µL, 0.6 mmol). The mixture was cooled at 0 °C and a solution of trisnorsqualenic acid (120 mg, 0.30 mmol) in anhydrous DCM (2 mL) was added dropwise. Mixture was stirred for 30 min at 0 °C and a solution of rhodamine B piperazine (181 mg, 0.33 mmol) in DMF (1 mL) was added dropwise. After being stirred at room temperature for 16h, DMF was removed under vaccum. The residue was taken up in sat. NaHCO3 aqueous solution (4 mL) and extracted with AcOEt (3 × 15 mL). The combined organic layers were washed with brine, dried over MgSO4 and concentrated under reduced pressure. The crude was then purified by flash chromatography on silica (CH2Cl2/Methanol from 100:0 to 90:10). Fraction containing the expected product were concentrated to provide rhodamine B 4-(1,1',2-trisnorsqualenoyl)piperazine (140 mg, 56%) as a dark purple glassy solid.

1 H NMR (300 MHz, MeOD, δ in ppm): 7.76 (2H, m, H-4', H-5'), 7.70 (1H, m, H3'), 7.52 (1H, m, H-6'), 7.27 (2H, d, J = 9.5 Hz, H-1, H-8), 7.09 (2H, dd, J = 9.5 Hz, J = 2.1 Hz, H-2, H-7), 6.97 (2H, d, J = 2.4 Hz, H-4, H-5), 5.06–5.20 (5H, m, HC=C(CH3)CH2), 3.71 (8H, q, J = 7.1 Hz, H3CCH2N), 3.35–3.50 (8H, m, NCH2CH2N), 2.44 (2H, t, J= 9 Hz NOCCH2CH2), 2.21 (2H, t,J= 9Hz NOCCH2CH2), 2.13–1.93 (16H, m, =C(CH3)CH2CH2CH=), 1.68 (3H, s, HC=C(CH3)2), 1.61 (12H, s, HC=C(CH3)), 1.31 (12H, t, J = 7.1 Hz, H3CCH2N)

Formulation of fluorescent SQAd/VitE NPs

Fluorescent SQAd/VitE NPs were prepared by the nanoprecipitation method (see Materials and Methods) after adding 1% of fluorescent probe (either DiD or SQRho) to the organic phase.

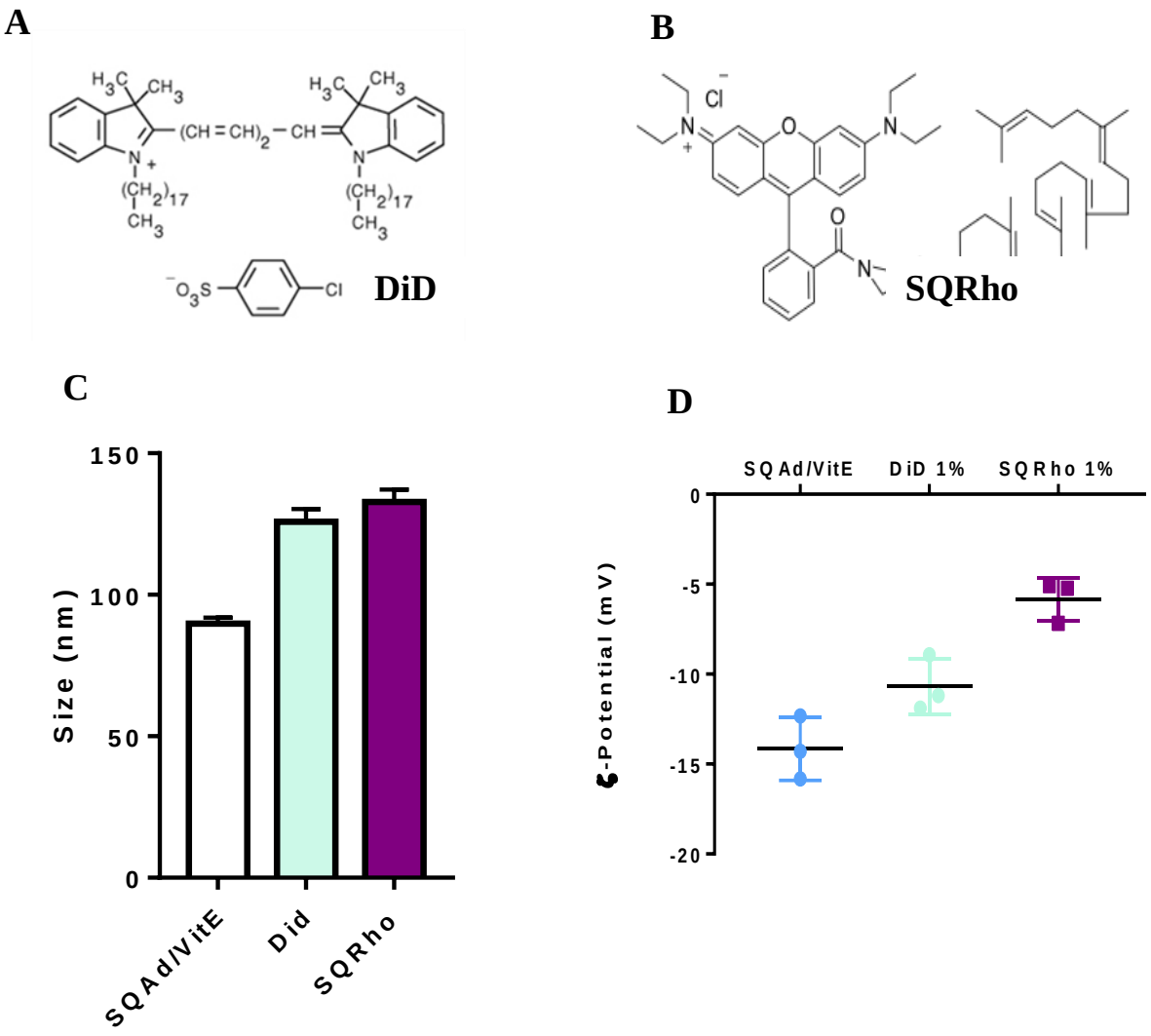

Supp. Fig. S2. Characterization of fluorescent SQAd/VitE NPs. (**A**) Structure of 1,1′-dioctadecyl-3,3,3′,3′- tetramethylindodicarbocyanine perchlorate (DiD) (**B**) Structure of SQRho (**C**) Hydrodynamic size of fluorescently labeled SQAd/VitE NPs (diameter, nanometers) measured by dynamic light scattering (DLS). (**D**) Measurement of surface ζ-potential of fluorescently labeled SQAd/VitE NPs.

Cellular uptake of fluorescent SQAd/VitE NPs

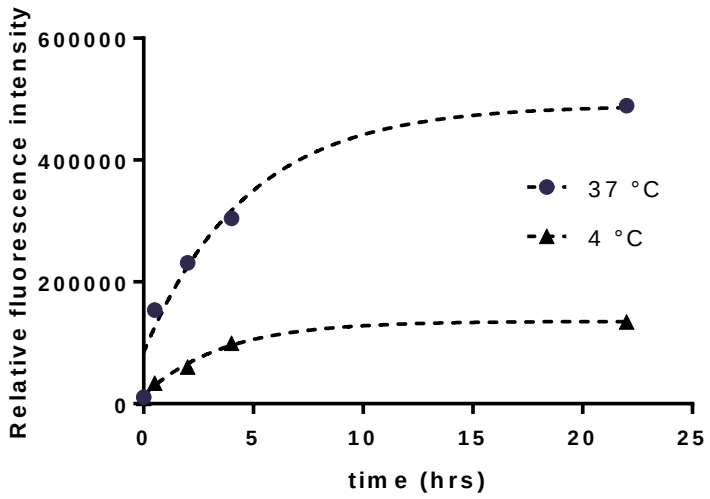

Supp. Fig. S3. H9c2 cells/well (26 000 cells/ cm2) were seeded in 12-well plates and cultured for 24 h at 37°C. The cells were then incubated at 37 °C or 4°C with fluorescent SQRho tagged SQAd/VitE NPs diluted in cell culture medium for different durations. At the end of the incubation period, cells were washed with 1 mL of PBS and then treated with 300 µL of 0.25% trypsin solution for 5 min at 37 °C and 5% CO2. Trypsin solution was diluted by adding 0.7 mL of medium, and the fluorescence of the cells was recorded using a flow cytometer C6 (Accuri Cytometers Ltd.). For fluorescence detection of SQ-Rho labeled NPs, excitation was carried out using a 488 nm argon laser and emission fluorescence was measured at 515 nm. 10 000 cells were measured for each sample. The results were expressed as the mean relative fluorescence intensity (MFI) ± SEM.

Pro and anti-inflammatory cytokine kinetics after LPS challenge

The levels of different cytokines were assessed in the plasma by ELISA after initial LPS challenge (7.5 mg/kg)

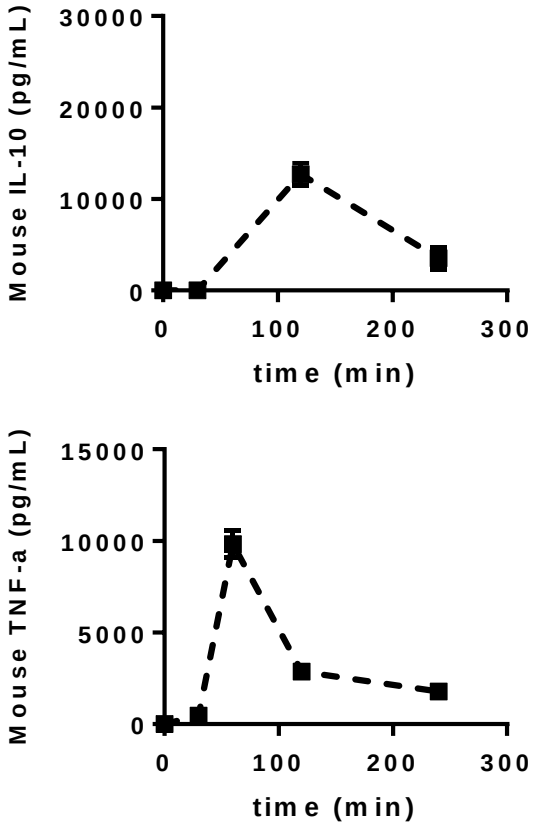

Supp. Fig. S4. TNF-α and IL-10 levels in plasma of untreated 8-wk-old male C57BL6 mice after LPS challenge. Endotoxemia was induced by intraperitoneal injection of a 7.5 mg/kg dose of LPS (Sigma O111:B4) diluted at 1.875 mg/mL in buffered saline. Following LPS injections, blood samples (~50 µL) were collected at predetermined time points via submandibular puncture. Plasma was obtained by centrifuging blood samples at 2000 rcf for 10 min and stored at –78°C before further analysis. Cytokines levels were quantified by Biolegend ELISA mouse kit per manufacturer instructions.

Dose dependency of SQAd/VitE NPs effect on cytokines in vivo.

Animals received SQAd/VitE NPs treatment (15 mg/kg or 30 mg/kg) after initial LPS challenge

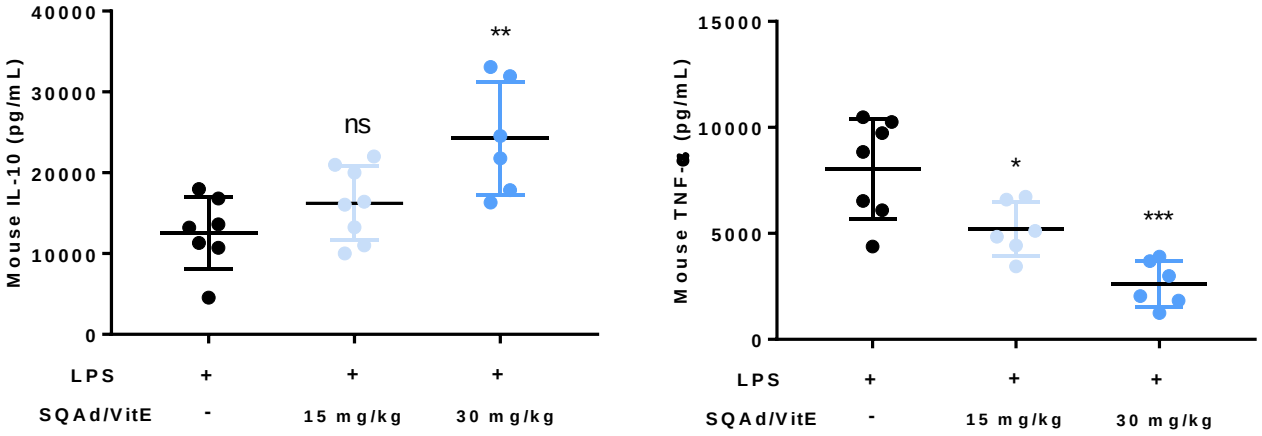

Supp. Fig. S5. Plasma TNF-α and IL-10 levels in 8-wk-old male C57BL6 mice after LPS challenge and SQAd/VitE NPs treatments at 15 mg/kg or 30 mg/kg. Endotoxemia was induced by intraperitoneal injection of a 7.5 mg/kg dose of LPS (Sigma O111:B4) diluted at 1.875 mg/mL in buffered saline. Following LPS injections, blood samples (~50 µL) were collected at 1h after NPs injection via submandibular puncture. Data are mean ± SD. ns: non significant,*P<0.05, **P<0.01,***P<0.001 (Student's t-test).

Anti-inflammatory efficacy of SQAd/VitE NPs.

After lethal LPS challenge, Liver of treated vs non treated animals were compared for signs of disease severity.

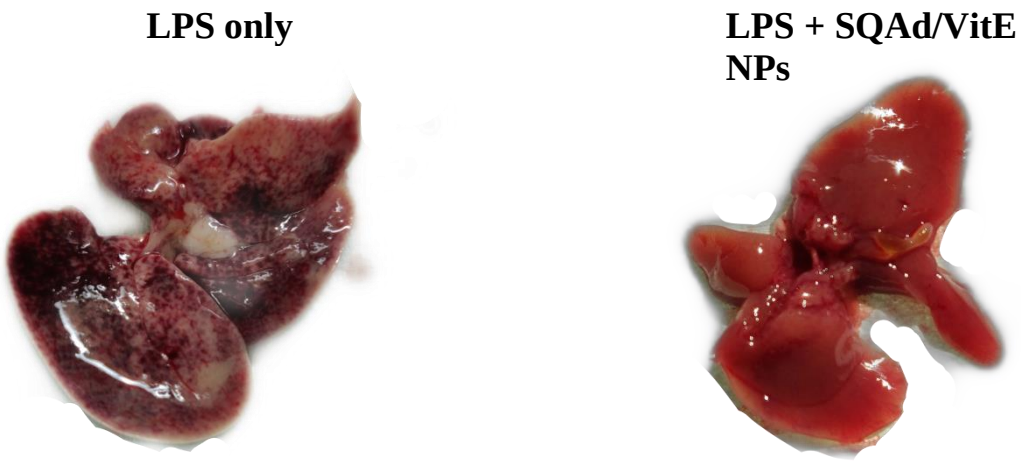

Supp. Fig. S6. Liver of non-treated vs treated animal in lethal LPS challenge model. C57BL/6J mice (n=10 animals/group) were sensitized to the lethal effects of LPS by i.p. injection of 8 mg of D-galactosamine hydrochloride. A single i.p. dose of LPS at 2 μg/kg caused 60% mortality within 48 hours. Mice in the treatment groups received SQAd/VitE NPs i.v. at a dose of 30 mg/kg and the liver was visually compared to LPS only treated animals.

Chapter 2

Squalene-based nanoparticles for the targeting of atherosclerotic lesions

Romain Brusini[a,1], Flavio Dormont[a,1], Catherine Cailleau[a], Arnaud Peramo[a], Mariana Varna[a], Patrick Couvreur[a]*

[1] These authors contributed equally to this work.

[a] Institut Galien Paris-Sud, CNRS UMR 8612, Université Paris-Sud, Université Paris-Saclay, 92296 Châtenay-Malabry, France

Squalene-based nanoparticles for the targeting of atherosclerotic lesions

Abstract

Native low-density lipoproteins (LDL) naturally accumulate at atherosclerotic lesions and are thought to be among the main drivers of atherosclerosis progression. Numerous nanoparticular systems making use of recombinant lipoproteins have been developed for targeting atherosclerotic plaque. These innovative formulations often require complicated purification and synthesis procedures which limit their eventual translation to the clinics. Recently, squalenoylation has appeared as a simple and efficient technique for targeting agents to endogenous lipoproteins through a bioconjugation approach. In this work, we develop a fluorescent squalene bioconjugate to evaluate the biodistribution of squalene-based nanoparticles in an ApoE$^{-/-}$ model of atherosclerosis. By accumulating in LDL endogenous nanoparticles, the squalene bioconjugation could serve as an efficient targeting platform for atherosclerosis. Indeed, in this proof of concept, we show that our squalene-rhodamine (SQRho) nanoparticles, could accumulate in the aortas of atherosclerotic animals. Histological evaluation confirmed the presence of atherosclerotic lesions and the collocalisation of SQRho bioconjugates at the lesions sites.

I. Introduction

The adequate management of atherosclerosis is one of the major health challenges in modern medicine. Although lipid-lowering drugs have been applied successfully for the past 25 years, novel strategies focused on directly detecting and treating vessel wall inflammation, a hallmark of atherosclerosis, are being developed(1, 2). In this context, therapeutic and diagnostic nanomaterials are being actively studied for their ability to target atherosclerotic lesions and specifically deliver molecules of interest(3-5). Among these, recombinant lipoprotein-based nanoparticles have garnered attention for their innate interaction with atherosclerotic plaque(6-8). Low-density Lipoproteins (LDL) are cholesterol-rich (40-50% w/w) cargo vehicles for the delivery of cholesterol to peripheral tissues. They consist of a lipid rich core surrounded by a monolayer of amphiphilic phospholipids and apolipoproteins (ApoB100 and ApoE). In the body, LDL naturally accumulate in atherosclerotic plaques, where they are modified by binding to proteoglycans or remnant reactive oxygen species, which enhances their recognition by macrophages via a number of unregulated receptors such as scavenger receptor A (SRA), lectin-like receptors (LOX-R) and toll-like receptors (TLR4)(9). This triggering of macrophage inflammatory pathways is a critical event in the atherosclerotic lesion development and fuels progression of the disease. Consequently, by taking advantage of this natural interaction between lipoproteins and atherosclerotic plaque several groups have described lipoprotein-like nanoparticles that aim at targeting atherosclerotic lesions. Although this represents a promising strategy, its industrial implementation and economic feasibility remain challenged by the complicated production of these LDL-like nanoparticles.

Recently, our laboratory has pioneered the exploitation of squalene, a metabolic precursor of cholesterol as a biomimetic carrier to specifically interact with LDL(10, 11). When conjugated to squalene, diverse therapeutic agents were shown to interact with lipoproteins in the circulation, thus demonstrating squalene to be an efficient targeting agent for these endogenous lipoproteins particles. This elegant approach exploiting LDL as indirect natural carriers towards LDL receptor expressing cells could therefore be used to direct diverse therapeutic agents to atherosclerotic plaque, exploiting the natural accumulation of LDL at these sites.

In this work, we investigated a proof-of-concept of this technology by using fluorescent squalene bioconjugates and evaluating their biodistribution in *in vivo* models of atherosclerosis

using ApoE$^{-/-}$ mice. Our preliminary data shows efficient targeting of atherosclerotic plaque although more studies are required to confirm our hypothesis.

II. Materials and Methods

1. Synthesis of SQRho

SQRho was synthesized by direct acylation of the piperazine-rhodamine B after *in situ* formation of chloroformate mixed anhydride of trisnorsqualenic acid. To a solution of ethyl chloroformate (30 µL, 0.33 mmol) in anhydrous DCM (1 mL) was added Et3N (90 µL, 0.6 mmol). The mixture was cooled at 0 °C and a solution of trisnorsqualenic acid (120 mg, 0.30 mmol) in anhydrous DCM (2 mL) was added dropwise. Mixture was stirred for 30 min at 0 °C and a solution of rhodamine B piperazine (181 mg, 0.33 mmol) in DMF (1 mL) was added dropwise. After being stirred at room temperature for 16h, DMF was removed under vaccum. The residue was taken up in sat. NaHCO3 aqueous solution (4 mL) and extracted with AcOEt (3 × 15 mL). The combined organic layers were washed with brine, dried over MgSO4 and concentrated under reduced pressure. The crude was then purified by flash chromatography on silica (CH2Cl2/Methanol from 100:0 to 90:10). Fraction containing the expected product were concentrated to provide rhodamine B 4-(1,1',2-trisnorsqualenoyl)piperazine (140 mg, 56%) as a dark purple glassy solid.

1 H NMR (300 MHz, MeOD, δ in ppm): 7.76 (2H, m, H-4', H-5'), 7.70 (1H, m, H3'), 7.52 (1H, m, H-6'), 7.27 (2H, d, J = 9.5 Hz, H-1, H-8), 7.09 (2H, dd, J = 9.5 Hz, J = 2.1 Hz, H-2, H-7), 6.97 (2H, d, J = 2.4 Hz, H-4, H-5), 5.06−5.20 (5H, m, HC=C(CH3)CH2), 3.71 (8H, q, J = 7.1 Hz, H3CCH2N), 3.35−3.50 (8H, m, NCH2CH2N), 2.44 (2H, t, J= 9 Hz NOCCH2CH2), 2.21 (2H, t,J= 9Hz NOCCH2CH2), 2.13−1.93 (16H, m, =C(CH3)CH2CH2CH=), 1.68 (3H, s, HC=C(CH3)2), 1.61 (12H, s, HC=C(CH3)), 1.31 (12H, t, J = 7.1 Hz, H3CCH2N)

2. Nanoparticle synthesis

Squalene-rhodamine nanoparticles (SQRho NPs) were prepared by nanoprecipitation, as previously described. Briefly, SQRho and squalenic acid (SQCOOH) were separately dissolved in absolute ethanol (6 mg/mL) and mixed in different ratios to obtain a final organic solution with constant 6 mg/mL concentration. This organic solution was added dropwise under moderate mechanical stirring to a 5% (w/v) dextrose solution (DXT 5%). The ethanol was then completely evaporated using a Rotavapor (90 rpm, 40 °C, 42 mbar) to obtain an aqueous suspension of pure NPs (2 mg/mL). NPs size (hydrodynamic diameter) and surface charge (zeta potential) were measured using a Malvern Zetasizer Nano ZS 6.12 (173° scattering angle, 25 °C,

Material RI: 1.49, Dispersant Viscosity RI: 1.330, Viscosity 0.8872 cP). For the size measurements by dynamic light scattering (DLS), a good attenuator value (7−9) was obtained when suspending 50 µL of NPs in 1 mL of distilled water. The mean diameter for each preparation resulted from the average of three measurements of 60 s each. For zeta potential measurements, 70 µL of NPs was dissolved in 2 mL of KCl 1 mM before filling the measurement cell. The mean zeta potential for each preparation resulted from the average of three measurements in automatic mode, followed by the application of the Smoluchowski equation. NP stability was assessed by measuring NP size by DLS at different time intervals after initial formulation up to five days.

3. **Cell Internalization of NPs.**

Flow Cytometry. A total of 50 000 Raw 264.7 cells/well (26 000 cells/ cm2) were seeded in 12-well plates and cultured for 24 h at 37°C. The cells were then incubated with 100 µM fluorescent SQRho NPs diluted in cell culture medium. At the end of the incubation period, cells were washed with 1 mL of PBS and then treated with 300 µL of 0.25% trypsin solution for 5 min at 37 °C and 5% CO2. Trypsin solution was diluted by adding 0.7 mL of medium, and the fluorescence of the cells was recorded using a flow cytometer C6 (Accuri Cytometers Ltd.). For fluorescence detection of SQ-Rho labeled NPs, excitation was carried out using all four available channels. 10 000 cells were measured for each sample. The results were expressed as the mean fluorescence intensity (MFI) ± SEM.

Confocal Microscopy. A total of 200 000 RAW cells/well (100 000 cells/cm2) were seeded on 12 mm glass coverslips in 6-well plates. Cells were grown for 24 hours in order to adhere to the glass slip, and then incubated with 100 µM of SQ-Rho labeled fluorescent SQAd NPs diluted in culture medium. At the end of the incubation period, cells were washed with 1 mL of PBS and fixed with 4% PFA for 15 min. Residual PFA was then neutralized by NH4Cl 50 mM for another 15 min before mounting on microscopy slides. Slides were imaged with an inverted LSM510 Zeiss confocal microscope using a PlanApochromat 63X objective lens (NA 1.40, oil immersion) and lasers at 488 nm (green NAs) or 543 nm (red NAs). Pinhole was set at 61 µm giving an optical section thickness of 0.6 µm. Numerical images were acquired with LSM 510 software version 3.2 and further image analysis was made using ImageJ software

4. *In vivo* experiments

The targeting efficacy of SQRho NPs was evaluated *in vivo* in a ApoE$^{-/-}$ knockout mouse model of atherosclerosis. 8 week-old male C57BL/6J ApoE$^{-/-}$ mice were fed with Western Diet chow for at least 12 weeks for the development of atherosclerotic lesions and used aged 52 weeks. Wild-type C57BL/6J 8-12 week old mice were used as controls. At the onset of the experiment, SQRho diluted at 4 mg/mL in 5% dextrose solution were intravenously injected at a dose of 15 mg/kg through the suborbital vein. After 24 hours, the mice were euthanized by intraperitoneal injection of a lethal dose of sodium pentobarbital, organs and aortas were harvested and immediately imaged using a IVIS Lumina LT Series III system (Caliper Life Science) using 540 nm excitation and 620 nm emission filters. Images and measures of fluorescence signals were acquired and analyzed with Living Imaging software (Caliper Life Sciences).

5. Immuno fluorescence stainings

To evaluate the targeted cells by the SQRho NPs, anti-alpha smooth muscle actin, anti-CD64 and anti-CD36 antibodies (BioLegend) were respectively used as markers of activated smooth muscle cells, macrophages or endothelial cells. Anti-CD36 antibody was diluted at 1/200, anti-CD64 and anti-alpha smooth muscle actin antibodies were diluted at 1/100, and corresponding secondary antibodies were diluted at 1/1000. For all the conditions tested, a negative control was performed by omitting the primary antibody.

Following IVIS imaging, the collected aortas were divided in small samples (from 2 to 10mm), fixed with 4% PFA solution for 24h and then frozen and stored at -80°C. The frozen samples were then cut in 5µm thick histological sections. Tissue sections were rehydrated in PBS, treated with 0.2% triton solution for 3 min at room temperature (RT) for membrane permeabilization, and blocked with 1% Bovine Serum Albumin (BSA) for 30min at RT. Then, diluted primary antibodies in TBS were applied for 2h to 3h at RT, followed by diluted secondary antibodies for 1h30 to 2h at RT. A gentle washing of the slides for 2 x 5min was performed between each steps and the slides were kept in the dark during all the treatments incubation times. Finally, slides were mounted using compatible mounting medium and coverslip.

III. Results and Discussion

1. Nanoparticle synthesis

Nanoparticle-based carriers enable target-specific drug delivery or imaging in a number of conditions. Previous studies from our lab have shown that squalene bioconjugate-based nanoparticles display unique LDL-targeting properties which could be exploited to accumulate these nano-vectors at sites of atherosclerotic plaque development. Fluorescent squalene nanoparticles were synthesized using a nanoprecipitation technique after synthesis of a squalene-rhodamine (SQRho) bioconjugate. Efficient conjugation of Rhodamine to squalene was achieved after functionalization of rhodamine with piperazine, affording Rhodamine-piperazine, which could then be coupled to squalene-acetic acid in satisfying yield (56%) (Figure 1A). SQRho does not form on its own nanoparticles with satisfying stability and physico-chemical features and needs to be stabilized by coprecipitation with squalenic acid (SQCOOH). In this approach, SQCOOH and SQRho were solubilized in an ethanolic solution at different ratios, and then nanoprecipitated in a 5% dextrose solution under vigorous stirring. Upon mixture of the different solutions, instatenous self-assembly of NPs occurred. Nanoparticle size was controlled by carefully modifying SQRho:SQCOOH ratios. Thus, SQRho NPs could be produced with a substantial hydrodynamic size range. By varying the SQRho:SQCOOH ratio from 50-90% we were able to synthesize stable nanoparticles ranging from 210 to 58 nm (Figure 1B). Zeta potential of the nanoparticles was also determined and ranged from +2.4 mV to + 40 mV (Figure 1C). This could be explained by the fact that, at physiological pH, SQCOOH bears a negative charge offsetting the positive charge of Rhodamine. With increasing SQCOOH content in the nanoparticles, the positive rhodamine charge is offset, leading to a lower absolute zeta potential and poorer colloidal stability. A ratio of SQRho:SQCOOH 82:18 wt% was found to be satisfying to obtain stable formulations of the desired mean hydrodynamic diameter and size distribution (thereafter named SQRho NPs). SQ-Rho nanoparticles stability was evaluated in PBS over 5 days by DLS (Figure 1D). Therefore, and as we have done previously, stable multi-bioconjugate nanoparticles were obtained and could allow to study squalene biodistribution.

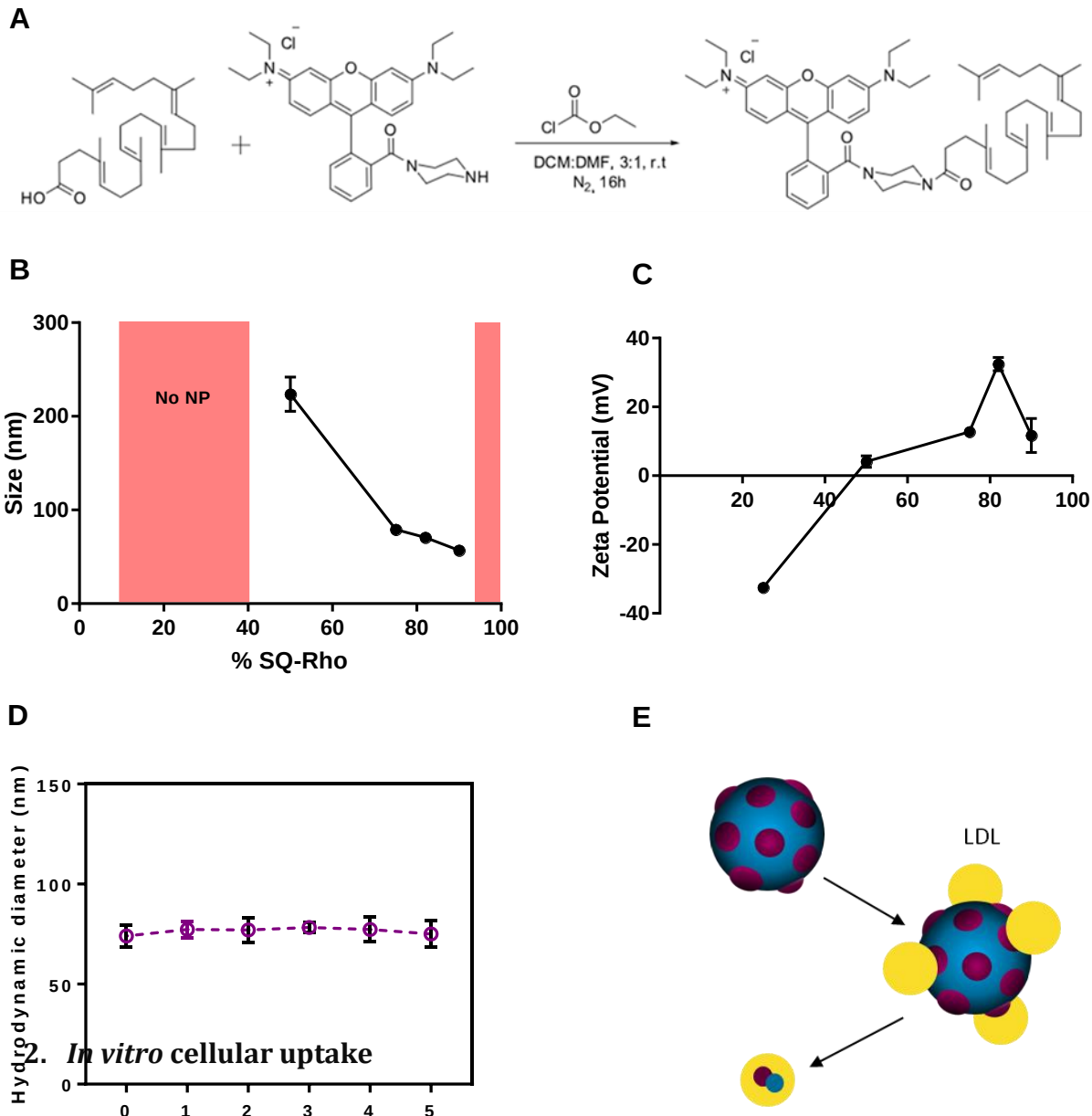

2. *In vitro* cellular uptake

We set out to investigate if our nanoparticle could take advantage of certain biological properties of LDL such as accumulation in plaque resident macrophages. Squalene is a

Figure 1 : (**A**) Scheme of rhodamine-piperazine coupling with squalenic acid. (**B**) Hydrodynamic size of SQRho:SQCOOH NPs (diameter, nanometers) measured by dynamic light scattering (DLS). (**C**) Measurement of surface ζ-potential of SQRho:SQCOOH Nps. (**D**) Stability study of SQRho: SQCOOH (82:18 wt %) in PBS over 5 days. (**E**) Supposed LDL interation of squalene-bioconjugate based nanoparticles with endogenous LDL.

found to gradually accumulate inside of cells over time (Figure 2C). This was confirmed by confocal imaging which showed pockets of fluorescence inside of RAW 264.7 cells where endosomes accumulate the fluorescent endocyted material (Figure 2A-B). When cells were incubated with SQRho at 4 °C instead of 37°C, cell fluorescence intensity dramatically decreased pointing to endocytosis as the major pathway of cell internalization for SQRho NPs.

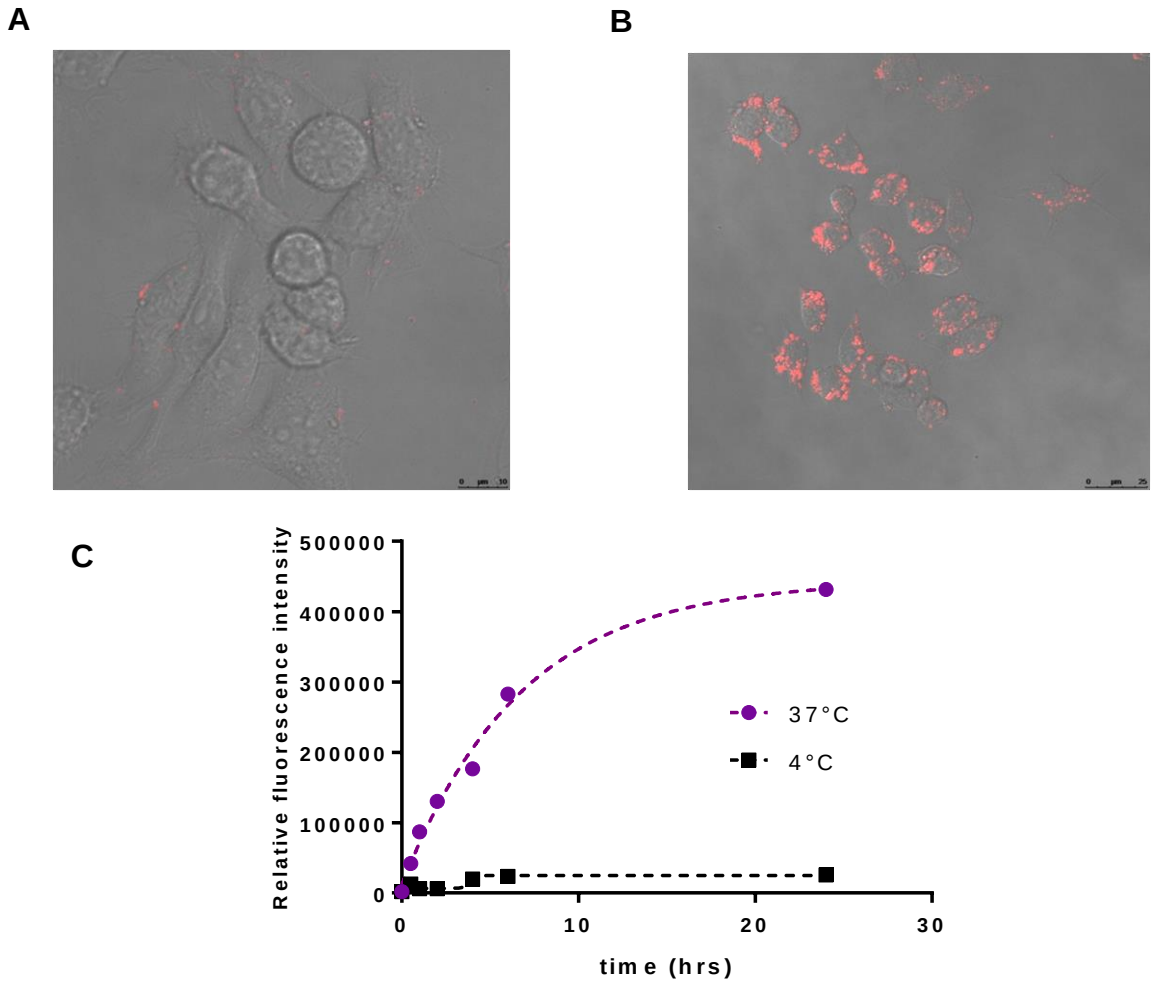

Figure 2: (**A**) Phase contrast confocal microscopy image of RAW 264.7 macrophages incubated with 100 µM of SQRho for 30 min. Scale bar= 10 µm. (**B**) Phase contrast confocal microscopy image of RAW 264.7 macrophages incubated with 100 µM of SQRho for 4 hrs. Scale bar= 10 µm. (**C**) Flow cytometry of RAW 264.7 microphages incubated with 100 µM of SQRho at different time intervals at 37 °C and 4 °C.

the LDL receptor expressed at the surface of macrophages, and are then endocytosed and trafficked to lysosomes, where cholesteryl ester is hydrolyzed to free cholesterol by acidic lipase. Here, we showed that SQRho bioconjugates accumulated inside of macrophages. Although other nanoparticle types are scavenged by macrophages, the structural similarity of squalene with cholesterol and its ability to specifically interact with endogenous LDL makes it an interesting candidate to target plaque resident macrophages. Another factor that remains to be evaluated is whether SQRho accumulated in macrophages as whole nanoparticles or after partition into LDL.

3. *In vivo* plaque targeting

To assess whether SQRho nanoparticles accumulated in atherosclerotic lesions and were taken up by plaque macrophages *in vivo*, we conducted a biodistribution study on a mouse model of atherosclerosis. ApoE$^{-/-}$ mice are a common model for human atherosclerosis, which features apparition of fatty streaks in atherosclerosis-prone regions and chronic inflammation of the lesions with monocyte infiltration(13, 14). In an initial experiment, the detection limit of our imaging system was evaluated by imaging directly the SQRho NPs in a DXT 5% solution or free SQRho bioconjugates in EtOH solution as % of initial dose (ie. the initial injected dose in a 25g mouse with 2 mL of blood ~ 200µg/mL). In DXT 5% the SQRho NPs fluorescence was found to be detectable to up to 0.01% of the initial dose. In EtOH fluorescence was found to be detectable up to 0.001% of the initial dose (Figure 3A). This pointed to possible quenching phenomena occurring in SQRho NPs as the fluorescent moieties are packed so close together compared to free SQRho bioconjugates in EtOH. Nevertheless-and as quenching might not occur once SQRho bioconjugates disperse in LDL- 0.01% of the initial dose seemed like an acceptable detection limit and we went forward with the *in vivo* experiment.

Wild type C57BL/6J mice or ApoE$^{-/-}$ mice were injected with SQRho nanoparticles and the biodistribution of the nanoparticles at atherosclerosis prone areas (namely the aorta) was investigated. The hypothesis was that if SQRho could accumulate in atherosclerotic plaque, an increase of fluorescence in the aortas of ApoE$^{-/-}$ mice would be observable. Thus, 24 hours post-injection, the mice were euthanized, their aortas excised and directly imaged on a IVIS Lumina imaging system. The *ex vivo* imaging showed that, in comparison with the control wild-type mice, an increase of up to 3 times in the aorta radiant efficiency could be detected after intravenous injection of SQRho NPs in ApoE$^{-/-}$ mice (Figure 3B-C). These data together point to a possible accumulation of SQRho bioconjugates at the sites of atherosclerotic plaque lesion.

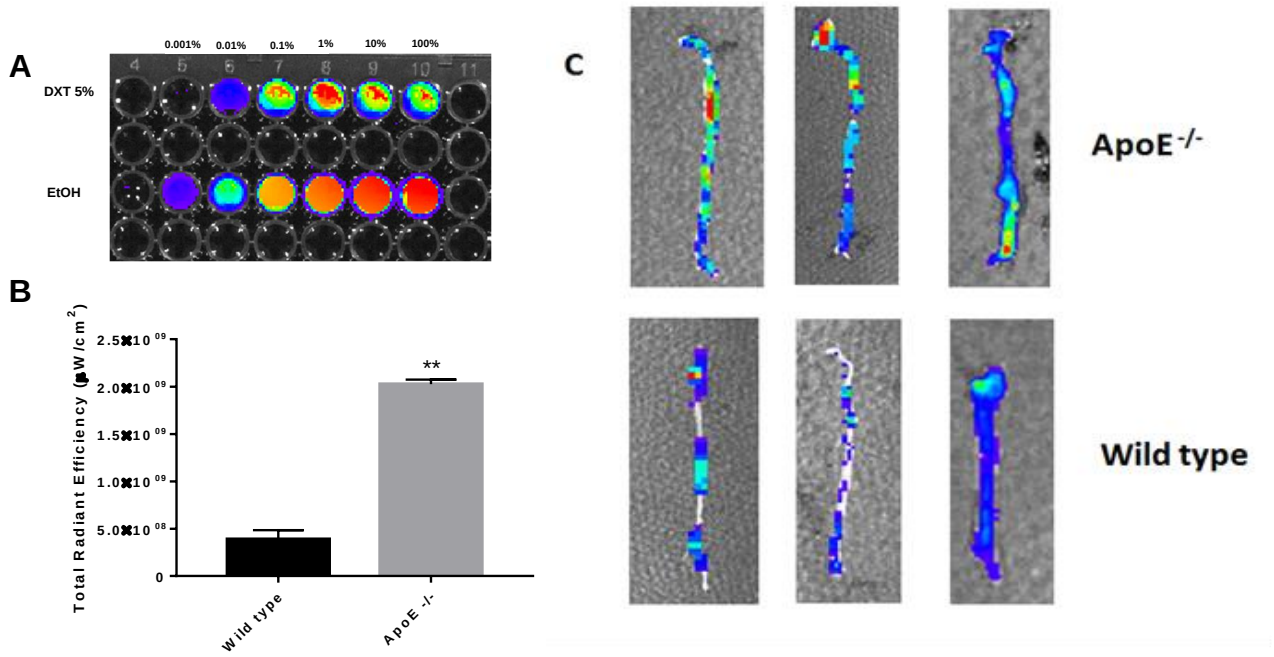

Figure 3: (**A**) Detection limit experiment. SQRho NPs were dispersed at 200 µg/mL in 5% DXT (top row) or EtOH (bottom row) and at different dilution factors. The plate was imaged in the IVIS Lumina system with excitation filter set at 540 nm and emission filter set at 620 nm. (**B**) Measured total radiant efficiency in the region of interest. *n*=3 mice per group. (C) Biodistribution of SQRho NPs in the aortas of ApoE$^{-/-}$ mice or wild type animals 24 hrs post-injection. Data are mean ± SD. **P*<0.05, ***P*<0.01 (Student's *t*-test).

histochemistry experiment on harvested aortas. After washing with PBS, aortas were freezed, cut in histological sections, and stained with DAPI and an anti-CD36 or anti-alpha smooth muscle actin antibody, used to determine whether NPs could accumulate in activated monocytes/macrophages or in activated smooth muscles. The experiment confirmed that substantial quantities of SQRho NPs could be found inside the atherosclerotic plaque but did not show significant co-localization of SQRho NPs with CD36-marked macrophages, or activated smooth muscles. Rather the SQRho NPs appeared to accumulate in the fatty region of the atheroma.

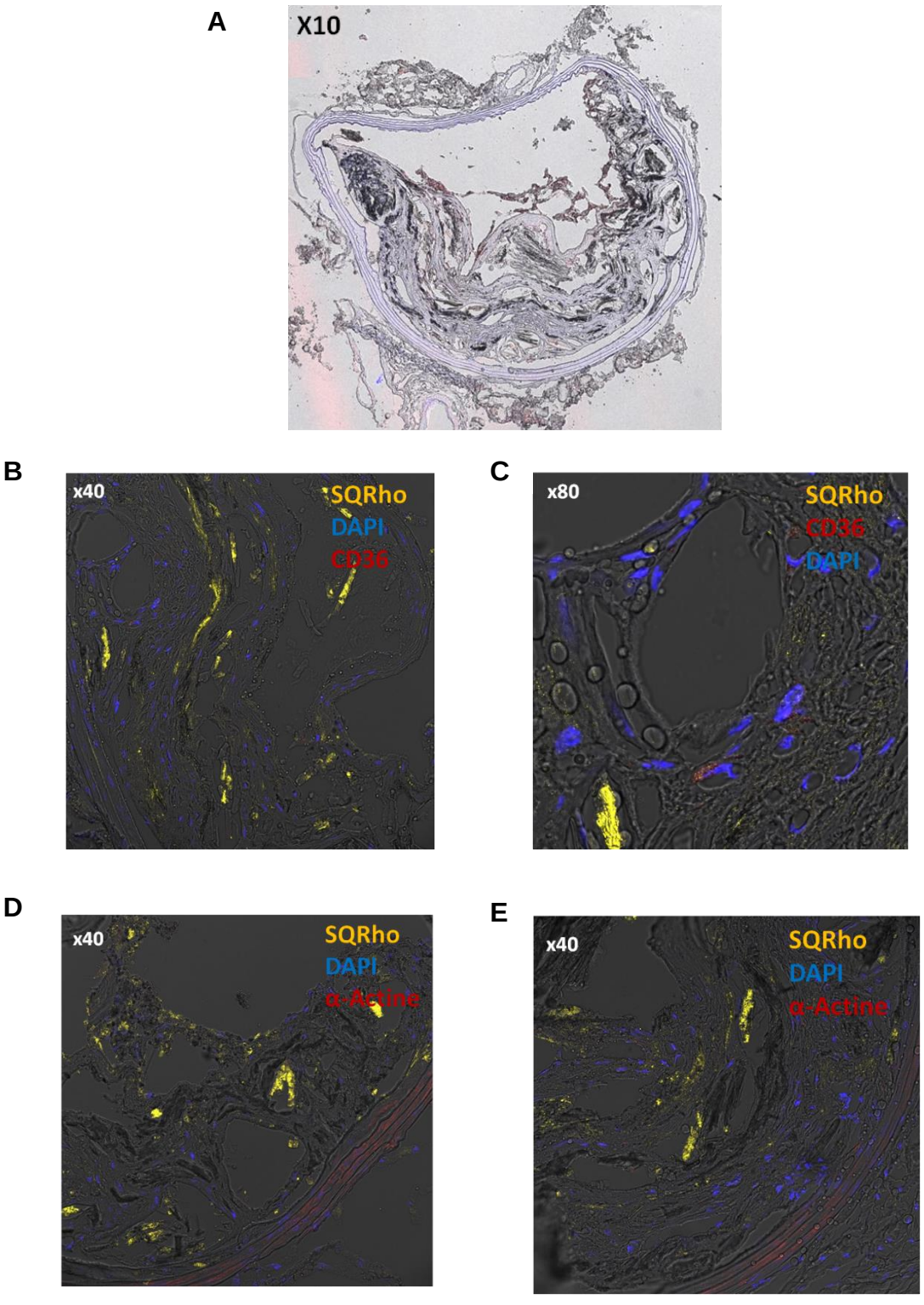

Figure 4: (**A**) Histology slide of a ApoE$^{-/-}$ aorta at x10 magnification. Atheroma clearly visible and reducing vascular lumen. (**B-E**) x40 or x80 magnification of atheroma with yellow fluorescence filter showing SQRho bioconjugates, blue filter showing DAPI staining, red fluorescence showing α-actin or CD36 staining.

IV. Conclusions

In this study, a proof-of-concept of atherosclerotic plaque targeting with SQ-based bioconjugates was investigated. Our preliminary results highlight a significant accumulation of SQRho NPs in the atherosclerotic plaque of ApoE$^{-/-}$ mice. Histological study confirmed the presence of fluorescent SQRho in the plaque but not that SQRho colocalized inside activated plaque resident macrophages.

Further studies will aim at confirming our initial result and conduct ex-vivo blood localization studies of SQRho NPs like the experiments that were undertaken with SQAd and SQGem bioconjugates (see General Discussion).

V. References

1. R. Paoletti, A. M. Gotto Jr,D. P. Hajjar, Inflammation in atherosclerosis and implications for therapy. *Circulation*. 109, III-20-III-26 (2004)
2. N. Kamaly, G. Fredman, J. J. R. Fojas, M. Subramanian*, et al.*, Targeted interleukin-10 nanotherapeutics developed with a microfluidic chip enhance resolution of inflammation in advanced atherosclerosis. *ACS nano*. 10, 5280-5292 (2016)
3. P. M. Winter, A. M. Morawski, S. D. Caruthers, R. W. Fuhrhop*, et al.*, Molecular imaging of angiogenesis in early-stage atherosclerosis with αvβ3-integrin–targeted nanoparticles. *Circulation*. 108, 2270-2274 (2003)
4. G. Fredman, N. Kamaly, S. Spolitu, J. Milton*, et al.*, Targeted nanoparticles containing the proresolving peptide Ac2-26 protect against advanced atherosclerosis in hypercholesterolemic mice. *Science translational medicine*. 7, 275ra220-275ra220 (2015)
5. M. E. Lobatto, C. Calcagno, A. Millon, M. L. Senders*, et al.*, Atherosclerotic plaque targeting mechanism of long-circulating nanoparticles established by multimodal imaging. *ACS nano*. 9, 1837-1847 (2015)
6. J. C. Frias, K. J. Williams, E. A. Fisher,Z. A. Fayad, Recombinant HDL-like nanoparticles: a specific contrast agent for MRI of atherosclerotic plaques. *Journal of the American Chemical Society*. 126, 16316-16317 (2004)
7. M. E. Lobatto, V. Fuster, Z. A. Fayad,W. J. Mulder, Perspectives and opportunities for nanomedicine in the management of atherosclerosis. *Nature Reviews Drug Discovery*. 10, 835 (2011)
8. B. L. Sanchez-Gaytan, F. Fay, M. E. Lobatto, J. Tang*, et al.*, HDL-mimetic PLGA nanoparticle to target atherosclerosis plaque macrophages. *Bioconjugate chemistry*. 26, 443-451 (2015)

9. M. F. Linton, P. G. Yancey, S. S. Davies, W. G. Jerome*, et al.* (2019) The role of lipids and lipoproteins in atherosclerosis. *Endotext [Internet]*, (MDText. com, Inc.).
10. D. Sobot, S. Mura, S. O. Yesylevskyy, L. Dalbin*, et al.*, Conjugation of squalene to gemcitabine as unique approach exploiting endogenous lipoproteins for drug delivery. *Nature communications*. 8, 15678 (2017)
11. D. Sobot, S. Mura, M. Rouquette, B. Vukosavljevic*, et al.*, Circulating lipoproteins: a Trojan horse guiding squalenoylated drugs to LDL-accumulating cancer cells. *Molecular Therapy*. 25, 1596-1605 (2017)
12. J. Kzhyshkowska, C. Neyen,S. Gordon, Role of macrophage scavenger receptors in atherosclerosis. *Immunobiology*. 217, 492-502 (2012)
13. A. S. Plump, J. D. Smith, T. Hayek, K. Aalto-Setälä*, et al.*, Severe hypercholesterolemia and atherosclerosis in apolipoprotein E-deficient mice created by homologous recombination in ES cells. *Cell*. 71, 343-353 (1992)
14. Y. Nakashima, A. S. Plump, E. W. Raines, J. L. Breslow*, et al.*, ApoE-deficient mice develop lesions of all phases of atherosclerosis throughout the arterial tree. *Arteriosclerosis and thrombosis: a journal of vascular biology*. 14, 133-140 (1994)

Chapter 3

Translation of Nanomedicines from Lab to Industrial Scale Synthesis: The Case of Squalene-Adenosine Nanoparticles

Flavio Dormont[a], Marie Rouquette[a], Clement Mahatsekake[b], Frédéric Gobeaux[c], Arnaud Peramo[a] Romain Brusini[a], Serge Calet[b], Fabienne Testard[c], Sinda Lepetre-Mouelhi[a], Didier Desmaële[a], Mariana Varna[a], Patrick Couvreur[a]

[a] Institut Galien Paris-Sud, CNRS UMR 8612, Université Paris-Sud, Université Paris-Saclay, 92296 Châtenay-Malabry, France

[b] HOLOCHEM, Voie de l'Innovation, 27100 Val-de-Reuil, France

[c] CEA Saclay, CNRS UMR 3685, Université Paris-Saclay, 91191 Gif sur Yvette, France

Published in Journal of Controlled Release

Translation of Nanomedicines from Lab to Industrial Scale Synthesis: The Case of Squalene-Adenosine Nanoparticles

Abstract

A large variety of nanoparticle-based delivery systems have become increasingly important for diagnostic and/or therapeutic applications. Yet, the numerous physical and chemical parameters that influence both the biological and colloidal properties of nanoparticles remain poorly understood. This complicates the ability to reliably produce and deliver well-defined nanocarriers which often leads to inconsistencies, conflicts in the published literature and, ultimately, poor translation to the clinics. A critical issue lies in the challenge of scaling-up nanomaterial synthesis and formulation from the lab to industrial scale while maintaining control over their diverse properties. Studying these phenomena early on in the development of a therapeutic agent often requires partnerships between the public and private sectors which are hard to establish.

In this study, through the particular case of squalene-adenosine nanoparticles, we reported on the challenges encountered in the process of scaling-up nanomedicines synthesis. Here, squalene (the carrier) was functionalized and conjugated to adenosine (the active drug moiety) at an industrial scale in order to obtain large quantities of biocompatible and biodegradable nanoparticles. After assessing nanoparticle batch-to-batch consistency, we demonstrated that the presence of squalene analogs resulting from industrial scale-up may influence several features such as size, surface charge, protein adsorption, cytotoxicity and crystal structure. These analogs were isolated, characterized by multiple stage mass spectrometry, and their influence on nanoparticle properties further evaluated. We showed that slight variations in the chemical profile of the nanocarrier's constitutive material can have a tremendous

impact on the reproducibility of nanoparticle properties. In a context where several generics of approved nanoformulated drugs are set to enter the market in the coming years, characterizing and solving these issues is an important step in the pharmaceutical development of nanomedicines.

I. Introduction

Nanostructured drug delivery systems have emerged over the last several decades as an important field of academic research and are set to bring momentous advances to human health through clinical and industrial developments. While a first generation of nanocarriers were successfully brought to market, notably in the oncology field, new classes of therapeutic agents making use of polymers, proteins, polysaccharides and other biomolecules have emerged for the treatment of numerous diseases(1, 2). Unfortunately, these new types of nanocarriers are facing difficulties in their translation to the clinics due to an absence of realistic industrial production, lack of reproducibility and insufficient cost-effectiveness(3). Part of the problem lies in the fact that nanostructured drug delivery systems have grown into increasingly complex structures with poorly understood biological fates(4). Size(5), surface charge(6), morphology(7), drug release profiles(8) and interaction with blood components(9) have all been shown to be key parameters that influence the biomedical outcome of nanocarriers *in vivo***.** Controlling these numerous parameters in a reproducible manner over intricate structures can be problematic, as well as difficult to bring to industrial standards. Accordingly, recent studies have highlighted the importance of developing simple and robust manufacturing methods that ensure the proper formulation of nanomaterials in large scales(10, 11).

Another critical issue lies in the challenge of scaling-up the synthesis of a nanocarrier's constitutive materials. Guidelines from the pharmaceutical industry in terms of good manufacturing practice and pharmaceutical quality can be applied, but the nature and complexity of nanomaterials carry their extra set of challenges. Indeed, while any scale-up of laboratory processes is difficult, nanomaterials production is made more challenging by the fact that subtle variations in the synthesis and manufacturing processes can result in significantly different products. The matter is further complicated when one considers that carriers (*e.g.* polymers, lipids, dendrimers) often inherently do not have a single pharmaceutical identity, but are constituted of a raft of different molecules which are difficult to individually characterize. This is contrary to conventional small-drug therapeutics, where the active pharmaceutical ingredient is the main concern. While regulations are still unclear regarding the plural identity of nanomedicines, special care should be taken when considering production of nanomaterials. Namely, there must be robust quality control systems in place, validating batch-to-batch consistency and biological equivalence. Identifying critical parameters that might affect the reproducibility of nanomaterial properties early on and monitoring these parameters on

multiple batches is a good practice which can minimize the appearance of reproducibility issues later on(12).

Recently, squalenoylation (i.e squalene loaded with active molecules) has emerged as a simple, safe and efficient method to produce nanoparticles encapsulating a vast range of therapeutic agents(13-15). Conjugating squalene, an endogenous, biocompatible and biodegradable lipid to a drug candidate yields nanocarriers with high drug loading efficiency, low toxicity, and high blood residence time(16). These nanoparticles have been used in pre-clinical models to treat a host of afflictions from cancer(17) to ischemic stroke(18) and pain(19). As with other nanomedicines, efforts now need to focus on the translation from lab-scale experiments to semi-industrial batches, allowing eventual regulatory approval for clinical trials.

In this article, through the example of squalene-adenosine (SQAd) nanoparticles, we wish to report on the challenges encountered in the process of scaling-up nanomaterial synthesis by comparing two batches, one synthesized at the gram scale in the laboratory, the other at the kilogram scale by an industrial partner. We highlight specific parameters which needed to be closely monitored to ensure batch-to-batch consistency. Notably, we demonstrate that scaling of lab scale synthetic processes can induce varying impurity profiles which can have tremendous impact on the reproducibility of the biological and physico-chemical properties of nanoparticle from batch-to-batch.

II. Materials and Methods

1. Materials

Squalene, adenosine, N-Bromosuccinimide (NBS), 1-hydroxybenzotriazole hydrate HOBt, 2-(1H-7-azabenzotriazol-1-yl)-1,1,3,3-tetramethyluronium hexafluorophosphate (HATU), tetrabutylammonium fluoride (TBAF), aluminium isopropoxide, propionic acid, triethyl orthoacetate, triethylamine (NEt_3), diisopropylethylamine (DIPEA), formic acid, 3-(4,5-dimethylthiazol-2-yl)-2,5-diphenyltetrazolium bromide (MTT), penicillin streptomycin solution, glutamine, norepinephrine, Claycomb's Medium, Dulbecco's Modifidied Eagle's Medium (DMEM) and dextrose (DXT) were purchased from Sigma-Aldrich (France). Ultra-pure water was prepared using a MilliQ system (Millipore Corporation, Billerica, MA). Reagents and HPLC grade solvents as ethanol, methanol, ethyl acetate, and acetonitrile were provided by Carlo Erba (France). Ammonium acetate $CH_3CO_2NH_4$ was from VWR.

2. Industrial Scale Synthesis of SQAd (Ind SQAd)

Synthesis of 3-bromo-2,6,10,15,19,23-Hexamethyl-tetracosa-6,10,14,18,22-pentaen-2-ol (squalene bromohydrine) **2.**

To a stirred solution of squalene **1** (1000 g, 2.4 mol) in THF (5 L), H_2O (200 mL) was slowly added until the solution became opalescent. To this mixture, THF (100 mL) was slowly introduced until solution became clear again. N-Bromosuccinimide (520 g, 2.9 mol) was then added and the reaction mixture was stirred 90 min at room temperature after which THF was removed and a liquid-liquid extraction was performed with 500 mL of brine and 1000 mL of diethyl ether. The organic phase was separated and the aqueous phase extracted with diethyl ether (3 x 800 mL). All the organic layers were combined, dried over $MgSO_4$, filtered and concentrated under reduced pressure. The resulting oily residue was purified by flash chromatography over silica gel (cyclohexane/ethyl acetate : 8/1 v/v) to provide 2,3-bromohydrine **2** (353 g, 29%) as a yellow oil. ^{1}H NMR (300 MHz, $CDCl_3$) δ: 5.25-5.10 (m,5H, *H*C=C(CH_3)), 4.01 (dd, *J* = 2.1, 11.3 Hz, 1H, CHBr), 2.32-2.35 (m, 1H), 1.95-2.19 (m, 18H, CH_2), 1.77-1.88 (m, 1H), 1.70 (s, 3H, CH_3), 1.63 (m, 15H, CH_3), 1.37 (s, 3H, CH_3), 1.36 (s, 3H, CH_3).

Synthesis of 2,3-epoxysqualene-2,2-dimethyl-3,7,12,16,20-pentamethylhenicosa-3,7,11,15,19-pentaen-1-yloxirane (epoxysqualene) **3.**

In a 10 L round bottom flask fitted with a mechanical stirrer and a calcium chloride guard tube, squalene bromohydrine **2** (350 g, 0.69 mol) was solubilized in MeOH (5 L) and K_2CO_3 (2eq) was added to this mixture. The reaction mixture was stirred 2 hours at room temperature and was then concentrated *in vacuo*. The residue was treated with H_2O and extracted with AcOEt (2 x 1 L). The combined organic layers were dried with $MgSO_4$, filtered and the solvent removed under reduced pressure to obtain a yellow oil (280 g, 95%) which was directly used in the next step without any further purification. ^{1}H NMR ($CDCl_3$) δ: 5.25-5.10 (m,5H, *H*C=C(CH_3)), 2.69 (t, *J* = 7.0 Hz, 1H, CH) 1.95-2.19 (m, 20H, CH_2); 1.68 (s, 3H, CH_3) 1.60 (s, 3H, CH_3); 1.58 (m, 12H, CH_3) 1.28 (s, 3H, CH_3); 1.24 (s, 3H, CH_3).

Synthesis of 2,6,10,15,19,23-Hexamethyl-tetracosa-1,6,10,14,18,22-hexaen3-ol 4.

To a stirred solution of 2,3-epoxysqualene **3** (280 g, 0.66 mol) in toluene (2.5 L) was added aluminium isopropoxide (430.8 g, 1.98 mol). The resulting mixture was stirred under reflux for 16 h. After cooling to room temperature, 1 N HCl was added until the whole solid was solubilized. The organic phase was collected and the aqueous phase extracted with diethyl ether (4 x 500 mL). The combined organic layers were washed with brine, dried over $MgSO_4$,

filtered and concentrated under reduced pressure. The resulting oily residue was purified by flash chromatographic purification over silica gel (petroleum ether/diethyl ether : 4/1 (v/v)) to provide allylic alcohol **4** (177.5 g, 63%) as a colourless oil. ^{1}H NMR (300 MHz, $CDCl_3$) δ: 5.25–5.10 (m, 5H, *H*C=C(CH_3)), 4.96 (m, 1H, =C*H*$_2$), 4.86 (m, 1H, =C*H*$_2$), 4.05 (t, *J* = 6.5 Hz, 1H, C*H*OH), 2.20–1.95 (m, 20H, CH_2), 1.75 (s, 3H, CH_3), 1.70 (s, 3H, CH_3), 1.64 (s, 3H, CH_3), 1.63 (s, 12H, CH_3).

Synthesis of 4,8,12,17,21,25-Hexamethyl-hexacosa-4,8,12,16,20,24-hexaenoic acid ethyl ester (squalene acetic ethyl ester) **5.**

A stirred solution of allylic alcohol **4** (175 g, 0.41 mol) and propionic acid (3.5 g, 0.047 mol) in triethyl orthoacetate (1 L) was heated under reflux for 3 h. After cooling to room temperature, triethylamine (7 g, 0.069 mol) was added and the mixture was concentrated under reduced pressure. The residue was stirred for 5 min with 0.1 N HCl solution and extracted with diethyl ether (4 x 500 mL). The combined organic phases were washed with brine, dried over $MgSO_4$, filtered and concentrated under reduced pressure to provide the crude ester **5** (202 g, quantitative) as a pale yellow oil which was directly used in the next step without further purification. ^{1}H NMR (300 MHz $CDCl_3$) δ: 5.20-5.02 (m, 6H, *H*C=C(CH_3)), 4.09 (q, *J* = 7.2 Hz, 2H, OC*H*$_2$$CH_3$), 2.40-2.20 (m, 4H, CO_2C*H*$_2$C*H*$_2$), 2.15-1.85 (m, 20H, CH_2), 1.66 (s, 3H, CH_3), 1.59 (s, 18H, CH_3), 1.23 (t, *J* = 7.2 Hz, 3H, OCH_2C*H*$_3$).

Synthesis of squalenylacetic acid 4,8,12,17,21,25-Hexamethyl-hexacosa-4,8,12,16,20,24-hexaenoic acid (squalenylacetic acid) **6.**

In a 10 L round bottom flask fitted with a mechanical stirrer, a reflux condenser and a calcium chloride guard tube, was introduced ester **5** (200 g, 0.4 mol) solubilized 3000 mL of EtOH and 1000 mL of THF. After stirring, LiOH,H_2O (92.5 g, 2.2 mol) was added at room temperature. The mixture was heated to reflux for 24 h. After cooling, the reaction mixture was concentrated under reduced pressure and MilliQ water was added. The mixture was acidified with HCl 3N to pH = 3-4 and was then extracted by MTBE (3 x 1 L). The combined organic extracts were dried over $MgSO_4$, filtered and concentrated under reduced pressure. The residue was purified by flash chromatography on silica gel (dichloromethane/petroleum ether : 1/1 (v/v)) to provide squalenylacetic acid **6** (121 g, 65%) as a yellow oil. ^{1}H NMR (300 MHz $CDCl_3$) δ: 5.15 -5.0 (m, 6H, *H*C=C(CH_3)), 2.49-2.30 (m, 4H, C O_2C*H*$_2$C*H*$_2$), 2.20-1.90 (m, 20H, CH_2), 1.70 (s, 3H, CH_3), 1.62 (s, 18H, CH_3).

Synthesis of N-9-2,3-bis[(tert-butyldimethylsilyl)oxy]-5 -[(tertbutyldimethylsilyl)oxy] methyloxolan-2-yl]-9H-purin-6-yl-4,8,12,17,21,25-hexamethylhexacosa-4,8,12,16,20,24-hexaenamide(Tri-silylated Squalene Adenosine) **7.**

To a stirred solution of squalenylacetic acid **6** (120 g, 0.25 mol) in anhydrous dichloromethane (1 L) and DMF (5 mL), was added under nitrogen HOBt (46 g, 0.3 mol), HATU (114 g, 0.3 mol), tris-O-silylated adenosine (130.2 g, 0.25 mol) and DIPEA (9.35 g, 0.075 mol). The reaction mixture was stirred 72 hours at room temperature and was then concentrated *in vacuo*. Aqueous sodium hydrogen carbonate was added and the mixture was extracted with ethyl acetate (3 × 500 mL) and dichloromethane (1 × 300 mL). The combined extracts were washed with brine, dried on $MgSO_4$, and concentrated under reduced pressure. The crude product was purified by flash chromatography on silica gel eluting with 10 % ethyl acetate in cyclohexane to give tri-silylated Squalene Adenosine **7** as a colourless oil (119 g, 45%); ^{1}H NMR (300 MHz, $CDCl_3$) δ : 8.70 (s,1H, H8), 8.64 (s, 1H NHCO), 8.35 (s, 1H, H2), 6.10 (d, , *J* = 5.2 Hz, 1 H, H1'), 5.20 (t, *J* = 6.4 Hz, 1 H, *H*C=C(CH_3)), 5.20-5.10 (m, 5H, *H*C=C(CH_3)), 4.67 (t, *J* = 4.7 Hz, 1 H, H2'), 4.3 (t, *J* = 4.7 Hz, 1 H, H2'), 4.15-4.11 (m; 1 H, H4'), 4.02 (dd, *J* = 11.2 Hz, *J* = 3.9 Hz, 1H, H5'), 3.78 (dd, *J* = 11.2 Hz, *J* = 2.7 Hz, 1H, H5'), 2.96 (t, *J* = 7.8 Hz, 2 H, $O_2CCH_2CH_2$), 2.45 (t, *J* = 7.8 Hz, 2 H, $O_2CCH_2CH_2$), 2.10-1.95 (m, 20 H, =C(CH_3)CH_2CH_2), 1.67 (s, 6 H, C=C(CH_3)$_2$), 1.58 (s, 15 H, C=C(CH_3)), 0.95 (s, 9 H, *t*-BuSi), 0.93 (s, 9 H, *t*-BuSi), 0.78 (s, 9H, *t*-BuSi), 0.15 (s, 3 H, CH_3Si), 0.14 (s, 3 H, CH_3Si), 0.10 (s, 6H, CH_3Si), −0.04 (s, 3 H, CH_3Si), −0.24 (s, 3 H, CH_3Si).

Synthesis of N-9-2,3-dihydroxy-5-(hydroxymethyl)oxolan-2-yl]-9H-purin-6-yl-4,8,12,17,21,25- hexamethylhexacosa-4,8,12,16,20,24-hexaenamide (Squalene-Adenosine) **8.**

To a solution of tris-O-silylated Squalene Adenosine **7** (100 g, 0.94 mol) in dry THF (1 L) was added TBAF (1M solution in THF, 340 mL, 0.34 mol) and the mixture was stirred for 3h at room temperature. The reaction was then quenched with brine and the mixture was extracted with ethyl acetate (3 × 500 mL). The combined extracts were dried on $MgSO_4$, and concentrated under vacuum. The crude product was purified by chromatography on silica gel eluting with 5 % methanol in dichloromethane to give Squalene-Adenosine **8** as a colourless oil (37.1 g, 55 %); ^{1}H NMR (300 MHz, $CDCl_3$) δ: 9,39 (broad s, 1 H, N*H*CO), 8.41 (s, 1 H, H8), 8.21 (s, 1 H, H2), 5.98 (d, 1 H, *J* = 5.4 Hz, H1'), 5.32 (t, 1 H, *J* = 6.3 Hz, *H*C=C(CH_3)), 5.05-4.93 (m, 5 H, *H*C=C(CH_3)),

4.61 (t, 1 H, *J* = 4.9 Hz, H2'), 4.18 (m, 1 H, H3'), 3.98 (m, 1 H, H4'), 3.69 (dd, 1 H, *J* = 11.9 Hz, *J* = 3.7 Hz, H5'), 3.57 (dd, *J* = 11.9 Hz, *J* = 3.3 Hz, 1 H, H5'), 2.98 (t, 2 H, *J* = 7.8 Hz, $O_2CCH_2CH_2$), 2.45 (t, 2 H, *J* = 7.8 Hz, $O_2CCH_2CH_2$), 2.11-1.93 (m, 20 H, $=C(CH_3)CH_2CH_2$), 1.62 (s, 3 H, $C=C(CH_3)$), 1.60 (s, 3 H, $C=C(CH_3)$), 1.54 (s, 15 H, $C=C(CH_3)$)

3. Lab Scale Synthesis of SQAd (Lab SQAd)

SQAd was synthesized as previously reported(18) starting from 20 g of squalene and obtaining 700 mg of SQAd for a total yield of 2.1 %.

4. HPLC-UV-ESI-MS analysis.

Chromatography Apparatus: A high-performance liquid chromatograph Waters Alliance 1695 (Waters, Milford, MA), equipped with a Waters DAD 2996 photodiode array detector, Hewlett-Packard computer with a Waters Empower 3 software and a Waters autosampler with a 50 μL loop was used, with simultaneous detection at 220 nm and 270 nm. The spectra (detection wavelengths from 200-600 nm) were recorded for all peaks. The HPLC system was coupled on line with a Waters TOF mass spectrometer.

Columns and Mobile Phase: A Waters Xselect LC-18 column (2.1 x 150 mm, 3.5 μm) was used. The solvents used were (A) 100% HPLC-grade acetonitrile (B) 0.1% formic acid in MilliQ water. Flow rate: 0.25 mL/min. Solvents and samples were filtered through a 0.45 μm Millipore filter type HA (Millipore Corp., Bedford, MA).

HPLC Conditions: SQAd and SQAd analogs phase (called Ph1) were separated using a gradient over 10 min from 80% to 100% of A. Peak assignments were made based on spectral data.

Electrospray Mass Spectrometry (ESI-MS). Mass spectrometry was performed using electrospray MS. The instrument was a Waters TOF LCT Premier mass spectrometer equipped with an ion spray interface with a capillary voltage of 2800 V. The mass spectrometer was operated in the positive-ion mode.

5. High Resolution HPLC-ESI-MS^n analysis.

Chromatography Apparatus: A ThermoFisher Scientific (ThermoFisher, Waltham, MA) chromatograph including a Dionex U-3000 RSLC system equipped with a WPS-3000 autosampler and a TCC-3000 column oven was used. The RSLC system was coupled on-line to a hybrid mass spectrometer LTQ-Orbitrap Velos Pro (ion trap and orbital trap) from ThermoFisher.

Columns and Mobile Phase: A Macherey-Nagel Nucleodur 100-5 C18 EC column (2.1 x 125 mm) was used. The solvents used were 50% HPLC-grade acetonitrile/ 50% HPLC-grade MeOH (solvent A) and 0.1% formic acid in MilliQ water (solvent B). Flow rate was 0.3 mL/min. Solvents and samples were filtered through a 0.45 μm Millipore filter type HA (Millipore Corp., Bedford, MA).

HPLC Conditions: SQAd and SQAd analogs were separated using a solvent gradient over 10 min from 80% to 100% of solvent A.

High Resolution Mass Spectrometry: Mass Spectrometry Full Scan analysis was performed in the Orbital Trap with a resolution of 30 000 in positive mode. The instrument was a ThermoFisher hybrid mass spectrometer LTQ-Orbitrap Velos Pro equipped with an electrospray ion source with a capillary voltage of 3400 V.

MS^n: MS^n was performed in the LTQ ion trap with Collision Induced Dissociation (CID) at an energy of 35 (arbitrary unit). Fragment detection was performed in the orbitrap with a resolution of 7500.

6. Preparative HPLC.

Preparative HPLC separation of Ph1 from SQAd was performed by injecting 1 mL of a filtered solution of 10 mg/mL Ind SQAd sample in ethanol onto a Waters Xselect LC-18 (30 × 150 mm, 2.1 μm) HR C-18 column. Elution was performed using Waters model 501 pumps to deliver a constant flow rate of 42 mL/min. The solvent system used was identical to prior HPLC experiments. SQAd was detected by absorbance at 270 nm using a Waters UV DAD 2996 photodiode array detector. The first product impurity phase (Ph1) was collected between 13.6 min and 15.3 min and SQAd was collected between 19 min and 21 min.

Peak Extraction.

Fractions of eluates containing compounds of interest were combined, filtered through a 0.22 μm Teflon filter, and concentrated at 50 °C under 0.01 hPa vacuum on a rotary evaporator to obtain purified compound.

7. Preparation and Physico-Chemical Characterization of NPs.

SQAd nanoparticles (SQAd NPs) were prepared by nanoprecipitation, as previously described[20,21] (Supp. Figure S1). Briefly, for both Lab SQAd and Ind SQAd, SQAd bioconjugates were dissolved in 1 mL of absolute ethanol (6 mg/mL) and added dropwise under moderate mechanical stirring to a 5% (w/v) dextrose solution (DXT 5%).The ethanol

was then completely evaporated using a Rotavapor (90 rpm, 40 °C, 42 mbar) to obtain an aqueous suspension of pure NPs (2 mg/mL). Ph1 nanoparticles were obtained from the analog chromatographic fraction using the same protocol. NPs size (hydrodynamic diameter) and surface charge (zeta potential) were measured using a Malvern Zetasizer Nano ZS 6.12 (173° scattering angle, 25 °C, Material RI: 1.49, Dispersant Viscosity RI: 1.330, Viscosity 0.8872 cP). For the size measurements by dynamic light scattering (DLS), a good attenuator value (7−9) was obtained when suspending 50 µL of NPs in 1 mL of distilled water. The mean diameter for each preparation resulted from the average of three measurements of 60 s each. For zeta potential measurements, 70 µL of NPs was dissolved in 2 mL of KCl 1 mM before filling the measurement cell. The mean zeta potential for each preparation resulted from the average of three measurements in automatic mode, followed by the application of the Smoluchowski equation. NP stability was assessed by measuring NP size by DLS at different time intervals after initial formulation up to seven days.

8. Cryo-Transmission Electron Microscopy (cryo-TEM).

The morphology of SQAd nanoparticles was observed with cryo-transmission electron microscopy. Drops of the solutions were deposited on electron microscope grids covered with a holey carbon film (Quantifoil R2/2) previously treated with a plasma glow discharge. The excess liquid on the grids was blotted out with filter paper, and the grids were quickly immersed in liquid ethane to form a thin vitreous ice film. The whole process was performed using a Vitrobot apparatus (FEI Company). Observations were conducted at low temperature (−180°C) on a JEOL 2010 FEG microscope operated at 200 kV. Images were recorded with a Gatan camera.

9. Small-Angle X-ray Scattering

SAXS experiments were performed on two different set-ups. Lab SQAd was studied at the SWAXSLab in CEA Saclay with a Xeuss 2.0 apparatus (Xenocs) equipped with a GeniX3D X-ray generator (λ = 1.542Å) and a PILATUS3 1M 2D detector. The detector to sample distance was chosen to attain the 0.01-0.5 $Å^{-1}$ q-range. Averaging and data treatment were performed with PYSAXS software (https://pypi.org/project/pySAXS/). The sample Ind SQAd was studied at the synchrotron SOLEIL (Saint-Aubin, France) on the SWING beamline. Data were recorded at 12keV with a 4M bi-dimensional Eiger detector in the chosen 0.014-1.9 $Å^{-1}$ q-range. The data

treatments were performed using FOXTROT software. For each set-up, the samples were inserted in 1.5 mm diameter quartz capillaries sealed with paraffin wax and analyzed with a counting time of 3600s and 250 ms for respectively the SWAXSLab and SWING beamlines.

10. Spiking experiment.

SQAd and Ph1 were separately dissolved in absolute ethanol (6 mg/mL). The SQAd and Ph1 ethanolic solutions were mixed in varying ratios as to obtain different 0.1 %, 1 %, 5 %, 10 % (w/w) solutions of Ph1 in SQAd. This organic solution was then nanoprecipitated as described above in a 5% (w/v) dextrose solution.

11. Cell Culture.

MCEC (Mouse Cardiac Endothelial Cells, TebuBio, France) cells were grown in DMEM medium supplemented with 10% FBS, 1% penicillin-streptomycin and 1% HEPES at 37 °C and 5% CO_2. HL1 (Cardiac Muscle cells, Sigma, France) were grown in Claycomb's medium supplemented with 10% FBS, 1% penicillin-streptomycin, 1% glutamine and 1% norepinephrine at 37 °C and 5% CO_2. HepG2 (Hepatocellular Carcinoma, Sigma, France), HUVEC (Human Umbilical Vein Endothelial cell, ATCC, France) and MiaPaca (Human Pancreatic Carcinoma Epithelial Cells, ATCC, France) cells were grown in DMEM medium supplemented with 10% FBS and 1% penicillin-streptomycin at 37 °C and 5% CO_2 atmosphere. For HL1 and MCEC cell lines, cells were divided to the tenth every 3-4 days. For MiaPaca, HepG2 and HUVEC cells, cells were divided to the fifth every 3-4 days.

12. Cytotoxicity of SQAd NPs.

Cytotoxicity was evaluated using an MTT (3-[4,5-dimethylthiazole-2-yl]-2,5-diphenyltetrazolium bromide) assay. For a typical 24 hours cytotoxicity study, cells were seeded in a 96 well plate at 8 000 cells/well (30 000 cells/cm^2) for 24 hours. Subsequently, cells were treated with different concentrations of nanoparticles ranging from 1 μM to 200 μM in 200 μL of complete cell medium. Cells were incubated for 24 hours before the MTT assay was performed. For the MTT assay, cells were washed with PBS, and incubated for 2 hours with medium containing 0.5 mg/mL of MTT. The medium was removed after 2 hours and 100 μL of DMSO were added to each well before measuring absorbance reading on a Perkin Elmer absorbance reader at 570 nm.

13. Rat Plasma Samples.

Rat blood samples were obtained from healthy male Sprague Dawley rats by cardiac puncture and collected into heparinated collection tubes. Plasma was obtained by centrifuging the blood samples at 2000 rcf for 10 min. Plasma samples were pooled, split into 5 mL aliquots and stored at -80 °C until further use. For protein binding experiments, the aliquots were thawed at room temperature and then incubated at 37 °C.

14. Protein Assay.

Plasma protein binding to SQAd nanoparticles was studied by incubating 250 μL of NP suspension (4 mg/mL) in DXT 5% with 250 μL of rat plasma. Incubation was carried on at 37 °C for 1 h to promote protein adsorption. The amount of adsorbed proteins on SQAd NPs after incubation in plasma was quantified using the Protein Assay reagent (Pierce, Thermo Scientific, Waltham, MA, USA) according to manufacturer's protocol. Briefly, after incubation, NP-protein complexes were centrifuged at 16 000 rcf for 10 min to pellet NP- protein complexes. The supernatant was removed and the pellet was resuspended in 500 μL of PBS. This procedure was repeated twice to remove any loosely bound proteins until final suspension in 500 μL of PBS. A plasma aliquot not incubated with nanoparticles was subjected to the same procedure as control. For the assay, 25 μL of each sample were placed in a 96-well plate and 200 μL of Protein Assay working solution were added. The measures were performed in triplicate. The plate was covered, mixed on an orbital plate shaker, and incubated at 37 °C for 30 min. The absorbance of each sample, standard and blank was measured with a Perkin Elmer absorbance reader at 570 nm. The protein concentration was calculated using interpolation with the standard curve obtained from PBS solutions of Bovine Serum Albumin.

15. Protein Separation by 1D-PAGE.

Proteins were separated by 1D-PAGE according to Laemmli(20) with some modifications. Proteins were desorbed from SQAd NPs by adding SDS-PAGE sample buffer to the pellet and heating the solution to 95 °C for 5 min. A Biorad Mini-PROTEAN® TGX Stain-Free™ 4%-15% Bis–Tris polyacrylamide gel was used as separating gel. Electrophoresis was carried out at a constant voltage of 300 V in electrophoresis buffer, until the dye front reached the lower end of the gel (20 min). Separated proteins were imaged using a Biorad ChemiDoc Imaging system and analyzed with Biorad Image Lab software. For quantification, total lane

fluorescence was measured and for each detected band the band fluorescence count was normalized over total lane fluorescence yielding the normalized percentage of fluorescence count (NpFlC %).

III. Results and Discussion

1. Scale-up and Reproducibility of NPs properties.

a) Synthesis of SQAd

At the onset of this study was a need to scale up the synthesis of the SQAd bioconjugates for use in multi-lab pre-clinical trials evaluating SQAd efficacy in different animal models. Starting from squalene, SQAd was first synthesized at a lab scale in limited amounts (*ie*. 100 mg) with a total yield of ~2 % (Lab SQAd) and then by an industrial partner in large scale using the same synthetic process (Ind SQAd). SQAd synthesized from industrial batches was obtained in a higher total yield (~5 %) through industrial optimization of the synthesis process. The synthetic route to SQAd **8** is illustrated in Figure 1A. Because of its lack of functional groups, conjugation to squalene **1** can only be achieved after functionalization of the squalene aliphatic chain. This functionalization process starts with the selective hydroxybromination of the terminal double bond with NBS in wet THF according to the method of Van Tamelen(21). The bromohydrine **2** pathway shows a proclivity for the formation of the terminal 2,3-bromohydrine which has been attributed in part to conformational changes of the squalene chain in a water containing solution. This hypothesis is strongly supported by the numerous observations that most epoxidation reactions performed in apolar organic solvents using peroxy acids or dimethyldioxirane give a mixture of internal epoxidation products(22, 23). The chemoselectivity of NBS/H_2O for the terminal double bond was, however, not perfect and the crude material needs to be thoroughly purified by silica gel chromatography before engaging the bromohydrine in the next step. Nevertheless, this synthetic path was considered preferable to other oxidative methods as the process didn't require the involvement of toxic reagents or heavy metals which would further complicate regulatory approval. As depicted in
Figure 1A, once the crucial terminal functionalization was obtained, 2,3-oxydosqualene was easily derived from the 2,3-bromohydrine by potassium carbonate treatment (b). The one isoprene-unit homologation was then achieved by sequential aluminium isopropoxide ring opening reaction (c) followed by Claisen-Johnson rearrangement with triethylorthoacetate (d)(24). After saponification, the obtained squalenyl acetic acid was coupled to 2',3',5'-trisilylated adenosine using HATU/HOBt as coupling agent with moderate yield. After extensive purification, the silyl protecting groups were removed upon TBAF treatment. Although the lipidic nature of squalene precluded crystallization of the

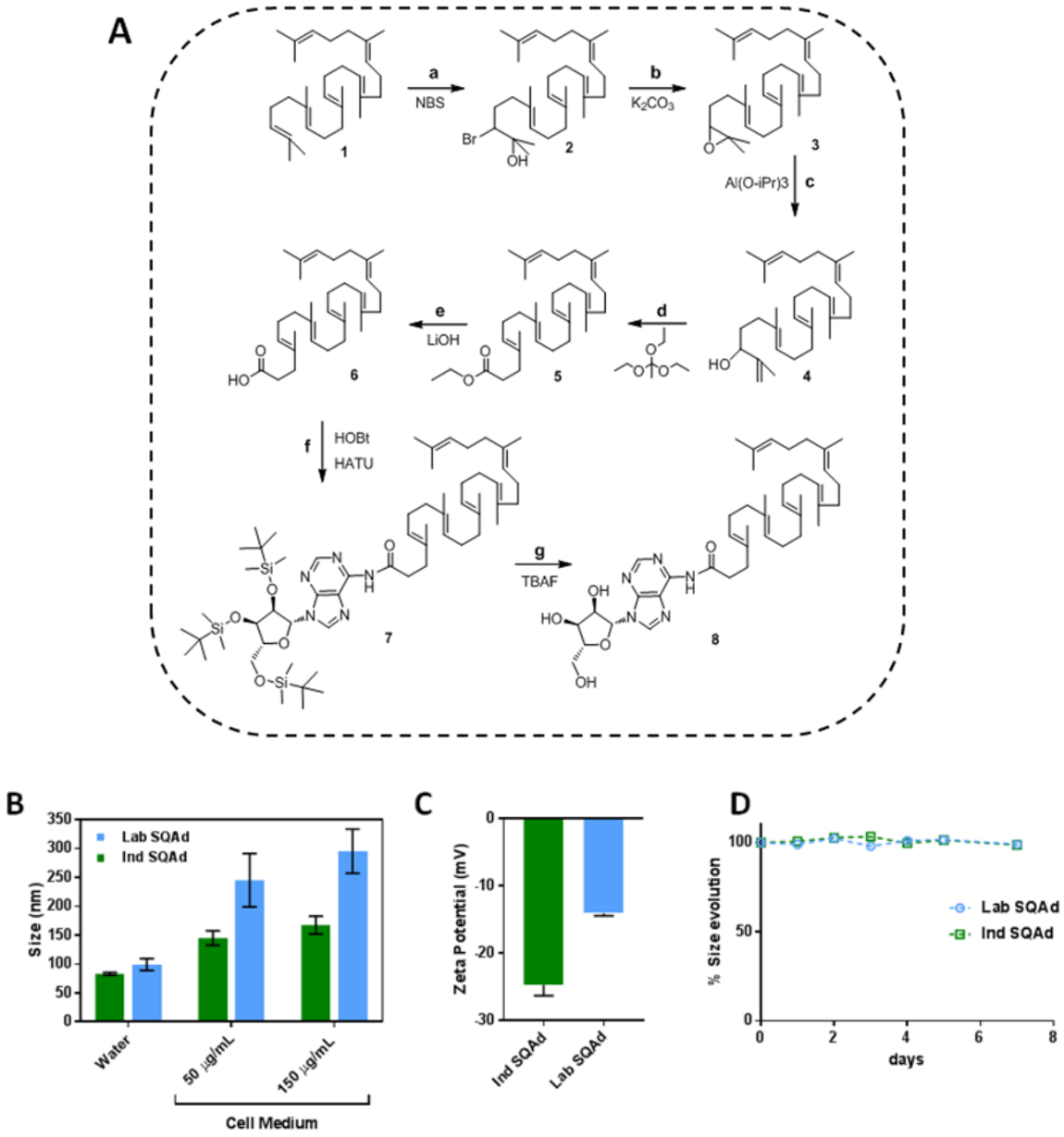

Figure 1: A. Scheme of SQAd synthesis: a) Squalene and NBS in THF/H_2O, 29%. b) 2 and K_2CO_3 in MeOH, 95%. c) 3, aluminium-isopropoxide in Toluene, reflux, 63%. d) 4, propionic acid in triethyl orthoacetate, reflux. e) 5, LiOH,H_2O in EtOH/THF, reflux, 65%. f) 6, HOBt, HATU and DIPEA in DCM, 45%. g) 7 and TBAF in THF, 55%. **B.** DLS measurement of NPs sizes for Lab SQAd and Ind SQAd batches. For measurements performed in cell medium, NPs were dispersed at a concentration of 50 µg/mL or 150 µg/mL in complete DMEM medium. **C.** Zeta-potential measurements of Lab SQAd and Ind SQAd. **D.** Stability of SQAd NPs in water determined by DLS monitoring of NP size

chromatographic conditions for both Lab SQAd and Ind SQAd. NMR analysis of both batches yielded spectra consistent with SQAd (Supp. Figure S2). Nanoparticles of both Lab SQAd and Ind SQAd were then formulated to evaluate the influence of industrial scale-up on NPs properties.

b) NP formulation and physico-chemical characterization

SQAd NPs were prepared by nanoprecipitation(18) of an ethanolic solution of SQAd in a 5% (w/v) aqueous dextrose solution. Once formulations of different SQAd batches were obtained, size and polydispersity index (PDI) of the NPs were measured by dynamic light scattering (DLS) (Figure 1B). The resulting measurements showed substantial differences in the colloidal

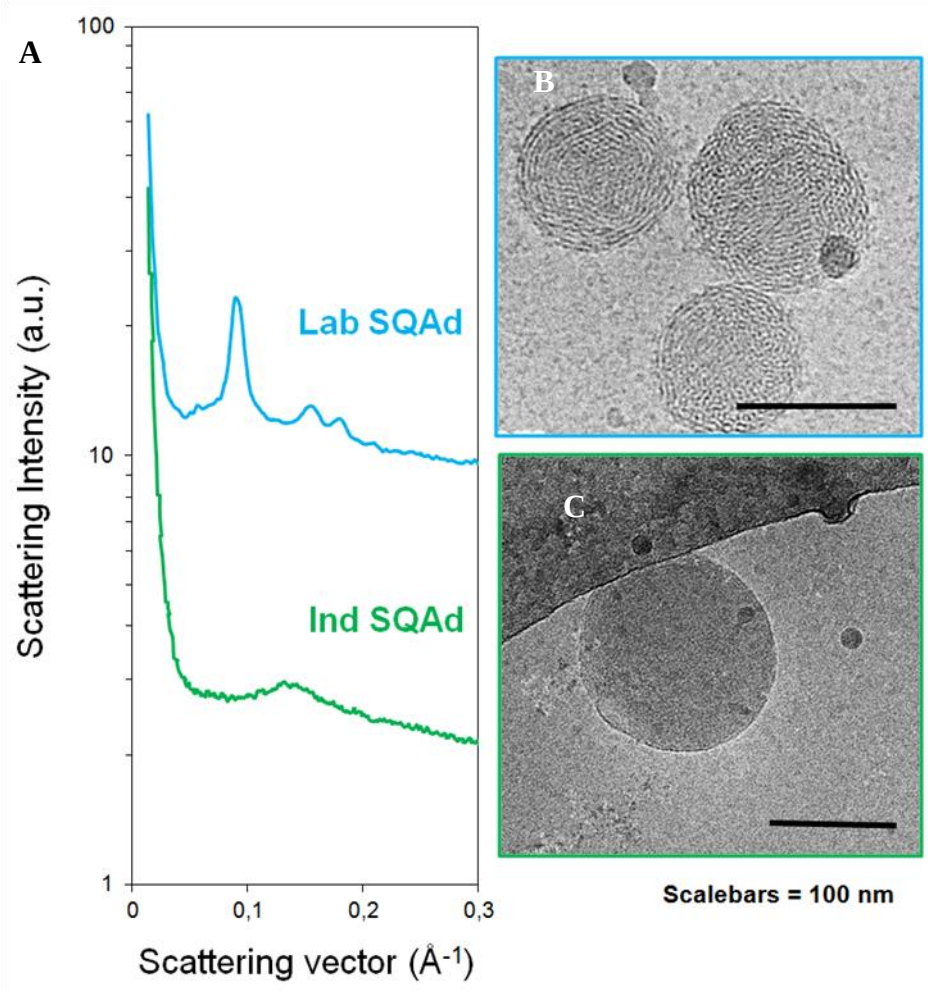

Figure 2: A. Small-angle X-ray diffraction patterns NPs recorded at room temperature. **B.** Selected Cryo-TEM image of Lab SQAd NPs obtained by nanoprecipitation of an ethanolic solution in DXT 5%. **C.** Selected Cryo-TEM image of Ind SQAd NPs obtained by nanoprecipitation of an ethanolic solution in DXT 5%.

behavior of formulations originating from different SQAd batches. Indeed, small variation in the mean size were observed (83 nm/ 99 nm for respectively Ind SQAd and Lab SQAd) while larger differences in the mean zeta potential were measured (from -25mV to -15mV for respectively Ind SQAd and Lab SQAd) (Figure 1C). Both formulations were stable for at least 7 days in water as measured by DLS (Figure 1D), while in cell culture medium Ind SQAd NPs were found to be

more stable than Lab SQAd NPs. This difference was most probably due to their stronger surface charge which inhibited NPs aggregation in a solution of high ionic strength such as cell medium. In addition, cryo-TEM imaging (Figures 2B-C) showed substantial differences concerning the NPs internal structure. Lab SQAd demonstrated apparent internal ordering while Ind SQAd produced NPs with less apparent structure. To further investigate this observation, the internal structure of SQAd NPs was studied by Small-Angle X-ray Scattering (SAXS) (Figure 2A). For Lab SQAd, the SAXS pattern displayed three Bragg reflections at q_0 = 0.091 Å^{-1}, q_1 = 0.158 Å^{-1} ($q_0\sqrt{3}$) and q_2 = 0.182 Å^{-1} ($2q_0$). These peaks indexed as the reflections of an inverse two-dimensional hexagonal phase with lattice parameter a = 78.0 Å. For Ind SQAd, however, SAXS data showed only one smooth Bragg peak without high order reflections, in agreement with a lower ordering of the internal structure, as observed by cryoTEM. The low ordering of Ind SQAd NPs suggested that some constituents of the SQAd NPs batches may influence NPs colloidal behavior and warranted further studies to evaluate if these physico-chemical differences may impact the biological behavior of NPs.

c) Cytotoxicity of Lab SQAd and Ind SQAd batches

In this study, HepG2, HUVEC, HL1 and MiaPaca cells lines were chosen as *in vitro* models of the influence of SQAd to account for cell subtype-specific variations. The cytotoxicity of different batches of SQAd NPs was determined after incubation with the various cell lines by performing an MTT assay (Figure 3). Ind SQAd batches were consistently found to be more toxic than lab SQAd NPs with IC_{50} values in the 100 μM range while Lab SQAd did not induce a strong cytotoxicity even at concentrations of 200 μM. This tendency was confirmed on the four tested cell lines and with NPs incubation times ranging from 24 to 72 hours. Also, the presence of dextrose in the formulations did not to influence the cytotoxicity of SQAd NPs (Supp. Figure S3).

Squalene is an endogenous precursor of cholesterol which is non toxic to cells. Once functionalized into squalenylacetic acid **6**, it has been shown to induce a moderate inhibition of cell proliferation in certain models with IC_{50} concentrations in the 180-200 μM ranges on HUVEC and MiaPaca cells(25). Adenosine, on the other hand, has a more controversial effect on cell proliferation(26-28). While it can induce apoptosis and cell death in certain types of cardiomyocytes(29) and neutrophils(30), adenosine provides important cytoprotective functions in the heart and brain tissue during ischemia, hypoxia or ischemia reperfusion (31,

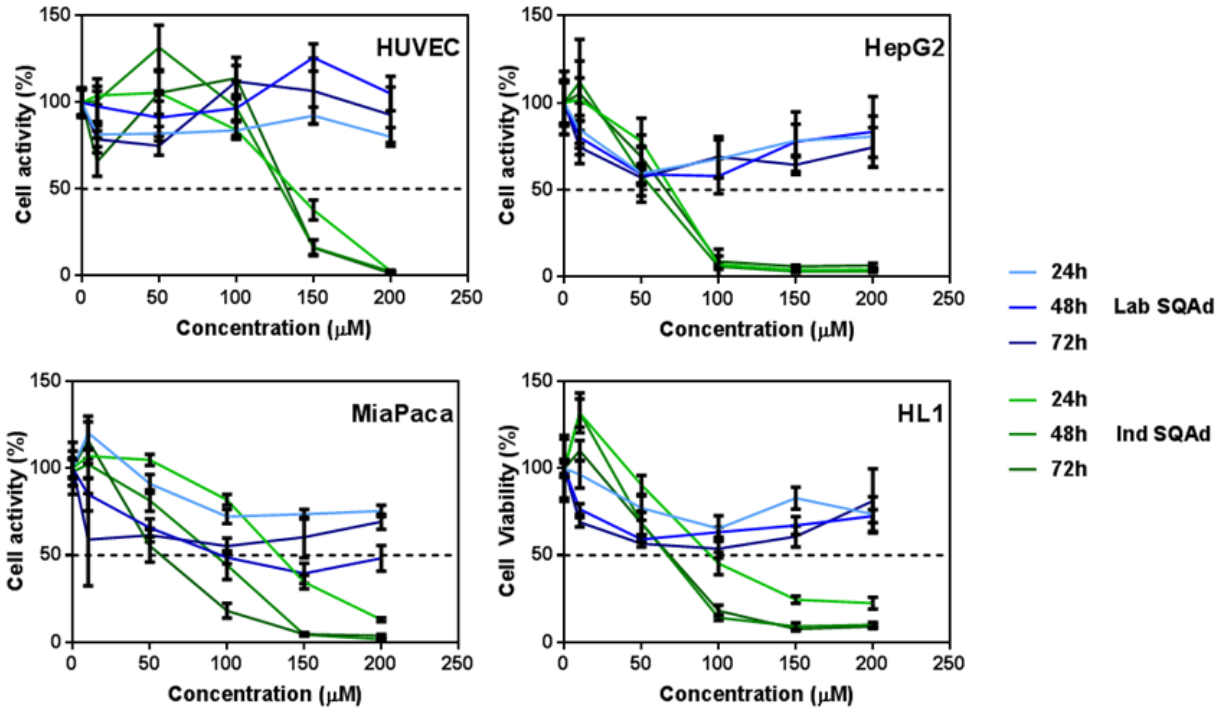

Figure 3: MTT assays of Lab SQAd and Ind SQAd on HUVEC, HepG2, MiaPaca and HL1 cell lines. Viability was expressed as % of viability of non treated cells as measured by formazan dye absorbance at 570 nm. Concentrations ranging from 5 μM to 200 μM were studied over 24 h, 48 h and 72 h of incubation.

32). A number of studies have reported that cell specific purinergic receptors contribute to the dual effects of adenosine on cell viability(33-35). SQAd has been shown not to be a direct agonist of these purinergic adenosine receptors but rather to act through accumulation of adenosine intracellularly(36). In any case, these subtle cytotoxic and cytoprotective effects of adenosine can hardly explain the gross differences displayed in the cytotoxicity profiles of the different SQAd batches observed in this study.

d) Plasma protein adsorption

Current understanding of nanoparticles interactions *in vivo* suggests that the protein corona (*ie* surface adsorbed proteins) formed on nanoparticles greatly influences their biological fate(37, 38). Consequently, plasma protein adsorption on Ind SQAd NPs and Lab SQAd NPs was

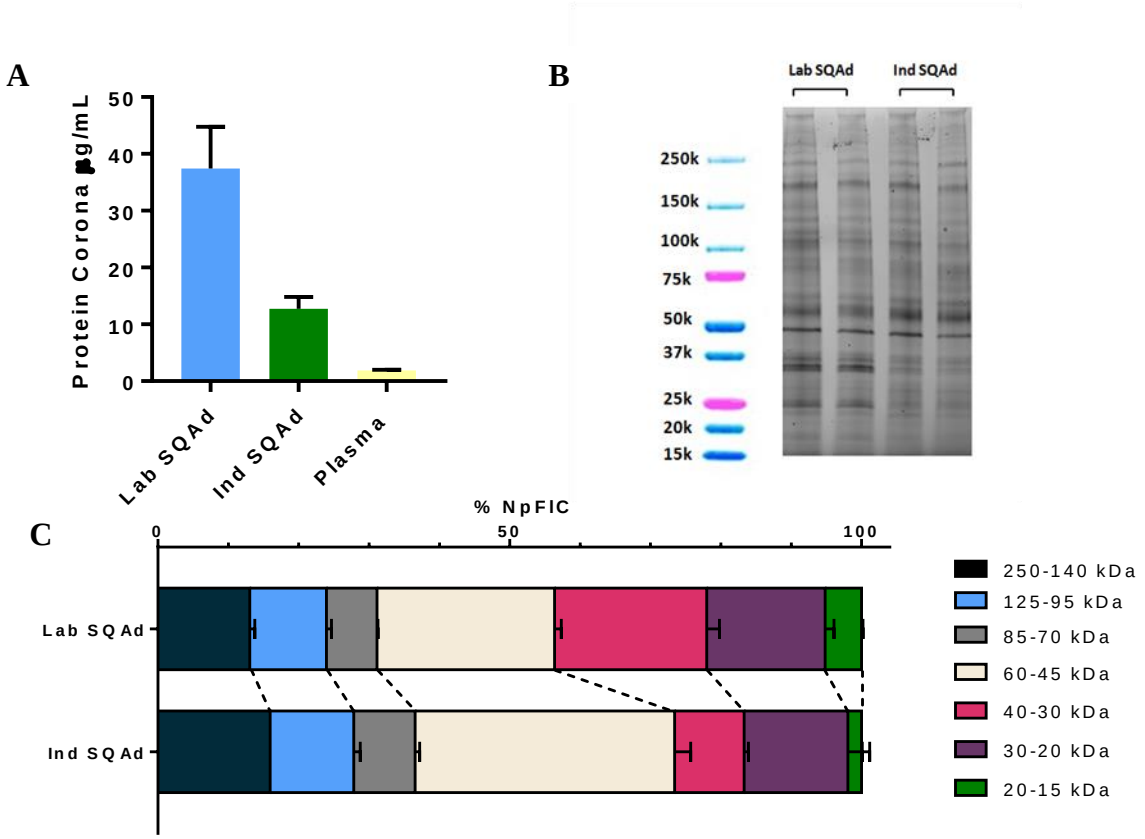

Figure 4: A. Concentration of protein corona isolated from different batches of SQAd NPs as measured by Pierce protein assay. For plasma control, the same procedure as for NPs corona evaluation was used but without the presence of nanoparticles. **B.** 1D-PAGE from two independent experiments of Lab SQAd and Ind SQAd protein corona. Molecular weight ladder was migrated with a pre-stained Biorad Precision Plus sample which is shown alongside the stain-free gel electrophoresis. **C.** Normalized percentage of fluorescence count for proteins found in the hard corona of Lab SQAd and Ind SQAd nanoparticles. Proteins were grouped following molecular weight expressed in kDa.

evaluated after incubation in rat plasma for 1 h at 37 °C. NP-protein complexes were isolated from excess plasma, washed thoroughly, and the amount of adsorbed proteins was quantified for each formulation. Lab SQAd formulations afforded an average of 37.4 µg/mL (i.e. 93.5

µg/mg NPs) adsorbed proteins, while Ind SQAd afforded an average of 12.8 µg/mL (i.e. 32 µg/mg NPs) adsorbed proteins (Figure 4A). These values refer to those proteins which strongly interacted with the nanoparticles surface, the so called "hard corona", which essentially confer the NPs their biological identity. Although previous studies have shown that strongly negative NPs had a tendency to adsorb higher amount of proteins(39), the main driving force in protein-NP interactions is not simply electrostatic but revolves also around complex colloidal and biochemical interactions which characterize the NPs *in vivo*(40, 41). For instance, it is possible that the crystal lattice of the Lab SQAd nanoparticles allowed greater access and interaction with the small proteins of the plasma. To better identify the influence of the industrial scale-up on the nature of the adsorbed proteins at the surface of the NPs, stain-free 1D-PAGE was performed on the hard corona isolated from NPs of both Lab SQAd and Ind SQAd batches (Figure 4B). 1D-PAGE resolves the corona proteins according to their molecular weight and afforded a basic evaluation of the different fractions of protein adsorbed to the NPs and their relative amounts. The relative abundance of each protein fraction on the surface of the nanoparticles was evaluated by Normalized Percentage of Fluorescence Count (%NpFlC, equivalent to the fraction of total fluorescence for all proteins found in the corona). The protein corona compositions shown in Figure 4C varied in subtle ways between the two SQAd batches. Mainly, low molecular weight protein fractions appeared to be significantly reduced in Ind SQAd and could account for the smaller quantities of protein corona found on Ind SQAd NPs. On the contrary, proteins of larger molecular weight (above 60 kDa) were found to be present consistently among the tested nanoparticles samples (lane profiles can be found in Supp. Figures S4-S5). While the determinants of corona composition are often underappreciated and hardly characterized, they are critical in determining the subsequent fate and effects of NPs in both *in vitro* and *in vivo* situations. Studies have shown that variations of less than 10 % in the makeup of a NP's protein corona could result in an alteration of the pharmacokinetic profiles and biodistribution (38).

2. Identification and characterization of impurities

a) Chromatography studies

Our previous physico-chemical and *in-vitro* studies seemed to point to the presence of formerly undetected impurities, especially in the Ind SQAd batches. As such, a more sensitive HPLC-MS approach of the different SQAd samples was carried out in order to identify and characterize eventual impurities responsible for batch-to-batch discrepancies. The results, shown in Figure 5, indicate that other than SQAd (peaks 3 and 4) a small quantity of detectable impurity phase, from now on named Ph1, corresponding to a mass of elution peaks around 20.8 min (peaks 1,2 and 5), was present in Ind SQAd batches. UV integration at 270 nm showed Ph1 peaks present at 1-2% in Ind SQAd and hardly detectable (<0.5%) in Lab SQAd. ES-MS data showed Ph1 as being composed of a mixture of SQAd analogs with major components having measured masses of 734.48 g/mol and 750.47 g/mol. Two minor impurities were also found in shoulder 6 for which a MS study can be found in Supp. Figure S6.

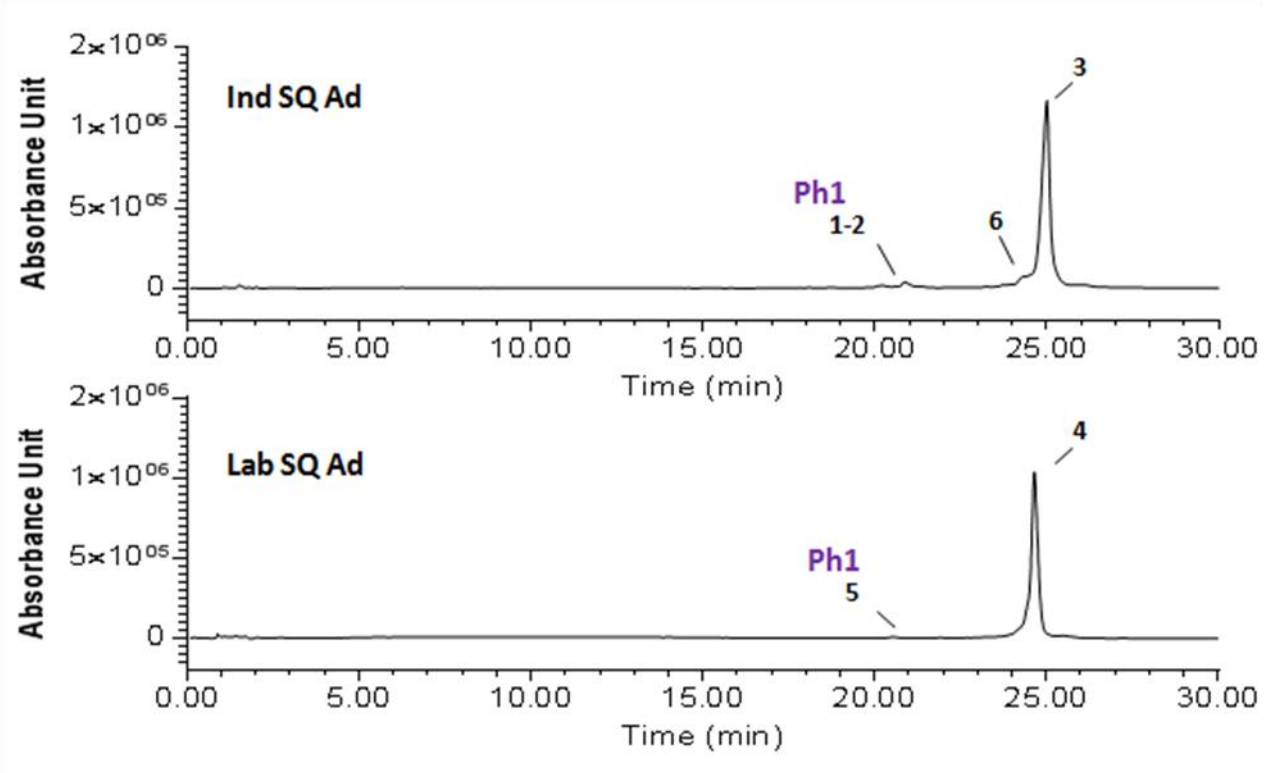

Figure 5: UV-HPLC spectra of Ind SQAd and Lab SQAd. UV spectra was recorded at 270 nm, corresponding to the maximum absorption peak of SQAd. At the end of the HPLC system, ES mass spectrometry was performed and the results reported in Table 1.

Peak no	Identification	t_R (min)	Proposal ions	Measured mass (m/z)	Elemental composition	UV Integration (%)
1	SQAd OH_2	20.22	$[M-H]^+$	750.47	$C_{42}H_{63}N_5O_7$	0.5
2	SQAd OH	20.87	$[M-H]^+$	734.48	$C_{42}H_{63}N_5O_6$	1.5
3	SQAd	25.00	$[M-H]^+$	718.49	$C_{42}H_{63}N_5O_5$	98
4	SQAd	24.73	$[M-H]^+$	718.49	$C_{42}H_{63}N_5O_5$	99.5
5	SQAd OH	20.52	$[M-H]^+$	734.48	$C_{42}H_{63}N_5O_6$	0.5

Table 1: Spectrometry data for Lab SQAd and Ind SQAd HPLC peaks.

This corresponded to SQAd (*m/z* = 718.49) with one or two additional oxygen atoms which we inferred to be -OH substituents present on the aliphatic squalene chain of SQAd. To elucidate this further, a collision induced dissociation (CID) MS^n study of these compounds was carried out (Table 2 and Supp. Figures S7-S9). CID of SQAd in the conditions used for this study usually yields a single major product ion with *m/z* = 586.44, corresponding to the fragmentation of a ribose residue from the adenosine moiety. When CID was carried out on Ph1, it showed that both compounds with *m/z* = 734.48 and *m/z* = 750.47 first demonstrated the usual pathway of parent ion fragmentation observed with secondary allylic alcohols, corresponding to a β-elimination of the hydroxyl group, resulting in CID products of m/z = 716.47 and m/z = 732.47 respectively (Figure 6A).

Peak no	Identification	t_R (min)	Proposal ions	Measured mass (m/z)	Elemental composition	UV Integration (%)
1	SQAd OH_2	20.22	$[M-H]^+$	750.47	$C_{42}H_{63}N_5O_7$	0.5
2	SQAd OH	20.87	$[M-H]^+$	734.48	$C_{42}H_{63}N_5O_6$	1.5
3	SQAd	25.00	$[M-H]^+$	718.49	$C_{42}H_{63}N_5O_5$	98
4	SQAd	24.73	$[M-H]^+$	718.49	$C_{42}H_{63}N_5O_5$	99.5
5	SQAd OH	20.52	$[M-H]^+$	734.48	$C_{42}H_{63}N_5O_6$	0.5

Table 2: Collision induced dissociation of the different SQAd compounds detected by MS^n.

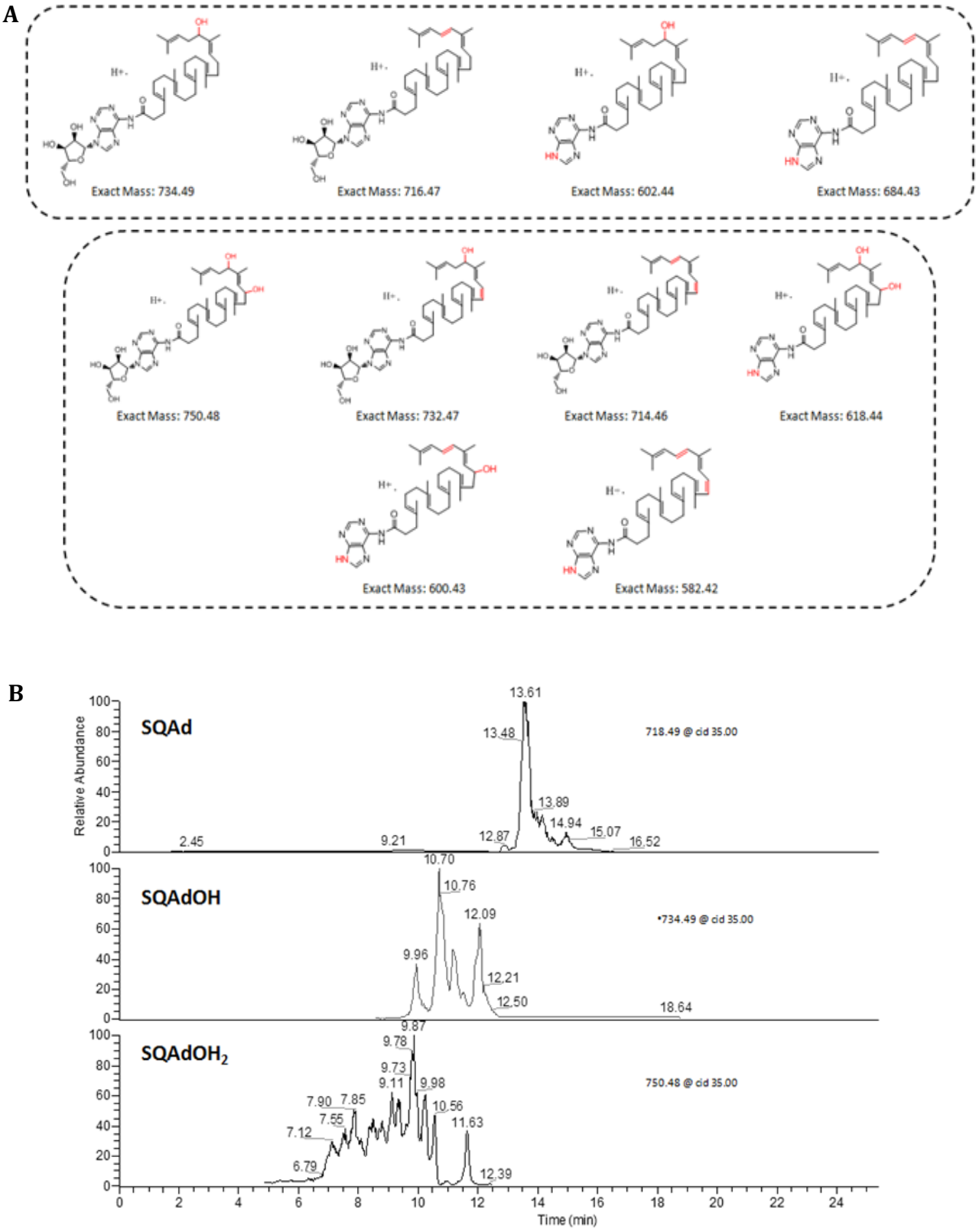

Figure 6: A. Presumptive structures for the detected SQAd analogs and their collision-induced product ions are shown. Upper box shows product ions for single –OH substituted SQAd analogs, lower box corresponds to double –OH substituted products. Exact masses were calculated with the ChemDraw software and fitted the experimental data. **B.** Chromatograms of the different SQAd analogs obtained during HPLC-ESI-MS^{n}.

This was followed by the expected product ions induced by SQAd ion fragmentation and loss of the ribose residue. Of note, chromatograms obtained from the high resolution HPLC-ESI-MS^n study additionally showed that slightly different elution peaks corresponded to compounds having identical molecular masses (Figure 6B). For single –OH substituted compounds SQAdOH, we found five elution peaks corresponding to the five possible substitution products over the available isoprenyl subunits, while double –OH substituted compounds $SQAdOH_2$ gave 10 elution peaks corresponding to the combination of two substitutions out of a set of five available isoprenyl subunits. This indicated that the SQAd analogs most probably existed as a mixture of isomers in Ph1, suggesting that the oxidative side-reaction which led to the additional hydroxyl groups occurred unselectively over all five isoprenyl subunits. Although, in the absence of an exact structural determination, the mechanism of formation of these minor byproducts remains speculative, it can be suggested that they result from the ring-opening reaction with aluminum isopropoxide of internal epoxides produced by over oxidation with NBS. Previous studies have shown that the main side product in the Van Tamelen procedure is the □□□-bis-bromohydrine(42, 43). During the purification process, using chromatography on silica gel, only the main side product corresponding to the □□□-bis-bromohydrine could be separated, while minor less polar internal bromohydrines are much more difficult to eliminate and could remain with the main product. Once formed, these highly hindered allylic alcohols would not act as substrates in the Claisen-Johnson transposition and thus would remain as minor components in the bulk main product.

b) Cytotoxicity of hydroxylated SQAd impurities

To elucidate the impact of Ph1 impurities on the observed batch-to-batch discrepancies in NPs properties, a preparative HPLC separation (HPLC-Prep) was performed to isolate Ph1 from SQAd. Practically, two series of experiments were performed (Figure 7). First, NPs were prepared from Ph1 only (Figure 7A) and tested as such for their cytotoxicity and physico-chemical properties. When prepared by nanoprecipitation, Ph1 yielded stable NPs and DLS data showed a strongly negative zeta potential of -35 mV and sizes of ca. 100 nm (Figure 7B). Further studies focused on the biological effects of Ph1 NPs which were found to be dramatically cytotoxic, with IC_{50} values around 5 μM, compared to isolated SQAd which barely induced cytotoxicity in the tested concentration ranges (Figures 7D-E). The influence of minor impurities on cytotoxicity was also studied and data reported in Supp. Figure S10. Later, a series of additional experiments were performed in which pure SQAd fractions from HPLC prep experiments were spiked with increasing concentrations of Ph1 (from 0.1 % w/w to 10 % w/w).

Remarkably, the amount of Ph1 was proportionally linked to cytotoxicity in SQAd nanoformulations (Figure 7F).

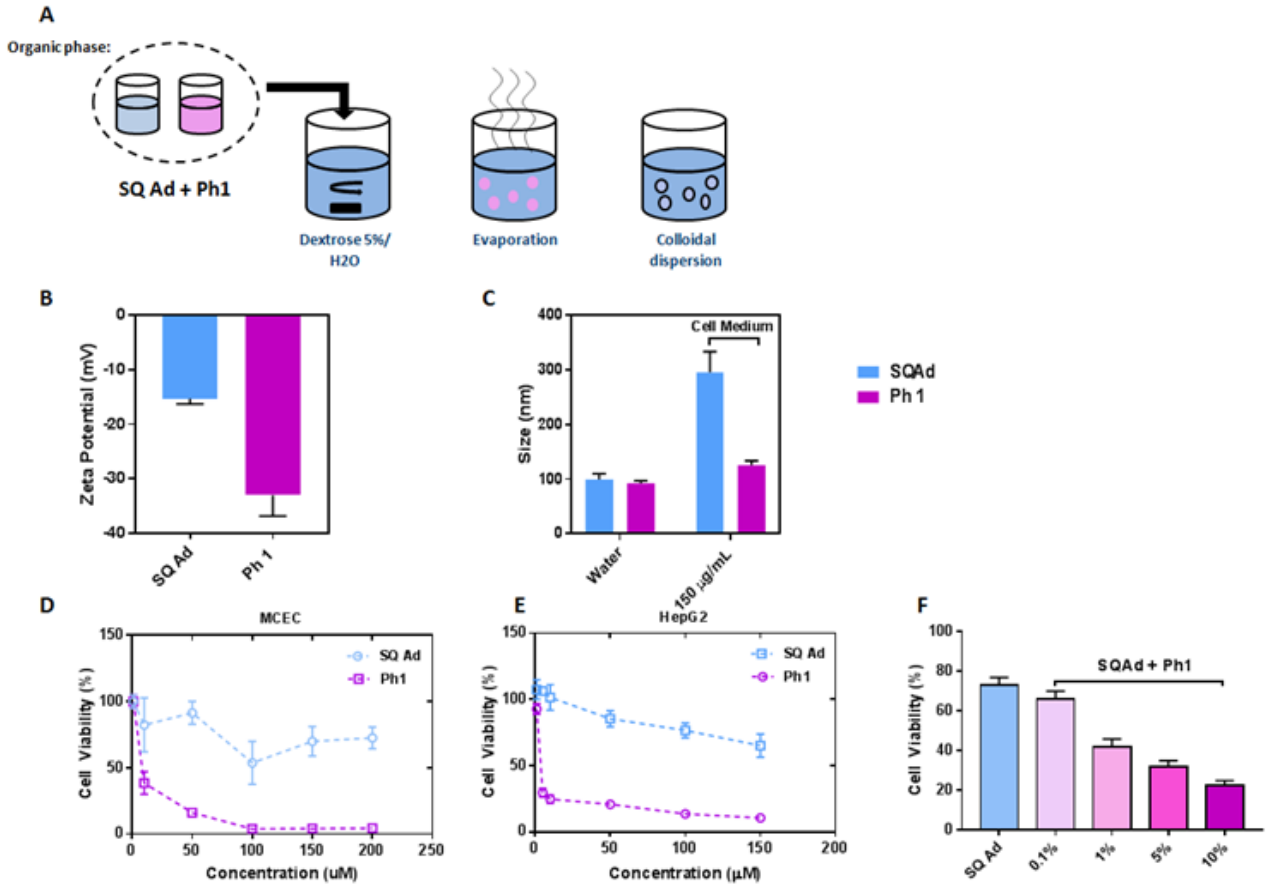

Figure 7: A. Representative scheme of spiking experiments, where isolated Ph1 and pure SQAd were combined in varying ratios. **B.** Zeta-potential measurements of SQAd and Ph1 NPs. **C.** DLS size measurement of SQAd and Ph1 NPs. For measurements performed in cell medium, NPs were dispersed at 150 µg/mL in complete DMEM medium. **D-E.** MTT assays of SQAd and Ph1 NPs on MCEC and HepG2 cell lines. Cell viability was measured as % viability of non treated cells. **F.** Cell viability after 24 hours incubation with 100 µM of SQAd eluate NPs or NPs of SQAd spiked with increasing concentrations of Ph1 from 0.1%-10% w/w.

These experiments confirmed that the Ph1 impurity, even when present in small quantity, was responsible for both the biological and physico-chemical alteration of SQAd NPs properties. It is not surprising that Ph1 forms a stable colloidal phase when nanoformulated, as other terpenoid derivatives of squalene have been shown to do so[46]. Ph1 yields NPs demonstrating low zeta potential and high toxicity which can help to explain the properties observed with Ind

SQAd batch NPs. We postulate that the observed cytotoxic effect of Ph1 is likely due to the aberrant squalene chains altering the cell membrane integrity. Indeed, squalene strongly interacts with lipid bilayers because of its structural similarity with cholesterol as well as through binding to LDL receptors on the cell surface(44-46). Additionally, it is also possible that hydroxylated SQAd analogs can participate in oxidative stress signaling through their similitude with lipid peroxidation by-products.

Ultimately, nanoparticle-based delivery systems are unique structures capable of accumulating bioactive molecules inside tissues and cells. This makes them a class of materials that is especially sensitive to the presence of residual manufacturing components or variations in purity from batch-to-batch(47-49). This has often lead to misjudgments concerning NP toxicities and poor reproducibility of results(50, 51). Here, even though special precautions were taken in using biocompatible reagents and formulation strategies, scaling-up the manufacturing process resulted in varying quantities of analogs of the lipid carrier chain which in turn were responsible for an unexpected cytotoxicity of SQAd NPs. These findings highlight the complexity of nanotechnology and the escalating level of expertise required to successfully generate safe and efficient nanomedicines. Not only does it require a thorough understanding of the chemistry and biocompatibility of compounds used for the initial formulation of the nanoparticles, but also full comprehension of the synthesis process and its implications on the aforementioned properties. In a context where the reproducibility of nanoformulations is put into question(52) and several generics of approved nanoformulated drugs are set to enter the market in the coming years(53), special care and regulatory oversight over these issues is of outmost importance.

IV. Conclusion

In this study, we showed that the scale-up of the bromohydrine synthetic pathway to SQAd can alter the impurity profile of the squalene bioconjugate which results in critical variations in SQAd NPs properties. Here, close analogs of the carrier lipid chain were found to be highly cytotoxic and strenuous to separate from SQAd bulk by conventional chromatographic methods. Surprisingly, these minor impurities had a strong impact on the colloidal properties, internal structure and biological properties of SQAd NPs. Identifying these issues was crucial in finally obtaining batches of SQAd that yield nanoparticles with consistent properties, which has now been achieved by the industrial partner.

Failure to properly characterize a material has afflicted the nanotechnology field for many years,

regularly leading to misjudgments about the properties of nanoparticles. The matter is often made worse in the case of nanocarriers because of the inherent polydispersity of their physico-chemical properties as well as their plural chemical identity. Identifying which parameters are most important for establishing the therapeutic and biological equivalence of two nanoparticle formulations is therefore important. As the field matures and a growing number of products seek regulatory approval, an especially careful approach in terms of toxicity and pharmaceutical development should be adopted in the maturation process of these innovative materials. Ultimately, understanding and solving these issues is a crucial part of the advancement of nanomedicines, and one which cannot be left for the industry to deal with alone.

Funding: The authors gratefully acknowledge the financial support from the 7th EuroNanoMed-II call for proposals, project NanoHeart n°ANR-16-ENM2-0005-01. This work was further supported by la Fondation pour la Recherche Médicale (FRM) grant number ECO20160736101. Cryo-TEM observations were made thanks to "Investissements d'Avenir" LabEx PALM (ANR-10-LABX-0039-PALM).

Acknowledgments: The authors wish to thank Karine Leblanc from the BioCIS platform for her expert technical advice on running and performing chromatography experiments as well as Audrey Solgadi from UMS-IPSIT SAMM platform for her help in designing and performing the MS^n experiments as well as helpful corrections in the manuscript. Jéril Degrouard is thanked for his technical help and discussions relating to cryo-TEM images.

V. References

1. S. Mura, J. Nicolas,P. Couvreur, Stimuli-responsive nanocarriers for drug delivery. *Nature materials*. 12, 991 (2013)
2. A. Kakkar, G. Traverso, O. C. Farokhzad, R. Weissleder*, et al.*, Evolution of macromolecular complexity in drug delivery systems. *Nature Reviews Chemistry*. 1, 0063 (2017)
3. V. J. Venditto,F. C. Szoka Jr, Cancer nanomedicines: so many papers and so few drugs! *Advanced drug delivery reviews*. 65, 80-88 (2013)
4. J.-B. Coty,C. Vauthier, Characterization of nanomedicines: A reflection on a field under construction needed for clinical translation success. *Journal of controlled release*. (2018)
5. J. Seiffert, F. Hussain, C. Wiegman, F. Li*, et al.*, Pulmonary toxicity of instilled silver nanoparticles: influence of size, coating and rat strain. *PloS one*. 10, e0119726 (2015)
6. H.-X. Wang, Z.-Q. Zuo, J.-Z. Du, Y.-C. Wang*, et al.*, Surface charge critically affects tumor penetration and therapeutic efficacy of cancer nanomedicines. *Nano Today*. 11, 133-144 (2016)
7. S.-Y. Qin, Y.-J. Cheng, Z.-W. Jiang, Y.-H. Ma*, et al.*, Morphology control of self-deliverable nanodrug with enhanced anticancer efficiency. *Colloids and Surfaces B: Biointerfaces*. 165, 345-354 (2018)

8. S. T. Stern, J. B. Hall, L. Y. Lee, L. J. Wood*, et al.*, Translational considerations for cancer nanomedicine. *Journal of Controlled Release*. 146, 164-174 (2010)
9. N. Bertrand, P. Grenier, M. Mahmoudi, E. M. Lima*, et al.*, Mechanistic understanding of in vivo protein corona formation on polymeric nanoparticles and impact on pharmacokinetics. *Nature communications*. 8, 777 (2017)
10. R. N. Mamidi, S. Weng, S. Stellar, C. Wang*, et al.*, Pharmacokinetics, efficacy and toxicity of different pegylated liposomal doxorubicin formulations in preclinical models: is a conventional bioequivalence approach sufficient to ensure therapeutic equivalence of pegylated liposomal doxorubicin products? *Cancer chemotherapy and pharmacology*. 66, 1173-1184 (2010)
11. H. Ragelle, F. Danhier, V. Préat, R. Langer*, et al.*, Nanoparticle-based drug delivery systems: a commercial and regulatory outlook as the field matures. *Expert opinion on drug delivery*. 14, 851-864 (2017)
12. R. M. Crist, J. H. Grossman, A. K. Patri, S. T. Stern*, et al.*, Common pitfalls in nanotechnology: lessons learned from NCI's Nanotechnology Characterization Laboratory. *Integrative Biology*. 5, 66-73 (2012)
13. D. Desmaële, R. Gref,P. Couvreur, Squalenoylation: a generic platform for nanoparticular drug delivery. *Journal of controlled release*. 161, 609-618 (2012)
14. E. Lepeltier, B. Loretz, D. DesmaëLe, J. Zapp*, et al.*, Squalenoylation of chitosan: a platform for drug delivery? *Biomacromolecules*. 16, 2930-2939 (2015)
15. P. Couvreur (2016) Squalenoylation: a novel technology for anticancer and antibiotic drugs with enhanced activity. *Nanosciences and Nanotechnology*, (Springer), 253-272.
16. L. H. Reddy, H. Khouri, A. Paci, A. Deroussent*, et al.*, Squalenoylation favourably modifies the in vivo pharmacokinetics and biodistribution of gemcitabine in mice. *Drug Metabolism and Disposition*. (2008)
17. A. Maksimenko, J. Mougin, S. Mura, E. Sliwinski*, et al.*, Polyisoprenoyl gemcitabine conjugates self assemble as nanoparticles, useful for cancer therapy. *Cancer letters*. 334, 346-353 (2013)
18. A. Gaudin, M. Yemisci, H. Eroglu, S. Lepetre-Mouelhi*, et al.*, Squalenoyl adenosine nanoparticles provide neuroprotection after stroke and spinal cord injury. *Nature nanotechnology*. 9, 1054 (2014)
19. J. Feng, S. Lepetre-Mouelhi, A. Gautier, S. Mura*, et al.*, A new painkiller nanomedicine to bypass the blood-brain barrier and the use of morphine. *Science Advances*. 5, eaau5148 (2019)
20. U. K. Laemmli, Cleavage of structural proteins during the assembly of the head of bacteriophage T4. *nature*. 227, 680 (1970)
21. E. Van Tamelen,T. Curphey, The selective in vitro oxidation of the terminal double bonds in squalene. *Tetrahedron Letters*. 3, 121-124 (1962)
22. M. Ceruti, F. Viola, F. Dosio, L. Cattel*, et al.*, Stereospecific synthesis of squalenoid epoxide vinyl ethers as inhibitors of 2, 3-oxidosqualene cyclase. *Journal of the Chemical Society, Perkin Transactions 1*. 461-469 (1988)
23. J. L. Abad, J. Casas, F. Sanchez-Baeza,A. Messeguer, Dioxidosqualenes: characterization and activity as inhibitors of 2, 3-oxidosqualene-lanosterol cyclase. *The Journal of Organic Chemistry*. 58, 3991-3997 (1993)
24. W. S. Johnson, L. Werthemann, W. R. Bartlett, T. J. Brocksom*, et al.*, Simple stereoselective version of the Claisen rearrangement leading to trans-trisubstituted olefinic bonds. Synthesis of squalene. *Journal of the American Chemical Society*. 92, 741-743 (1970)
25. E. Buchy, S. Valetti, S. Mura, J. Mougin*, et al.*, Synthesis and Cytotoxic Activity of Self-Assembling Squalene Conjugates of 3-[(Pyrrol-2-yl) methylidene]-2, 3-dihydro-1H-indol-2-one Anticancer Agents. *European Journal of Organic Chemistry*. 2015, 202-212 (2015)
26. S. M. Schrier, E. W. Van Tilburg, H. Van Der Meulen, A. P. Ijzerman*, et al.*, Extracellular adenosine-induced apoptosis in mouse neuroblastoma cells studies on involvement of adenosine receptors and adenosine uptake1. *Biochemical pharmacology*. 61, 417-425 (2001)
27. M. F. Ethier, V. Chander,J. G. Dobson Jr, Adenosine stimulates proliferation of human endothelial cells in culture. *American Journal of Physiology-Heart and Circulatory Physiology*. 265, H131-H138 (1993)
28. P. Fishman, S. Bar-Yehuda,L. Vagman, Adenosine and other low molecular weight factors released by muscle cells inhibit tumor cell growth. *Cancer research*. 58, 3181-3187 (1998)

29. V. Shneyvays, K. Jacobson, A. Li, H. Nawrath*, et al.*, Induction of apoptosis in rat cardiocytes by A3 adenosine receptor activation and its suppression by isoproterenol. *Experimental cell research*. 257, 111-126 (2000)
30. Y. Kohno, Y. Sei, M. Koshiba, H. O. Kim*, et al.*, Induction of Apoptosis in HL-60 Human Promyelocytic Leukemia Cells by Adenosine A3Receptor Agonists. *Biochemical and biophysical research communications*. 219, 904-910 (1996)
31. S. Bès, B. Ponsard, M. El Asri, C. Tissier*, et al.*, Assessment of the cytoprotective role of adenosine in an in vitro cellular model of myocardial ischemia. *European journal of pharmacology*. 452, 145-154 (2002)
32. V. Ramkumar, D. M. Hallam,Z. Nie, Adenosine, oxidative stress and cytoprotection. *The Japanese Journal of Pharmacology*. 86, 265-274 (2001)
33. J. Barankiewicz, A. M. Danks, E. Abushanab, L. Makings*, et al.*, Regulation of adenosine concentration and cytoprotective effects of novel reversible adenosine deaminase inhibitors. *Journal of Pharmacology and Experimental Therapeutics*. 283, 1230-1238 (1997)
34. K. A. Jacobson, Adenosine A3 receptors: novel ligands and paradoxical effects. *Trends in pharmacological sciences*. 19, 184-191 (1998)
35. T. Imura,S. Shimohama, Opposing effects of adenosine on the survival of glial cells exposed to chemical ischemia. *Journal of neuroscience research*. 62, 539-546 (2000)
36. M. Rouquette, S. Lepetre-Mouelhi, O. Dufrancais, X. Yang*, et al.*, Squalene-adenosine nanoparticles: ligands of adenosine receptors or adenosine prodrug? *The Journal of pharmacology and experimental therapeutics*. (2019)
37. M. P. Monopoli, C. Åberg, A. Salvati,K. A. Dawson, Biomolecular coronas provide the biological identity of nanosized materials. *Nature nanotechnology*. 7, 779 (2012)
38. P. Grenier, I. M. De Oliveira Viana, E. M. Lima,N. Bertrand, Anti-polyethylene glycol antibodies alter the protein corona deposited on nanoparticles and the physiological pathways regulating their fate in vivo. *Journal of controlled release*. 287, 121-131 (2018)
39. C. D. Walkey, J. B. Olsen, F. Song, R. Liu*, et al.*, Protein corona fingerprinting predicts the cellular interaction of gold and silver nanoparticles. *ACS nano*. 8, 2439-2455 (2014)
40. A. Bigdeli, S. Palchetti, D. Pozzi, M. R. Hormozi-Nezhad*, et al.*, Exploring cellular interactions of liposomes using protein corona fingerprints and physicochemical properties. *ACS nano*. 10, 3723-3737 (2016)
41. R. Liu, W. Jiang, C. D. Walkey, W. C. Chan*, et al.*, Prediction of nanoparticles-cell association based on corona proteins and physicochemical properties. *Nanoscale*. 7, 9664-9675 (2015)
42. R. Hauptfleisch,B. Franck, Stereoselective syntheses of 1, 24-dihydroxy squalene 2, 3; 22, 23-dioxides by double sharpless epoxidation. *Tetrahedron letters*. 38, 383-386 (1997)
43. T. Hoshino, S.-I. Nakano, T. Kondo, T. Sato*, et al.*, Squalene–hopene cyclase: final deprotonation reaction, conformational analysis for the cyclization of (3 R, S)-2, 3-oxidosqualene and further evidence for the requirement of an isopropylidene moiety both for initiation of the polycyclization cascade and for the formation of the 5-membered E-ring. *Organic & biomolecular chemistry*. 2, 1456-1470 (2004)
44. A. Peramo, S. Mura, S. O. Yesylevskyy, B. Cardey*, et al.*, Squalene versus cholesterol: Which is the best nanocarrier for the delivery to cells of the anticancer drug gemcitabine? *Comptes Rendus Chimie*. (2018)
45. D. Sobot, S. Mura, S. O. Yesylevskyy, L. Dalbin*, et al.*, Conjugation of squalene to gemcitabine as unique approach exploiting endogenous lipoproteins for drug delivery. *Nature communications*. 8, 15678 (2017)
46. A. Gaudin, O. Tagit, D. Sobot, S. Lepetre-Mouelhi*, et al.*, Transport mechanisms of squalenoyl-adenosine nanoparticles across the blood–brain barrier. *Chemistry of Materials*. 27, 3636-3647 (2015)
47. A. P. Leonov, J. Zheng, J. D. Clogston, S. T. Stern*, et al.*, Detoxification of gold nanorods by treatment with polystyrenesulfonate. *ACS nano*. 2, 2481-2488 (2008)
48. J. Liu, D. A. Sonshine, S. Shervani,R. H. Hurt, Controlled release of biologically active silver from nanosilver surfaces. *ACS nano*. 4, 6903-6913 (2010)

49. S. Zhu, E. Oberdörster,M. L. Haasch, Toxicity of an engineered nanoparticle (fullerene, C60) in two aquatic species, Daphnia and fathead minnow. *Marine Environmental Research*. 62, S5-S9 (2006)
50. R. Cortesi, E. Esposito, E. Menegatti, R. Gambari*, et al.*, Effect of cationic liposome composition on in vitro cytotoxicity and protective effect on carried DNA. *International Journal of Pharmaceutics*. 139, 69-78 (1996)
51. E. Oberdörster, Manufactured nanomaterials (fullerenes, C60) induce oxidative stress in the brain of juvenile largemouth bass. *Environmental health perspectives*. 112, 1058 (2004)
52. J. C. Leroux, Drug delivery: too much complexity, not enough reproducibility? *Angewandte Chemie International Edition*. 56, 15170-15171 (2017)
53. M. Davenport, Closing the gap for generic nanomedicines. *Chemical Engineering News*. 92, 10-13 (2014)

Supplementary Materials

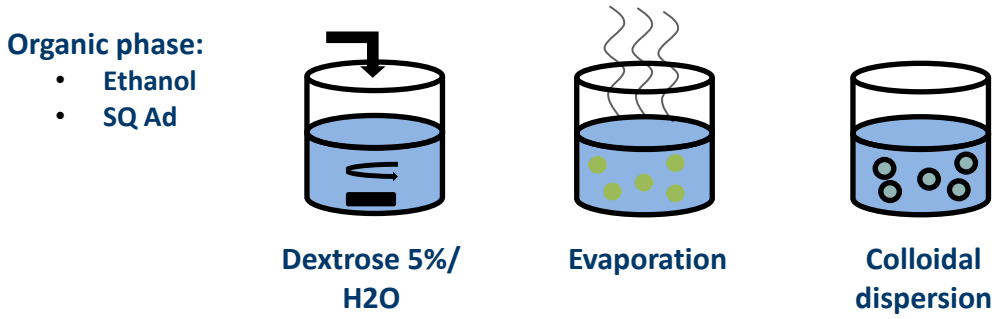

Figure S1: Overview of SQAd NP synthesis. Bioconjugates are dispersed in Ethanol at the concentration of 6 mg/mL. The organic phase is nanoprecipitated in an acqueous DXT 5% solution under vigorous stirring. The ethanol is evaporated under reduced pressure leaving a colloidal dispersion of SQAd NPs.

Lab SQAd

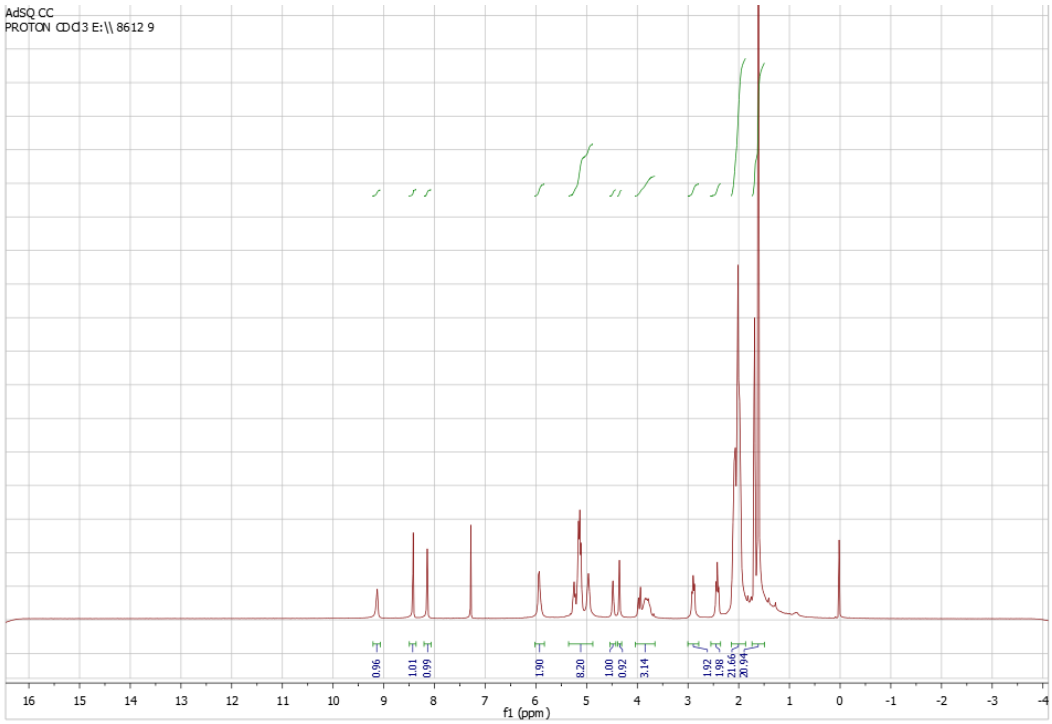

Ind SQAd

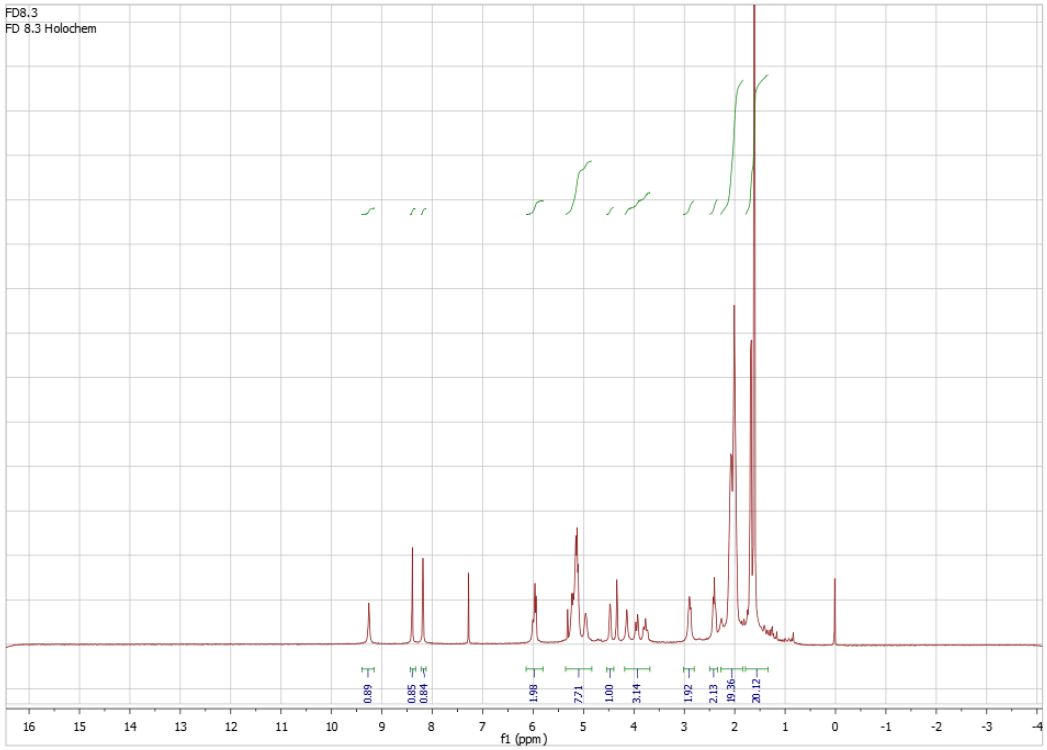

Figure S2: NMR spectra of Lab SQAd and Ind SQAd

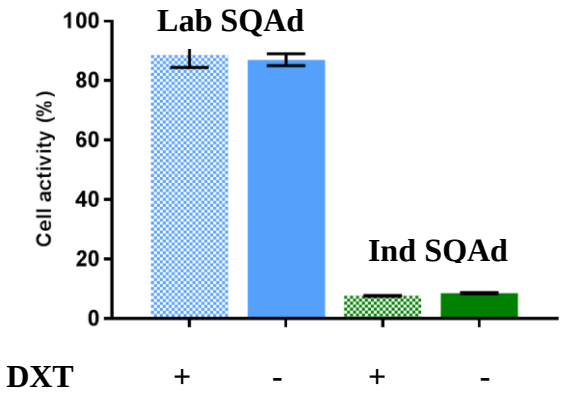

Figure S3: Cytotoxicity of Lab SQAd vs Ind SQAd at 100 μM on HepG2 cells over 24 hrs with different formulations methods to control for DXT influence.

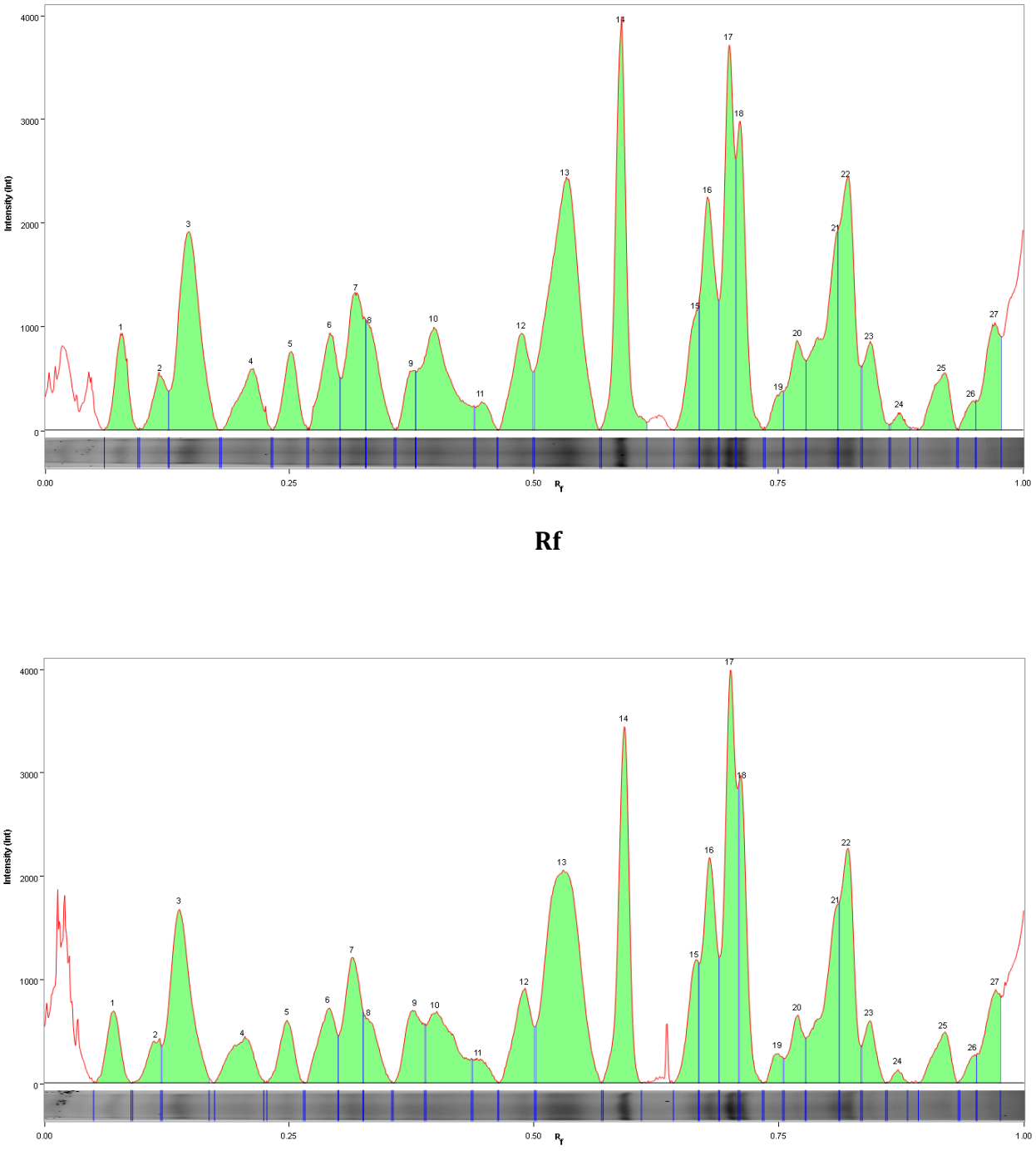

Figure S4: 1D-PAGE experiment lane profiles from Image Lab software analysis of Lab SQAd gel electrophoresis of two independent Lab SQAd protein corona isolation experiments. Intensity peaks indicate presence of protein in the gel for a given elution ratio (Rf). Higher elution ratios correspond to lower molecular weight proteins. Peak numbers correspond to user defined band numbers.

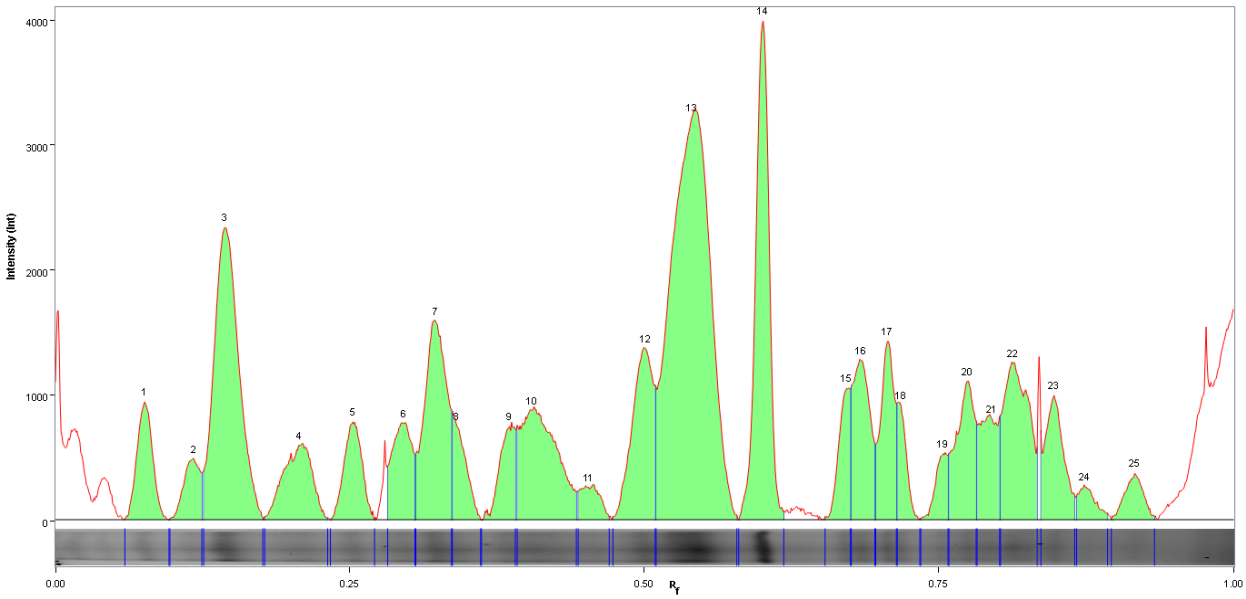

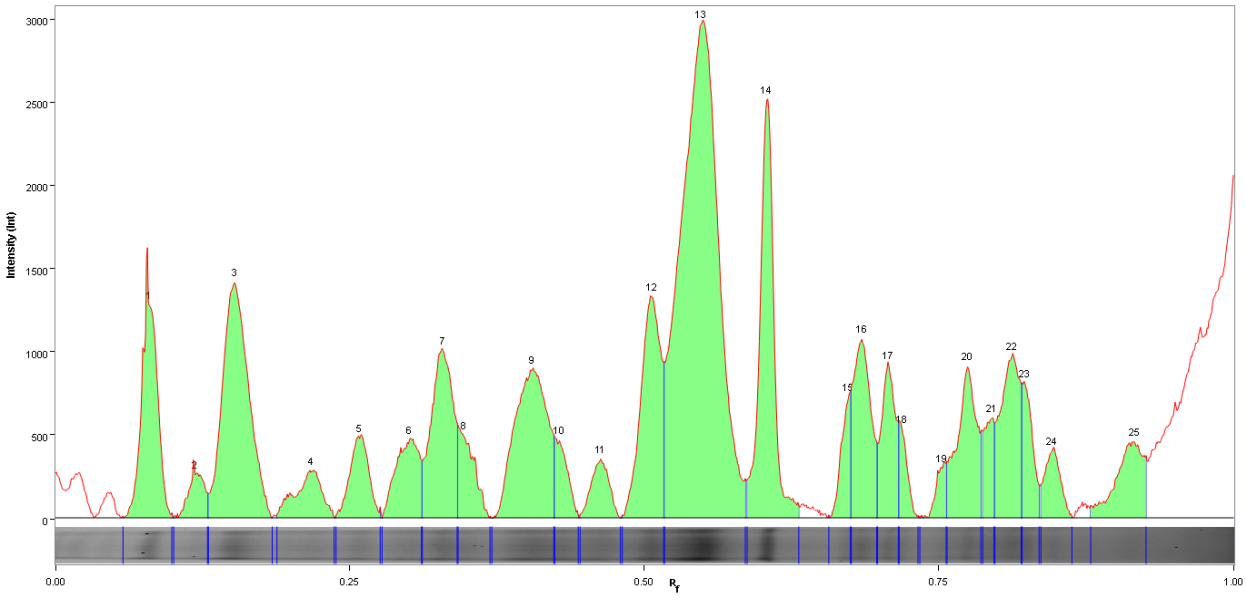

Figure S5: 1D-PAGE experiment lane profiles from Image Lab software analysis of Ind SQAd gel electrophoresis of two independent Ind SQAd protein corona isolation experiments. Intensity peaks indicate presence of protein in the gel for a given elution ratio (Rf). Higher elution ratios correspond to lower molecular weight proteins. Peak numbers correspond to user defined band numbers.

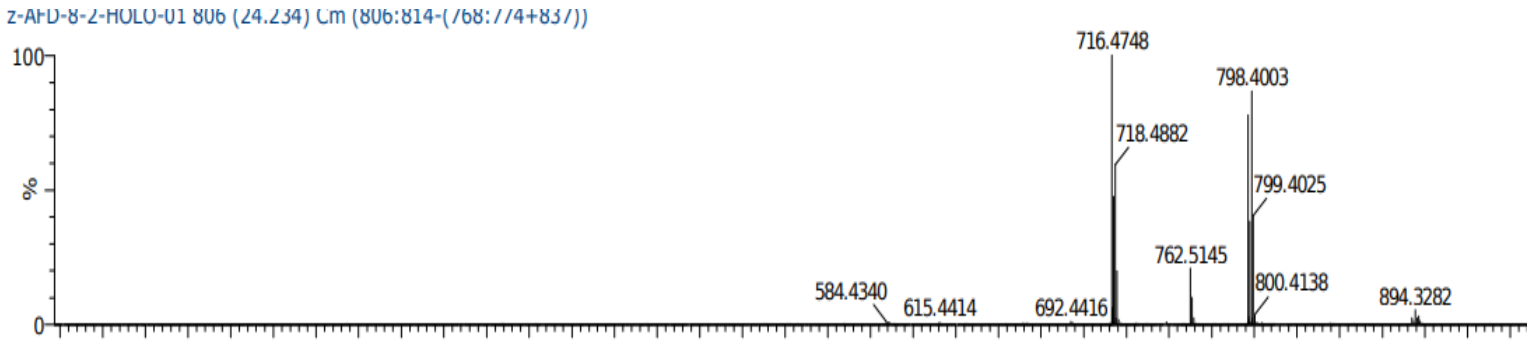

Figure S6: MS of minor impurities found in Lab SQAd shoulder **6**. The compound with m/z= 798.40 g/mol is a Br containing SQAd analog recognizable by its characteristic "dual" MS peaks caused by the similar abundances of Br isotopes ^{79}Br and ^{81}Br. The compound found at m/z= 716.47 g/mol is most probably a triene derivative of SQAd with an additional insaturation on the aliphatic chain.

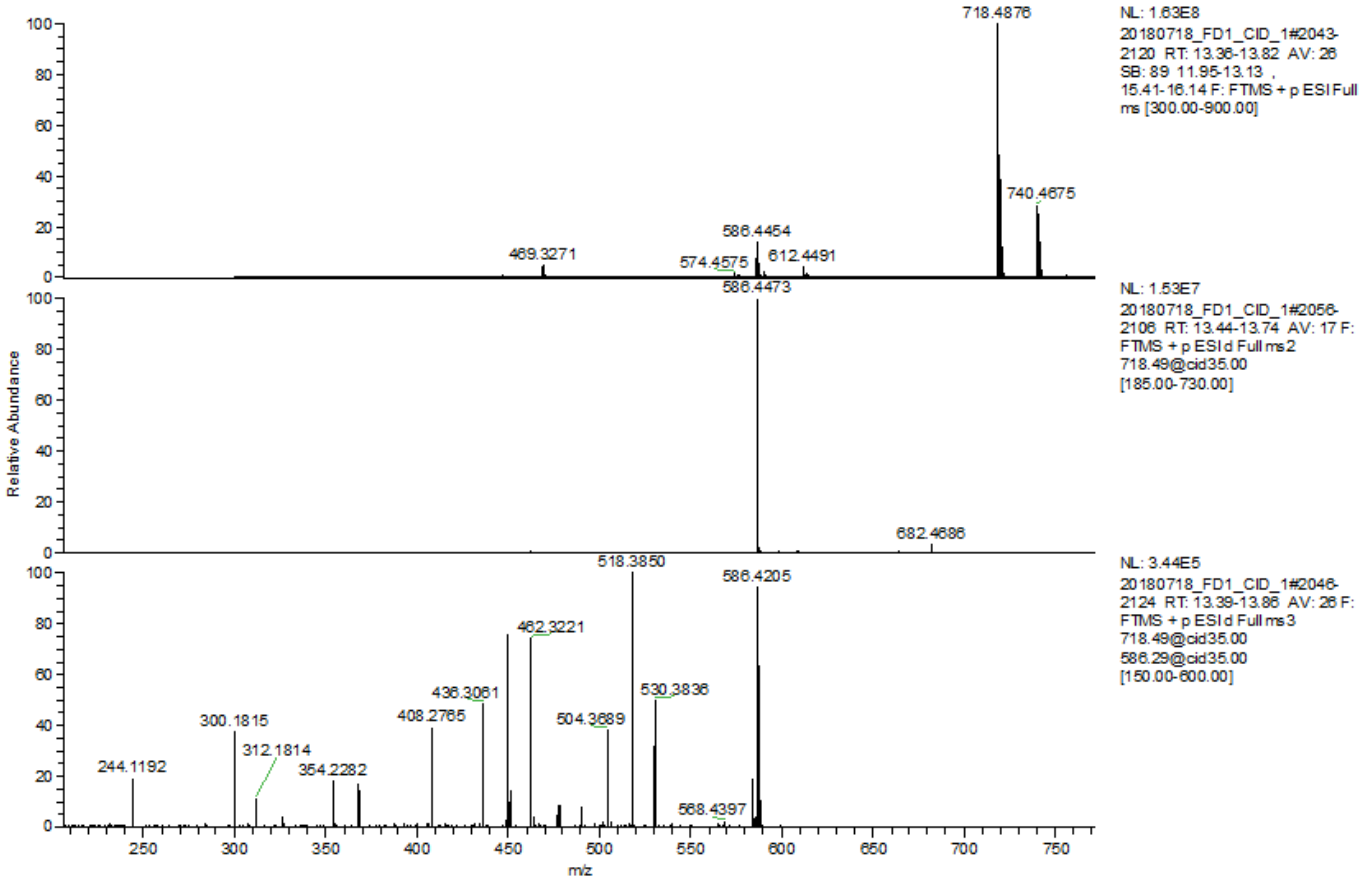

Figure S7: ESI-MS^n of SQAd (*m/z*= 718.49) with full scan ions (top) MS CID product (middle) and MS^2 CID products (bottom).

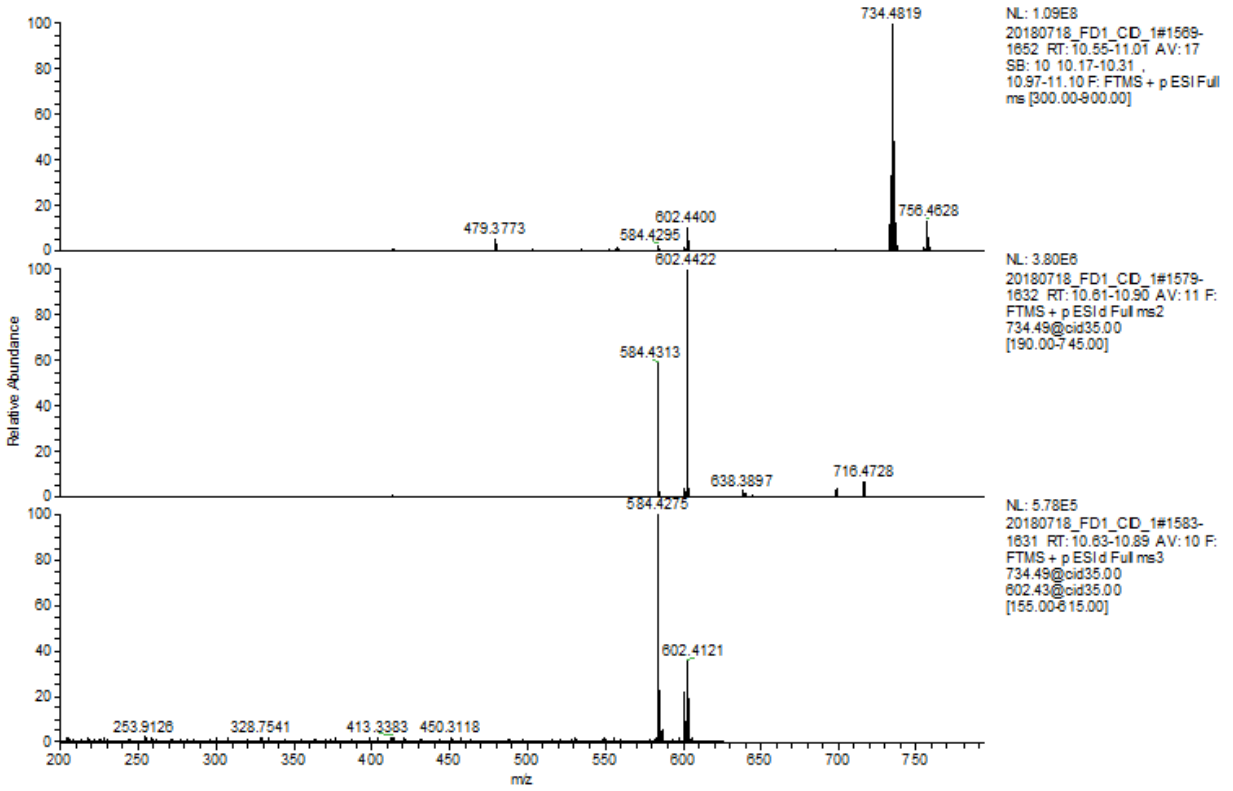

Figure S8: ESI-MS^n of "SQAdOH" analog (*m/z*= 734.48) with full scan ions (top) MS CID product (middle) and MS^2 CID products (bottom).

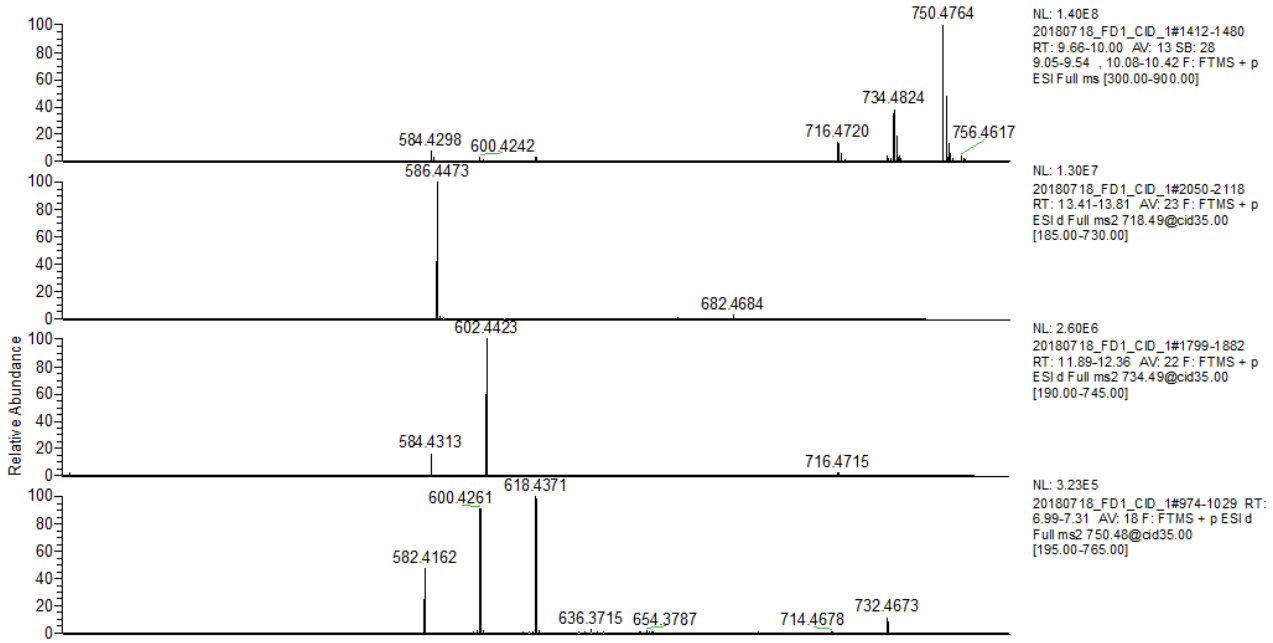

Figure S9: ESI-MS^n of "SQAdOH2" analog (*m/z*= 750.48) with full scan ions (top) MS (middle top), MS^2 CID product (middle bottom) and MS^3 CID products (bottom).

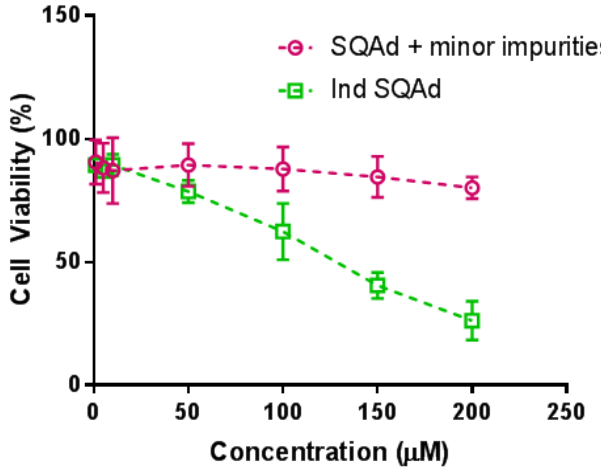

Figure S10: Cytotoxicity of SQAd containing the minor bromine and triene impurities on HL1 cells over 24 hours.

General Discussion

The goal of this doctoral thesis was to evaluate the pharmacological potential of squalene-adenosine based therapies in inflammatory disorders. The hypothesis was that the specific micro-environment reigning in inflamed tissues would allow our nanoparticular formulations to differentially target the foci of inflammation and provide a promising adenosine based therapeutic intervention. This was supported by several arguments.

In a seminal study published by our laboratory, SQAd NPs were shown to have promising therapeutic properties against cerebral ischemia and reperfusion injuries in a murine carotid ligation model. At the time, the main protective effects were thought to have been provided by the action of adenosine on the vascular endothelium. However, some early signs of lowered inflammation were detected and indication of a lower inflammatory response in this model was encouraging for future work on the use of SQAd derived nanoparticles in inflammatory disorders.

In another recent study evaluating Squalene-Leu-enkephalin (SQ-LENK) nanoparticles as efficient painkillers to bypass the use of central opioid receptors antagonists, SQ-LENK nanoparticles were first observed to accumulate at local sites of inflammation. This accumulation occurred in a carrageenan-induced paw inflammatory pain model and enabled the nanoparticles to enact a targeted analgesic action without inducing measurable side effects. Although inflammatory micro-environment targeting was not the main point of this study, we considered that the accumulation of the SQ-LENK derivatives at the site of inflammation was interesting enough to warrant further exploration in more pathological expressions of inflammation such as sepsis or endotoxemia.

In this general discussion, we will discuss first the use of adenosine in inflammatory disorders and what advantages or limitations the squalenoylation technology affords for endogenous purine therapy. Secondly, we will discuss multidrug nanoparticles, their potential use in

inflammatory disorders and important developments and limitations. Thirdly, how the different results of SQ NPs biodistribution studies present in this work can be interpreted in light of recent literature, what they mean for the understanding of squalene-based targeting technology and potential investigation avenues. Finally, we will discuss the industrial scale-up of nanomedicines, its stakes and challenges for the eventual successful application of nanoparticle-based technologies in the clinics.

I. Adenosine in the treatment of inflammatory disorders

Adenosine immunomodulation

The adenosine receptor system has evolved as both a rapid sensor of tissue injury and the major 'first-aid' machinery of tissues and organs(1). Adenosine receptor activation thus preserves tissue function and prevents further tissue injury following an acute insult, hyper inflammation or reperfusion injury, conditions in which the immune system has a paramount role(2). During these inflammatory phases, adenosine plays an important role in regulating inflammation. It can be formed endogenously in response to metabolic stress through the extracellular action of two key ectoenzymes CD39 and CD73 which sequentially dephosphorylate pro-inflammatory ATP into pro-resolving adenosine. Inhibition of the final step of this cascade by genetic depletion of CD73 in mice is associated with a pro-inflammatory phenotype showing exacerbated severity in numerous rodent models of inflammatory diseases(3). In macrophages and neutrophils, adenosine inhibits the release of pro-inflammatory cytokines such as TNF-α while stimulating production of anti-inflammatory cytokines such as interleukin 10 (IL-10). Four ubiquitous G protein–coupled receptors (A_1, A_{2A}, A_{2B} and A_3) are responsible for mediating adenosine signaling. Recent advances in understanding the role of the distinct adenosine receptors and the complex network of cellular players that determine the adenosine response to tissue injury have helped identify novel pharmacological targets to restore tissue function in various inflammatory conditions(4, 5). Although adenosine receptor subtypes play complicated and sometimes opposing roles in inflammation, central administration or continuous intravenous infusion of adenosine have generally been shown to be protective against inflammatory insults(6). However -and despite progress in the development of several specific agonists of adenosine receptors- these approaches remain largely limited by the side-effects that unchecked adenosine receptor activation affords, as well as rapid metabolization(7). Hence, any modification in adenosine delivery that may alleviate adverse reactions without losing its immunomodulatory action may prove beneficial.

Squalenoylation

Systemic injection of adenosine usaully causes arterial hypotension and a baroreceptor reflex tachycardia mediated in part by withdrawal of vagal tone from the sinoatrial node(8). In this work, we showed that squalenoylation can protect against adenosine-related cardiodepressive

side effects (Figure 1B).

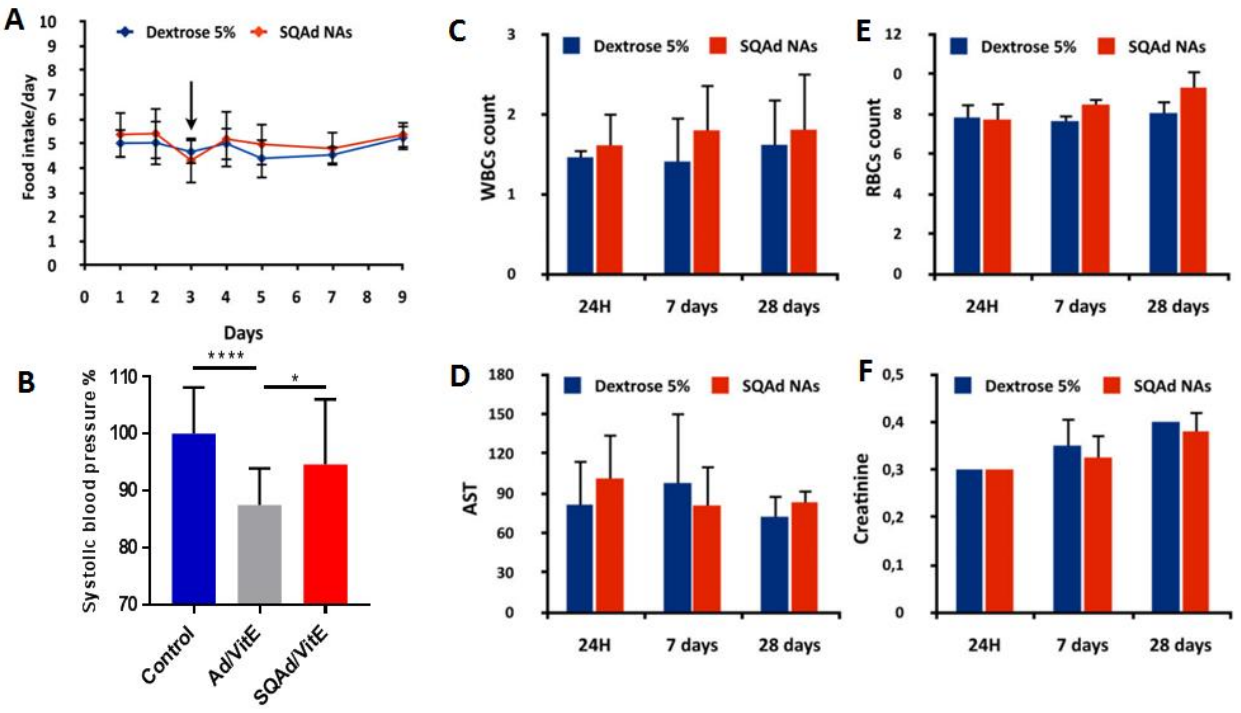

Figure 1: (**A**) Daily food intake of SQAd treated animals comparatively to controls.(**B**) Systolic blood pressure determination as % of control. *n*=3 animals per group, five measurements per animal. (**C-F**) Work done by A.Gaudin evaluating the acute (day 1 and day 7) and long term (day 28) toxicity of the SQAd upon systemic administration were then assessed. SQAd administration did not induce any increase nor decrease of the white (**C**, data are presented as mean ($\times 10^3/\mu L$) ± SD, N = 5 animals/group) and red blood cells counts (**E**, data are presented as mean ($\times 10^6/\mu L$) ± SD, N = 5 animals/group). Similarly, no differences in aspartate aminotransferase (**D**, data are presented as mean (UI/L) ± SD, N = 5 animals/group) and creatinine (**F**, data are presented as mean (mg/dL) ± SD, N = 5 animals/group) were observed between the animals injected with SQAd and the controls (dextrose 5%).

This adds itself to previous work from our laboratory showing that SQAd did not induce significant variations in white blood cell counts, red blood cells, food intake or markers of hepatic or renal stress. Essentially, SQAd nanoparticle administration caused no measurable side-effects, contrary to administration of the free drug. To refine this data, and in an additional study with collaborators at University of Namur, we evaluated the influence of SQAd and SQAd/VitE NPs on hematologic parameters. Both formulations were found to induce no toxicity, as measured by hemolysis, and did not induce platelet aggregation or coagulation (Figure 2-3). In the presence of platelet aggregation inducers, adenosine showed an anti-aggregation effect,

in accordance with the literature. This anti-aggregation effect was diminished after encapsulation of adenosine in SQAd nanoparticles.

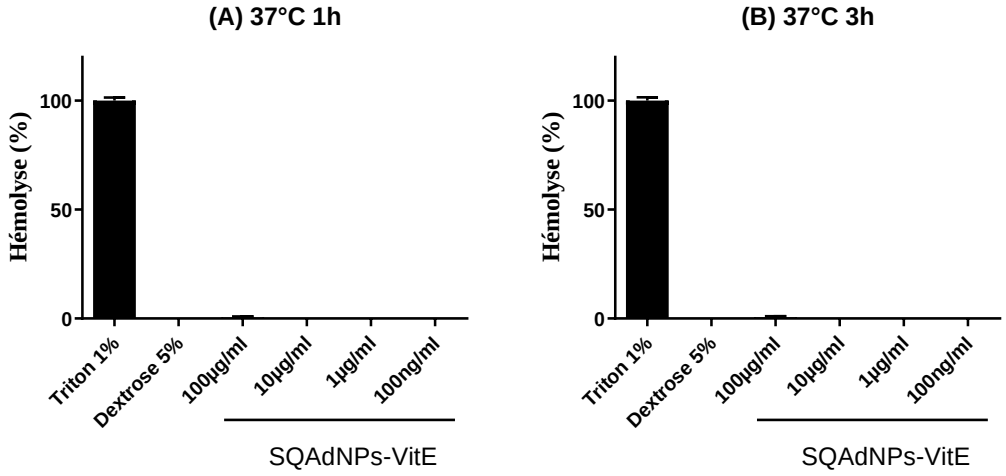

Figure 2: Washed red blood cells from 3 healthy donors were incubated in presence of SQAd/VitE NPs during 1h, 3h or 24h at 37°C in presence of 5% CO_2. After centrifugation, supernatant is collected and hemoglobin content is determined by spectrometric detection at 540nm. Formulations were tested at concentrations ranging from 100 µg/ml to 1ng/ml. No hemolysis of the tested formulations was observed from 100µg/ml to 1ng/ml, in washed red blood cells, Triton X100 1% is the positive control, inducing 100% of red blood cell lysis.

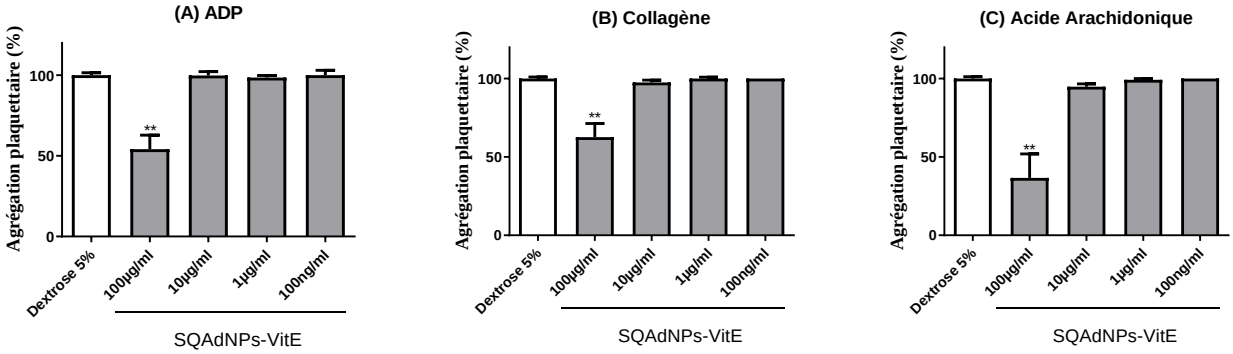

Figure 3: Platelet aggregation following incubation with platelet aggregation inducers. Aggregation was studied using a chronometric aggregometer by measuring the optical density at 620 nm in a glass cuvette (at 37°C under continuous stirring (1,000 rpm). Platelet-rich plasma (PRP) at 300,000 platelets/µL were incubated with SQAd/VitE NPs in presence or absence of platelet aggregation inducers (ADP, collagen or arachidonic acid). Data were collected with the Chronolog two-channel recorders connected to a computer. PRP were obtained from healthy

donors and used freshly within 3 hours to maintain platelet reactivity. A significant anti-aggregation effect is observed with SQAd/VitE NPs at concentration of 100 µg/mL when platelet aggregation is induced by ADP, Collagen or Arachidonic Acid. *n*=6 Data are mean ± SD. ns: non significant,**P*<0.05, ***P*<0.01,****P*<0.001 (Student's *t*-test).

Taken together, these data paint the picture of a highly improved therapeutic index for adenosine, and represent a significant step forward in the use of adenosine for inflammatory conditions. Along with the added targeting afforded by the nanoparticle formulation, and the possibility to co-encapsulate different drugs to synergize with adenosine therapy, SQAd NPs appear as a truly promising platform for purinergic based inflammation therapy.

Further studies

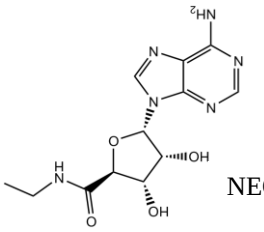

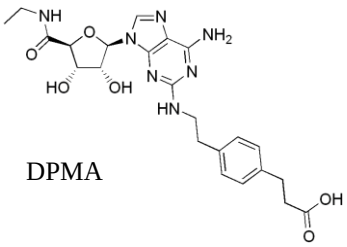

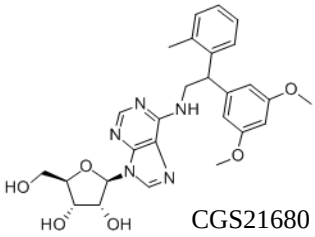

Some elements to consider remain in the above mentioned contradictory effects of unspecific activation of the adenosine receptor system. Indeed, it has been recognized that adenosine receptor subtypes play complicated and sometimes opposing roles in inflammation (Figure 4). Activation of one or the other receptor systems seems to be predicated, in part, on extracellular adenosine concentrations. Indeed, adenosine can induce signaling through all four of its cognate receptors, however, it does so with varying effective concentrations (EC_{50}). While A_1 and A_3 are high affinity receptors with EC_{50} values that are between lower than 1 µM, A_{2A} and A_{2B} receptor activation generally requires adenosine levels that between 1-10 µM. Because physiological adenosine concentrations are lower than 1 µM, physiological levels of adenosine cannot activate A_2 receptors which require pathophysiological conditions. Prolonged exposure of cells to elevated levels of adenosine is thus often associated with tissue stress and induces a response which aims at reestablishing homeostasis. Perhaps, the high local doses that SQAd therapy allows to attain could be the key that afforded the important therapeutic improvements observed in our endotoxemia models. An interesting perspective which could be explored using squalenoylation technology would be the use of specific adenosine receptor agonists such as

NECA, CGS21680 or DPMA. These compounds could gain from the squalene based nanoformulation in terms of improved bioavailability, all the while activating only a specific subset of adenosine receptors with higher affinity.

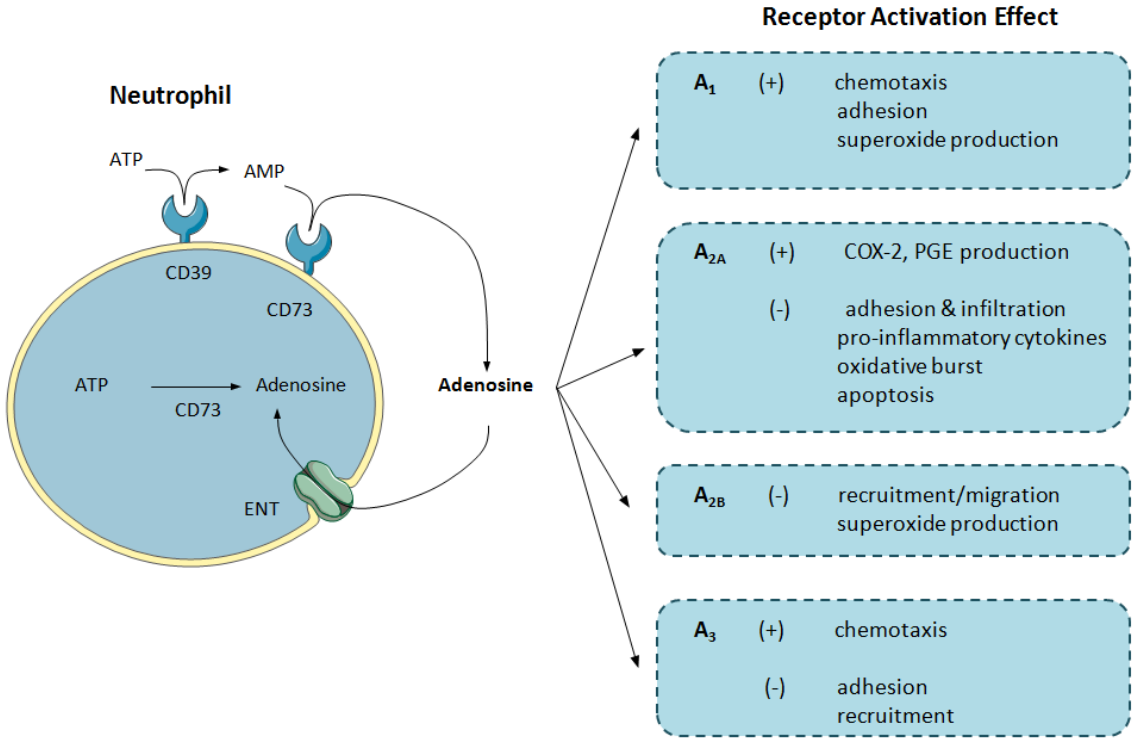

Figure 4: Overview of adenosine regulation of neutrophils.

II. Multidrug nanoparticles

In this section, we will discuss multidrug nanoparticles and their use in therapeutic interventions. Here, the term 'multidrug nanoparticles' will be used to describe those nanomaterial based systems that encapsulate multiple drugs for a synergistic pharmacological effect but exclude theranostic devices.

Where multidrug nanoparticles have a role to play

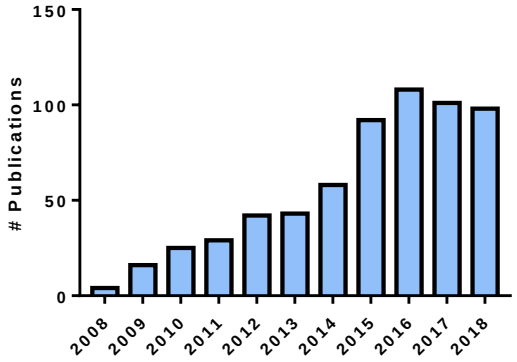

Figure 5: Number of publications related to multidrug nanoparticles in the pharmacology field from the past ten years as referenced by Web of Science.

Over the last ten years, nearly 20 000 research articles were published in the field of pharmacology describing the use of nanoparticles. Among these, about 700 mentioned multidrug therapies, which represent about 3.5% with a declining trend in the last two years (Figure 5). In fact, despite their interesting design, it is becoming increasingly difficult to publish multidrug-based studies because of their inherent complexity. Multidrug nanoparticle studies make the assumption that not only two particular drugs will act at their intended sites with the intended mechanism, but that their action will be synergistic and that the encapsulation of both drugs in the same nanoparticular system facilitates this synergistic action. This markedly enhances the number of hypothesis that need to come true for a certain system to work, and the number of experiments and controls that need to be used to prove the studies' main points with any kind of significance.

With this in mind, where do multidrug nanoparticles have a role to play? Historically, the first studies evaluating multidrug nanoparticle systems were undertaken in the context of oncology

and antibiotics, evaluating their effect against the appropriately named, multi-drug resistant cancers or organisms. If these cancers were resistant to different drugs maybe tackling them with different drugs simultaneously could be the key to overcome their pharmacological resistance. Following this idea, for instance paclitaxel has been delivered to cancer cells in vivo with different co-drugs to overcome drug resistance(9, 10). One could ask, what is it about these particular types of cancer that makes the use of multidrug nanoparticles adequate? Their properties could be surmised as follows: (i) Precise spatial location that NPs can (ideally) target (ii) Resistance to single drug treatments that can be improved by multidrug formulation (iii) Importance of spatial and temporal delivery of drugs together for synergistic action. (iv) Existence of a particular micro-environment that allows differential accumulation of nanoparticles in the disease space or specific targeting.

This, in essence, gives us a roadmap for the development of relevant multidrug nanoparticle formulations. Indeed, if all of the above conditions are met, then multidrug nanoparticles could and should be developed for the disease and may improve therapeutic outcomes. Here, we would argue that these conditions are met in acute, uncontrolled inflammatory disorders which provide the following:

1. Resistance to single drug treatments due to multifactorial influence (inflammatory cascades, ROS, pathogens)
2. A specific enzymatic, chemical and biological microenvironment (inflammatory microenvironment with increased endothelial permeability)
3. Importance of spatial and temporal co-distribution of drugs (especially for countering ROS which act very quickly at the sites where they are produced)
4. Precise location of inflammation foci.

Recognizing the first parameter, *ie* the multifactorial pathogenesis of uncontrolled inflammatory processes and the importance of oxidative stress, other groups have started to develop multidrug antioxidant and anti-inflammatory based therapies(11).

Recognizing the other three parameters prompted us to study a multidrug nanoparticle system in the context of sepsis. As far as we know, our study was the first to evaluate such a combination of anti-inflammatory and antioxidant agents with a nanoparticle based system. Because of the pro-drug based design of SQ based nanoparticles, another drug could easily be incorporated in the nanoparticle and actually augment total drug loading, which is one the particularities of squalenoylation technology (Figure 6).

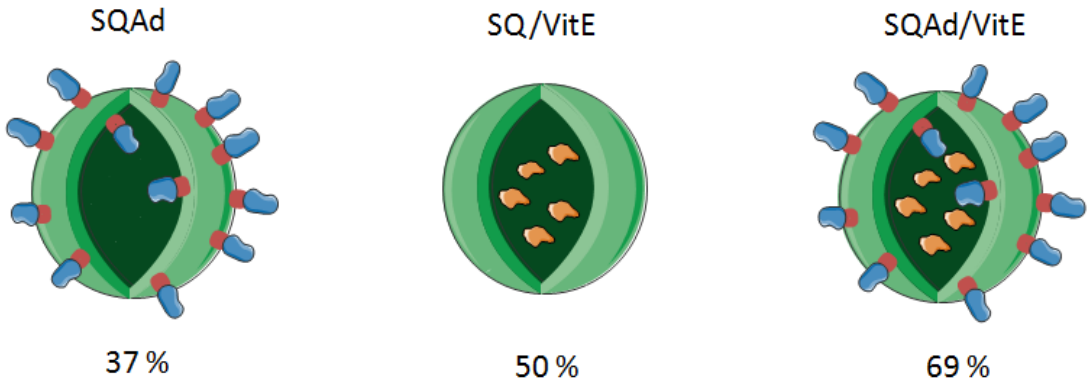

Figure 6: Total drug loading of SQAd monodrug nanoparticles vs VitE encapsulated in squalene-only nanoparticles vs SQAd/VitE nanoparticles

Further Studies

Another condition in which multidrug nanoparticles could be of use is in ischemia-reperfusion injuries. After an ischemic event, reperfusion induces a rush of blood and nutrients to ischemic tissue and cells which triggers a host of abnormal reactions leading to mitochondrial respiratory chain dysfunction(12), oxidative stress(13), apoptotic cell death(14) and an inflammatory reaction(15, 16). The ischemic endothelium is also characterized by increased permeability and some groups have shown that this can be exploited by nanoparticles to target the diseased tissue after reperfusion(17). As we can see, this meets all the criteria that we articulated above for the use of multidrug nanoparticles. Reperfusion injuries are localized, multifactorial events that are often difficult to treat and induce a specific micro-environment that can be target by nanoparticles.

Accordingly, in collaboration with the group of Pr. Maria José Blanco Prieto at the University of Navarra, a rat model of ischemia-reperfusion injury was developed to test these hypotheses. Briefly, rat left anterior descending artery was transiently occluded with a polyethylene (PE-10) tube for one hour to induce ischemia. Reperfusion was afforded by removing the PE-10 tube, at which point SQAd/VitE NPs, SQAd NPs, dextrose 5% controls were injected right after reperfusion. In a first experiment, SQAd nanoparticles were fluorescently labelled to evaluate whether these could accumulate at the site of ischemia-reperfusion. The animals were sacrificed 24 hours after NP treatment. As can be seen in Figure 7, some fluorescence signal can be detected in the heart infarcted area, which confirmed accumulation of the NPs.

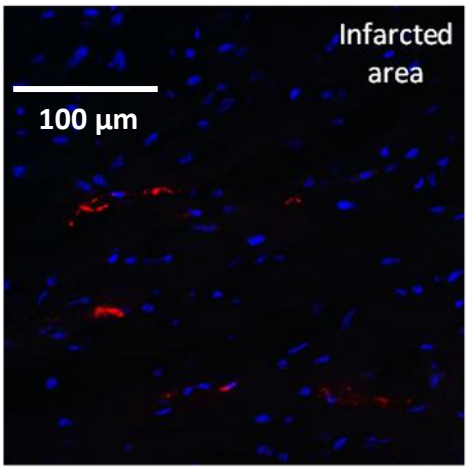

Figure 7: Study performed by L.Saludas evaluating the biodistribution of SQAd nanoparticles to infarcted myocardium. Fluorescent nanoparticles were injected 4 hours after reperfusion and animals sacrificed 24 hours after NP injection. Heart tissue was collected, frozen and included in OCT. Sections were stained with DAPI for cell marking.

To evaluate the effect of NP treatments on heart function, the ejection fraction and fractional shortening parameters were evaluated using a non-invasive echocardiography apparatus. Figure 8 represents the measured ejection fraction and fractional shortening of the left ventricular diameter between diastole and systole at two days after ischemia and three months. The larger the values of these two important parameters, the healthier the animals are. The important thing to observe here being the difference between these values at three months compared to two days, which describe the recovery of the animal after initial trauma. In the case of both SQAd and SQAd/VitE groups, we see that a significant improvement of cardiac function was observed, while the DXT 5% control treat group did not display any significant improvement of cardiac function over the three month period.

One important caveat to not here is that in multidrug SQAd/VitE NPs system, contrary to our endotoxemia studies, the dose of SQAd was twice lower than in the SQAd group, which could partly explain the observed results. Further studies at the therapeutic doses that were found in chapter 2 should be undertaken. For now these data allow us to simply say that the multidrug system is as efficient as single drug SQAd at 2x lower dose, which is still a promising result.

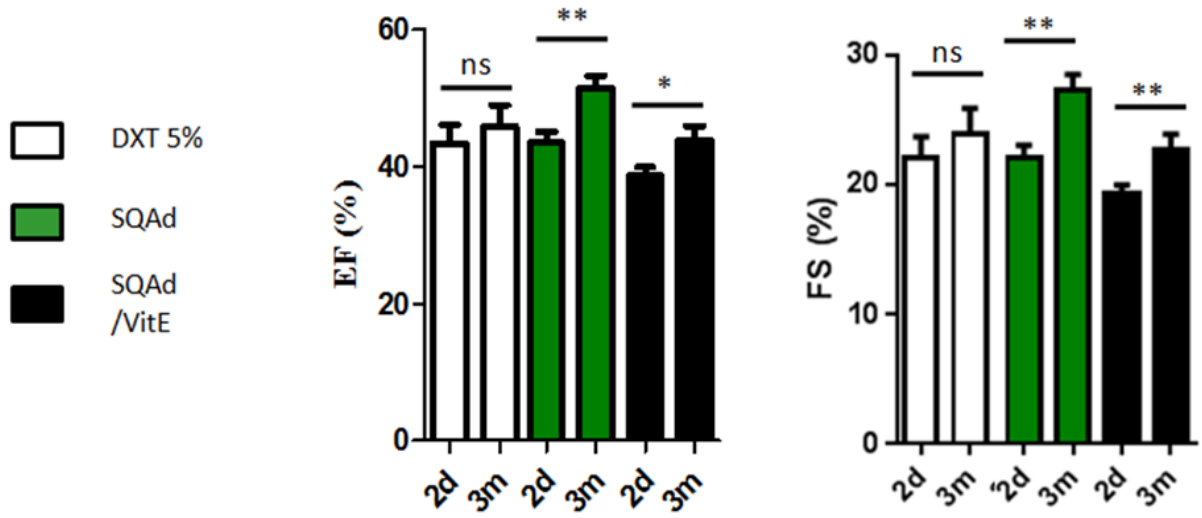

Figure 8: Heart function of rats after ischemia reperfusion injury measured by non-invasive echocardiography. The left graph represents ejection fraction EF% of SQAd/VitE NPs treated group, SQAd treated group and DXT 5% treated group. N=6 animals/group. Right graph represents the fractional shortening FS%

These interesting studies indeed confirmed the potential of multidrug squalene based nanoparticles, which opens the way to a myriad of drug combinations to be explored. Some interesting developments for multidrug SQAd based therapy could be found in drugs that slow metabolization of adenosine, such as adenosine deaminase inhibitors like dipyridamole, which allow the accumulation of adenosine. Used in a multidrug nanoparticular system, this compound could limit local breakdown of adenosine while avoiding common side-effects of dipyridamole (flushing, nausea, dizziness).

III/Differential SQ-based nanoparticles biodistribution in inflammatory disorders

As presented in Chapters 1 and 2, SQ-based nanoparticles biodistribution was evaluated in three murine models of inflammation: A local LPS induced paw inflammation model, a systemic LPS induced endotoxemia model and an ApoE -/- knockout atherosclerotic vascular inflammation model. In each model, an augmented accumulation of SQ based nanoparticles in the inflamed area was observed (Figure 9).

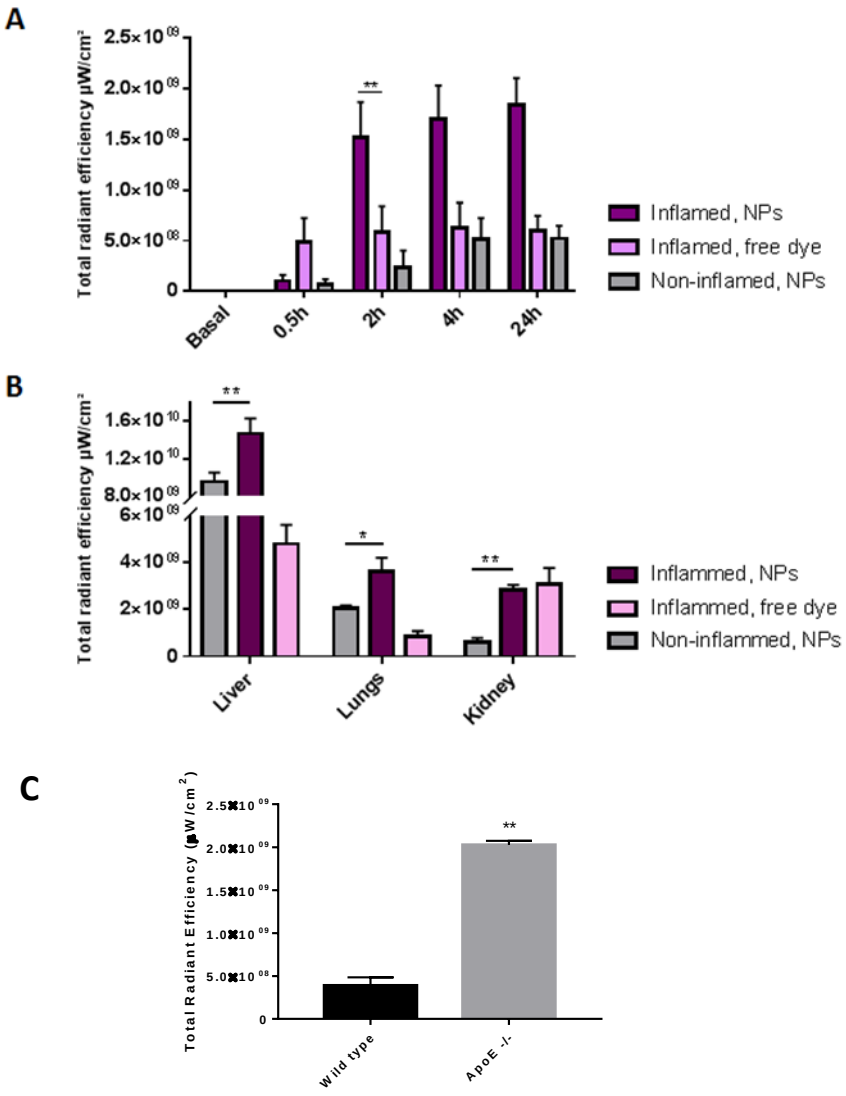

Figure 9: (**A**) Analysis of the measured total radiant efficiency in the paw. *n*=3 mice per group. (**B**) Analysis of the measured total radiant efficiency in the different organs. *n*=3 mice per group. Data are mean ± SD. **P*<0.05, ***P*<0.01 (Student's *t*-test). (**C**) Analysis of measured total radiant efficiency in aorta of ApoE -/- atherosclerotic mice vs wild type mice.

Possible mechanisms of accumulation

There are essentially three mechanisms that could explain this differential accumulation of SQ based NPs at the sites of inflammation:

i. Accumulation in LDL and indirect targeting by LDL accumulation at the site of inflammation.

ii. Capture by the immune system and localization at inflammation site

iii. EPR effect caused by leaky vasculature at the site of inflammation

1. Accumulation in LDL

In a previous paper from our laboratory, squalene-based bioconjugates were found to be efficient targeting moieties for LDL endogenous lipoproteins(18). In an interesting study, both Squalene-Gemcitabine (SQGem) and SQAd nanoparticles were found to accumulate into LDL (Figure 10), indirectly conferring a targeting capacity towards LDL-receptor (LDLR) expressing cells. This targeting approach was validated in another study where SQGem nanoparticles were used to specifically target MDA-MB-231 breast cancer cells in vivo, which overexpress LDLR(19). Interestingly, the LDLR synthesis pathway is also upregulated in immune cells during conditions of acute inflammation and in the metabolic disorders involved with the pathogenesis of atherosclerosis(20, 21). It followed that squalene-based nanoparticles could preferentially accumulate at the sites of acute inflammation and atherosclerotic plaque development, warranting further studies in this context. This led us to extend our investigations on inflammation to targeting atherosclerotic plaque, via the observed accumulation of SQ bioconjugates in LDL particles and their subsequent accumulation in atherosclerotic plaques. This was the main hypothesis behind our atherosclerosis study. The study seemed to confirm that SQ based NPs accumulated inside atherosclerotic plaque. Current work in our lab is aimed at establishing whether this accumulation is due to the specific nature of our squalene nanoparticles or occurs through a more passive mechanism common to other nanoparticular systems. Another question that remains is whether all SQ NPs accumulate in LDL, and if not, what fraction remains as “free NPs”.

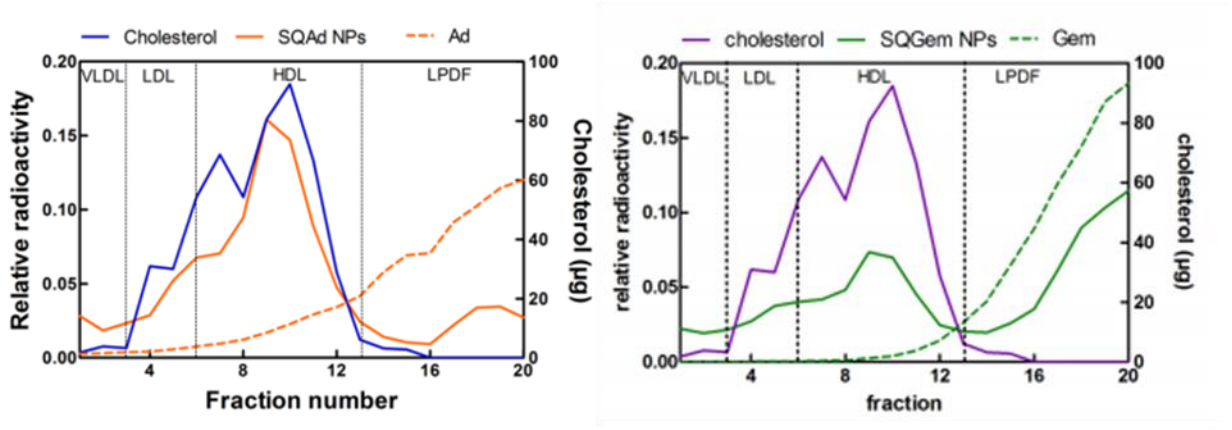

Figure 10: Work by Dunja Sobot on distribution of SQNPs in the blood. ^{3}H-SQGem, ^{3}H-SQAd, ^{3}H-Ad and ^{3}H-Gem distribution in plasmatic fractions – in vivo. Radioactivity (green and yellow curves) and cholesterol (violet and blue curve) distribution among the collected fractions of plasma obtained from rats treated with 3 H-SQGem (solid green curve), 3 H-SQAd (solid yellow curve), free 3H-Ad (dashed yellow curve) or free 3 H-Gem (dashed green curve)), 5 min post administration. Results are expressed as relative radioactivity compared to total plasma (mean values, n=6).

An important concept here, is the importance of the relative concentration of LDL to NPs. LDL usually have a concentration of around ~1.3 µM in the blood, which is almost 100x lower than the usual initial dose injected with SQ based nanoparticles of around 100 µM. Even given an initial capture by the reticular endoplasmic system (RES), one can easily imagine a rapid saturation of LDL capacity to transport SQ based treatments. There probably exists an equilibrium between stable nanoparticles in the circulation and accumulated SQ bioconjugates inside of LDLs, with further studies that are being undertaken to evaluate this hypothesis.

2. Capture by immune system

If SQ NPs remain in the circulation then capture by the immune system can be another eventual outcome. This phenomenon has been exploited by different research groups to forward nanoparticles to the sites of inflammation by “hitchhiking” on neutrophils for instance(22, 23). This kind of system usually requires nanoparticles that are recognized by immune cells with specific targeting motifs and induce some kind of inflammatory response of their own. While SQAd NPs did not induce an inflammatory response on their own, they do get recognized by RAW 264.7 macrophages in vitro and after i.v. injection a certain amount can be detected in the

spleen. As of now, further studies are needed to conclude on this question.

3. EPR Effect in inflammation

In acute inflammation, vascular hyperpermeability dominates and numerous research groups have demonstrated the use of this leaky vasculature to deliver therapeutic agents in inflammatory disorders ranging from rheumatoid arthritis to hepatitis. The increase in endothelial permeability has also been unequivocally demonstrated in sepsis and atherosclerosis, where it allows the migration and accumulation of different macromolecules in cells at the sites of inflammation(24-27). For these reasons, there is little doubt that increased endothelial permeability is at the root of the targeting mechanism observed in our studies. Whether squalene-nanoparticles diffuse out of the circulation as whole nanoparticles or after capture by different structures such as LDL or immune cells is still unknown. The question then is whether a significant amount of SQ NPs can stay stable in the circulation long enough to efficiently accumulate at the site of inflammation through this mechanism. Our in vivo data presented in **chapter 1** showed that SQ NPs displayed significant accumulation in the inflamed tissue two hours after i.v. injection (Figure 11). Although we could not test in vivo the stability of the SQAd and SQAd/VitE NPs evaluated in that study, our ex vivo data showed that for at least the two hours needed for initial tissue accumulation, a certain amount of nanoparticles could remain stable as measured by DLS. Whether this is relevant for *in vivo* experiments is debatable.

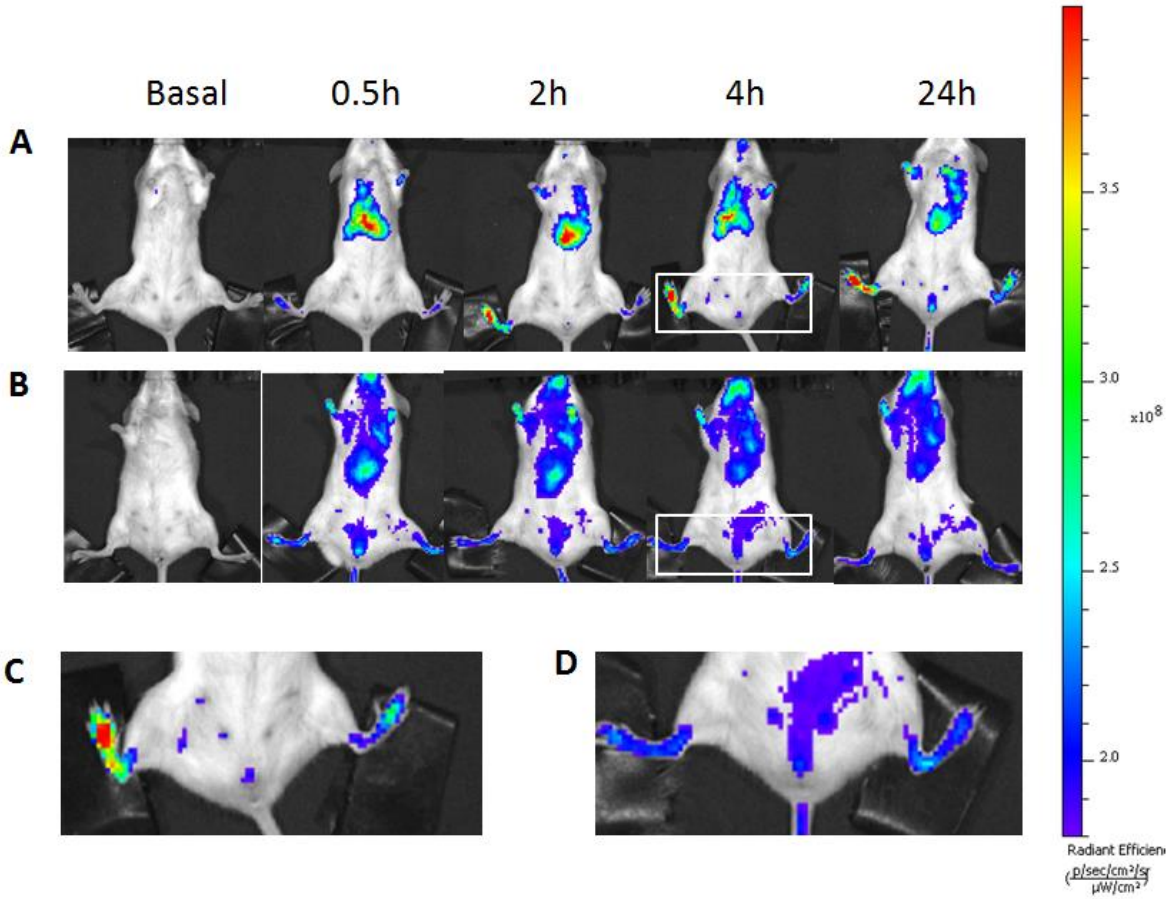

Figure 11: IVIS Lumina scan of mice after intravenous administration of fluorescent SQAd/VitE NPs or control fluorescent dye solution (ventral view). (A) Biodistribution of fluorescent SQAd/VitE NPs in mice with inflamed right hind paw and non-inflamed left hind paw. (B) Biodistribution of the free dye in mice with inflamed right hind paw. (C) Zoom of group A at 4 hours. (D) Zoom of group B at 4 hours.

IV. Industrial Scale up of Nanomedicines

The challenges and stakes of scaling up nanomaterial synthesis

Scaling up the production of any chemical entity be it small drug molecule, polymer or protein has always been a challenge with its own dedicated fields of process engineering, materials engineering, or industrial engineering. Numerous guidelines from different regulatory agencies have been set in place for the industrial production of molecules selected for use in humans. Agencies such as the FDA ensure the quality of drug products by carefully monitoring drug manufacturers' compliance with its Current Good Manufacturing Practice (CGMP) regulations. The CGMP regulations for drugs contain minimum requirements for the methods, facilities, and controls used in manufacturing, processing, and packing of a drug product. The regulations make sure that a product is safe for use, and that it has the ingredients and strength it claims to have.

These form a base from which the field of nanomedicine needs to elaborate to develop a common framework of guidelines for the successful translation from laboratory work to industrial production. This is now a key issue for the field which is starting to be viewed as an infertile playground for chemists and biologists rather than a productive incubator for the medicines of the future. Simplicity, efficiency, consistency, reproducibility these are all essential attributes which are for now lacking from the usual formulations churned out by the hundreds of nanomedicine labs around the world, which limit their industrial translation and the probability of one ever making it to the market.

So what has been lacking?

When a putative nanomedicine first shows initial positive results, it has to be produced in large scale for eventual study by different labs and for toxological evaluation in different animal models. While rodent models are still usually within the means of laboratory production, non-murine models such as dogs or pigs usually require 100x of active pharmaceutical ingredient (API) quantity than what rodents do and currently, very few nanomedicines ever make it to this stage. Indeed, to attain these types of trials, a scale up in both chemical synthesis and formulation processes has to be set up. When achieved, quality evaluation is performed to test

the drug formulation. However, due to the novel nature of nanomedicines, their manufacturing is challenged by potential issues related to: (i) scalability complexities; (ii) incomplete purification from contaminants (such as by-products or starting materials); (iii) high production costs; (iv) low yield; (vi) insufficient batch-to-batch reproducibility; (vii) consistency and storage stability of the final compound; (viii) lack of infrastructure and expertise; (ix) low interest from venture funds and pharmaceutical industry investment. Therefore, an essential requirement for clinical translation is to have access to a preparation method that allows the production of large, scalable quantities of nanomedicine, which is also consistently manufactured at the same high level of quality from batch-to-batch. It follows that the careful rational design of nanomedicines from the early phase of material selection, production method optimization, and product purification is of fundamental importance to increase their clinical translation potential. Any grant for the development of new nanomedicines should be accompanied by a crude economical and process design feasibility study to assess ease of industrial translation. This would force researchers, not only to think about the issue, but also design materials and projects which have a chance to make it to the clinics one day.

Regulatory oversight

Even when all these challenges are met, new nanomedicines are faced with somewhat of a regulatory void. As of now, regulatory agencies have issued no specific guidelines for nanomedicines, which could give a common framework of drug development. Indeed, there is a regulatory need for validated, sensitive and standardizable assays incorporating *in vitro*, *ex vivo* and *in vivo* protocols to appropriately assess the nanotoxicology of nanomedicines during the early stages of clinical development. Protocols should be in place to detect any toxicity caused not only by the encapsulated therapeutic compounds, but also novel mechanisms unique to nanotechnology. For example, the effects of nanomedicine accumulation in RES organs (liver, kidneys, spleen) should be investigated for each new formulation to ensure its safety. This is complicated further by the fact that nanomedicines often do not have a single chemical identity but are formed of numerous different molecules. For example, polymers have been widely investigated as an effective platform for nanomedicine strategies; however, their safety and efficacy is highly dependent on the polymer molecular weight, polydispersity, molecular structure, and conjugation chemistry.

Nanomedicines encompass such a large array of materials and structures that it is still unknown whether it will ever be possible to develop standardized testing protocols. Effective clinical translation will most probably require an interdisciplinary approach to ensure GMP manufacturing, characterization, toxicology evaluation and trial design. An effective way to fast-track promising novel nanomedicines would be the use of laboratories and centres that have expertise in nanoparticle characterization or scale up according to regulatory and industrial standards.

V. References

1. G. Haskó, B. Csóka, Z. H. Németh, E. S. Vizi*, et al.*, A2B adenosine receptors in immunity and inflammation. *Trends in immunology*. 30, 263-270 (2009)
2. M. Y. Zuidema,C. Zhang, Ischemia/reperfusion injury: the role of immune cells. *World journal of cardiology*. 2, 325 (2010)
3. U. Flögel, S. Burghoff, P. L. Van Lent, S. Temme*, et al.*, Selective activation of adenosine A2A receptors on immune cells by a CD73-dependent prodrug suppresses joint inflammation in experimental rheumatoid arthritis. *Science translational medicine*. 4, 146ra108-146ra108 (2012)
4. K. A. Jacobson,Z.-G. Gao, Adenosine receptors as therapeutic targets. *Nature reviews Drug discovery*. 5, 247 (2006)
5. A. Tsuchida, T. Miura, T. Miki, K. Shimamoto*, et al.*, Role of adenosine receptor activation in myocardial infarct size limitation by ischaemic preconditioning. *Cardiovascular research*. 26, 456-461 (1992)
6. G. Haskó,B. N. Cronstein, Adenosine: an endogenous regulator of innate immunity. *Trends in immunology*. 25, 33-39 (2004)
7. G. Haskó, J. Linden, B. Cronstein,P. Pacher, Adenosine receptors: therapeutic aspects for inflammatory and immune diseases. *Nature reviews Drug discovery*. 7, 759 (2008)
8. I. Biaggioni, J. Onrot, A. S. Hollister,D. Robertson, Cardiovascular effects of adenosine infusion in man and their modulation by dipyridamole. *Life sciences*. 39, 2229-2236 (1986)
9. S. Ganta,M. Amiji, Coadministration of paclitaxel and curcumin in nanoemulsion formulations to overcome multidrug resistance in tumor cells. *Molecular pharmaceutics*. 6, 928-939 (2009)
10. Y. Patil, T. Sadhukha, L. Ma,J. Panyam, Nanoparticle-mediated simultaneous and targeted delivery of paclitaxel and tariquidar overcomes tumor drug resistance. *Journal of Controlled Release*. 136, 21-29 (2009)
11. P. E. Marik, V. Khangoora, R. Rivera, M. H. Hooper*, et al.*, Hydrocortisone, vitamin C, and thiamine for the treatment of severe sepsis and septic shock: a retrospective before-after study. *Chest*. 151, 1229-1238 (2017)
12. E. J. Lesnefsky, S. Moghaddas, B. Tandler, J. Kerner*, et al.*, Mitochondrial dysfunction in cardiac disease: ischemia–reperfusion, aging, and heart failure. *Journal of molecular and cellular cardiology*. 33, 1065-1089 (2001)
13. K. A. Kaminski, T. A. Bonda, J. Korecki,W. J. Musial, Oxidative stress and neutrophil activation—the two keystones of ischemia/reperfusion injury. *International journal of cardiology*. 86, 41-59 (2002)
14. M. A. Daemen, C. Van'T Veer, G. Denecker, V. H. Heemskerk*, et al.*, Inhibition of apoptosis induced by ischemia-reperfusion prevents inflammation. *The Journal of clinical investigation*. 104, 541-549 (1999)

15. C. Szabó, The pathophysiological role of peroxynitrite in shock, inflammation, and ischemia-reperfusion injury. *Shock (Augusta, Ga.)*. 6, 79-88 (1996)
16. J. Li, C. Xie, J. Zhuang, H. Li*, et al.*, Resveratrol attenuates inflammation in the rat heart subjected to ischemia-reperfusion: Role of the TLR4/NF-κB signaling pathway. *Molecular medicine reports*. 11, 1120-1126 (2015)
17. D. Verma, T. Levchenko, E. Bernstein,V. Torchilin, ATP-loaded liposomes effectively protect mechanical functions of the myocardium from global ischemia in an isolated rat heart model. *Journal of controlled release*. 108, 460-471 (2005)
18. D. Sobot, S. Mura, S. O. Yesylevskyy, L. Dalbin*, et al.*, Conjugation of squalene to gemcitabine as unique approach exploiting endogenous lipoproteins for drug delivery. *Nature communications*. 8, 15678 (2017)
19. D. Sobot, S. Mura, M. Rouquette, B. Vukosavljevic*, et al.*, Circulating lipoproteins: a Trojan horse guiding squalenoylated drugs to LDL-accumulating cancer cells. *Molecular Therapy*. 25, 1596-1605 (2017)
20. M. F. Linton, P. G. Yancey, S. S. Davies, W. G. Jerome*, et al.* (2019) The role of lipids and lipoproteins in atherosclerosis. *Endotext [Internet]*, (MDText. com, Inc.).
21. R. Ross, Atherosclerosis—an inflammatory disease. *New England journal of medicine*. 340, 115-126 (1999)
22. D. Chu, Q. Zhao, J. Yu, F. Zhang*, et al.*, Nanoparticle targeting of neutrophils for improved cancer immunotherapy. *Advanced healthcare materials*. 5, 1088-1093 (2016)
23. D. Chu, J. Gao,Z. Wang, Neutrophil-mediated delivery of therapeutic nanoparticles across blood vessel barrier for treatment of inflammation and infection. *ACS nano*. 9, 11800-11811 (2015)
24. L. Hakanpaa, E. A. Kiss, G. Jacquemet, I. Miinalainen*, et al.*, Targeting β1-integrin inhibits vascular leakage in endotoxemia. *Proceedings of the National Academy of Sciences*. 115, E6467-E6476 (2018)
25. W. L. Lee,A. S. Slutsky, Sepsis and endothelial permeability. *The New England journal of medicine*. 363, 689 (2010)
26. J. Huynh, N. Nishimura, K. Rana, J. M. Peloquin*, et al.*, Age-related intimal stiffening enhances endothelial permeability and leukocyte transmigration. *Science translational medicine*. 3, 112ra122-112ra122 (2011)
27. M. Friedman,S. Byers, Endothelial permeability in atherosclerosis. *Arch. Pathol.* 76, 99-105 (1963)

Introduction Générale

Les syndromes auto-inflammatoires, marqués par une réaction excessive du système immunitaire, sont associés à de nombreuses conditions pathologiques comme le sepsis, les accidents d'ischémie/reperfusion ou l'athérosclérose. En effet, une réponse inflammatoire excessive à l'encontre des tissus caractérise souvent l'apparition et la pathophysiologie de ces maladies complexes pour lesquelles ils manquent toujours des traitements efficaces. Ainsi, la plupart des thérapies disponibles pour adapter la réponse inflammatoire sont limitées la plupart du temps par des effets secondaires indésirables, une mauvaise spécificité et par l'apparition d'états d'immunodéficience.

Des avancées en délivrance de médicaments ont permis le développement de nombreux outils qui aident à adapter la stratégie d'administration d'agents pharmaceutiques. Notamment, les "nanomédecines" ont permis d'obtenir de nombreuses innovations en oncologie et en technologie diagnostique. En améliorant le ciblage des médicaments et en protégeant l'agent pharmaceutique d'une métabolisation précoce, les nanomedicines permettent d'améliorer l'index thérapeutique de certaines molécules, résultant en une amélioration du prognostic patient. Néanmoins, avec ces promesses viennent des limitations notables, comme le faible taux de chargement en drogue de certaines nanoformulations, un développement industriel compliqué ou un mauvais contrôle du relargage.

Pour répondre à ces limitations, l'équipe du Pr. Couvreur développe depuis 2004 une nouvelle stratégie d'encapsulation des médicaments, appelée « squalenoylisation ». Ainsi, le couplage d'agents actifs avec des dérivés du squalène, un lipide endogène, biocompatible et biodégradable, permet d'obtenir des nanoparticules stables, avec haut taux de chargement et faible toxicité. Les nanoparticules obtenues présentent dans de nombreux cas une pharmacocinétique plus avantageuses ainsi que distribution plus ciblée aux zones pathologique. L'application de cette technique à l'adénosine, une molécule au potentiel thérapeutique important mais limité par un temps de demi-vie plasmatique extrêmement court, a fourni des résultats particulièrement prometteurs dans le cadre du traitement de l'ischémie cérébrale et du traumatisme de la moëlle épinière.

Un autre avantage des nanoparticules à base de squalène est qu'elles rendent possible l'encapsulation de plusieurs agents thérapeutiques au sein d'un même système, permettant ainsi des traitements multi-drogue. Ceci est un outil important dans le contexte d'une réponse excessive du système immunitaire, où convergent souvent plusieurs facteurs pour faire progresser la maladie. Par exemple, il a été établi que l'auto-inflammation est souvent maintenue par des cercles vicieux entre stress oxydant et cascades pro-inflammatoires, ces deux voies de signalisation contribuant l'une à l'autre et inhibant le retour à l'homéostasie. Il n'existe pour l'instant pas de thérapies efficaces contre ce couplage pathologique. Part conséquent, un des objectifs de cette thèse était de développer et de tester sur de modèles précliniques d'inflammation excessive, des nanoparticules à base de squalène encapsulant deux agents thérapeutiques : l'adénosine, comme médiateur endogène des réponses inflammatoires et un antioxydant comme inhibiteur du stress oxydant. Notre hypothèse étant qu'une thérapie multi-drogue pourrait être avantageuse pour contrer les nombreux processus pathogènes qui se renforcent mutuellement lors des réponses inflammatoires ; mais aussi qu'une formulation sous forme de nanoparticules pourrait fournir des propriétés de ciblage intéressantes.

Dans une introduction bibliographique, nous décrivons dans un premier temps les différents systèmes qui ont été étudiés jusqu'aujourd'hui pour mitiger les processus inflammatoires non contrôlés qui se produisent lors du sepsis. Nous y résumons brièvement la pathogénèse de la maladie, évaluons où les thérapies actuelles ont échoué et examinons les différentes avancées faites en nanomédecine dans le domaine. Dans un second chapitre bibliographique, nous évaluons l'utilisations de biomatériaux dans le contexte des maladies cardiovasculaires, qui présentent souvent des désordres inflammatoires sous-jacents. Cette revue étudie les nanosystèmes qui ont été évalués pour la prévention de l'athérosclérose ainsi que le traitement de sa manifestation aiguë, l'ischémie cardiaque. Nous y analysons comment ces deux maladies évoluent, où et comment les nanomatériaux peuvent jouer un rôle thérapeutique et des pistes de recherche prometteuses dans le domaine.

Notre partie expérimentale est divisée en trois chapitres.

Dans le premier chapitre expérimental, nous décrivons le développement d'une nouvelle formulation de nanoparticules multidrogues à base de squalène pour l'atténuation de réponses inflammatoires excessives. En encapsulant l'adénosine et le tocopherol dans un même agent

thérapeutique, ces nanoparticules ont le potentiel de lutter efficacement contre le couplage en inflammation et stress oxydant tout en limitant les effets secondaires liés à l'administration de fortes doses d'adénosine. Après avoir caractérisé les propriétés physico-chimiques de notre formulation, ses effets anti-inflammatoires et anti-oxydants ont été évalués dans des modèles *in vitro* sur cellules tissulaires ou immunitaires. En parallèle, nous avons évalué la biodistribution de ces nanoparticules de squalène *in vivo* qui s'est révélée posséder une forte capacité de ciblage pour les tissus inflammés. Par conséquent, le potentiel thérapeutique de ces nanoparticules de squalène-adénosine/tocophérol (SQAd/VitE) a été évalué dans deux modèles *in vivo* d'inflammation systémique suite à une infection par endotoxine. Nos résultats montrent que les animaux traités avec les nanoparticules SQAd/VitE ont une survie significativement améliorée à l'endotoxémie générée et souffrent moins d'effets secondaires néfastes que les animaux traités avec les contrôles drogue libre.

Dans le deuxième chapitre expérimental, nous étudions si la capacité de ciblage des nanoparticules de squalène pour les tissus inflammés peut être translaté à d'autres modèles de maladie inflammatoire. Pour cela, nous avons étudié une preuve de concept la biodistribution de nanoparticules de squalène fluorescentes dans un modèle *in vivo* d'athérosclérose sur souris ApoE-/-. Nos résultats initiaux montrent que les nanoparticules de squalène s'accumulent bien dans les zones riches en lipide de la plaque d'athérome et pourrait interagir avec les macrophages résidents. Des études en cours cherchent à élucider plus précisément ce mécanisme d'accumulation.

Enfin, dans un troisième chapitre expérimental, nous évaluons la faisabilité du scale-up industriel de la synthèse de bioconjugués à base de squalène. En effet, bien que les nanomédecines puissent apporter de nombreuses avancées dans le traitement de diverses maladies, elles sont encore limitées par une production industrielle irréaliste, et par la création de systèmes qui sont devenus trop complexes ou trop onéreux à produire à grande échelle. Dans l'optique de faciliter la translation des nanoparticules de squalène d'une échelle de laboratoire à l'échelle industrielle nécessaire aux larges études multicentriques inéluctables pour une éventuelle mise sur le marché, nous nous sommes associés à un partenaire industriel pour produire en grande quantité des bioconjugués de squalène-adénosine (SQAd). Nos analyses ont démontré que des faibles différences dans la composition des profils d'impuretés de SQAd pouvait engendrer des propriétés physicochimiques et biologiques radicalement différentes, résultant en une mauvais reproductibilité des résultats d'études précliniques.

L’ensemble de ces travaux constitue une avancée dans le développement pharmaceutique des nanoparticules d’adénosine-squalène et ouvrent de nouvelles perspectives de recherche en démontrant comment les propriétés de ciblage que cette formulation nanoparticulaires octroie peuvent améliorer le traitement de réactions inflammatoires excessives.

Titre : Développement de nanomédicaments pour les troubles inflammatoires: évaluation de l'effet protecteur dans des modèles précliniques
Mots clés : Inflammation, nanoparticules, adénosine, squalène

Des avancées en délivrance de médicaments ont permis le développement de nombreux outils qui aident à adapter la stratégie d'administration d'agents pharmaceutiques. Notamment, les "nanomédecines" ont permis d'obtenir de nombreuses innovations en oncologie et en technologie diagnostique. En améliorant le ciblage des médicaments et en protégeant l'agent pharmaceutique d'une métabolisation précoce, les nanomedicines permettent d'améliorer l'index thérapeutique de certaines molécules, résultant en une amélioration du prognostic patient. Néanmoins, avec ces promesses viennent des limitations notables, comme le faible taux de chargement en drogue de certaines nanoformulations, un développement industriel compliqué ou un mauvais contrôle du relargage. Les nanoparticules à base de squalène ont été développé pour répondre à ces limitations. Un autre avantage des nanoparticules à base de squalène est qu'elles rendent possible l'encapsulation de plusieurs agents thérapeutiques au sein d'un même système permettant ainsi des traitements multi-drogue. Ceci est un outil important dans le contexte d'une réponse inflammatoire excessive, où convergent souvent plusieurs facteurs pour faire progresser la maladie. Part conséquent, un des objectifs de cette thèse était de développer et de tester sur de modèles précliniques d'inflammation, des nanoparticules à base de squalène encapsulant deux agents thérapeutiques : l'adénosine, comme médiateur endogène des réponses inflammatoires et un antioxydant comme inhibiteur du stress oxydant. Notre hypothèse étant qu'une thérapie multi-drogue pourrait être avantageuse pour contrer les nombreux processus pathogènes qui se renforcent mutuellement lors des réponses inflammatoires, mais aussi qu'une formulation sous forme de nanoparticules pourrait fournir des propriétés de ciblage intéressantes. Au cours des travaux de cette thèse, nous avons également la faisabilité de translation industrielle de la synthèse des bioconjugués à base de squalène.

Titre: Development of nanomedicines for inflammatory disorders: evaluation of squalene-based nanoparticles in pre-clinical models
Mots clés : Inflammation, nanoparticules, adenosine, squalene

Advances in drug delivery have led to the development of many tools that help tailor the drug delivery strategy. In particular, "nanomedicines" have made it possible to obtain numerous innovations in oncology and diagnostic technology. By improving drug targeting and protecting the pharmaceutical agent from early metabolism, nanomedicines improve the therapeutic index of certain molecules, resulting in improved patient prognosis. However, with these promises come notable limitations, such as the low drug loading rate of certain nanoformulations, complicated industrial development or poor release control. Squalene-based nanoparticles have been developed to meet these limitations. Another advantage of squalene-based nanoparticles is that they make it possible to encapsulate several therapeutic agents within the same system, thus allowing multi-drug treatments. This is an important tool in the context of an excessive inflammatory response, where many factors often converge to advance the disease. Therefore, one of the objectives of this thesis was to develop and test on preclinical models of inflammation, squalene-based nanoparticles encapsulating two therapeutic agents: adenosine, as an endogenous mediator of inflammatory responses and an antioxidant as an inhibitor of oxidative stress. Our hypothesis is that a multi-drug therapy could be advantageous to counter the many pathogenic processes which reinforce each other during inflammatory responses, but also that a formulation in the form of nanoparticles could provide interesting targeting properties. During the work of this thesis, we also have the feasibility of industrial translation of the synthesis of squalene-based bioconjugates.

Université Paris-Saclay
Espace Technologique / Immeuble Discovery
Route de l'Orme aux Merisiers RD 128 / 91190 Saint-Aubin, France